USGS
science for a changing world

Eruptive History of Mammoth Mountain and its Mafic Periphery, California

Professional Paper 1812

U.S. Department of the Interior
U.S. Geological Survey

Cover. Photograph of east side of dacitic Mammoth Mountain, showing steep former glacial headwall, several discrete lava domes, and numerous cleared ski runs. Complex edifice consists of 24 separate extrusions, all erupted between 100 ka and 50 ka. Total relief in image ~970 m. Lincoln Peak is large dome at right. Part of residential district of Town of Mammoth Lakes at right center. See figure 1 for more details.

Eruptive History of Mammoth Mountain and its Mafic Periphery, California

By Wes Hildreth and Judy Fierstein

Professional Paper 1812

U.S. Department of the Interior
U.S. Geological Survey

U.S. Department of the Interior
SALLY JEWELL, Secretary

U.S. Geological Survey
Suzette M. Kimball, Director

U.S. Geological Survey, Reston, Virginia: 2016

For more information on the USGS—the Federal source for science about the Earth, its natural and living resources, natural hazards, and the environment—visit http://www.usgs.gov or call 1–888–ASK–USGS.

For an overview of USGS information products, including maps, imagery, and publications, visit http://www.usgs.gov/pubprod/.

Suggested citation:
Hildreth, Wes, and Fierstein, Judy, 2016, Eruptive history of Mammoth Mountain and its mafic periphery, California: U.S. Geological Survey Professional Paper 1812, 128 p., 2 plates, scale 1:24,000, http://www.dx.doi.org/10.3133/pp1812

ISSN 1044-9612 (print)
ISSN 2330-7102 (online)

ISBN 978-1-4113-4065-7

Acknowledgments

Garniss Curtis introduced Wes Hildreth to Long Valley in 1960, Ian Carmichael motivated his work on the caldera-forming eruption in the 1970s, Gail Mahood and Colin Wilson kept him busy there for decades, and Dave Hill drew him into Mammoth Mountain investigations in 2003. Our work built upon that of our late friend and colleague, Roy Bailey, whose 1:62,500-scale geologic map provided a guide to our investigations. Hill and Margaret Mangan have ably overseen USGS research and monitoring at Long Valley, today as part of the California Volcano Observatory (http://volcanoes.usgs.gov/observatories/calvo/). Duane Champion led our paleomagnetic investigations, and Andy Calvert provided the new $^{40}Ar/^{39}Ar$ age determinations. We are grateful to Deanna Dulen and Wymond Eckhardt for engaging us in the geology, ecology, and history of Devils Postpile National Monument, which they have overseen with dedication and good judgment; to Clifford Mann for a wealth of information on the history and logistics of the Mammoth Mountain Ski Area; to Gene Suemnicht and Mike Sorey for advice on well logs and the geothermal system; to Brent Turrin and Dean Miller for contributions in the field and the lab; to John Gottwald and Scott Lee for access to the Arcularius and Alpers Ranch properties; and to Sally and Bob Drake of Old Mammoth for hospitality, companionship, and imagination and vigor on the mountainside. The manuscript was constructively reviewed by Charlie Bacon, Margaret Mangan, and Dave Hill.

Contents

Plates

[In pocket and available online at http://www.dx.doi.org/10.3133/pp1812]

Figures

Tables

Appendix

Eruptive History of Mammoth Mountain and its Mafic Periphery, California

By Wes Hildreth and Judy Fierstein

Introduction

This report and accompanying geologic map portray the eruptive history of Mammoth Mountain and a surrounding array of contemporaneous volcanic units that erupted in its near periphery. The moderately alkaline Mammoth eruptive suite, basaltic to rhyodacitic, represents a discrete new magmatic system, less than 250,000 years old, that followed decline of the subalkaline rhyolitic system active beneath adjacent Long Valley Caldera since 2.2 Ma (Hildreth, 2004). The scattered vent array of the Mammoth system, 10 by 20 km wide, is unrelated to the rangefront fault zone, and its broad nonlinear footprint ignores both Long Valley Caldera and the younger Mono-Inyo rangefront vent alignment.

The Mammoth Lakes area of Mono County, owing to its spectacular alpine landscape, has become one of California's busiest recreational playgrounds and a regional center of real estate development. The name applies to the town of Mammoth Lakes as well as to the cluster of lakes in a large cirque southwest of town that is now locally called the Lakes Basin. The town has spread around the eastern base of Mammoth Mountain, a late Pleistocene pile of silicic lava domes, and has locally expanded onto lower slopes of the mountain itself (fig. 1). Looming nearly 1,000 m above the downtown area, much of the 5-km-wide volcanic edifice has been laced with chair lifts, gondolas, ski runs, and bike paths by the Mammoth Mountain Ski Area, a corporate entity under permit from Inyo National Forest. In addition to skiing, long-established, snowboarding and summertime mountain biking have recently become major activities. Tourism to Mammoth Lakes is estimated to be 1,300,000 visitors per winter and 1,500,000 per summer. Some of America's top long-distance runners also live and train in Mammoth Lakes, attracted by its elevation and its variety of challenging trails.

At the western base of Mammoth Mountain, along the canyon of the Middle Fork San Joaquin River, lies the Devils Postpile National Monument, a National Park Service enclave surrounded by extensive wilderness areas administered by the U.S. Forest Service. As many as 2,000 visitors per day enter the monument during the summer season. The area also contains several of the busiest trailheads in the Sierra Nevada, providing wilderness access for hikers, pack animals, mountaineers, and fishermen.

Many geographic names that appear in this report are informal despite having been in local use for decades. Most appear on maps distributed by the Town of Mammoth Lakes or the Mammoth Mountain Ski Area and can be found here on map figures 2–5, on several photo figures, and on the geologic map.

Recent Unrest

Geophysical unrest beneath Mammoth Mountain and in adjacent parts of the Sierra Nevada and Long Valley Caldera has generated concern among residents, stakeholders, and geoscientists since at least 1980, when four magnitude 6 earthquakes shook the area. Extensive monitoring for three decades has documented numerous earthquake swarms, ground uplift and deformation, changes in hydrothermal systems, and emission of magmatic CO_2 at several sites that semiencircle Mammoth Mountain (Evans and others, 2002; Farrar and others, 1995; Foulger and others, 2003, 2004; Gerlach and others, 2001; Hill, 1996, 2006; Hill and others, 1990, 2003; Hill and Prejean, 2005; Julian and others, 1998; Langbein, 2003; Pitt and Hill, 1994; Pitt and others, 2002; Prejean and others, 2002, 2003; Rogie and others, 2001; Sorey and others, 1993, 1998; Tizzani and others, 2009). Such investigations led the U.S. Geological Survey, in cooperation with Federal, State, County, and local authorities, to prepare a response plan for any future episodes of unrest, calibrated for progressively more intense premonitory activity (Hill and others, 2002).

Unrest specific to Mammoth Mountain, 1979–2003, was reviewed thoroughly by Hill and Prejean (2005), who included interpretation of the midcrustal mafic magma system inferred to drive deep long-period (LP) seismicity, CO_2 exsolution, and fluid ascent into the brittle upper 4–6 km where swarms of brittle-failure earthquakes have been recurrent for more than three decades. The varied and persistent unrest also prompted scrutiny of volcanological data already in hand and critical review of our understanding of the region's volcanic history (Hildreth, 2004). That review led us into intensified geological and laboratory investigations, the results of which are reported here.

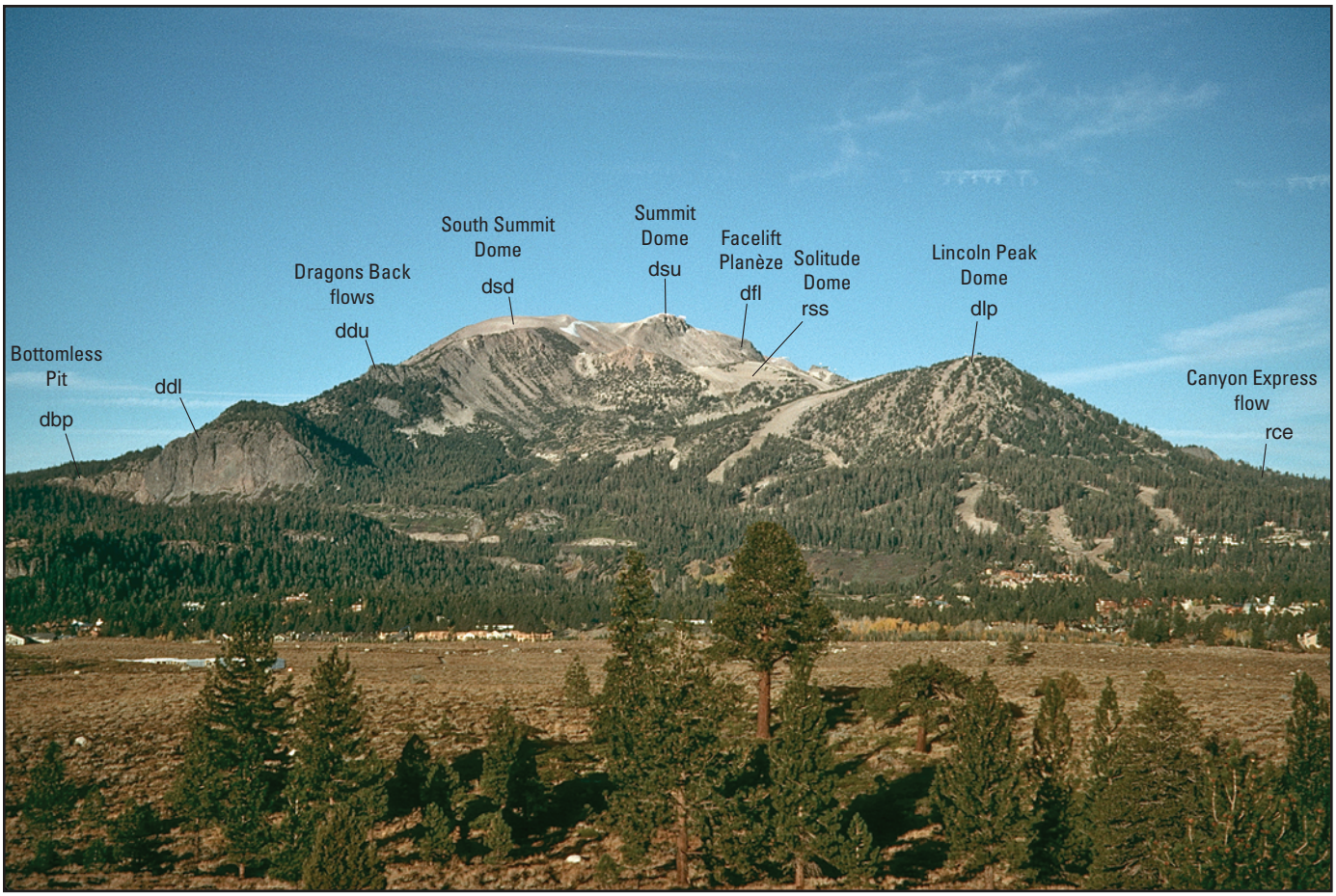

Figure 1. East side of Mammoth Mountain, showing steep former glacial headwall and numerous cleared ski runs. Several extrusive units are identified and are fully described in text. Dragons Back flows (ddl, ddu) and Solitude Dome (rss) are youngest eruptive units on edifice (~58–50 ka). $^{40}Ar/^{39}Ar$ ages include 64±7 ka for Lincoln Peak dome (dlp), 61.4±2 ka for Summit Dome (dsu), and 87±6 ka for South Summit Dome (dsd), one of oldest and largest units on edifice. Subhorizontal roadcut across center of image is Lake Mary Road, which links upper residential neighborhood of Mammoth Lakes (at right) to Lakes Basin (out of view to left). Housing development at right center is built on forested coulee of rhyodacitic unit rce (~80 ka). Total relief in image ~970 m. View is westward from moraine crest near Sherwin Creek.

Physiography and Access

Mammoth Mountain straddles the principal drainage divide (figs. 2–4) that separates the San Joaquin River system, which drains to the Pacific Ocean, from tributaries of the Owens River system, which is landlocked. The volcano grew atop one of the lowest saddles along the crest of the central Sierra Nevada, and the 2,800-m passes adjacent to the 3,369-m volcanic edifice remain among the lowest in the range. Here, the divide also marks the structural transition between the Basin and Range extensional region and the tectonically rigid Sierra Nevada microplate. Where adjoined by lavas of Mammoth Mountain, the divide is also the southwest topographic rim of Long Valley Caldera (although the ring-fault structural margin of the caldera lies buried ~5 km northeast).

Major regional Highway 395, which extends from southern California to Reno (Nevada) and beyond, transects the eastern part of the map area. About 6 km east of the town of Mammoth Lakes, Highway 203 branches from 395 and extends into town and an additional 9 km through the Mammoth Mountain Ski Area to Minaret Summit on the divide. From there, a narrow paved mountain road (open only in summer) descends into the San Joaquin River canyon for ~11 km, reaching Devils Postpile National Monument and Reds Meadow Pack Station at road's end. In town, Lake Mary Road and Old Mammoth Road branch from Highway 203 and extend separately ~7 km southwest into the Lakes Basin, where they rejoin. Starting from the Lakes Basin, San Joaquin canyon, and Mammoth Mountain, numerous trails lead off into the John Muir and Ansel Adams Wilderness areas of the High Sierra. The Sierra has been called a "gentle wilderness," and for experienced hikers this is generally true during the summer months, although black bears, cougars, precipitous terrain, and stream crossings do introduce risks.

Annual precipitation in downtown Mammoth Lakes (2,380 m elevation) averages ~59 cm (23 inches), and

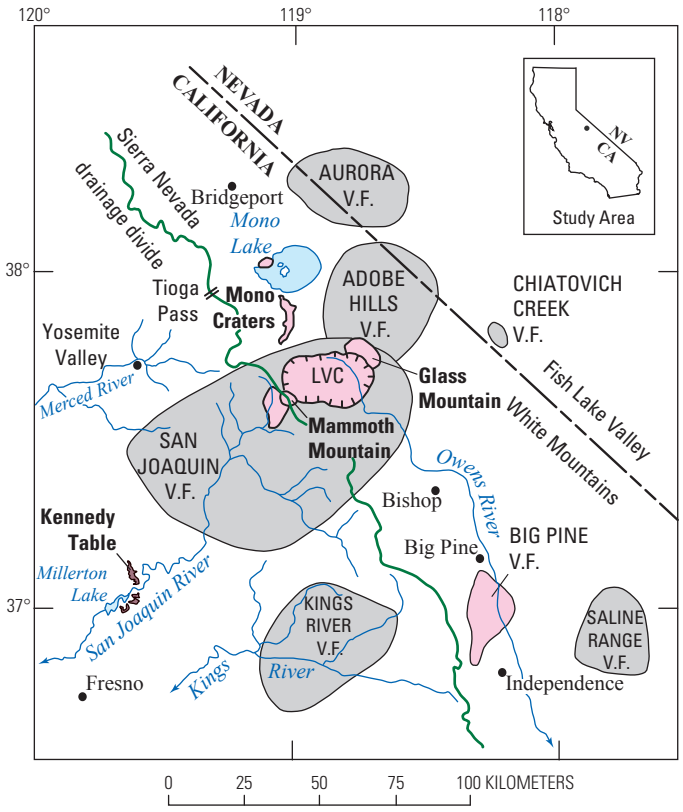

Figure 2. Regional location map and volcanic setting of Mammoth Mountain and Long Valley Caldera (LVC). Fields in pink delimit areas having vents for Quaternary volcanic rocks. Shaded fields enclose vents for predominantly Pliocene volcanic fields (v.f.). Aurora field also contains a few Pleistocene vents (Lange and Carmichael, 1996), and San Joaquin field includes a few Miocene vents (Moore and Dodge, 1980). Late Miocene Kennedy Table and related intracanyon andesite lava-flow remnants are correlated with unit Tasj ~80 km upstream near Mammoth Mountain. Other Miocene and older volcanic rocks not shown.

average annual snowfall is ~533 cm (210 inches). Mammoth Mountain Ski Area (based 7 km farther west, at 2,700 m) has average annual snowfall of 884 cm (348 inches) and, in 2005–06, it had a record snowfall of 1,468 cm (578 inches). Precipitation is greatest from November through April but scanty from June through September. East of the Sierra Nevada, precipitation falls off steeply to 19 cm (7.5 inches) at Benton and to only 13.5 cm (5.3 inches) at the Bishop airport. Location of Mammoth Mountain at a low point on the rangecrest and at the head of the major southwest-trending San Joaquin canyon system accounts for its high snowfall and unusually long skiing season, which commonly lasts from October through June. In downtown Mammoth Lakes, average daily maximum and minimum temperatures are 78 °F (26 °C) and 46 °F (8 °C) in July and 39 °F (4 °C) and 16 °F (–9 °C) in February.

Seven modest streams drain much of the map area east of the main divide. Largest is Mammoth Creek, which drains the Lakes Basin and the east flank of Mammoth Mountain. Sherwin, Laurel, and Convict Creeks drain northward from Sierran cirques and down the south wall of Long Valley Caldera into Long Valley. Deadman and Glass Creeks drain the northwest wall, flow generally eastward to their confluence near Crestview and join the Owens River near Big Springs. Dry Creek drains the north slope of Mammoth Mountain, flows (seasonally) northeastward for 18 km to join the Owens River northeast of Lookout Mountain. Although ephemeral today, Dry Creek cut gorges 40–50 m deep through the lavas of several units during the Pleistocene. West of the main divide, the southwest flank of Mammoth Mountain is drained steeply by Reds and Boundary Creeks, and the Pumice Butte area is drained more circuitously by Crater Creek; all three join the Middle Fork San Joaquin River. King Creek and Minaret Creek are western tributaries of the Middle Fork that cut through volcanic units at the west edge of the map area.

Total relief in the map area is ~1,500 m. The floor of Long Valley at the northeastern and southeastern margins of the map is lower in elevation than 2,150 m, and late Pleistocene lavas are preserved along the floor of the Middle Fork San Joaquin canyon to as low as 2,000 m. Bloody Mountain at the head of Laurel Creek stands 3,823 m high; the divide at the head of Sherwin Creek reaches 3,680 m; Mammoth Crest locally exceeds 3,500 m; Mammoth Mountain is 3,369 m; and San Joaquin Mountain on the principal divide reaches 3,536 m. Vegetation zones, accordingly, range from barren alpine through pine-fir forests to semiarid sagebrush steppe.

Settlement and Development

There are many cities on volcanoes (Auckland, Kagoshima, Napoli, Hilo), but few have expanded so fast and recently as Mammoth Lakes. Thousands of prospectors, miners, and camp followers first swarmed the Lakes Basin area in 1878–79 when gold was reported in the Mesozoic metavolcanic rocks of Red Mountain, stained reddish brown by oxidation of disseminated pyrite. The boom camps were largely abandoned after 1880, although small-scale operations persisted intermittently through the 1950s, as summarized by Rinehart and Ross (1964). Total production of Au and Ag from the several mines in the district probably did not exceed $1 million, but the ballyhoo to attract investors gave rise to the name “Mammoth Mine,” which spread with time to the Mammoth Rock, Lakes, Creek, and Mountain.

Homesteading began on Mammoth Meadow (also called Arcularius Meadow) by 1897, and the first hotel to accommodate tourists was built by 1905. Building a good road up Sherwin Grade in 1916 shortened to 2.5 hours the drive from Bishop to Mammoth Lakes, opening the way for construction of lodges and expansion of fishing, hiking, and pack-train recreation throughout the 1920s and 1930s. Inyo National Forest was established in 1907 and Devils Postpile National Monument in 1911. Mammoth Lakes opened its first post


119°15'
119°'
118°45'
37°50'
37°40'
Mono Lake
Cowtrack Mountain
Granite Mountain
Adobe Valley
Mt Dana
Mt Gibbs
Bloody Canyon
TIOGA PASS RD
Rush Creek
120
Pumice Valley
Mono Craters chain
395
Grant Lake
Koip Peak
mjl
June Lake
158
Wilson Butte
Obsidian flow
HSF
Crestview
Bald Mountain
Dexter Canyon
Taylor Canyon
Black Mtn
Benton Range
Glass Mountain
Gem Lake
Carson Peak
June Mountain
Glass Creek
White Wing Mtn
Thousand Island Lake
Agnew Pass
Tmel
San Joaquin Mountain
Deadman Creek flow
Lookout Mountain
bar
Dome 7403
Cone Peak
Long Valley
Dry Creek
Deer Mountain
WEST MOAT
rwm
Gilbert Peak
Resurgent Dome
Benton Crossing
Banner Ridge
Mt Ritter
Tmcl
Tmwc
Deadman Pass
The Minarets
Minaret Summit
203
CDHS
Hot Creek
Mammoth Mountain
ML
SOUTH MOAT
rhc
North Fork
Iron Mtn
Devils Postpile
Lakes Basin
Sherwin Creek
Laurel Mountain
Convict Creek
McGee Mountain
Lake Crowley
Owens River Gorge
Casa Diablo Mountain
HCE
Lion Point
Middle Fork
Mammoth Crest
Pumice Butte
Bloody Mountain
Mt Morrison
Toms Place
McGee Ck
San Joaquin River
Fish Creek
0
10
KILOMETERS

office in 1923, but the town was not incorporated until 1984. In 1920–21, the Forest Service made the trails to Lakes Basin suitable for automobile traffic. In the 1930s and 1940s, the Forest Service supported growth of recreational skiing, leading to establishment of numerous rope tows along the Eastern Sierra, including some set up by the locally iconic entrepreneur Dave McCoy as early as 1946 along Minaret Road at the toe of Mammoth Mountain.

In 1953, McCoy was awarded a 25-year permit to develop what became the Mammoth Mountain Ski Area (MMSA), building a warming hut at the site of the present Main Lodge and three rope tows in series to the top of North Knob. The first chair lift, Chair 1, was erected in 1955, and others were added or improved during succeeding decades, proceeding to Chair 27 in 1994. The gondola to the summit took three summers to construct, opening in 1967. By the 1980s, MMSA had 40 snow "cats" to groom ski runs and 250 ski instructors. In 2005, when McCoy (by then 90 years old) sold it to Starwood Capital Group, MMSA had 400 ski instructors and 3,000 permanent and seasonal employees.

Growth of MMSA engendered a sustained boom in real estate development. The year-round population of Mammoth Lakes had been 26 in 1946 but grew to 7,100 by 2000 and 8,234 in 2010. Tourism to Mammoth Lakes has expanded to reach an annual total of 2.8 million. There are about 9,000 housing units in Mammoth Lakes and 4,800 rental units. Residential neighborhoods have crept as high as 2,630 m on the east flank of the volcano, and numerous cabins are at 2,600–2,800 m in the Lakes Basin at its southeastern toe. There are lodges at elevations of 2,450, 2,530, and 2,720 m around the base of the mountain as well as restaurants at McCoy Station (2,930 m) and on the summit (3,360 m). From the summit of Mammoth Mountain, it is 2.4 km to Mammoth Mountain Inn, 2.6 km to Tamarack Lodge, 3.1 km to Canyon Lodge, and 6 km to the downtown corner of Main Street and Old Mammoth Road. Nearly all of these facilities could be at risk were volcanic activity to resume on or near the edifice.

Figure 3. (facing page) Shaded relief map centered on Long Valley Caldera, showing Mammoth Mountain at caldera's southwest margin. Rugged terrain to west and south is glacially sculpted Sierra Nevada. Green line indicates Sierran drainage divide between Pacific slope and internally drained Great Basin. Selected peaks along main divide are Bloody Mountain (3,826 m), Mammoth Mountain (3,369 m), San Joaquin Mountain (3,536 m), Mount Gibbs (3,893 m), and Mount Dana (3,981 m). Other notable Sierran peaks are Mount Morrison (3,942 m), Iron Mountain (3,398 m), Mount Ritter (4,008 m), Carson Peak (3,325 m), and Koip Peak (3,951 m). Volcanic highs on caldera rim include Bald Mountain (2,775 m), Glass Mountain (3,390 m), and Cone Peak (3,094 m). High point on caldera's resurgent uplift is Gilbert Peak (2,619 m). Surface level of Mono Lake fluctuates around 1,945 m, and that of Lake Crowley on the caldera floor around 2,062 m. Downtown Mammoth Lakes (ML) has an elevation of ~2,400 m. Four red stars indicate vents for important eruptive units outside the map area but described in the text. Additional abbreviations: CDHS, site of Casa Diablo Hot Springs, now replaced by a geothermal plant; HCF, Hilton Creek Fault; HSF, Hartley Springs Fault. Three nonglaciated Pleistocene lava flows prominent on image are basalt of Arcularius Ranch (bar), rhyolitic Hot Creek flow (rhc), and rhyolitic West Moat Coulee (rwm).

Previous Geological Work

Comprehensive geologic mapping of the current study area was first completed in the 1950s at a scale of 1:62,500 by Rinehart and Ross (1964) and Huber and Rinehart (1965a). At the same scale, Bailey (1989) adapted their regional mapping while elaborating in more detail the volcanic and structural history of Long Valley Caldera and its surroundings. A useful map of volcanic and surficial deposits in the Mammoth Lakes area is part of a fine thesis by Lipshie (1974). An excellent map of the volcanic rocks in and near Devils Postpile National Monument was prepared on behalf of the National Park Service as an undergraduate mapping project at Fresno State University (Clow and Collum, 1983).

Topical and preliminary studies in the area have been many and varied. Mayo (1930, 1934a) made a reconnaissance geologic map of a large region that included the Mammoth Lakes and Long Valley areas, and he coined the term "Mammoth embayment" for the rangefront reentrant now known to have been magnified by subsidence of Long Valley Caldera. Mayo (1934b) also drew attention to wave-cut terraces and Pleistocene lake deposits produced by intracaldera Long Valley Lake. Mayo and others (1936) first described the alignment of Holocene vents (later called the Inyo Chain) and noted its proximity but ambiguous relationship to Sierran rangefront faults, an issue revisited by Bursik and others (2003). Erwin (1934) mapped the upper San Joaquin Basin and the Ritter Range, focusing on basement rocks but also contributing early observations on the volcanic rocks of Devils Postpile, Red Cones, and Pumice Butte. Benioff and Gutenberg (1939) investigated the young fissure called the "Earthquake Fault" near Mammoth Lakes. Chelikowski (1940), in the course of studying the early post-caldera rhyolites (our unit rer), also noted the sites of several mafic vents and the extent of Pleistocene intracaldera lake deposits; Chelikowski may have been first to propose explicitly that the "Mammoth embayment" is the collapsed caldera source of the Bishop Tuff, although Mayo (1935, p. 674–5; 1937, p. 184) and Gilbert (1938, p. 1860) had already flirted with the idea. While concentrating on older volcanics to the north and east, Gilbert (1941) also made reconnaissance observations on the late Pleistocene volcanic rocks of the Mammoth Lakes area.

Matthes (1960) reconnoitered the geomorphology and glacial geology of the upper San Joaquin Basin. Kesseli (1941a, b) and Curry (1968, 1971) did the same for the Mammoth Lakes side of the main divide, both of them recognizing that lava flows near Mammoth Creek separated tills of

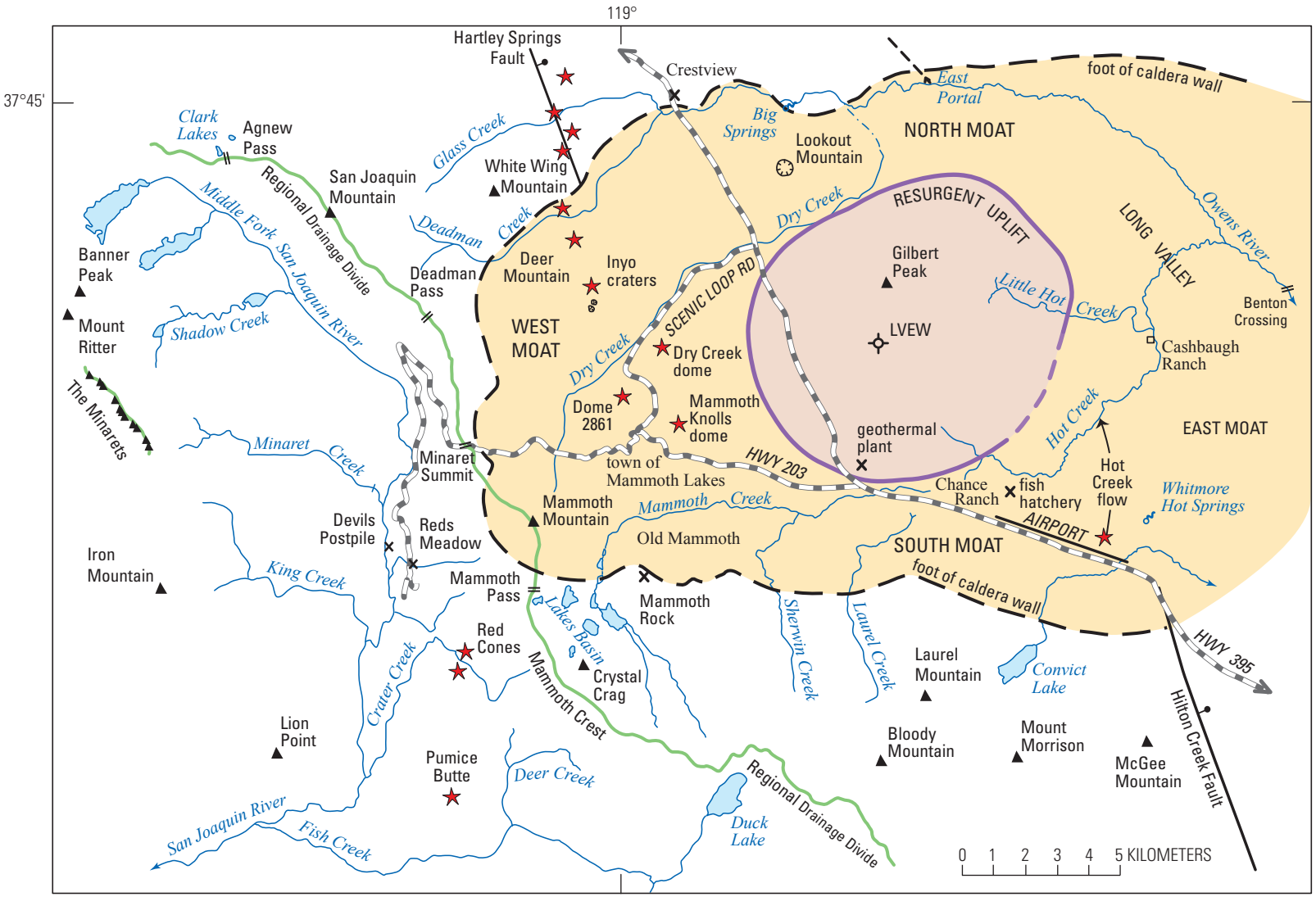

Figure 4. Principal drainages, highways, and geographic names in and near geologic map area. Regional drainage divide, locally higher than 3,500 m, separates streams flowing to Pacific Ocean via San Joaquin River from those flowing to Owens River system, which is ultimately landlocked within Basin and Range Province. Dashed line approximates topographic floor of Long Valley Caldera, equivalent to base of present-day topographic wall except where wall has been buried by Mammoth Mountain and several moraines. Structural wall (ring-fault zone) on which caldera subsidence took place is deeply buried far inboard, roughly along an arcuate trend linking vents indicated for Hot Creek flow, Dry Creek and Mammoth Knolls domes, and Lookout Mountain (Hildreth, 2004). Selected vents are shown by stars. North-trending alignment of six vents north of Deer Mountain is Holocene Inyo Chain. The term "moat" refers to the annular lowland that encircles the caldera's 10-km-wide resurgent uplift (outlined in purple), the center of which is marked by site of 3-km-deep corehole LVEW (Long Valley Exploratory Well; McConnell and others, 1995). Geothermal plant is at site of former Casa Diablo Hot Springs.

different ages. Putnam (1949) mapped the June Lake district, just north of our map area, describing the north end of the Inyo Chain and relationships between mafic lavas northeast of June Lake and the glacial deposits that sandwich them. Huber (1981) summarized evidence for the timing and magnitude of uplift of the central Sierra Nevada, for incision of the San Joaquin River canyon, and for Pliocene closure of the local segment of the Sierran drainage divide.

Publications dealing with aspects of volcanic rocks investigated in the current report also include: Huber and Rinehart (1965b, 1967); Rinehart and Huber (1965), Bailey and others (1976), Chaudet (1986), Mankinen and others (1986), Vogel and others (1994), and Mahood and others (2010). Studies of such rocks that were principally geochemical-petrological include: Cousens (1996), Reid and others (1997), Heumann and Davies (1997), Heumann and others (2002), and Bailey (2004). Studies of the volcanology and petrology of the late Holocene Inyo Chain have been numerous: Eichelberger and others (1985, 1988), Gibson and Naney (1992), Mastin and Pollard (1988), Mastin (1991), Miller (1985), Nawotniak and Bursik (2010), Sampson and Cameron (1987), Sampson (1987), Varga and others (1990), Vogel and others (1989), and Wood (1977).

Investigations of the Long Valley hydrothermal system (Lachenbruch and others, 1976a; Sorey and others, 1978, 1991, 1993, 1998; Sorey, 1985; Shevenell and others, 1987; Suemnicht and Varga, 1988; Farrar and others, 2003; Suemnicht and others, 2006) have made clear that the principal heat source lies not deep beneath the widespread surface manifestations in the south-central and southeastern parts of Long Valley Caldera but, instead, near the caldera's western margin, within the area of younger volcanic rocks addressed here.

Methods

Sampling began in 1998 and 2003 in support of efforts at Stanford University to expand the Ar-geochronological database for Pleistocene volcanic rocks in the Mammoth Mountain area, culminating in the report by Mahood and others (2010). For an interdisciplinary workshop on volcanic processes in and near Long Valley Caldera, held at Mammoth Mountain in October 2003, Hildreth was asked to prepare a comprehensive volcanological overview that was presented orally and later published (Hildreth, 2004). The review led to recognition that Mammoth Mountain and its mafic periphery represent a new magmatic system, compositionally, temporally, and spatially separate from contiguous Long Valley Caldera. Field reconnaissance soon made clear that numerous eruptive units, both mafic and silicic, had been lumped in the course of previous mapping, despite being distinguishable in age, composition, and petrography. Recognition that a better understanding of the eruptive history would be readily achievable by means of field scrutiny and high-precision Ar geochronology nucleated the detailed remapping presented here at a scale of 1:24,000. From 2004 through 2012, 294 days of fieldwork were devoted to the project, generally in two-week intervals scattered each year between May and October.

Because most of the area is either glaciated and till-strewn or mantled with 1350 C.E. pumice-fall deposits, aerial photographs were of only minor utility, and our detailed mapping was done directly on USGS 1:24,000 topographic quadrangle maps (Bloody Mountain, Convict Lake, Crestview, Crystal Crag, Dexter Canyon, June Lake, Mammoth Mountain, Old Mammoth, and Whitmore Hot Springs). A hand-held GPS device was commonly useful in the woods. Much of the work was conducted as day hikes, but multinight backpack trips were made in the San Joaquin canyon and the Pumice Butte area. Most of the Quaternary map units were cored and their paleomagnetic directions measured in the USGS lab at Menlo Park, California, by D.E. Champion. The data were used to help correlate or distinguish scattered exposures. Mammoth Mountain Ski Area permitted vehicular access and paleomagnetic drilling of volcanic outcrops.

One or more thin sections of each volcanic map unit were examined microscopically. The observations are summarized in the unit descriptions and tabulated in table 1. All eruptive units are listed in table 1, along with the 3-letter unit labels by which each is identified on the geologic map and cited in the text. Most samples were analyzed chemically, and the data are listed in appendix 1.

New radioisotopic ages were determined in the U.S. Geological Survey geochronology laboratory in Menlo Park, California, supervised by A.T. Calvert. Most samples in this study were dated using $^{40}Ar/^{39}Ar$ incremental heating techniques following methods described in Calvert and Lanphere (2006), and Muffler and others (2011), and the results are listed in table 2. Because most samples for which $^{40}Ar/^{39}Ar$ ages reported by Mahood and others (2010) were collected with Hildreth's participation, sites and stratigraphic relations cited here for those units are equally well known to us. Mahood and others (2010) showed that Mammoth Mountain biotite contains excess Ar and yields ages much older than those of coexisting feldspar, thus demonstrating that published middle Pleistocene K-Ar biotite ages (Bailey and others, 1976; Mankinen and others, 1986) for Mammoth Mountain are untenable.

Geologic Setting

Basement Rocks

Mammoth Mountain formed at the convergence of four significant structural boundaries (fig. 5). The volcanic edifice grew (1) within a scalloped reentrant of the topographic wall of 767-ka Long Valley Caldera (Bailey, 1989), and (2) it overlies the intrusive contact of a Late Cretaceous granite pluton against steeply foliated Mesozoic metavolcanic rocks (Huber and Rinehart, 1965a). The edifice also buries (3) a regional

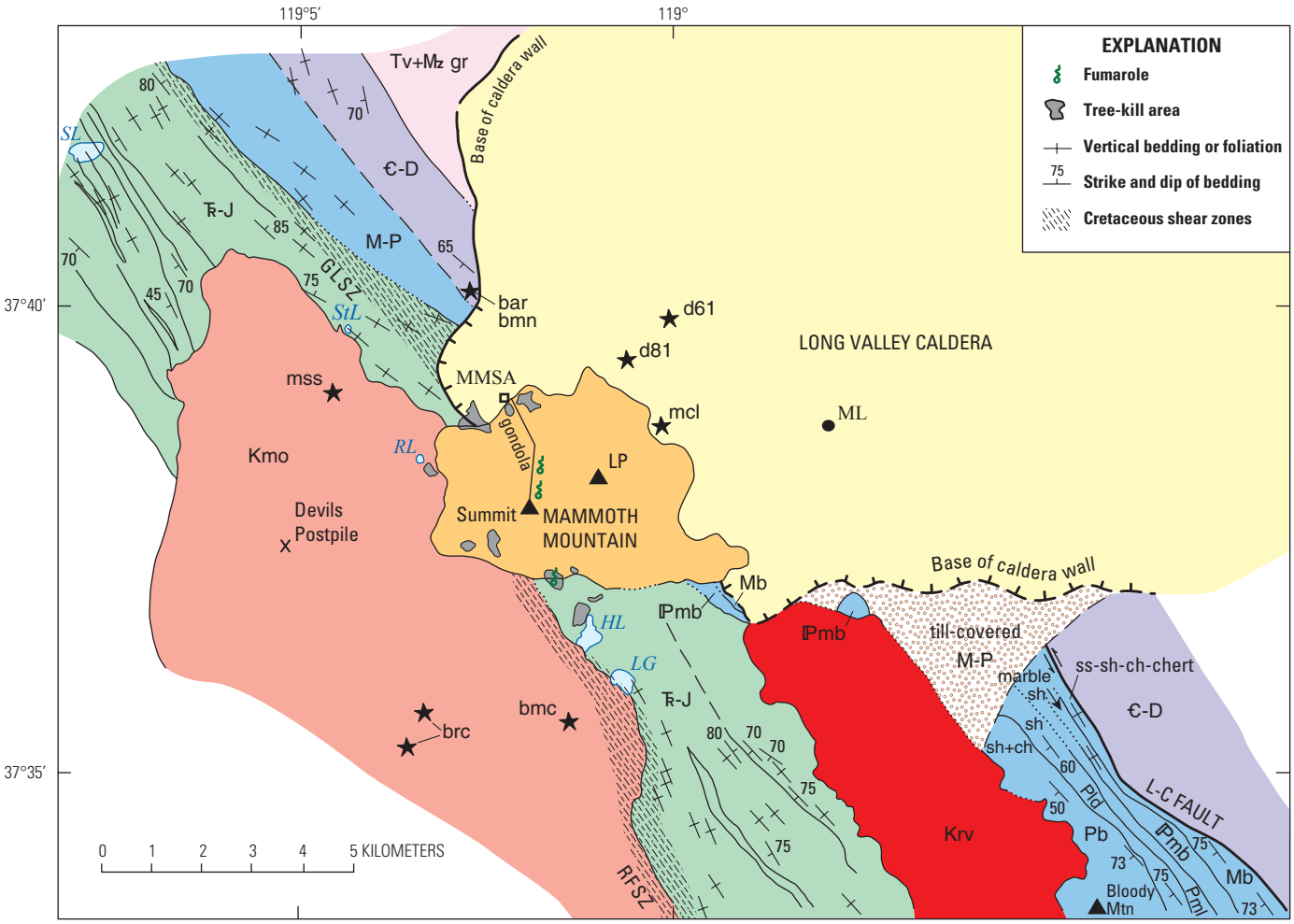

Figure 5. Simplified map of basement structure beneath late Pleistocene Mammoth Mountain. Two Late Cretaceous granitoid plutons (Kmo, Krv) and near-vertical belts of Paleozoic metasedimentary and Mesozoic metavolcanic strata strike northwest beneath the volcanic edifice. Gem Lake shear zone (GLSZ) and Rosy Finch shear zone (RFSZ), ductile belts of Late Cretaceous dextral transpression (Greene and Schweikert, 1995; Tikoff and Greene, 1997), also pass beneath Mammoth Mountain. The Laurel-Convict Fault (L-C) is a Permian-Triassic high-angle fault zone that juxtaposes sequences of lower and upper Paleozoic marine strata (Greene and others, 1997). Mammoth Mountain edifice was built against topographic wall of 767-ka Long Valley Caldera, which may influence distribution of CO_2 gas to tree-kill areas (10 gray patches) around western half of edifice (see fig. 14). Several vents peripheral to edifice are indicated by stars and identified by unit label (table 1). Abbreviations: HL, Horseshoe Lake; LG, Lake George; LP, Lincoln Peak; ML, downtown Mammoth Lakes; MMSA, Main Lodge of Mammoth Mountain Ski Area; RL, Reds Lake; SL, Shadow Lake; StL, Starkweather Lake. Late Paleozoic lithologies indicated: ch, calc-hornfels; sh, siliceous hornfels; ss, sandstone. Basement structure and simplified stratigraphy generalized from Greene and Stevens (2002), Huber and Rinehart (1965a), and Rinehart and Ross (1964).

contact (Morgan and Rankin, 1972; Brook and others, 1974) between the metavolcanic belt and Paleozoic metasedimentary rocks of the Mount Morrison pendant (Rinehart and Ross, 1964; Greene and Stevens, 2002). Finally, Mammoth Mountain overlies (4) the Rosy Finch shear zone segment of the Sierra Crest Shear Zone System (Tikoff and Teyssier, 1992; Greene and Schweickert, 1995; Tikoff and Greene, 1997), a north-northwest striking dextral transpressional structure of Late Cretaceous age that foliates both metavolcanic and granitic basement rocks nearly vertically. There may additionally be a right-stepping offset in the shear zone beneath the edifice (fig. 5), an inherited structure that might also help focus crustal transport of magmatic fluids.

Pre-Quaternary rocks beneath and near Mammoth Mountain can be summarized fourfold: Paleozoic metasedimentary rocks, Mesozoic metavolcanic rocks, Late Cretaceous granitoid plutons, and late Neogene volcanic rocks.

The Paleozoic metasedimentary rocks extend along the south rim of the caldera as what is called the Morrison block or Mount Morrison pendant, which was mapped in detail by Rinehart and Ross (1964) and Greene and Stevens (2002). The steeply dipping strata consist of Cambrian through Permian marine formations that extend as a northwest-striking series of pendants and septa for ~115 km from Bishop Creek to Mono Lake. The sequence underlies the eastern part of Mammoth Mountain and western half of Long

Valley Caldera, as indicated by metasedimentary remnants on the north and west rims of the caldera (Bailey, 1989) as well as the major pendant that forms much of the south rim, from Mammoth Rock to the Hilton Creek Fault. The belt of near-vertical Paleozoic strata is ~10 km wide, represents a stratigraphic thickness of ~7 km, and was severely folded and faulted during the Permian and Mesozoic (Greene and Stevens, 2002). The rocks include siliceous, calcsilicate, and pelitic hornfels, argillite and slate, fine-to-coarse sandstone and quartzite, black chert, and limestone/marble, all metamorphosed in the hornblende-hornfels facies at ~200 MPa during pluton emplacement. The fine-grained clastic sediments are interpreted to have been deposited in deep water on the continental slope or rise, the chert hemipelagically, the sands on submarine fans, and the limestone on a carbonate platform (Stevens and Greene, 1999).

The Mesozoic metavolcanic rocks that strike beneath Mammoth Mountain form a steeply southwest-dipping sequence dominated by silicic pyroclastic rocks of Triassic and Jurassic age. South of Mammoth Mountain, they form a septum 2.5–4 km wide that extends 12 km southeast, separating the two large Cretaceous plutons described below (Rinehart and Ross, 1964). North of Mammoth Mountain, they form a 5-km-wide belt that extends more than 40 km northwest, separating the Paleozoic metasedimentary section on the east from the Cretaceous metavolcanic complex of the Ritter Range on the west (Huber and Rinehart, 1965a). Both belts are complexly stratified homoclines that young southwestward, having foliation and bedding that typically dip 60º–80º SW. Lithologically, massive to stratified intermediate-to-rhyolitic tuffs predominate, including a few quartz-bearing ignimbrites—some of them hundreds of meters thick. Stratified tuffs rich in crystals and lithic clasts include fallout, pyroclastic-flow, and reworked deposits. Also present are aphanitic and porphyritic lava flows, shallow intrusives, and subordinate interbeds and lenses of shale, sandstone, siltstone, calcsilicate hornfels, marble, and tuffaceous sedimentary rocks (Rinehart and Ross, 1964). Major ignimbrite sheets and plane-parallel bedding of intercalated sandy sediments and tuffs suggests subaerial and shallow subaqueous depositional environments of low relief. The entire sequence is in the hornblende-hornfels facies, locally schistose, and was deformed and metamorphosed before and during emplacement of the Late Cretaceous batholith.

The east wall of upper Mammoth Creek from Arrowhead Lake to Lake Mary is a high ridge called Red Mountain (also known locally as Gold Mountain) that consists of hornfelsed Mesozoic metavolcanic rocks that are stained reddish brown by oxidation of disseminated pyrite. Associated weak mineralization, said to be principally vein-hosted gold and silver, has attracted intermittent prospecting and minor production (Rinehart and Ross, 1964). The northwest-trending upland surface of Red Mountain, 4 km long, 0.3–1 km wide, and 3,000–3,400 m in elevation, is an unglaciated remnant of a preglacial Sierran erosion surface of only modest relief. Called the “Solitude surface” by Curry (1971), Pleistocene erosion has isolated it 300 m above Lake Mary, 600 m above downtown Mammoth Lakes, and nearly 1,000 m above the caldera floor. In addition to remnants of Pliocene basaltic units Tbmm and Tbrm that occupy shallow paleochannels atop the surface, there are pebbles, cobbles, and boulders of aphyric felsite and obsidian, hornblende-biotite dacite, and phenocryst-poor olivine-plagioclase basalt scattered across the surface, probably reflecting precaldera stream transport from a volcanic field that collapsed into Long Valley Caldera.

The Mono Creek Granite (Bateman, 1992a, b) is one of the great Late Cretaceous plutons of the Sierra Nevada, a 50-km-long, northwest-elongate, medium-to-coarse-grained biotite granite, rich in alkali-feldspar megacrysts. Near Mammoth Mountain, the granite forms Mammoth Crest, Crystal Crag, the north wall of Fish Creek canyon below Pumice Butte, and both walls of the Middle Fork San Joaquin canyon, terminating against metavolcanic rocks 6 km north of Devils Postpile. The western half of Mammoth Mountain banks against and conceals a northeast-sloping granite wall that formed a steep scalloped alcove in the caldera margin. The scallop had probably been a middle Pleistocene cirque during Marine Isotope Stage 6 (MIS 6), before being filled by the trachydacite edifice in the late Pleistocene. Mammoth Mountain does not drape the caldera rim; it grew within the scallop and its lava flows bank against the granite wall. The granite crops out as far east as Lake George and Horseshoe Lake in Lakes Basin. West of Mammoth Mountain, most of the Tertiary and Quaternary volcanic units along the Middle Fork rest on Mono Creek Granite.

Two discrete plutons correlated lithologically (by Rinehart and Ross, 1964) with the Round Valley Peak Granodiorite (Bateman, 1965; 1992a, b) crop out on the caldera wall at the south edge of the map area. The western one, 3–5 km wide, encloses the canyon of Sherwin Creek, intrudes along the contact between the metavolcanic and metasedimentary sequences, and extends 15 km southeastward as far as Lee Lake. The smaller eastern pluton is roughly equant in plan view, only 3 km across, and intrudes the Paleozoic metasedimentary rocks on the north slope of Laurel Mountain. Both plutons consist of Late Cretaceous medium-grained, hornblende-biotite granodiorite.

Neogene Volcanic Rocks

Remnants of numerous Pliocene mafic and trachydacitic volcanic rocks (and a few of late Miocene age) survive within 15 km north, west, and south of Mammoth Mountain (Huber and Rinehart, 1965a; Bailey, 1989, 2004). Northwest of Mammoth Mountain, 14 Pliocene vents were indicated by Bailey (1989) along the 12-km-long reach of the Sierran drainage divide between Minaret Summit and Gem Lake that includes Deadman Pass and San Joaquin Mountain (figs. 3, 4).

Across the northwest to north-central rim of Long Valley Caldera, Bailey mapped an additional 19 Pliocene mafic and

intermediate precaldera vents. For these and other precaldera lavas east of the caldera, Bailey (2004, his fig. 3) compiled numerous ages that range from 4.5 to 2.3 Ma, predominantly 3.7 to 2.7 Ma. Some of these have been reinvestigated by us, but many lie outside our map area, and all are far older than the largely late Pleistocene vent array around Mammoth Mountain. Judging from surviving circumcaldera outcrops, however, Pliocene volcanic rocks were probably distributed densely across what are now the western and northern parts of the caldera, prior to glaciation and caldera collapse. Such rocks are as thick as 466 m beneath the Long Valley Caldera floor just southeast of Inyo Craters, where they were penetrated by a geothermal well (fig. 6) at depths of 1,168 to 1,634 m (Suemnicht, 1987), sandwiched between metasedimentary basement rocks and intracaldera Bishop Tuff. Sparse fragments of concealed intracaldera Pliocene basalt have also been brought up in the ejecta ring of unit rwm (~150 ka) adjacent to Mammoth Knolls.

South and west of Mammoth Mountain, we have investigated the Neogene mafic and intermediate lavas in more detail (and we have dated some), because they are spatially associated with the Quaternary lavas and have not been clearly distinguished from them by previous investigators.

Altogether, we have described 32 Neogene volcanic units around the periphery of the map area. They are summarized here in the following seven geographic groupings:

1. Lakes Basin. Three units are olivine-rich remnants of mafic lava flows (units Tbmm, Tbrm, and Tmmc) on the cirque rim of Lakes Basin just south of Mammoth Mountain; one of them gave a K-Ar age of 3.15±0.1 Ma. Source vents are unidentified, and only small fractions of the flows are preserved.

2. Pumice Butte area. Four Neogene units (Tasj, Tacc, Tmcm, Tmsd) rest on Mesozoic granite in the Pumice Butte area, 8–10 km south of Mammoth Mountain. Unit Tasj is a thick stack of phenocryst-rich olivine-clinopyroxene-plagioclase trachyandesite (9.16±0.02 Ma), partly intrusive, that rims the canyon of the Middle Fork San Joaquin River and is preserved as intracanyon remnants as far as 80 km downstream, near Millerton Lake Reservoir, almost to the Great Valley. The second unit, Tacc, is a pair of phenocryst-poor, glacially scoured, trachyandesite domes (4.3±0.2 Ma) in the headwaters of Crater Creek. Third is unit Tmcm, a small remnant of olivine-rich basaltic trachyandesite (3.36±0.02 Ma) near Upper Crater Meadow. Last of the four, unit Tmsd, is a substantial remnant of an undated olivine-rich mafic shield on the divide between Deer and Fish Creeks, 4–5 km east of Pumice Butte.

3. High Sierra. High on the west wall of the Middle Fork are vents for four olivine-bearing mafic units, so glacially ravaged that all are inferred to be pre-Quaternary. Unit Tbld, resting on granite, consists of a pair of basaltic lava-flow remnants (3.35 Ma) and an agglutinated vent complex at Knoll 2836, 2.5 km west of Devils Postpile and ~7 km west of the summit of Mammoth Mountain. The other three are glaciated plugs of basaltic trachyandesite, each of which intrudes metavolcanic basement. Although all three lie just west of the map area (fig. 3), they were investigated, analyzed (appendix 1), and described in order to eliminate them as possible vents for mafic lavas along the Middle Fork. Unit Tmwc is a small plug (UTM 123/712) that forms Crag 10640 (3,243 m), 700 m west of Castle Lake and 9.5 km northwest of the summit of Mammoth Mountain. Unit Tmcl is a plug (UTM 099/731) that lies 300 m northwest of Cabin Lake on the south wall of upper Shadow Creek. Unit Tmel is a third plug (UTM 095/774), cropping out above the east shore of Emerald Lake (~1 km east of Thousand Island Lake) in the headwaters of the Middle Fork. None of these correlate with any of the intracanyon lava remnants preserved downstream within the map area. Our reconnaissance likewise excludes correlations with any of numerous mafic lava flows that vented and crop out near Agnew Pass (Huber and Rinehart, 1965a; Bailey, 1989) at the head of the Middle Fork.

4. Middle Fork. On and near the floor of the Middle Fork canyon southwest of Mammoth Mountain, glaciated remnants of mafic lava flows, rich in clinopyroxene and olivine (with or without plagioclase) and locally columnar, are preserved on both sides of the river. On the west wall, unit Tbtb is a thick stack of several conformable basaltic lava flows (The Buttresses) dated at 3.75±0.01 Ma and having reversed paleomagnetic polarity. On the east wall, 2 km downstream, unit Tmcw is a pair of petrographically similar but slightly more evolved basaltic trachyandesite lava flows, undated but yielding a reversed paleomagnetic direction similar to that of unit Tbtb. Five kilometers still farther downstream on the lower southeast wall of the Middle Fork above its convergence with Fish Creek, a 300-m stack of ~20 undated phenocryst-rich olivine-clinopyroxene basaltic lava flows (unit Tbpl) crops out extensively, just east of Pond Lily Lake. All three units rest directly on granite. Despite wide search, source vents have been located for none of them.

5. West Wall. The caldera's west rim is capped by a thick stack of Pliocene mafic lava flows (unit Tbdp), which (along with overlying trachydacitic lavas and tuffs) extend ~11 km northwest along the San Joaquin Ridge as far as Agnew Pass and Gem Lake. The complex was mapped and described by Chaudet (1986), Bailey and others (1990), and Bailey (2004), but only its southern half is covered by the present map area. About 1 km south of Deadman Pass, the stack is locally as thick as 450 m and apparently fills a paleochannel (cut in basement rocks) that crossed the modern Sierran drainage

divide from northeast to southwest. The basal flow in the paleochannel yielded an $^{40}Ar/^{39}Ar$ age of 3.71 Ma, and a flow capping the 450-m stack gave 3.28 Ma (table 2). It was proposed by Huber (1981) that this paleochannel linked the Neogene San Joaquin River to former tributaries that drained a catchment area within and east of the site of present-day Mono Basin. Extensional opening of Mono Basin and Adobe Valley and rangefront faulting younger than the Pliocene mafic lava flows created the Quaternary divide and beheaded the river system.

Overlying the mafic stack (unit Tbdp) along the crest of the San Joaquin Ridge is a set of hornblende-biotite trachydacite lava domes that includes San Joaquin Mountain and Two Teats (both just northwest of the map area; Bailey, 1989) as well as Dome 3321 (our unit Tdsd), which gave a K-Ar age of 2.8 Ma. Eruption of these domes was accompanied by emplacement of comagmatic pyroclastic-density-current deposits (units Tdpd, Tdsj) that are preserved extensively along the ridgecrest (Bailey and others, 1990). East of the ridgecrest, a chain of four more hornblende-biotite trachydacite domes (units Tdud, Td65, Tdww) extends 4 km northeast toward White Wing Mountain, where the distal dome yielded a K-Ar age of 2.6 Ma. Although bulk compositions range from 64 to 71 percent SiO_2, all 7 domes and their associated pyroclastic deposits are lithologically similar in being crystal-rich and plagioclase-dominated. An additional Neogene eruptive unit on our map is a large scoria cone of clinopyroxene-olivine basaltic trachyandesite (unit Tmww) that lies high on the south slope of White Wing Mountain, southeast of the 2.6-Ma dome (unit Tdww). Just north of the map area, a few more Pliocene mafic and dacitic units crop out at June Mountain (Bailey, 1989).

6. North Wall. Many Neogene volcanic units also crop out along and near the north wall of Long Valley Caldera (Bailey, 1989). We have mapped and described nine of them because of the need to distinguish them clearly from contiguous Quaternary volcanic units. Just west of the Obsidian Flow (unit ric), 2 km north of the caldera wall, glacially ravaged unit Tmwo includes a vent complex and lava-flow remnants of phenocryst-rich basaltic trachyandesite, which, though remarkably fresh, yielded a $^{40}Ar/^{39}Ar$ age of 3.15±0.03 Ma. A derivative lava flow that crops out along the canyon walls of Glass Creek 1.7–3.0 km east of the vent is merely the shallow surface manifestation of a concealed stack of mafic lavas 300 m thick that rests on granitic basement and is recognized only in drill core (Eichelberger and others, 1985).

   Cone 8478, just north of Crestview, is a 300-m-high Pliocene edifice (unit Tb84; 3.44 Ma) around which varied mafic and andesitic lava flows (units Taec, Taww, and Tmcv) extend ~4 km southwest as well as south into the later site of Long Valley Caldera, whence they supplied abundant lithic fragments during ring-fracture eruption of the Bishop Tuff (Hildreth and Mahood, 1986). Just east of mafic Cone 8478, two more Pliocene domes of crystal-rich hornblende-biotite trachydacite (units Td83 [3.42 Ma] and Td78) crop out on the caldera wall; they are chemically similar (65–68 percent SiO_2) to parts of the large Bald Mountain dome complex just east of the map area. All these units are either lapped by the Bishop Tuff (unit rbt; 767±2 ka) or demonstrably older than it.

   At the foot of the caldera's north wall, between Big Springs and Alpers Canyon, densely welded crystal-rich rhyolitic ignimbrite (unit Trac; 11.7 Ma) overlies severely weathered phenocryst-poor basalt (unit Tbbs), which is recognized only locally. The ignimbrite is a remnant of an extensive unit inferred to have erupted from a Miocene source far northeast of the map area.

7. South Rim. High on the south rim of Long Valley Caldera, a tiny precaldera remnant of a phenocryst-poor orthopyroxene-plagioclase-hornblende trachydacite lava flow, unit Tdlm (3.6 Ma), has been erosionally isolated at the top of the caldera wall. Its source vent is unknown but probably foundered with the caldera. Its similarity to some of the hornblende-bearing trachydacite domes on the north and west rims of the caldera supports the likelihood that a formerly continuous field of Pliocene mafic and dacitic lavas spanned what later became the western half of the caldera. The inference is strengthened by the presence of scattered blocks of hornblende-biotite dacite, aphyric rhyolite, and various mafic lavas strewn across the unglaciated low-relief Pliocene erosion surface cut on Mesozoic basement (units Mzmv and Krv) high above the southwest rim of the caldera. The source of such blocks can only have been a precaldera highland above the site of the present-day caldera.

   The distribution of pre-Quaternary volcanic units and many more mapped by Bailey (1989) east of our map area shows that an extensive volcanic field (fig. 2) blanketed the later sites of Long Valley Caldera and Mammoth Mountain during the Pliocene. Starting in the early Quaternary, however, and for the next 2 million years (2.2 to 0.2 Ma), only rhyolite is known to have erupted in the Long Valley region.

Long Valley Rhyolites

Precaldera Mafic and Dacitic Magmatism

The Pliocene-to-Quaternary volcanic field that includes Long Valley and Mammoth Mountain (fig. 2) is part of an active regional transtensional zone at the Sierra Nevada–Basin and Range transition. Its eruptive history overlaps in time with smaller mafic-to-silicic volcanic fields along this

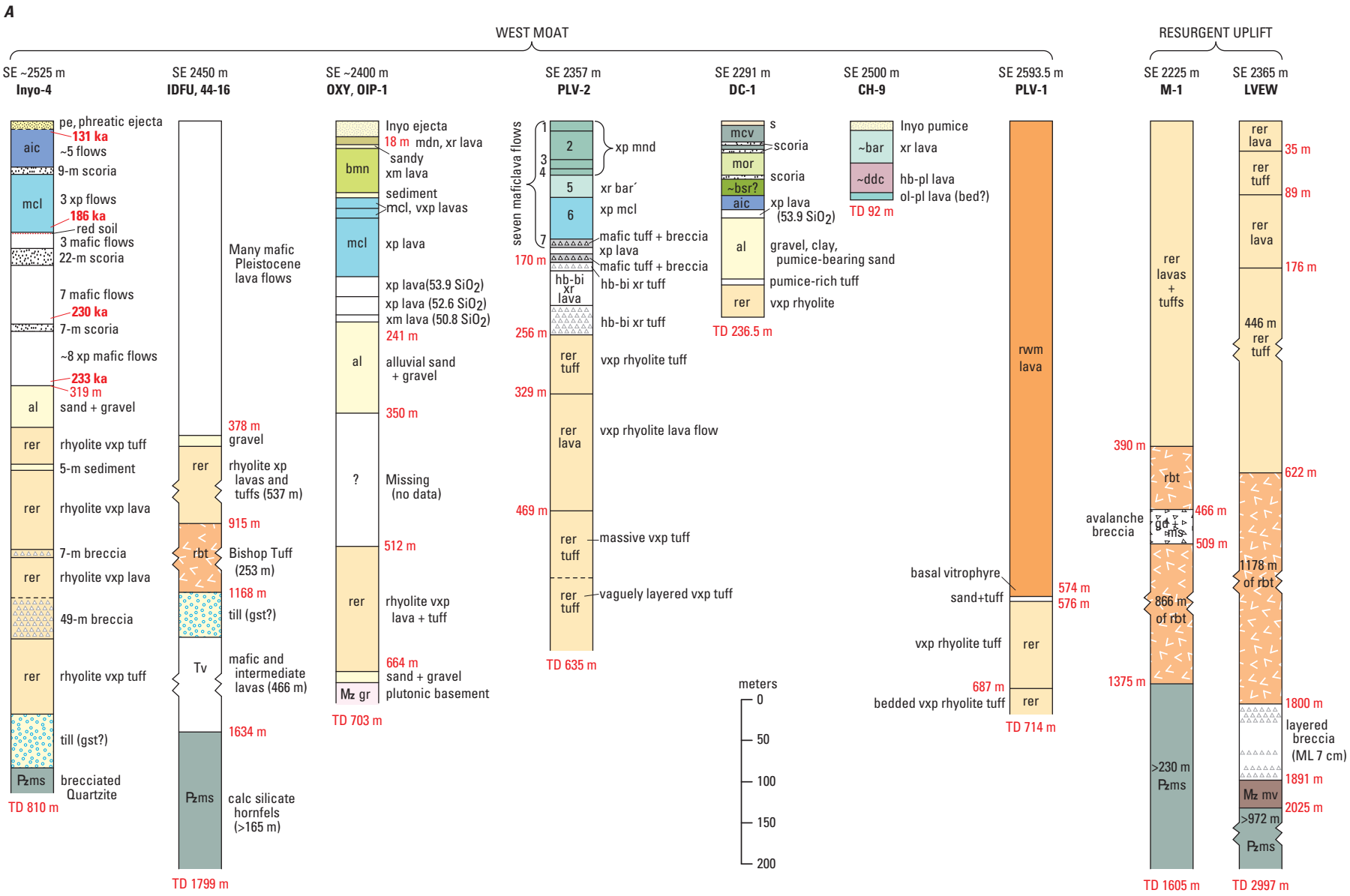
A
WEST MOAT
RESURGENT UPLIFT
SE ~2525 m
Inyo-4
pe, phreatic ejecta
131 ka
aic
~5 flows
9-m scoria
mcl
3 xp flows
186 ka
red soil
3 mafic flows
22-m scoria
7 mafic flows
230 ka
7-m scoria
~8 xp mafic flows
233 ka
319 m
al
sand + gravel
rer
rhyolite vxp tuff
5-m sediment
rer
rhyolite vxp lava
7-m breccia
rer
rhyolite vxp lava
49-m breccia
rer
rhyolite vxp tuff
till (gst?)
Pzms
brecciated Quartzite
TD 810 m
SE 2450 m
IDFU, 44-16
Many mafic Pleistocene lava flows
378 m
gravel
rer
rhyolite xp lavas and tuffs (537 m)
915 m
rbt
Bishop Tuff (253 m)
1168 m
till (gst?)
Tv
mafic and intermediate lavas (466 m)
1634 m
Pzms
calc silicate hornfels (>165 m)
TD 1799 m
SE ~2400 m
OXY, OIP-1
Inyo ejecta
18 m
bmn
mdn, xr lava
sandy xm lava
sediment
mcl, vxp lavas
mcl
xp lava
xp lava(53.9 SiO2)
xp lava (52.6 SiO2)
xm lava (50.8 SiO2)
241 m
al
alluvial sand + gravel
350 m
?
Missing (no data)
512 m
rer
rhyolite vxp lava + tuff
664 m
sand + gravel
Mz gr
plutonic basement
TD 703 m
SE 2357 m
PLV-2
seven maficlava flows
1
2
3
4
xp mnd
5
xr bar´
6
xp mcl
7
mafic tuff + breccia
xp lava
170 m
mafic tuff + breccia
hb-bi xr lava
hb-bi xr tuff
256 m
hb-bi xr tuff
rer tuff
vxp rhyolite tuff
329 m
rer lava
vxp rhyolite lava flow
469 m
rer tuff
massive vxp tuff
rer tuff
vaguely layered vxp tuff
TD 635 m
SE 2291 m
DC-1
mcv
s
scoria
mor
scoria
~bsr?
aic
xp lava (53.9 SiO2)
al
gravel, clay, pumice-bearing sand
pumice-rich tuff
rer
vxp rhyolite
TD 236.5 m
SE 2500 m
CH-9
Inyo pumice
~bar
xr lava
~ddc
hb-pl lava
ol-pl lava (bed?)
TD 92 m
SE 2593.5 m
PLV-1
rwm lava
basal vitrophyre
574 m
sand+tuff
576 m
vxp rhyolite tuff
rer
687 m
bedded vxp rhyolite tuff
rer
TD 714 m
meters
0
50
100
150
200
SE 2225 m
M-1
rer lavas + tuffs
390 m
rbt
avalanche breccia
gd
mfs
466 m
509 m
866 m of rbt
1375 m
>230 m
Pzms
TD 1605 m
SE 2365 m
LVEW
rer lava
35 m
rer tuff
89 m
rer lava
176 m
446 m
rer tuff
622 m
1178 m of rbt
1800 m
layered breccia (ML 7 cm)
1891 m
Mz mv
2025 m
>972 m
Pzms
TD 2997 m

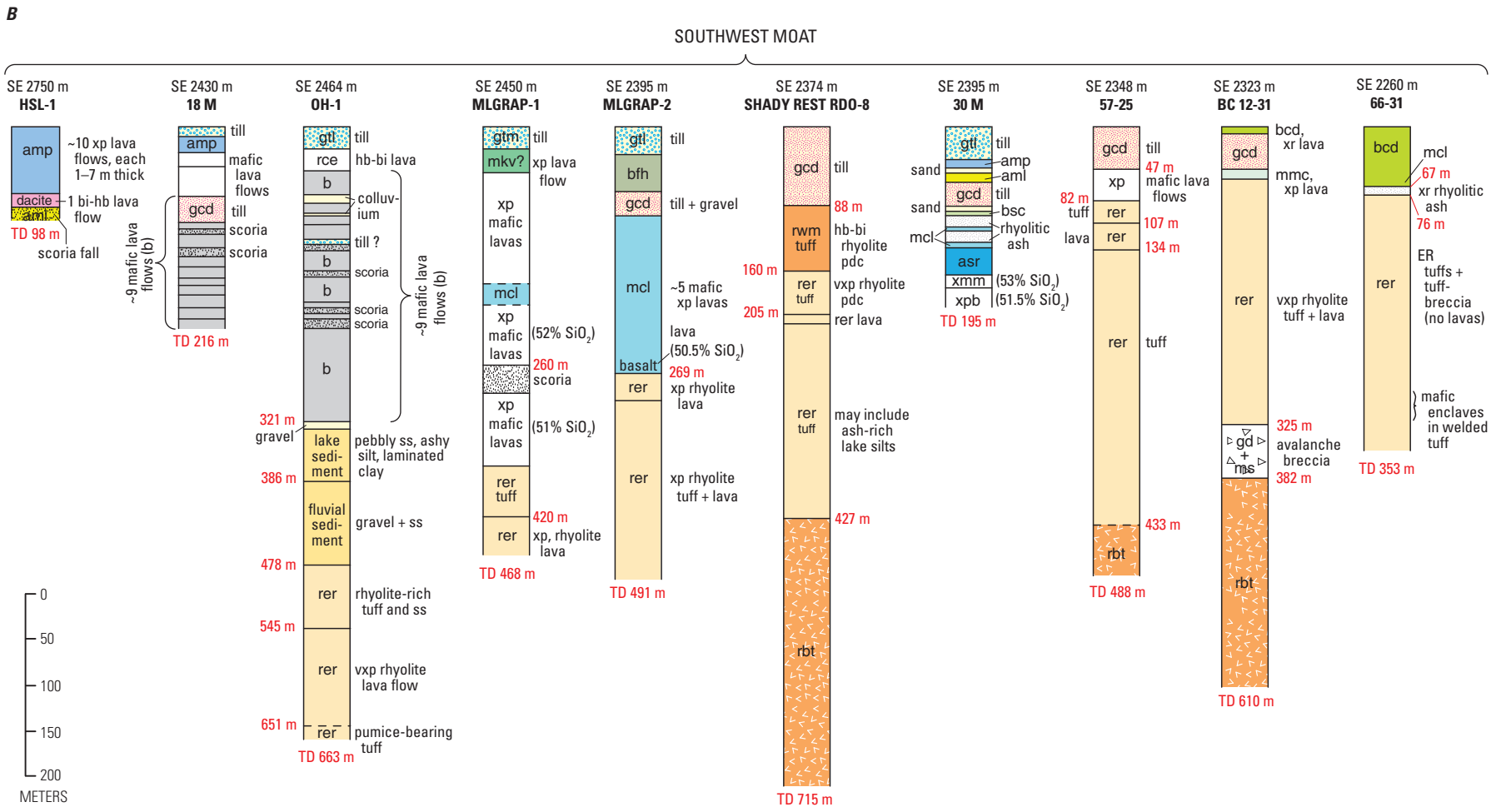

Figure 6. Well logs for selected drill holes within map area. All drill sites are located on figure 8. Unit labels as in tables 1, 2, and in Description of Map Units. Labelled units identified by Hildreth by microscopic examination and chemical analysis of cuttings or core. SE, surface elevation; TD, total depth of well. A, Wells in west moat or on resurgent uplift. Sources of well-log data: Inyo-4, Eichelberger and others, 1988; IDFU 44–16, Suemnicht, 1987; OXY OIP-1, geothermal corehole, 1984, logged and sampled by R.A. Bailey, 1984, unpublished; PLV-1 and PLV-2, Benoit, 1984; DC-1, Sorey and others, 1978, logged and sampled by R.A. Bailey, 1973; CH-9, Sorey and others, 1978; M-1, Suemnicht and Varga, 1988; LVEW, McConnell and others, 1995. For Inyo-4, $^{40}Ar/^{39}Ar$ ages (ka) for core samples are labeled in red and given in table 2. B, Wells in or near southwest moat. Sources of well-log data: HSL-1, cuttings taken by C. Farrar, logged by R.A. Bailey, 1996, unpublished; 18 M, cuttings logged for Mammoth Community Water District (MCWD) by driller, 1992; OH-1, cored for town of Mammoth Lakes, logged by E.V. Ciancanelli, 1991, unpublished; MLGRAP-1 and -2, Town of Mammoth Lakes geothermal coreholes, Sorey and others, 1991, partially logged and sampled by R.A. Bailey, 1988; Shady Rest RDO-8, Wollenberg and others, 1987, partial log by R.A. Bailey, 1986; 30 M, water well for MCWD; cuttings logged and collected by A.K. Ardell and T.D. McCarthy (MCWD), 2005, unpublished; 57–25, Ormat geothermal well, 2005, logged by R. Dunlap, J. Pollard, and K. Clark; Suemnicht and Sorey, 2007; BC 12–31, Mammoth Pacific geothermal corehole, 2002, Suemnicht and others, 2006, Fowler and others, 2011; 66–31, Mammoth Pacific geothermal corehole, 1992, Suemnicht and others, 2006, logged by R.A. Bailey, 1992, unpublished. Abbreviations: bi, biotite; hb, hornblende; ms, metasedimentary rocks; gd, granodiorite; ss, sandstone; Tv, Tertiary mafic and intermediate volcanic rocks; xr, crystal-rich; xm, crystal content intermediate; xp, crystal-poor; vxp, very crystal-poor (≤1 percent but not aphyric).

transition zone, as at Big Pine (Bateman, 1965) and Coso (Duffield and Bacon, 1981), respectively 50 and 110 km south-southeast of Long Valley. Around 4 Ma, decompressing upper mantle began leaking modest batches of mafic magma to the surface across a broad belt (Moore and Dodge, 1980) that extended from the later site of Long Valley for 40 km southwest into the Sierra Nevada and 30 km northeast into the Adobe Hills (fig. 2). Only close to Long Valley, which coincides with a major left-stepping offset in the Sierran rangefront, were the precaldera mafic products accompanied by eruptions of dacite (3.6–2.6 Ma). Precaldera magmatism close to Long Valley was reviewed by Bailey (2004), and all precaldera eruptive units included in our map area were summarized in the section above. Bailey noted that the mafic and dacitic magmas ceased erupting by ~2.5 Ma, somewhat before the onset of rhyolitic eruptions at 2.2 Ma. For ~2 million years thereafter, an increasingly molten deep-crustal environment evidently favored entrapment of mantle-derived basaltic magma, which in turn amplified crustal melting, initiating a prolonged interval of rhyolitic magmatism (which included caldera collapse at 767 ka). Not until after 250 ka did mafic eruptions resume and, even then, their vents have been limited to an area west of the structural caldera (Hildreth, 2004), a new magmatic focus herein called the Mammoth system.

Glass Mountain Rhyolites

Glass Mountain (fig. 3) is a sprawling precaldera complex (2.2–0.79 Ma) of more than 60 overlapping eruptive units, exclusively high-silica rhyolite (76.6–77.7 percent SiO_2), at the northeast periphery of Long Valley Caldera, where the rhyolites are exposed to a thickness greater than 1,050 m on the caldera wall (Metz and Mahood, 1985, 1991; Metz and Bailey, 1993). At least 50 km^3 of rhyolitic material is preserved as lava flows, domes, proximal tuff, and fans of mixed pyroclastic and reworked debris. Based on the pattern of intersection of caldera faults with the Glass Mountain edifice and the abundance of Glass Mountain lithic fragments in the Bishop Tuff (Hildreth and Mahood, 1986), we estimate that roughly 10–20 km^3 more is downfaulted beneath the caldera floor. As many as 17 plinian and subplinian events distributed Glass Mountain fallout from the Pacific Ocean to Utah (Izett and others, 1988), though the total volume is hard to estimate from the scattered remnants. The aggregate thickness of fall units is several meters in pumice quarries 15–20 km east of Glass Mountain (Sarna-Wojcicki and others, 2005), which, along with preservation of ash layers as far as 470 km south and 550 km east, suggests a dispersed volume of tephra in the range 50–100 km^3 (equivalent to 25–50 km^3 of hydrous high-silica-rhyolite magma). Total magma volume released by the Glass Mountain center may thus have been 100±20 km^3, all of it high-silica rhyolite. A few individual fall units may have exceeded 10 km^3, whereas only a few of the lavas are as voluminous as 1 km^3.

Compositional data for Glass Mountain lavas fall into two groups: (1) an older sequence (2.2–1.3 Ma) of at least 24 eruptive units, all high-silica rhyolite but chemically varied, tapped sporadically at different stages of evolution, including some units considerably more evolved than the Bishop Tuff in trace-element contents; and (2) a younger sequence (1.2–0.79 Ma) of at least 35 eruptive units, all of them geochemically similar to the more evolved end of the compositionally zoned Bishop Tuff array, and presumably tapped from a common, by-then-integrated, expanding magma chamber (Metz and Mahood, 1991; Metz and Bailey, 1993). All but one of the Glass Mountain rhyolites are crystal-poor; a dozen have 6–8 percent phenocrysts, but the great majority have 0–5 percent. Phenocryst abundances, species, and compositions (Metz, 1987) resemble those of the evolved, first-erupted part of the zoned Bishop Tuff, most units having quartz, sanidine, plagioclase, biotite, allanite, zircon, apatite, and Fe-Ti oxides. Glass Mountain lies just northeast of the present map area, but it represented a major component of the Long Valley rhyolitic system.

Climactic Eruption and Caldera Formation

The caldera-forming eruption of the Bishop Tuff at 767 ka began as a plinian outburst along or near the Hilton Creek Fault in the south-central part of what soon became the caldera (Hildreth and Mahood, 1986). The roof of the growing chamber, then about 5 km deep (Wallace and others, 1999), ultimately failed catastrophically, releasing more than 600 km^3 of gas-rich rhyolitic magma, compositionally and thermally zoned (Hildreth, 1979; Hildreth and Wilson, 2007), in a virtually continuous eruption about 6 days long (Wilson and Hildreth, 1997), thereby permitting 2–3 km subsidence of the roof, creating the caldera. About half the Bishop Tuff volume was emplaced radially as a set of sectorially distributed ignimbrite outflow sheets (unit rbt) along with concurrent plinian and coignimbrite fallout. The other half ponded inside the subsiding caldera, where welded intracaldera ignimbrite as thick as 1,500 m was subsequently buried by 500–800 m of postcaldera rhyolite tuffs, lavas, and sedimentary fill (Bailey, 1989). Pumice clasts in the Bishop Tuff range from ~1 to 25 weight percent phenocrysts and define compositional continua from 78 to 73 percent SiO_2 and 2 to 600 ppm Ba (Hildreth, 1979). The main suite of white pumice is accompanied by a sparse population of crystal-poor gray-to-black pumice that extends the ranges to 65 percent SiO_2 and to 1,350 ppm Ba (Hildreth and Wilson, 2007).

The 17 by 32 km depression called Long Valley Caldera owes its dimensions and the physiography of its walls to large-scale syneruptive slumping and to subsequent secular erosion. As inferred from gravity, drill holes, and vent distribution, the ring-fault zone—outlining the area of steep structural collapse of the cauldron (roof) block into the magma reservoir—encloses a subsided oval 12 by 22 km across. This encompasses an area of ~220 km^2 or roughly 55 percent of the

400-km^2 floor of the topographic-hydrographic basin conventionally portrayed as Long Valley Caldera (fig. 3 of Hildreth, 2004). The magma chamber had to be somewhat wider than the roof plate that sank into it. Nonetheless, clarity in definition of the structural caldera can help avoid misleading conceptualizations. For example, the Inyo rhyolites (unit ric) are commonly said to have invaded the caldera in 1350 C.E., and Mammoth Mountain is often said to straddle the caldera rim. In reality, both are extracaldera volcanoes, well outside the ring-fault zone. Despite proximity, Mammoth Mountain is compositionally and spatially independent of the Long Valley magma reservoir.

Seismic refraction profiles (Hill, 1976; Hill and others, 1985) and gravity models (Kane and others, 1976; Carle, 1988) indicate that the caldera fill thickens substantially toward the north and east, as confirmed in drill holes that show the intracaldera Bishop Tuff thickening from 0.9–1.2 km centrally to ~1.5 km in the eastern third of the caldera (Bailey, 1989). What fractions of the deepening may reflect precaldera topography, differential magma withdrawal, or tilting of the cauldron block during collapse remain uncertain. Where the caldera-forming eruption began, the Hilton Creek Fault system may have had several hundred meters of northeast-facing precaldera relief, and, where the caldera center is now, a left-stepping north-sloping ramp may have separated the en-echelon Hilton Creek and Hartley Springs Faults (figs. 3, 4). Greater subsidence in the north and east is also consistent with stratigraphic and petrological evidence that the final eruptive packages of the Bishop Tuff, which preferentially flowed toward those sectors, were withdrawn from deeper, hotter levels of the magma reservoir (Hildreth, 1979; Hildreth and Mahood, 1986; Wilson and Hildreth, 1997; Wallace and others, 1999; Hildreth and Wilson, 2007).

Postcaldera Eruptive History of the Long Valley System

Compositions of postcollapse eruptive units (760 to 100 ka) that vented inside or near the caldera's ring-fault zone are consistent with derivation from a reorganized, convectively mixed, and thermally restructured Long Valley magma reservoir. Compositions of silicic units on and near Mammoth Mountain, outside the ring-fault zone, are clearly distinct.

Postcaldera units of Long Valley compositional affinity (Bailey, 1989; Hildreth, 2004) are (1) rhyodacite Dome 7403 (east of map area), (2) the voluminous crystal-poor early postcaldera rhyolite (unit rer), and (3) three sets of what Bailey and others (1976) called "moat rhyolites"—the north-central rhyolite chain (unit rnc), the southeastern rhyolite cluster (unit rhc and associated lavas shown by Bailey, 1989, just outside our map area), and several rhyolites in the west moat (units rdc, rdm, rmk, and rwm). A caldera *moat* is a physiographic term for the annular trough in resurgent calderas (Smith and Bailey, 1968) that separates the intracaldera structural uplift from the caldera wall (see figure 3). Typically the site of postcaldera sedimentation and ring-fracture eruptions, a moat conceals and is broader than the structural zone of caldera ring faults.

Early Postcaldera Rhyolite

What Bailey and others (1976) termed the "Early rhyolite" (our unit rer) consists of ~100 km^3 of fairly uniform, phenocryst-poor rhyolite (74–75 pecent SiO_2; ~5.2 percent K_2O) that erupted during the 100,000-year interval following caldera collapse. This enormous eruptive volume is comparable to that of precaldera Glass Mountain and an order of magnitude greater than the total of all subsequent Long Valley rhyolites erupted in the last 600,000 years. Released in many eruptions from several vents (Bailey, 1989), the Early rhyolite includes as many as 12 exposed lava flows and domes, a few more intersected by drilling, and a predominance of rhyolite tuffs—mostly nonwelded pyroclastic-flow deposits (subunits rtav and rtcd)—that make up as much as three-quarters of the assemblage. Eight lava flows (but no tuffs) were K-Ar dated (Mankinen and others, 1986), yielding ages from 751±16 ka to 652±14 ka. The Early rhyolite extends far beyond its outcrop area, as documented in numerous wells (fig. 6; Suemnicht and Varga, 1988; Bailey, 1989; Sorey and others, 1991). At least 622 m thick near its center of outcrop, the Early rhyolite assemblage is still thicker than 350 m where deeply buried in the southeast moat and 230–537 m thick in wells in the west moat.

Because no correlative layers of distal ash have been identified outside Long Valley, it seems likely that individual eruptions of Early rhyolite tephra, though numerous, were subplinian and moderate in volume. This might be interpreted to mean that the residual rhyolite magma had been relatively depleted in volatiles during the caldera-forming eruption. On the other hand, the observations that three-quarters of the assemblage is pyroclastic and that much of it is nearly aphyric but biotite-bearing suggest that the magma was not water-poor. Perhaps the abundance of medium-scale Early rhyolite eruptions reflected relative ease of magma escape through the downfaulted and broken roof plate, thereby preventing by frequent eruptive release (and perhaps also by passive degassing) any postcaldera recurrence of severe gas overpressure.

Compositions of early postcaldera rhyolite lavas are similar in most respects to the last-erupted part of the zoned Bishop Tuff, except that Zr (170–200 ppm) and Ba (950–1,230 ppm) significantly extend the range of Bishop zoning (fig. 4 of Hildreth, 2004). Phenocryst contents of Early rhyolite are low, only 0–2 percent, compared to 15–25 percent in the directly preceding, last-erupted part of the Bishop Tuff. The dominant minerals in the Bishop Tuff, sanidine and quartz, are absent in Early rhyolite, and the sparse crystals present appear to be new, euhedral to subhedral, and unresorbed. These include plagioclase, orthopyroxene, Fe-Ti oxides, and sparse biotite, as well as traces of apatite, zircon, and pyrrhotite (Bailey, 1978, 1989). Processes that may have produced the contrast in crystal content between late Bishop Tuff and (compositionally

similar) postcollapse Early rhyolite were discussed by Hildreth (2004). The greatly elevated Ba contents of Early rhyolites relative to the Bishop Tuff may be attributable, at least in part, to resorption of accumulative sanidine.

Postcaldera Resurgent Uplift

Intracaldera resurgence was defined by Smith and Bailey (1968) as structural uplift of a caldera floor by renewed buoyancy of the viscous magma remaining in the postcollapse reservoir (or replenishment thereof), but the term has sometimes been inappropriately applied to postcaldera eruptive activity that may or may not accompany such uplift. A resurgent dome is a structural and physiographic feature that need not be accompanied by extrusion of lava domes. Bailey and others (1976) argued that structural uplift at Long Valley was important during the 100,000-year interval of Early rhyolite eruptions and may have been largely over by ~600 ka. Some Early rhyolite vents may lie along or close to faults associated with the uplift, but the relative timing of individual eruptive units and offsets along long-active faults is seldom clear. The roughly circular area of uplift is ~10 km across (figs. 3, 4) and dips radially outward at 10–25º (as inferred by Bailey, 1989). Lookout Mountain (subunit rlm; 692±14 ka), a cratered shield of Early rhyolite in the northwest moat, is outside the uplift, as are thick sections of Early rhyolite concealed beneath other sectors of the moat.

The high point of the uplift is Gilbert Peak (2,626 m elevation) and, if Early rhyolite thickness there is similar to that (622 m) in the Long Valley Exploratory Well (LVEW; fig. 6) ~2 km south, then the top of the subjacent Bishop Tuff would be at ~2,000 m, probably its maximum intracaldera elevation. This is 261 m higher than the top of the Bishop Tuff in the LVEW (a site downfaulted within the graben system atop the uplift), 469 m higher than in well 44-16 in the west moat, and 575 m higher than in well 66-29 in the southeast moat (Suemnicht and Varga, 1988; Bailey, 1989; McConnell and others, 1995). It seems likely that the (initially fluidized) primary surface of the Bishop Tuff that ponded inside the caldera was virtually horizontal at the close of its eruption. Therefore, even though part of the excess elevation of the resurgent structure owes to the constructional pile of proximal Early rhyolite, and part to differential compaction of the Bishop Tuff (which is much thicker in the low eastern third of the caldera; Hill, 1976; Bailey, 1989), doming of the top surface of the Bishop Tuff clearly demonstrates central uplift of at least 400 m. The net effect on surface elevation of transfer of ~100 km^3 of Early rhyolite magma from chamber to surface is uncertain; unknowns include magma recharge volume and strength of the roof plate as well as relative aspect ratios of the magma domain withdrawn and the extrusive rhyolite pile and its moat-filling apron.

Much of the uplift appears to have taken place during Early rhyolite time, but what fraction has continued episodically is unquantified. As shown on our map, mafic lava flows as young as 180–125 ka are displaced by faults of the graben system that crosses the resurgent uplift. If most of the uplift had indeed been roughly contemporaneous with eruption of Early rhyolite, as proposed by Bailey (1989), then uplift of ~400 m in ~100,000 years yields an average rate an order of magnitude smaller than that of the ~80 cm of renewed uplift that took place between 1980 and 2000 (Savage and Clark, 1982; Langbein, 2003).

Drill core from the LVEW (virtually central to the uplift) revealed within the 1.2-km-thick Bishop Tuff some ten phenocryst-poor intrusions, apparently sill-like and not present in wells drilled peripheral to the uplift (McConnell and others, 1995). Compositionally, the sills are Ba-rich rhyolite much like the Early rhyolite and, having a cumulative thickness of ~330 m, they could account for most of the resurgent uplift. For a 10-km-wide domical uplift of 400 m, the apparent volume of inflation is about 15.7 km^3 or merely ~16 percent of the volume of Early rhyolite erupted. The conventional model that a resurgent residual magma chamber buoyantly upwarps the cauldron block by reinflation or upward stoping is, therefore, for Long Valley, no more compelling than a model of central uplift by injection of shallow sills or laccoliths into the thick intracaldera fill (McConnell and others, 1995).

The fault system on the resurgent uplift is dominated by north-northwest trends essentially parallel to those of rangefront faults north and south of the caldera, but also parallel to the strike of steeply dipping structures and bedding in the metamorphic basement rocks (Rinehart and Ross, 1964). Radial and dome-concentric faults are absent. Thus, the structure of the uplift may have been influenced more by regional precaldera structures and susceptibility of the shallow, subhorizontally layered Bishop Tuff to sill injection rather than by chamber-wide buoyancy. Location of the uplift nonetheless surely reflects the main locus of the reorganized postcaldera magma reservoir, which so voluminously supplied the Early rhyolite erupted. For the past 500,000 years, however, despite paths provided by the complex fault system, there have been no more eruptions centered on the resurgent structure.

Rhyodacite Dome 7403

In the northeast corner of the caldera floor (fig. 3), a small rhyodacite lava dome stands alone at the foot of the Glass Mountain scarp (Hildreth, 2004). Only 110 m high and ~0.01 km^3 in volume, this glassy, coarsely blocky to polygonally jointed dome, subcircular in plan, is not a downfaulted precaldera mass but an unequivocally postcaldera eruptive unit. It extruded in three pulses, the summit dome rising ~40 m higher than southwest and northwest lobes. Bailey (1989) suggested that its glassy exterior reflected eruption into a Pleistocene intracaldera lake, but we observe only angular indigenous scree, no rounded or exotic pebbles, and no wave-cut features on its widely micropumiceous surface. The dome is compositionally homogeneous (67.9 percent SiO_2 with ~1,500 ppm Ba and ~800 ppm Sr) but unique in being the only nonrhyolite

postcaldera eruptive unit from the Long Valley reservoir. Unlike the trachydacites of similar SiO_2 content at Mammoth Mountain, the dome is subalkaline (Hildreth, 2004). Containing abundant euhedral plagioclase (<1 mm) and hornblende needles as long as 1 mm, it contrasts with Glass Mountain, Bishop Tuff, and early postcaldera rhyolites in having hornblende (instead of biotite or pyroxene) as the principal mafic silicate phase. The lava is compositionally somewhat like the rare dacite pumice ejected toward the end of the Bishop Tuff eruption (Hildreth and Wilson, 2007), which was probably withdrawn from a level beneath the thick capping rhyolite in the magma reservoir.

An attempt was made to determine its age by $^{40}Ar/^{39}Ar$ dating of clean euhedral plagioclase. Although sparse granite-derived xenocrysts were avoided, excess Ar was indicated by an erratic incremental-fusion spectrum. An attempt to date its tiny acicular hornblende euhedra also failed. Although a few accordant steps in the middle of the Ar-release spectrum are consistent with a middle Pleistocene age, the absence of lakeshore features suggests extrusion after shrinkage of the intracaldera lake, probably after MIS 6.

North-Central Rhyolite Chain

The earliest of three clusters of postresurgence rhyolites that Bailey (1989) termed moat rhyolite is a northwest-trending chain (unit rnc) that crosses the northeast sector of the Early rhyolite and is, therefore, not really in the caldera moat at all, nor aligned along the ring-fault zone. In contrast to the voluminous Early rhyolite, all components of unit rnc are phenocryst-rich and of small eruptive volume, totalling ~1 km^3. About 100 ºC lower in Fe-Ti-oxide temperature than the nearly aphyric Early rhyolite (Bailey, 1978), the north-central rhyolites are rich in plagioclase, sanidine, quartz, hornblende, and biotite. SiO_2 contents (73.9–75.3 percent) are similar to Early rhyolite, but K_2O (4.7 percent) and Ba (680–715 ppm) contents are significantly lower, probably as a result of sanidine fractionation. Mafic enclaves (53.3–54.9 percent SiO_2) occur in lava flows and domes along the north-central chain, but none have been found in any of the younger (southeast and west moat) rhyolites. Four discrete components of unit rnc yielded sanidine K-Ar ages of 527±12, 523±11, 505±15, and 481±10 ka (Mankinen and others, 1986). Simon and others (2014) recently published sanidine ages of ~570 ka for one of the domes and a derivative lava flow, apparently lengthening the time interval spanned by eruptions of unit rnc.

Southeastern Rhyolite Cluster

After an apparent hiatus of ~120,000 years, another set of rhyolite lavas erupted over an interval as long as ~35,000 years, from a cluster of six vents in the caldera's low southeast moat (Bailey, 1989). Two of these vents arguably extend the trend of the north-central chain just discussed, and two lie along the ring-fault zone, the others inboard of it. The extensive (12 km^2) Hot Creek flow (unit rhc) is the only one within our map area; the other five lie 0.5–5 km east of the Hot Creek flow (Bailey, 1989), where their limited outcrops are partly buried by caldera-lake sedimentary deposits. Four of the six lavas are crystal-poor (1–2 percent feldspars plus trace biotite, quartz, pyroxene, and Fe-Ti oxides), whereas two are phenocryst-rich hornblende-biotite rhyolites like the north-central chain. All six have 75–77 percent SiO_2 and 500–700 ppm Ba where fresh, although parts of several of them were altered by interaction with saline-alkaline lake water and sediment.

Altogether, the lavas exposed add up to only ~1.5 km^3, the Hot Creek flow being most of it. Five have been dated (Mankinen and others, 1986; Heumann, 1999; Simon and others. 2014). Sanidine yields ages of 362±8 ka and 333±10 ka for the two crystal-rich units. For crystal-poor units, sanidine gave ages of 329±23 ka and 329±3 ka, and for the Hot Creek flow, obsidian gave 288±31 ka and sanidine gave 333±2 ka. Whatever process promoted reversion to crystal-poor rhyolite at about 330 ka, it was unique in the post-Early rhyolite evolution of the Long Valley magma reservoir, because all other Long Valley rhyolites (527 to 100 ka) are rich in phenocrysts. Thermal rejuvenation by basalt injection is an unlikely explanation for these low-temperature rhyolites, because the crystal-poor units are marked by small euhedral phenocrysts and lack xenocrysts or partly resorbed relicts of an earlier generation. A more likely process, high-silica melt extraction from crystal-rich felsic mush, was discussed by Hildreth (2004).

West Moat Rhyolites

After another hiatus of about 180,000 years, a third cluster of rhyolites erupted, this time west of the resurgent uplift. It consists of three modest lava domes (units rdm, rdc, and rmk) and the extensive West Moat Coulee (unit rwm; 8.5 km^2; as thick as 574 m; Benoit, 1984). The coulee represents ~2 km^3 of rhyolite lava but the domes add up to only ~1 km^3 more. Three of the rhyolite vents are along the ring-fault zone, whereas that of Deer Mountain apparently lies ~2.5 km outboard of it. All four have been dated (Mankinen and others, 1986; Heumann, 1999; Mahood and others, 2010). Oldest is the West Moat Coulee, for which four ages range from 163 to 147 ka, while the Dry Creek dome, the bilobate Mammoth Knolls dome, and the Deer Mountain dome yield overlapping ages in the range 115–97 ka. All are phenocryst-rich (15–30 percent) low-temperature rhyolites containing plagioclase, sanidine, quartz, biotite, hornblende, Fe-Ti oxides, and trace amounts of zircon, apatite, allanite (± pyroxenes and pyrrhotite), but chemically they are of two kinds. Deer Mountain and the coulee have high Ba (700–860 ppm) and only 72–73 percent SiO_2, whereas the Dry Creek and Mammoth Knolls domes are more evolved, with 76–77 percent SiO_2 and lower Ba (110–200 ppm). Like all Long Valley rhyolites, all four are subalkaline, in contrast to the Mammoth Mountain suite. That Deer Mountain and the West Moat Coulee are chemically less evolved than the voluminous Early rhyolite (unit rer;

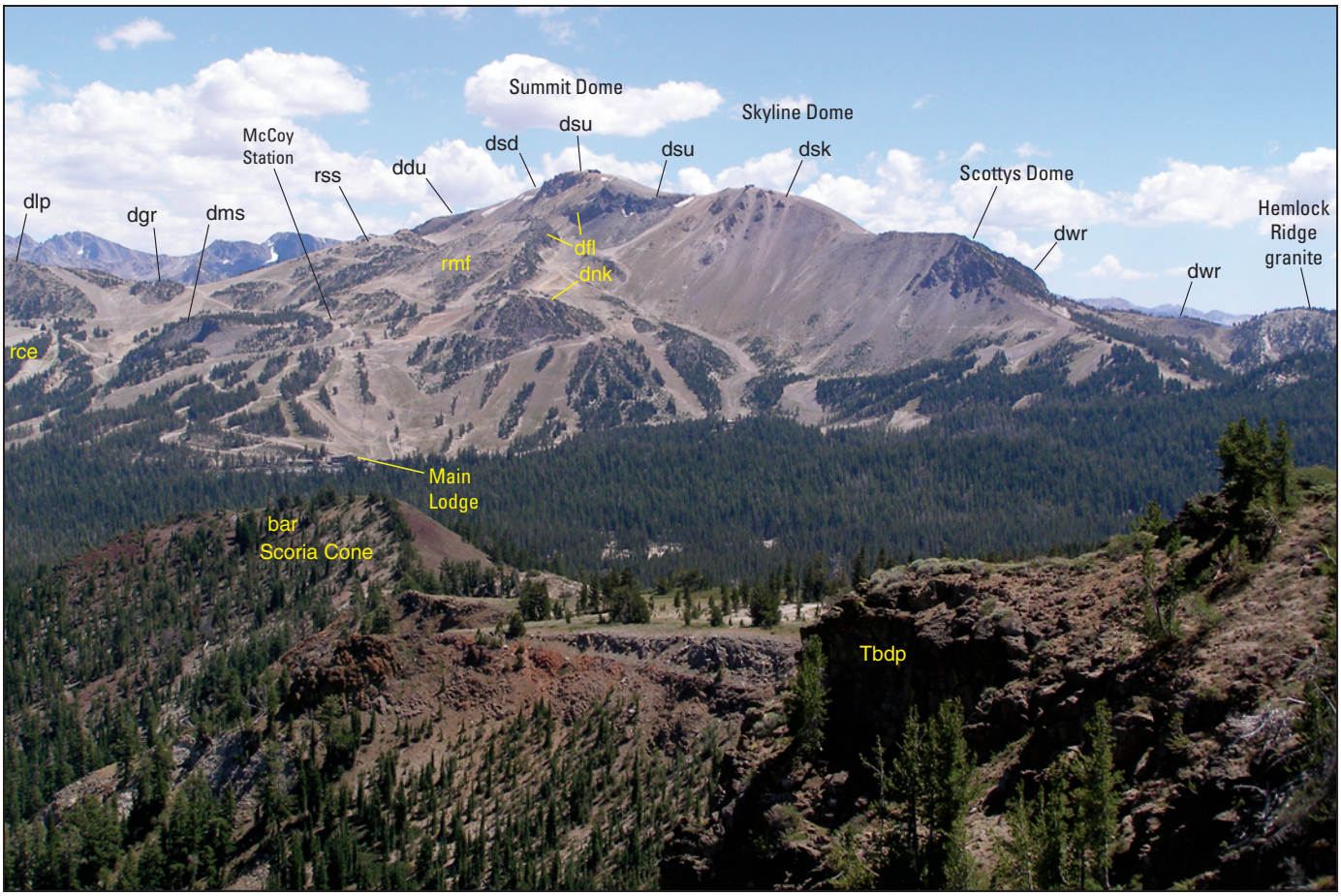

Figure 7. North side of Mammoth Mountain, viewed from caldera rim 5.5 km north-northwest of summit. Northwest-trending dome alignment supports crest, and several more silicic domes and flows are identified by unit label on northeast slope. All units visible erupted in interval 90–55 ka. In left foreground, red scoria cone, source of extensive lava flows of unit bar, erupted ~90 ka. Cliffs in near foreground are stack of Pliocene basalts of precaldera unit Tbdp. Summit of Mammoth Mountain is 650 m higher than MMSA Main Lodge, which can be seen at foot of edifice, just beyond scoria cone, where ski runs meet forest. Scottys Dome marks vent for extensive set of lava flows. Skyline Dome is widely acid-altered, as is notch to left of Summit Dome (see fig. 12).

750–650 ka) suggests mafic input to the Long Valley magma reservoir during the long intervening interval.

Mammoth Mountain and Contemporaneous Peripheral Volcanism

Mafic Periphery

The central complex at Mammoth Mountain consists of 25 distinguishable silicic units that erupted between 100 ka and 50 ka, an interval ~50,000 years long. The silicic edifice (fig. 7) accumulated near the center of a distributed field (fig. 8) of small monogenetic mafic and intermediate vents, the products of which we have divided into 38 separate map units (plus a few subunits). This peripheral monogenetic volcanic field, which consists predominantly of mildly alkalic basalt and its differentiates, produced a total eruptive volume in the range 7–12 km^3. Its activity began around 230 ka and has continued sporadically into the Holocene. Growth of the trachydacitic Mammoth Mountain edifice (~4±1 km^3) thus began near the middle of the basalt-driven volcanic field, in time and in space. Vents for the volcanic units peripheral to Mammoth Mountain scatter within a well-defined field only 10 by 20 km across, evidently reflecting a new domain of mantle-derived melt ascent, compactly circumscribed and unrelated to the range-front fault system. Before initiation of the Mammoth system, there had been no nonrhyolitic eruptions nearby since the Pliocene. Contemporaneous with the well-circumscribed Mammoth volcanic field, there has been no mafic or intermediate volcanism any closer than June Lake (20 km north of Mammoth Mountain) and Big Pine (85 km southeast). The Mammoth volcanic field is thus a new magmatic system that started up after 250 ka. It contrasts with the adjacent Long Valley system in that it lacks high-silica rhyolite and is consistently more alkaline (fig. 4 of Hildreth, 2004).

Vents for the 38 peripheral units are distributed within 4.6 km west, 6.8 km northeast, 8.5 km north, and 9 km south

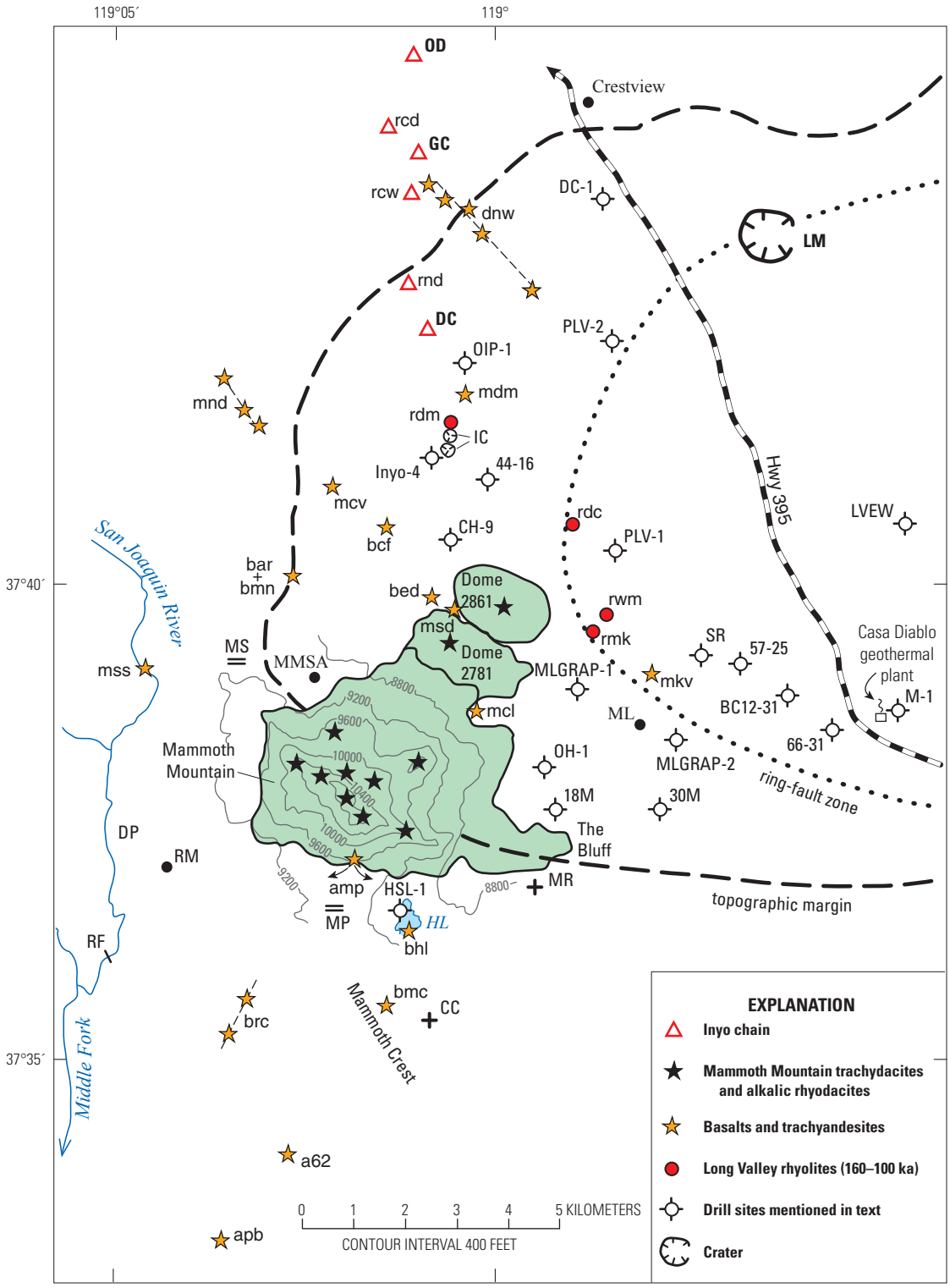

Figure 8. Distribution of volcanic vents exposed on and near Mammoth Mountain at southwest margin of Long Valley Caldera. Mammoth Mountain edifice is colored green, and its exposed vents are indicated by black stars. Peripheral mafic and intermediate vents are represented by orange stars. Four subalkaline Long Valley rhyolites contemporaneous with the alkaline Mammoth system are indicated by red dots. Red triangles represent Holocene rhyolitic Inyo chain; those indicated by bold letters erupted in 1350 C.E. All other vents are identified by 3-letter unit labels (see tables 1 and 2). Logs for drill holes located on map given in figure 6. Abbreviations: CC, Crystal Crag; DC, Deadman Creek flow; DP, Devils Postpile; GC, Glass Creek flow; HL, Horseshoe Lake; IC, Inyo (phreatic) Craters; LM, Lookout Mountain; ML, downtown Mammoth Lakes; MP, Mammoth Pass; MR, Mammoth Rock; MS, Minaret Summit; OD, Obsidian Dome; RF, Rainbow Falls; RM, Reds Meadow.

of the summit of Mammoth Mountain (fig. 8). Some exposed vents are as close as 4.6 km southwest, 4.4 km north, 3 km northeast, and 3 km southeast of the summit, a few of them right at the toe of the edifice. Vents for several other mafic and intermediate units are buried by the edifice itself, by adjacent surficial deposits, or by the cluster of 150- to 87-ka rhyolite and trachydacite domes at the northeast toe of the edifice. A few additional vents indicated on the map of Bailey (1989) and on figure 4 of Hildreth (2004) have proven, on renewed investigation, to be either of Neogene age, rootless secondary vents on late Pleistocene lava fields, or imaginary.

230–150 ka

The 38 peripheral units include 13 basalts, 16 mafic andesites, 6 andesites, and 3 dacites. Nine of them erupted before ~150 ka. The oldest exposed unit dated is unit mcl, an apron of lava flows that issued at the Canyon Lodge scoria cone and spread as far as 9 km northeast and 8 km east (fig. 9). Extensively concealed by younger lavas, its distal exposures have yielded ages as old as ~190 ka, but the most precise are 175–180 ka. Beneath unit mcl, a window of undated lava-flow unit asr is exposed near Shady Rest Campground, and several wells in the west moat and in Mammoth Lakes township have penetrated units mcl, asr, and a few underlying mafic lava flows that are uncorrelated and nowhere exposed (fig. 6). In the Inyo-4 core hole near Inyo Craters (Eichelberger and others, 1988), a set of flows compositionally identical to unit mcl (upper Group II of Vogel and others, 1994) yields a $^{40}Ar/^{39}Ar$ age of 186±2 ka. This is underlain by a 170-m-thick stack of ~18 mafic lava flows (Groups II to IV of Vogel), nowhere exposed, for which three $^{40}Ar/^{39}Ar$ ages (table 2) are as old as 233±4 ka. These unexposed mafic lavas below unit mcl are the oldest known products of the Mammoth volcanic system. Their vents are unknown but certainly buried in the west moat or beneath Mammoth Mountain.

On the south slopes of Knolls Vista (hill 2517), adjacent to downtown Mammoth Lakes, units asr and mcl are successively overlain by one lava flow of unit bsm (165±2 ka) and a set of fountain-fed flows of unit mkv (153±1 ka) from its nearby vent complex, against which lavas of unit msc (154±2 ka) apparently banked. Vents for units bsm and msc were buried by effusion of the rhyolitic West Moat Coulee (unit rwm; ~150 ka). Eastward along the south moat, exposures of lava-flow unit mmc (160±2 ka) are compositionally indistinguishable from those of vent complex mkv. Still farther east, near Chance Ranch, the stratigraphically lowest lava exposed in the south moat sequence (unit bsc) gave an age of 172±2 ka; it overlies units mcl and asr in water wells near town (fig. 6). In the west moat ~3 km north of the toe of Mammoth Mountain, a glacially scoured spatter cone (phenocryst-poor unit bcf) erupted at 164±2 ka.

The earliest of several mafic monogenetic eruptions south of Mammoth Mountain also took place during this opening interval. About 7 km south of the edifice, basaltic lava flows of unit bdc (155±2 ka), rich in olivine and plagioclase, form a platform that extends south from beneath andesitic Cone 2962 (unit a62; 118±2 ka).

150–100 ka

The next 50,000-yr-long interval, from ~150 ka to ~100 ka, was marked by eruption of Long Valley's west moat rhyolites (units rwm, rdm, rdc, and rmk), the first phenocryst-rich Mammoth Mountain trachydacite (unit d81; 99±7 ka), and 9 more peripheral mafic and andesitic units. Among these were a pair of 200-m-high andesite scoria cones, units apb (called Pumice Butte; 142±5 ka) and a62 (Cone 2962; 118±10 ka) that erupted 7–9 km south of Mammoth Mountain (fig. 10). A mafic scoria cone (unit mss; 121±2 ka) erupted through the bed of the Middle Fork San Joaquin River, which then incised its interior, exposing two dikes on the riverbank opposite Soda Springs Campground.

In the south moat, phenocryst-rich lava-flow unit mlc (130±1 ka) is exposed only at its rugged distal terminus, there sandwiched by basaltic lavas of units bsc and bfh; its source vent is buried by younger units and unlocated—but must lie many kilometers to the west. Also in the south moat, the flats around the geothermal plant and highway cloverleaf are floored by phenocryst-rich basaltic lavas of unit bcd (125±2 ka), which appears to have erupted at spatter-cone unit bed (121±3 ka) in the west moat, near the toe of Mammoth Mountain, prior to extrusion of three lava domes (units d81, rmk, and d61) that now separate the cone from exposures of its apron lavas.

Also in the west moat, unit aic (131±1 ka) is a stack of trachyandesitic lavas that crops out near and on the walls of South Inyo Crater, but its source vent is buried by younger deposits and remains unlocated. An eroded mafic scoria cone (unit mdm) nearby is undated but apparently older than the adjacent Deer Mountain rhyolite dome (unit rdm; 101±8 ka). A fourth west moat unit that erupted during this time interval is a glacially scoured coulee of weakly porphyritic pyroxene-plagioclase trachydacite (unit ddc; 103±9 ka) that appears to have issued from a vent subsequently buried by the Mammoth Mountain edifice.

100–50 ka

The next 50,000-yr-long interval included incremental construction of the Mammoth Mountain edifice (~87 ka to ~50 ka) and eruption of 14 peripheral units—5 basalts, 6 mafic andesites, 2 andesites, and 1 dacite. Two of the oldest in this interval are extensive lava flows on opposite sides of Mammoth Mountain—unit bsr (99±1 ka) in the south moat and unit drf (98±1 ka) along the Middle Fork San Joaquin River; both may have erupted from vents now covered by Mammoth Mountain. Both were subsequently overrun by

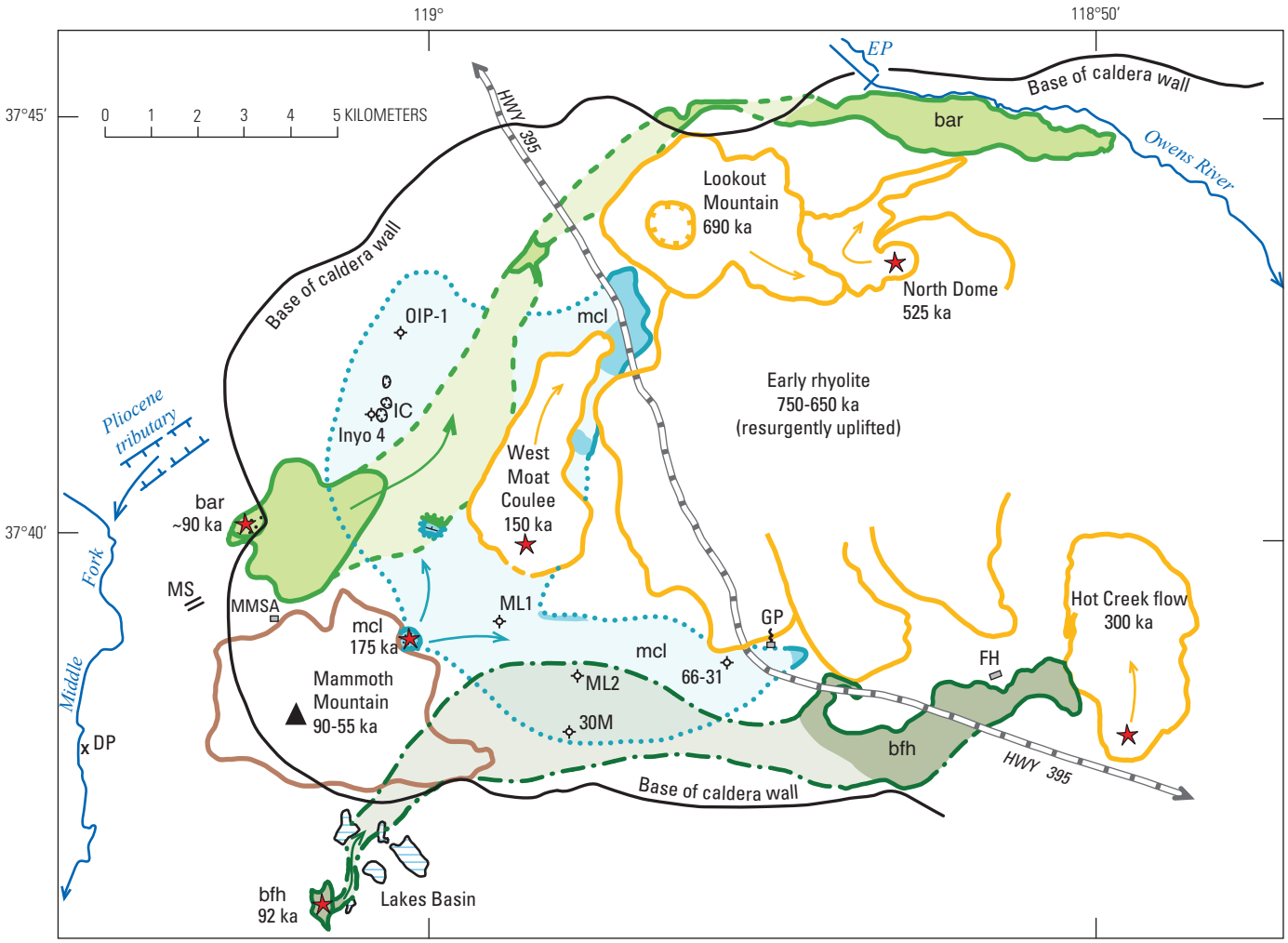

Figure 9. Map of three major mafic lava-flow units in western half of Long Valley Caldera. Because each is extensively covered by younger volcanic and glacial deposits, this diagram is provided to illustrate their original continuity. Scoria cone at source of each is shown by red star: unit mcl (~175 ka) in blue, bfh (~92 ka) in gray, and bar (~90 ka) in green. Colors are strong where unit is exposed but pale where unit is covered or eroded away. Small two-colored rectangle north of mcl scoria cone is north-dipping slab of mafic lavas (units mcl and bar) uplifted on roof of trachydacite Dome 2861 (~87 ka). Six wells are shown in which one or more of the three mafic units has been identified in drill cores (see fig. 6). Long Valley rhyolites outlined in orange predate the three mafic units, except that unit mcl is older than West Moat Coulee (~150 ka). Trachydacitic Mammoth Mountain is largely younger than the three, but its growth began quasi-contemporaneously with two of them. On west rim of caldera, Pliocene tributary of Middle Fork San Joaquin River (incised through pre-Cenozoic rocks) was filled and permanently blocked by 3.7-to-3.2-Ma stack of basaltic lava flows. Abbreviations: DP, Devils Postpile; EP, East Portal; FH, Hot Creek Fish Hatchery; GP, Casa Diablo Geothermal Plant; IC, Inyo Craters; MMSA, Main Lodge of Mammoth Mountain Ski Area; MS, Minaret Summit, road crossing from Mammoth Lakes township to Middle Fork.

aprons of phenocryst-poor lava flows of unit amp (97±1 ka), which erupted on the drainage divide at the later site of Mammoth Mountain and poured both eastward along Mammoth Creek and westward into the Middle Fork. Undated unit aml is a glaciated remnant of the phenocryst-poor orthopyroxene-hornblende silicic andesite at McLeod Lake, just south of the Mammoth Mountain edifice; its vent is not exposed, but its identification directly beneath unit amp in wells drilled near Horseshoe Lake and downtown Mammoth Lakes suggests that it is not much older than 97 ka (fig. 6). The colonnade called Devils Postpile (fig. 11) is part of an intracanyon mafic lava flow (unit mdp) along the floor of the Middle Fork, where it overlies units mss, drf, and amp and yielded an age of 82±1 ka.

A basaltic scoria cone (unit bmc) atop the Sierran drainage divide at Mammoth Crest, above Lakes Basin and only 4 km south of the summit of Mammoth Mountain, yielded an age of 92.7±2.4 ka. It was the source of an apron of lava flows (unit bfh) rich in large plagioclase phenocrysts that extended along Mammoth Creek as far as 18 km (fig. 9) but is exposed for only its distal 6 km (though also identified in intermediate water wells). Although the apron was glacially eroded and covered by till and younger lavas for the first 12 km away from the cone, the distal flow near the Hot Creek fish

Figure 10. Peripheral vent cluster 5–9 km south of Mammoth Mountain. Pair of small red scoria cones (unit brc) erupted in early Holocene. Pair of large forested scoria cones (units a62 and apb) erupted in interval 110–150 ka. Pair of off-white lava domes (unit Tacc) erupted in Pliocene. Low-relief forested foreground is Mammoth Pass, which is floored by lava-flow apron of unit amp (97 ka). Confluence of glacial canyons of Fish Creek and Middle Fork San Joaquin River is hidden behind Pumice Butte (apb). Canyon walls and steep nose at left center (northwest end of Mammoth Crest) are Mesozoic granite. View is southward from summit of Mammoth Mountain.

hatchery is chemically, petrographically, and paleomagnetically identical to the cone, and it yielded an indistinguishable age—92.4±2.4 ka.

Another basaltic scoria cone is well preserved on the caldera wall 2 km northeast of Minaret Summit and 4 km north of Mammoth Mountain (fig. 7). It was the source of two distinctive aprons of lava flows in the west moat, unit bmn (87±7 ka) and the overlying phenocryst-richer unit bar, which has given several ages, the most precise of which is 88±5 ka. A slab of unit bar was uplifted on the roof of trachydacite Dome 2861 (unit d61; 87±2 ka). In addition to spreading across much of the southwest moat, flows of unit bar extended 13 km northeast to bank against the north wall of the caldera, thence 10 km eastward to a terminus along the Owens River (fig. 9).

A multilobate flow field of mafic lavas extends 10 km northeast from the west moat near Dome 2861 to the north wall of the caldera near Big Springs. The southern half is exposed as a series of windows through late Pleistocene till of unit gdc and, beyond the glacial limit, the northern half branches into three lobes, the central one thickening and widening into a steep-sided coulee. We tried to separate the lobate field into two map units (mnd and mor)—variants that range in phenocryst content from aphyric to 4–5 percent plagioclase—but we found gradational areas and numerous rootless vents and fissures that complicate the outflow sequence. The mapped variants turned out to have overlapping ranges of composition (51.2–54.2 percent SiO_2) and indistinguishable paleomagnetic directions. The coulee, unit mor, gave an age of 66±2 ka. Map unit mns is a poorly exposed patch of scoria lapilli and bombs as big as 50 cm that is largely covered by glacial and colluvial deposits in the saddle between trachydacitic Domes 2861 and 2781; similar to units mor and mnd compositionally and mineralogically, the scoria may mark a concealed vent for those lava flows.

Unit msj is a small window of moderately porphyritic (clinopyroxene-plagioclase-olivine), subalkaline basaltic andesite lava that crops out directly beneath unit mnd at the

Figure 11. Devils Postpile, designated a National Monument in 1911, lies 4.5 km west of summit of Mammoth Mountain. Colonnade of phenocryst-rich basaltic trachyandesite, in this photo as high as 20 m, consists of prismatic columns 50–100 cm thick. Mapped as unit mdp, single intracanyon lava flow is altogether as thick as 110 m and may have taken 20–25 years for fractures to advance inward while it cooled and solidified. Eruption age 82±1 ka.

north end of the complex graben followed by Highway 395. Its source vent is unknown, and it crops out nowhere else. Nor has a source vent has been recognized for a lithic-rich mafic scoria-fall deposit (unit mic), several meters thick and exposed only on the walls of the Inyo Craters, where it rests directly atop unrelated unit aic (131±1 ka). Scoriae are mostly lapilli (but as big as 20 cm), contain 54.3–55.8 percent SiO_2, and are overlain by Mono Craters ashfall, then by magmatic and phreatic ejecta of the 1350 C.E. Inyo episode. Unit mic may be a phreatomagmatic or purely phreatic deposit; its vent was probably nearby but not identical to Inyo Craters.

50–0 ka

Subsequent to growth of the Mammoth Mountain edifice, there have been four mafic eruptions in its periphery as well as extrusion of a chain of five trachydacite lavas in the caldera's northwest moat. One is a glaciated sheet of phenocryst-rich olivine-clinopyroxene-plagioclase basaltic lava (unit bhl; 31±1 ka) that banked against the southeast toe of Mammoth Mountain near Horseshoe Lake. Remnants floor part of Lakes Basin, and abundant erratics of unit bhl occur in all of the numerous nested moraines along Mammoth Creek (unit glb), demonstrating that the till was deposited during MIS 2.

A large mafic scoria cone just west of Crater Flat and 6 km north of the summit of Mammoth Mountain produced a lava-flow apron (unt mcv; 31±2 ka, 34±1 ka) that extends 9 km northeast and banks against the caldera wall at Crestview. All but the distal 3 km of the apron lavas are concealed by younger lavas and surficial deposits.

A northwest-trending chain of three glacially ravaged remnants of comagmatic mafic scoria, agglutinate, and fountain-fed lava (unit mdn) is the product of aligned vents,

probably dike-fed, on the caldera wall, 2 km northeast of Deadman Pass and 8 km north of the summit of Mammoth Mountain. Banked against the toe of Lookout Mountain 9 km northeast, a surficial deposit (2 km beyond the glacial limit) consists entirely of angular clasts of unit mdn. One of many meter-sized blocks in the deposit gave an age of 17±1 ka, and a dense vent-proximal lava gave an age of 16±2 ka.

Red Cones is a pair of 120-m-high basaltic scoria cones, 3–4 km southwest of Mammoth Mountain (fig. 10). They jointly fed a 1.2-km^2 lava-flow field southwest of the cones (unit brc). The most recent eruption in the Mammoth Mountain periphery, this episode released ~0.025 km^3 of magma, equally divided between lavas and fragmental deposits. Small bits of charcoal in sediment beneath the ashfall gave a radiocarbon age of about 8.5 ka (Browne and others, 2010).

A southeast-trending nonglaciated chain of five comagmatic trachydacite domes and coulees (unit dnw) crosses the northwest moat, 11–12 km north of Mammoth Mountain. All five are glassy and rich in phenocrysts of plagioclase, sanidine, hornblende, and biotite, but they are variably contaminated with mafic enclaves, microdioritic blebs, and disequilibrium crystals, thus ranging in bulk composition from 67.3 to 60.4 percent SiO_2. Although the five vents are roughly aligned, their $^{40}Ar/^{39}Ar$ ages range from 42±1 ka to 27±1 ka. The two southeastern coulees, despite being the most contaminated, gave younger ages than the three northwestern units.

Trachydacitic Focus at Mammoth Mountain

Mammoth Mountain is a pile of overlapping silicic domes and coulees (figs. 1, 7) that extruded from a vent cluster only ~2.5 km across and spread laterally into a 5-km-wide volcanic edifice that has ~850 m of relief. The edifice exposed consists of 22 compositionally distinguishable extrusive units, among which only five (units dfl, dnh, dsd, dwr, and rce) represent more than a single flow. In addition, two comagmatic extrusions (units d81 and d61) form contiguous off-edifice domes, centered respectively 3.5 and 4.5 km northeast of the summit of Mammoth Mountain. The 24 extrusive units range in SiO_2 content from 63 to 71 percent, and all are mildly alkaline, widely glassy, and generally flow foliated. Nineteen are phenocryst-rich trachydacites, and five that have 70–71 percent SiO_2 and fewer phenocrysts (units rce, rmf, rrc, rsq, and rss) are designated alkalic rhyodacites. A thick, complex pumice-fall deposit (unit rfp) preserved at several sites scattered northeast and east of the glaciated edifice is compositionally similar to edifice unit rce.

Every bit of Mammoth Mountain was ice-covered and thus either surficially scoured or deeply excavated during late Pleistocene glaciation. As a result, most of the silicic lava flows and domes that make up the edifice were substantially reduced in size. Confirming correlations among lava remnants has thus required accumulation of chemical, petrographic, and paleomagnetic data. Except for unit rfp, any pyroclastic flow and fall deposits that accompanied extrusion of the 24 silicic lava units exposed have been eroded away or concealed by younger units.

Petrography

All 25 units (table 1) contain Fe-Ti oxides, biotite, sanidine, and plagioclase; the dominant phenocryst phase in every sample is plagioclase. Although it is more abundant than sanidine in all Mammoth Mountain products, unit descriptions give only the percent of total feldspar in each unit, owing to intrasample inhomogeneities in plagioclase/sanidine proportions, multigrain feldspar intergrowths, and wide ranges in sizes and disequilibrium morphologies of coexisting feldspar populations. Hornblende is the dominant mafic phenocryst in units dbp, ddl, ddu, and dom (all east of the summit) and in off-edifice unit d61. On the other hand, hornblende is sparse in units dgr, dnh, dsk, dsu, dwr, and virtually absent in all the rhyodacites (units rce, rfp, rmf, rrc, rsq,and rss). In the remaining trachydacite units (dfl, dlp, dml, dms, dnk, drc, dsd, dtl, and d81), biotite and hornblende are similar in abundance and either one may exceed the other in particular samples. Although subordinate to other mafic phases, pyroxene microphenocrysts (and sparse prisms 0.5–2 mm long) are common (0.5–2 percent) in units dfl, dgr, dlp, dml, dms, dnh, drc, dsd, dsu, dtl, d61, and d81. Pyroxenes appear to be absent in units dbp, dnk, dom, rce, and rfp, and they have been observed in merely trace amounts in the remaining eight silicic units at Mammoth Mountain. Most pyroxenes occur in clusters or in clots with other phases, suggesting entrainment from crystallizing rinds at the margins of conduits or magma pods. Orthopyroxene is more abundant than clinopyroxene, but both are present in some units. Many of the clinopyoxene crystals may have been released from andesitic enclaves that disaggregated in host dacites. Sparse enclaves (1–5 cm) were seen at some outcrops, and fine-grained mafic blebs, typically 2–5 mm across, were observed in thin sections of 13 of the 24 units; they are especially common in units dml and dtl. Groundmasses of all 100-odd Mammoth Mountain silicic samples sectioned are at least partly glassy and charged with microlites.

Some petrographic data based on thin-section examination are given in unit descriptions and summarized in table 1. In addition, the following generalizations can be noted.

- Mammoth Mountain trachydacites carry 15–35 percent crystals and the alkalic rhyodacites only 5–15 percent. Size ranges of the several mineral species are given in each unit description.

- Crystal clots (mostly 1–3 mm), containing interstitial glass and any combination of the phases present, occur in all samples.

- More than one population of plagioclase is typically present in every sample. Crystals with sieve

textures, internal resorption surfaces, and more sodic (or sometimes potassic) overgrowths are common in all trachydacites and present even in most samples of alkalic rhyodacite.

- Sanidine is more often inclusion-free and euhedral, especially in the most evolved units. Microprobe reconnaissance on about 10 samples from Mammoth Mountain by Ring (2000) showed all or most of the sanidine to be sodic (along with lesser anorthoclase), contrasting with the potassic sanidine present in the subalkaline rhyolites of the Long Valley suite.

- Ring (2000) also identified abrupt increases in Ba content of feldspars just outboard of resorption surfaces, possibly reflecting episodes of mixing with Ba-enriched hotter magma that had induced the resorption.

Eruptive Sequence

The 25 silicic units were erupted in several episodes between ~100 ka and ~50 ka, an interval ~50,000 years long (1) First was Dome 2781 (unit d81) at the northeast toe of the subsequent Mammoth Mountain edifice. There is no evidence of further activity after its extrusion at 99±7 ka until (2) an interval around 85±5 ka when off-edifice Dome 2861 (unit d61) and the oldest units exposed on the edifice erupted. The latter group includes the earliest alkalic rhyodacites (units rrc, rce, and rfp) and the large South Summit Dome (unit dsd; ~68 percent SiO_2), which may be the most voluminous eruptive unit on Mammoth Mountain. Initiation of edifice growth closely followed (or may have overlapped in time with) the interval of elevated peripheral activity that produced units amp, bar, bfh, bmc, bmn, bsr, ddc, and drf, all of which erupted close to or beneath the subsequent site of the Mammoth Mountain edifice.

(3) There followed extrusion of relatively low-silica (63–64 percent SiO_2), pyroxene-bearing trachydacite (unit dtl [76±1 ka]), now exposed at the east base of the edifice along Mammoth Creek.

(4) An episode of higher-silica trachydacite extrusions (66–70 percent SiO_2) ensued, producing the western flow-dome complex (unit dwr, 73±2 ka), the easternmost coulee at The Bluff (unit dom, 73±1 ka), and the Skyline Dome on the crest of the mountain (unit dsk, 71±1.5 ka).

(5) Another silicic trachydacite episode (66–70 percent SiO_2) subsequently produced two coulees on the north flank (units dml [67±1 ka] and dms [68±1 ka]). The age of the small dome, unit dgr (68.8 percent SiO_2), is poorly constrained but likely to have erupted during this episode or the next. Poorly exposed unit dnh (65±1 ka) crops out low on the southeast slope of the edifice, where it is overlain by the undated Bottomless Pit flow (unit dbp; 67 percent SiO_2), which forms much of the 150-m-high scarp above Twin Lakes.

(6) After a respite of a few thousand years, a short interval of renewed activity yielded a variety of silicic lavas, all of which erupted near or north of the summit. Low-silica (63–65 percent SiO_2) pyroxene-bearing flows of units drc and dfl (61±3 ka); pyroxene-free North Knob dome (unit dnk; 60±1 ka; 66.5 percent SiO_2); Lincoln Peak dome (unit dlp, 64±7 ka); and two alkalic rhyodacite lava flows (units rmf [61±1 ka] and rsq [63.7±4 ka]). These rhyodacites erupted from separate vents, but unit rsq issued atop the same site where rhyodacite unit rce had erupted ~15,000 years earlier and where unit rss subsequently built Solitude Dome (~50 ka). All four rhyodacites are readily distinguishable compositionally and are thus inferred to represent four separately evolved magma batches.

(7) After a brief interval, the Summit Dome (unit dsu, 68–70 percent SiO_2) extruded on the crest, where it overlies units dsd, dsk, drc, and dfl (61±3 ka). It rests directly atop unit dfl (fig. 12), and its radioisotopic age (61±2 ka) is indistinguishable.

(8) The pair of coulees capping the Dragons Back arete (units ddl [58±2 ka] and overlying ddu), both thick trachydacites (66–67 percent SiO_2), are among the youngest lavas erupted at Mammoth Mountain. Both flows continue eastward across the narrow glacial outlet of Lakes Basin, beyond which they were ice-sculpted to form the smooth till-mantled hill called Panorama Dome.

(9) Youngest of all is apparently Solitude Dome (rhyodacite unit rss), which grew atop the vent for older units rce (80±1 ka) and rsq (63.7±4 ka); it yields a sanidine age of 50±3 ka. The entire multiepisode growth of Mammoth Mountain thus lasted about 50,000 years, and it has been another ~50,000 years since the final eruption of the edifice.

Vent Locations

Vents for many of the 25 eruptive units distinguished at Mammoth Mountain are obscure or have been deeply eroded glacially. Dome 2781 (unit d81), Dome 2861 (unit d61), Skyline Dome (unit dsk), North Knob (unit dnk), Solitude Dome (unit rss), Gold Rush Express knob (unit dgr), and Lincoln Peak (unit dlp) are lava domes that emerged from subjacent conduits, and Scottys Dome likewise covers the vent for the White Bark Ridge complex (unit dwr). In common with Skyline Dome, the crestal regions of South Summit Dome (unit dsd) and Summit Dome (unit dsu) are extensively acid altered, indicating fluid flux from below, which is also consistent with subjacent conduits. The apron of rhyodacite lava flows (unit rce) that covers much of the northeast slope of the mountain apparently issued from a vent that was later covered by Solitude Dome (unit rss), which had also been the site from which the lava-flow unit rsq issued ~15,000 years after unit rce.

The glacially excavated trough (The Chasm) that separates the summit ridge of Mammoth Mountain from both Solitude Dome and the north-dipping planèze named "Face Lift" by the ski area (fig. 12) is apparently where several of the

remaining lavas originated. The upper end of the planèze and the narrow north-trending rib (of unit dsd) that closes the east end of the trough are both severely acid altered, as are parts of the colluvial fill that floors the trough. The steep northeast face of the summit ridge was the principal glacial headwall, away from which ice flowed east, north, and northwest during the late Pleistocene (MIS 2). Glacial action excavated a trough ~200 m deep and more than 1 km long, removing as much as 20 million cubic meters of lava, some large fraction of which had been altered fumarolically. From the distribution of orphan lava flows that extend north and southeast from the trough, it is inferred that the excavated region was the central hub, a multivent complex for units dbp, ddl, ddu, dml, dms, dfl, dnh, drc, and rmf. Adjacent to the inferred vent complex is the Summit Dome (unit dsu), lobes of which rest directly atop unit dfl on both walls of The Chasm (fig. 12 and geologic map).

Trachydacite units dtl and dom are exposed only distally, extending eastward from beneath the Dragons Back coulees. Less certainly linked to the excavated near-summit vent complex, they are nonetheless likely to have originated there, because both are younger than the massive South Summit Dome, which precludes outflow along alternatively plausible azimuths. Unit rrc is one of the oldest on the edifice, and, because it is exposed only locally beneath the toe of South Summit Dome, its vent is thoroughly concealed and thus unlocated.

Postglacial Phreatic Activity

Four small postglacial pits interpreted as phreatic craters were mapped by Huber and Rinehart (1965a, 1967) at elevations near 2,800 m just north of Lincoln Peak. Simplified to

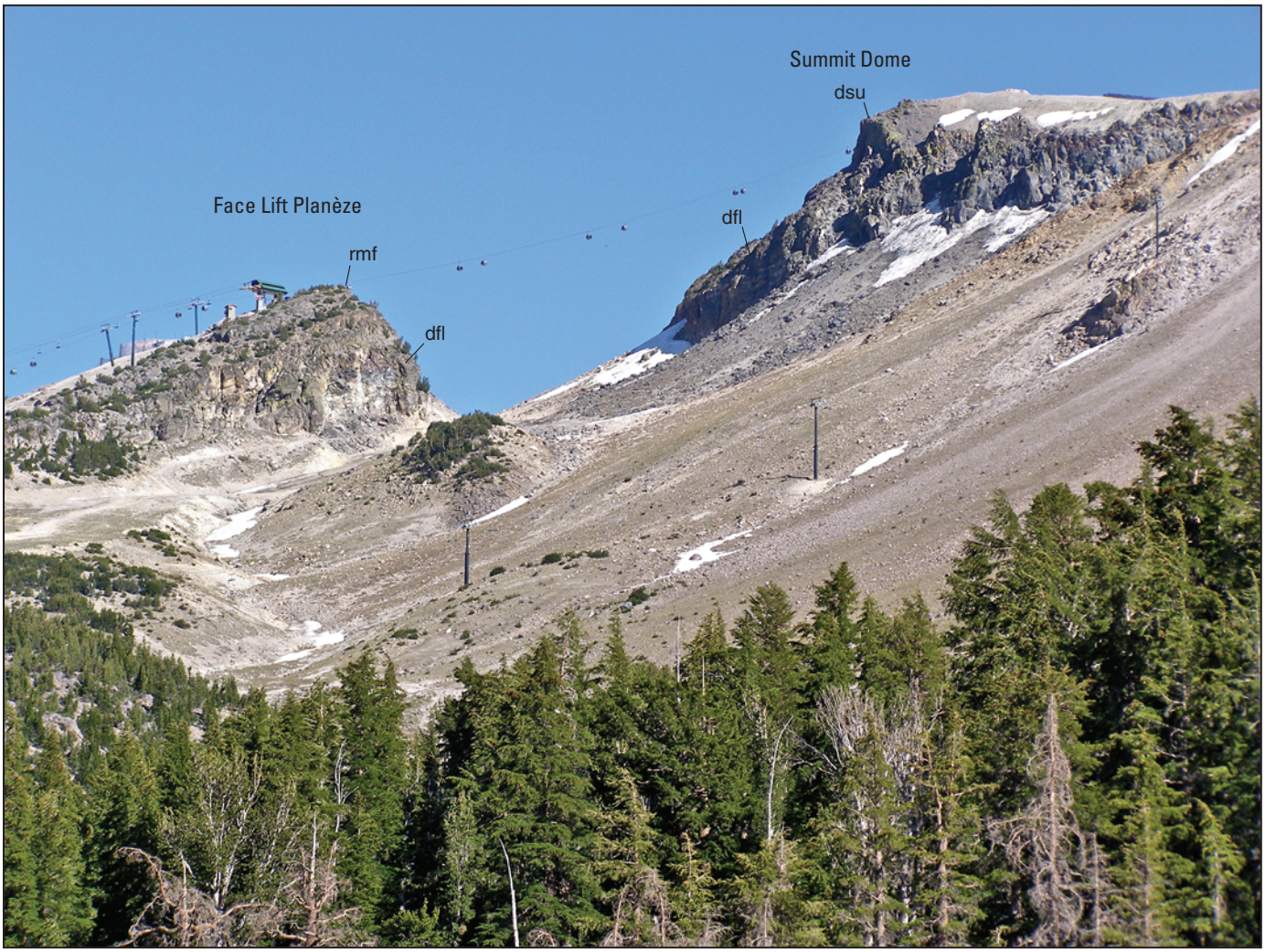

Figure 12. The Chasm, glacially eroded notch below summit headwall of Mammoth Mountain, viewed toward southeast. At upper right, thick flow of unit dfl spills northward from beneath Summit Dome (unit dsu), is erosionally cut out along glacial trough, and resumes on Face Lift planèze at left, where unit dfl is overlain by a flow of unit rmf. Original continuity of dfl flow, dipping 20° NNE., precludes invoking a fault. Summit crest at right is as much as 190 m above floor of notch. Aerial góndola spans notch and ends at visitor center, hidden behind cliff of false summit.

three pits, they were reproduced on the map of Bailey (1989), but they were never described. Although the sites have been partly bulldozed for ski runs, our repeated scrutiny of undisturbed areas around and between them has turned up no evidence for craters, ejected diamict, juvenile clasts, or thermal or fluid alteration. Undisturbed forested ground within and adjacent to the sites formerly depicted as craters are covered by combinations of thin colluvium, patchy ground moraine, bedrock and regolith of unit rce, and the 1350 C.E. Inyo pumice-fall deposit (with or without a thin aeolian sand layer beneath it). We conclude that explosion pits never existed there. Because the Mammoth Mountain Ski Area (MMSA) widely and repeatedly excavates, modifies, and replaces numerous shallow water-holding pits for erosion control and production of artificial snow, it seems likely that abandoned pits were interpreted as phreatic craters.

A contiguous pair of authentic phreatic craters beneath Chair 11 was mapped by Huber and Rinehart (1965a) and Bailey (1989), ~300 m southwest of the Main Lodge (at UTM 200/685). Although partly bulldozed for ski runs and construction of a reservoir, their phreatic (nonjuvenile) apron deposits are locally intact, 1–10 m thick, fines-rich, and thermally discolored (see unit pe). The phreatic diamict directly underlies 1350 C.E. Inyo pumice-fall deposits and directly overlies a thin organic layer containing charcoal dated at 850±60 cal yr B.P. (fig. 13). A stump buried in the phreatic deposit gave radiocarbon ages in the range 659–737 cal yr B.P. (Sorey and others, 1998).

Present-day fumarolic discharge on and near Mammoth Mountain is weak, and sites are few but widely scattered. Diffuse emission of water vapor carrying CO_2 and sulfur gases is detectable (1) along the upper gorge of Dry Creek (UTM 210/670), (2) along a small fault at the south toe of the edifice (UTM 211/652), and (3) more vigorously from cracks in bedrock of unit rmf at elevation 3,030 m on the Face Lift planèze (UTM 209/673) ~800 m north of the summit (Sorey and others, 1998). Several fumaroles along the summit ridge of Mammoth Mountain were said to have been active in the 1950s (Huber and Rinehart, 1967), and patches of early snowmelt along that ridge (over acid-altered areas of units dsd, dsu, dsk, dwr) are today observed annually and attributed by MMSA personnel to warm ground. Off the edifice, ~1 km east of Twin Lakes, the persistent odor of H_2S is detectable (without visible emission) along a zone of altered ground that extends 250 to 500 m northwest of Mammoth Rock, coinciding with a Mesozoic fault.

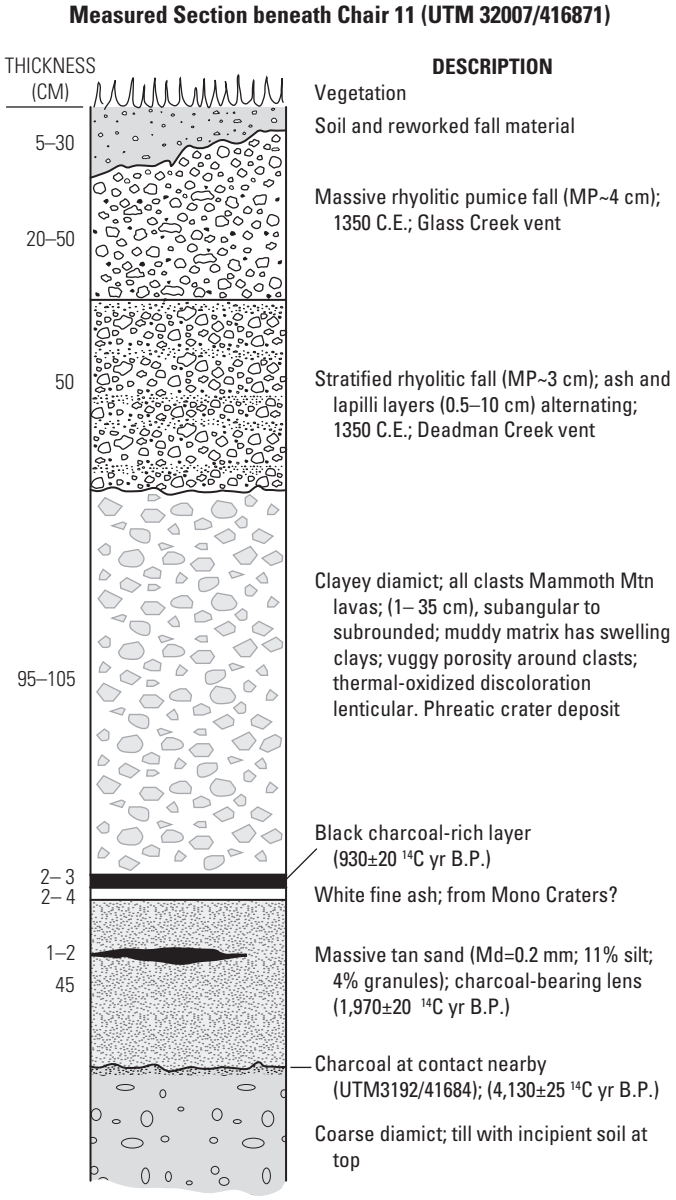

Figure 13. Measured section of surficial deposits beneath Chair 11, ~300 m west-southwest of Main Lodge of Mammoth Mountain Ski Area. Late Holocene phreatic crater deposit, here ~1 m thick and as thick as 10 m nearby, is overlain, with slight unconformity, by two southward-dispersed rhyolitic fall deposits of multipulse Inyo eruption of 1350 C.E. (see units ric and p, table 1). Three uncalibrated radiocarbon ages are indicated. When calibrated by program of Stuiver and Reimer (1993; update of 2014), the 2σ ages become 850±60, 1,910±40, and 4,690±130 yr B.P. Abbreviations: MP, maximum pumice size—average diameter of five largest clasts found in layer; Md, median diameter of sand by sieve analysis.

Diffuse CO_2 Emissions

About ten sites (fig. 5) around the base of the Mammoth Mountain edifice have, since 1990, developed cold soil-gas CO_2 concentrations great enough to kill trees (Farrar and others, 1995; Sorey and others, 1998, 2000; Cook and others, 2001; Evans and others, 2002). None of these have produced craters, visible orifices, or sulfur-bearing discharge, but some of the tree-kill areas do overlap the older Chair 11 phreatic craters and the pre-existing fumarolic area at the south toe of the edifice. Elevated CO_2 was also detected above tree line in MMSA vaults on the summit ridge and along the trough below its northeast face. Emissions are diffuse but substantial (Sorey and others, 1998; Lewicki and others, 2012).

The tree-kill areas form a half-circle that extends from Horseshoe Lake on the southeast around the south and west margins of the edifice to the vicinity of the MMSA Main Lodge at the northwest toe. No tree-kill areas are found around the eastern half of the edifice. It seems likely that the principal gas flux ascends centrally beneath the edifice, as manifest in the high-elevation fumaroles and the near-summit diffuse discharge. Some fraction of the ascending gas is evidently diverted to the south and west periphery, probably along a highly permeable layer of rubble (till and talus) that separates the edifice lavas from the northeast-sloping scallop of the Long Valley Caldera wall, against which the edifice was built (fig. 14). The partly concealed wall here is largely granitic (unit Kmo) but includes Mesozoic metavolcanic components as well. Such a semiannular buried slope of permeable scree would explain why the tree-kill areas are distributed only on sides of the edifice that bank against basement rocks. The northeast-facing caldera wall had been glaciated repeatedly between its creation at 767 ka and burial by Mammoth Mountain lavas starting ~85 ka.

As recounted in the reports cited above, tree-killing emissions began soon after an 11-month interval of persistent earthquake swarms (attributed to dike intrusion; Hill and Prejean, 2005) beneath Mammoth Mountain in 1989. Evans and others (2002) identified a substantial magmatic component in the dissolved inorganic carbon of virtually every spring and groundwater source, mostly cold and dilute, in the vicinity of the mountain. They infer that CO_2 now discharging in the tree-kill areas is gas that exceeds the dissolving capacity of the groundwater, and they hypothesize that the excess CO_2 began to be released in 1989 owing to disruption of a low-permeability seal atop an intracrustal reservoir of secularly stored basalt-derived gas.

Postglacial Diamicts

In addition to the late Holocene ejecta sheet surrounding the twin phreatic craters near Chair 11, various thin colluvial diamicts have been exposed in numerous MMSA water pits, typically 2–4 m deep and 10–30 m wide, that are widely distributed across the northern base of Mammoth Mountain between Reds Lake and Chair 4 (UTM 228/683). Most such exposures are tan or orange-brown, 0.5–3 m thick, vaguely stratified in layers 5–50 cm thick defined by slight grain-size variations, and might at first glance be taken for thin nonwelded pyroclastic-flow deposits. They overlie Mammoth Mountain lavas or discontinuous sheets of Pleistocene ground moraine, and they are generally overlain by 1350 C.E. Inyo pumice-fall deposits, either directly or with an intervening sheet of aeolian sand. Virtually all clasts are Mammoth Mountain dacite and rhyodacite, glassy or partly so, typically dense and nonvesicular, subrounded to subangular, and mostly 0.5–4 cm across but rarely and locally 10 cm or larger. Neither prismatically jointed clasts nor thermal/oxidation effects of clasts on the sandy-silty matrix were observed.

In some pits, the diamicts also contain granules and lapilli as big as 4 cm of biotite-feldspar pumice. Pumice clasts analyzed are strongly hydrated (LOI >10 weight percent), deficient in silica and alkalies, and enriched in Al_2O_3 (> 23 weight percent), suggesting long residence in wet colluvium. The pumices were probably reworked from unit rfp and soaked in groundwater for as long as 80,000 years. In 2004, two former pits (near UTM 211/688 and 226/684) on flats at the north toe of Mammoth Mountain exposed ashy diamicts, 0.5–1.5 m thick, rich in such hydrated/altered pumice lapilli; these may

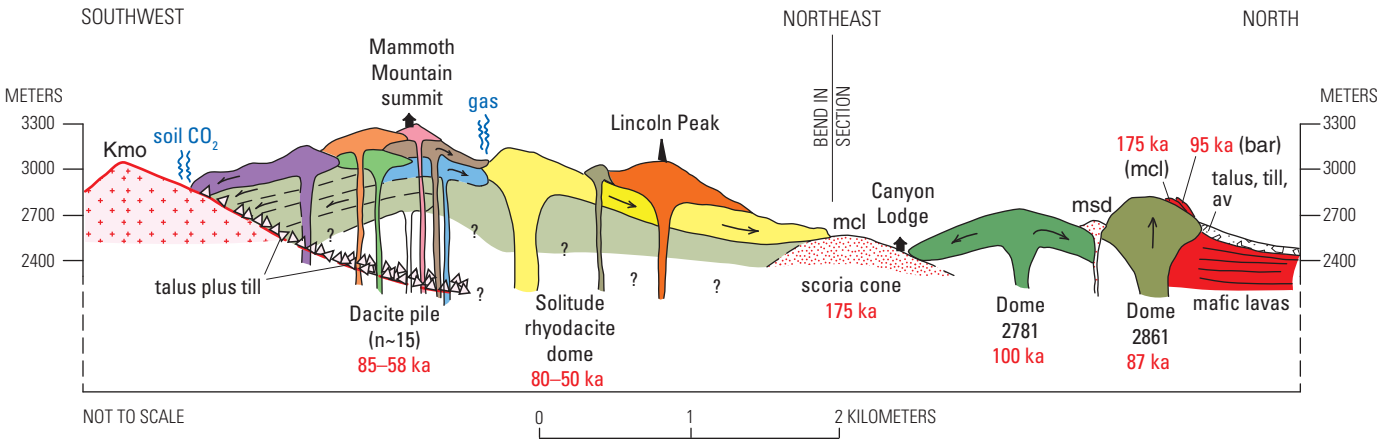

Figure 14. Schematic cross-section (cartoon) across summit of Mammoth Mountain, simplifying surface units and hypothesizing a permeable layer of buried rubble that drapes the granitic caldera wall against which the edifice was constructed. Some fraction of the CO_2 ascending from a deep basalt-fed reservoir toward near-summit fumaroles is diverted laterally toward the half-ring of tree-kill areas, which are limited to the side of the edifice in contact with basement rocks (fig. 5). Section bends northward at Canyon Lodge scoria cone to transect the two off-edifice domes of Mammoth Mountain lithology. No vertical exaggeration.

have been remnants of nonwelded pyroclastic-flow deposits related to units rce or rfp (~80 ka) or colluvially remobilized equivalents.

The diamicts as a whole we interpret as thin postglacial colluvium that, by creep, slumping, or sheetwash, has filled minor depressions on low-relief surfaces. As well as near the break-in-slope at the toe of the edifice, similar diamict is exposed in water pits on a 2,930-m plateau, ~300 m southeast of McCoy Station, where sparse clasts of dense, variably rounded, dacite and rhyodacite are as big as 9 cm but mostly 0.5–4 cm across. Here, as at the lower sites, an orange-brown layer of massive or lenticular crystal-vitric sand, 30–110 cm thick, lies between the diamict and the capping 1350 C.E. Inyo pumice falls. From site to site, its median grainsize (Md) ranges from 0.3 to 0.7 mm—fine to medium sand. It contains granules and sparse pebbles as big as 4 cm of dacite, granite, and biotite-feldspar pumice. We interpret the sand to have resulted from aeolian reworking of postglacial diamicts.

Volcanic Evidence for Glacial History

Glacial ice accumulated upon and blanketed Mammoth Mountain following its construction in the late Pleistocene. Although the volcanic edifice existed only for the last major glaciation (during Marine Isotope Stage [MIS] 2), glaciers had earlier advanced at least twice (and probably several times) into lowland parts of the map area from cirques on the Sierran rangecrest. Although the classic sequence of four glaciations defined for the eastern Sierra Nevada by Blackwelder (1931) has been scrutinized and provisionally amended many times, it remains remarkably robust in the Mammoth Lakes area. The McGee Till, which lies high on the south rim of the caldera just outside the map area, rests on basalt that gave a K-Ar age of 2.6±0.1 Ma, implying glaciation early in the Pleistocene (Putnam, 1962; Dalrymple, 1963). The Sherwin Till (probably MIS 22), which directly underlies the 767-ka Bishop Tuff, crops out in the northwest wall of the caldera (unit gst), more extensively just southeast of the caldera (Sharp, 1968), and may be buried by younger moraines at Convict Creek (Sharp, 1969). It was probably also deposited in the Mammoth embayment, where it was later engulfed by caldera collapse and buried during postcaldera volcanism. The Tahoe Till, inferred by Blackwelder to be of early Wisconsin age, has recently been shown to be complex (Phillips and others, 1996, 2009; Gillespie and Zehfuss, 2004) but largely to represent MIS 6. The only correlative glacial deposit in the map area is the Casa Diablo Till (unit gcd; Curry, 1968, 1971), which is here bracketed by dated lava flows to the interval 160–125 ka (MIS 6). The Tioga Till, youngest of Blackwelder's sequence, dominates glacial deposits in the Mammoth Lakes area, principally as a piedmont lobe of ~40 nested morainal ridges. Because they all include clasts of basaltic unit bhl (31±1 ka), the entire Tioga assemblage had to be deposited during MIS 2, irrespective of how many ice-front fluctuations and stillstands are represented. In the eastern Sierra, north and south of the Mammoth embayment, Phillips and others (1996, 2009) have dated by surface exposure methods moraines representing four Tioga advances between 28 ka and 14.5 ka, terminating in rapid retreat at 15–14.5 ka.

The Pliocene "Deadman Pass till" of Curry (1971) was shown to be a nonglacial diamict by Bailey and others (1990). Deposits of any glacial advances between MIS 22 and MIS 6 were obliterated here by the later advances that deposited the Casa Diablo and Tioga Tills. No deposits assignable to MIS 4, to a minor Recess Peak readvance (14.2–13.1 ka; Clark and Gillespie, 1997), to a Younger Dryas readvance (12.9–11.5 ka; Gillespie and Clark, 2011), or to Little Ice Age (~1350–1850 C.E.) cirque glaciers have been identified in the map area. Rock glaciers (see unit rg) here are thought to be of Holocene age, although parts of the heavily debris-laden moraines of Sherwin Creek (see unit gud) may have moved like rock glaciers in the late Pleistocene.

Erratic boulders of Sierran origin have been found overlying unglaciated Early rhyolite (unit rer) at many sites along the southwest side of the caldera's resurgent uplift. On ridge 2362, ~3 km east of downtown Mammoth Lakes (UTM 299/681), boulders of porphyritic granite (unit Kmo), granodiorite (unit Krv), leucogranite, and metavolcanics (unit Mzmv) are scattered in abundance at elevations as high as 2,345 m. As the site is slightly above but adjacent to the highest distal deposits of Casa Diablo Till (unit gcd), the boulders may have tumbled from the glacier front at its maximal advance. Accompanying boulders of phenocryst-poor mafic lavas (almost certainly younger than 200 ka) support emplacement of the erratics during MIS 6.

Erratics found at several other sites are well outboard of exposed moraines, however, and erratics of Quaternary lavas are absent. The highest site is on the east side of Peak 2506 (BM 8224 ft on older maps), ~3 km northeast of downtown Mammoth Lakes (UTM 293/696); boulders of the same four Mesozoic rock types just mentioned form an isolated cluster ~20 m across at an elevation of 2,495 m. If these were transported by an iceberg, as seems likely, it was prior to resurgent uplift of the Early rhyolite lava upon which they rest, because the closest lakeshore gravels are 270 m lower, at an elevation of 2,225 m near the geothermal plant, 3 km southeast.

Abundant erratics are also scattered along the ridge east of Sawmill Cutoff (road), 1.5–2 km northwest of Peak 2506, at elevations of 2,430–2,465 m, as far north as UTM 283/713. Boulders of granite, leucogranite, and metavolcanics are common, but the granodiorite (from unit Krv) is absent at these northerly sites. Another area of scattered erratics is within a 700-m-long strip at 2,300–2,365 m elevation along the ridge ~1 km east-northeast of the geothermal plant (UTM 318–323/681–688), where clusters of boulders of leucogranite, granodiorite, and metavolcanics are common. They are accompanied there by blocks of welded Bishop Tuff, many 20–60 cm across, which were certainly not transported by ice. As the Bishop Tuff is not preserved around the Mammoth

embayment, and intracaldera Bishop Tuff is buried by >400 m of caldera fill (fig. 6), the welded blocks were probably excavated from below during explosive phases of Early rhyolite (unit rer) activity (760–650 ka). Explosive ejection of the granitoid and metavolcanic boulders from buried till is less likely than a glacial origin, owing to the great size of many (1–2.5 m), to their small patchy occurrences, and to concentration of sites on the southwest side of the resurgent uplift, which faces Sierran sources of the Pleistocene glaciers. Our preferred interpretation is that the basement boulders were transported by icebergs from calving glaciers across an arm of Long Valley Lake and beached against the Early rhyolite prior to full structural uplift of the resurgent dome.

Inyo Chain

The 10-km-long Holocene Inyo chain (Bailey, 1989; Hildreth, 2004) consists of seven rhyolitic lava flows and domes, several phreatic craters, and a composite apron of pyroclastic fall and flow deposits (Miller, 1985; Sampson and Cameron, 1987; Nawotniak and Bursik, 2010). The oldest unit is North Deadman dome (unit rnd; ~0.04 km^3), undated but probably middle Holocene, followed by Wilson Butte (~0.05 km^3), which erupted just north of the map area about 1.3 ka. Both domes are aphyric glassy rhyolite. Wilson Butte (76.6 percent SiO_2) is similar compositionally and petrographically to the Mono Craters domes (Kelleher and Cameron, 1990) and should be called a Mono dome were it not for its position on the north-south trend of the Inyo chain rather than the arcuate trend of the Mono chain (fig. 2 of Hildreth, 2004). North Deadman dome (74.7 percent SiO_2) is compositionally intermediate between Wilson Butte and the crystal-poor lower-silica rhyolite (Sampson and Cameron, 1987) that dominated the youngest Inyo eruptive episode in 1350 C.E. Two phenocryst-poor minidomes (each <0.001 km^3) just north and south of the large Glass Creek flow erupted after Wilson Butte but prior to the 1350 C.E. Inyo eruption, the most evolved products of which they compositionally resemble (Sampson and Cameron, 1987). These are units rcd (73.2 percent SiO_2) and rcw (72.2 percent SiO_2), which both carry 1–2 percent feldspar phenocrysts and trace amounts of biotite, pyroxene, hornblende, and Fe-Ti oxides.

Injection of the Inyo dike (Eichelberger and others, 1985) in late summer of 1350 C.E. (Millar and others, 2006) led to sequential eruption of the Deadman Creek, Obsidian, and Glass Creek flows (all unit ric), each preceded by substantial pyroclastic outbursts (Miller, 1985), the last of which was followed by phreatic eruptions (unit pe) at nearby Inyo Craters (Mastin, 1991). Total magma volume erupted during the multipulse episode was estimated by Miller (1985) to be 0.4 km^3 as lava, 0.17 km^3 as fallout, and >0.05 km^3 as pyroclastic density currents.

Compositionally, the mid-14th century Inyo eruption was unusually complex (Sampson and Cameron, 1987; Vogel and others, 1989). In addition to the crystal-poor (2–3 percent crystals; "finely porphyritic") zoned rhyolite (70–74 percent SiO_2) that dominated the eruptive products, a very crystal-rich rhyodacite (71.3±1 percent SiO_2; 25–40 percent crystals; "coarsely porphyritic") piled up over the vents of the Deadman Creek and Glass Creek flows late in their extrusive episodes and mingled (to a limited extent) locally with the coerupted crystal-poor magma. Evidently having been stored separately, the crystal-rich magma was ~100 ºC cooler and chemically unrelated to the crystal-poor one, which has much higher K, Rb, Zr, Y, and REE (and lower Ti, Mg, Ca, and Sr) at equivalent SiO_2 contents. In addition to the silicic magmas, andesitic enclaves (~60 percent SiO_2) are present in the crystal-rich central parts of both flows (Varga and others, 1990).

The main crystal-poor magma was itself zoned (70–74 percent SiO_2), yielding smoothly linear compositional arrays (for example, 1.3–2.6 FeO and 265–1420 ppm Ba), which are continuous but show an apparent tendency toward volumetric bimodalism (Sampson and Cameron, 1987; Vogel and others, 1989). To explain the arrays, Sampson and Cameron (1987) suggested back-mixing between two slightly zoned silicic magmas that had earlier fractionated at higher pressure, while Vogel and others (1989) called for mixing between dacitic and rhyolitic end-members. Bailey and others (1976) had suggested that the crystal-poor phase might be Mono Craters magma (which may thus be partly right) and that the crystal-rich phase is Long Valley magma (which appears to be wholly right). The compositional and petrographic similarity of the crystal-rich Inyo phase and the nearby Long Valley rhyolite of Deer Mountain (unit rdm) was pointed out by Sampson and Cameron (1987). Moreover, Reid and others (1997) identified, in both the 1350 C.E. crystal-rich Inyo phase and 100-ka Deer Mountain lava, zircon populations with crystallization ages that cluster around 230 ka. Residual or thermally rejuvenated Long Valley magmatic mush is apparently implicated.

During the 1350 C.E. sequence, four closely spaced subplinian pumice eruptions issued from the three vents now covered by the lava flows (Miller, 1985), mantling the western part of the map area with substantial pumice-fall and derivative reworked deposits (unit p). Isopachs were drawn by Miller (1985), and grain size and componentry were given by Nawotniak and Bursik (2010). Along Glass Creek gorge between the Obsidian and Glass Creek flows, the cumulative sheet of coarse ejecta is >50 m thick, and it may also be as thick adjacent to the Deadman Creek flow where it is little incised. Many rhyolitic ejecta of varied textures are larger than 1 m proximally, and abundant rounded boulders of granite and basalt entrained from glacial deposits (buried during the eruption) are as big as 1–2.5 m. Poorly sorted tack-welded agglutinate is several meters thick in proximal fall deposits along Glass Creek. The fall deposits thin to 10–15 m by 1–2 km away from the vents, and the combined thickness of the pair of fall units that dispersed southward (fig. 13) is still ~1 m at Mammoth Mountain and Devils Postpile, 7–10 km south of the Deadman Creek flow. No paleosols or erosion surfaces separate the four fall units, and no fallout mantles the lava flows.

Faults

Several small faults have displaced young volcanic rocks within the map area. All appear to be normal faults with scarps generally 1–10 m high, and most are north-striking, consistent with ongoing Basin-and-Range extension and with continuation of the Hartley Springs rangefront fault, buried beneath the west moat. Exposure is poor owing to the mantle of pumiceous fallout from the Inyo eruptions of 1350 C.E., but it is clear that most of the faults displace late Pleistocene glacial deposits and numerous lava flows dated between 180 and 60 ka.

The *Upper Dry Creek Fault*, located ~1 km west of Dome 2861, extends for ~2 km, striking north in its southern third before bending toward N. 10º E. Displacement, which is normal and east-side-down, ranges from 5–10 m in unit ddc (103±9 ka) to 1–6 m where its northern splays cut units bmn (87±7 ka) and bar (88±5 ka). In several places along its strike, there are open clefts 1–5 m wide.

The *Inyo Craters Fault System* is a family of subparallel extensional faults and fissures, encompassing the Inyo Craters alignment. The principal fault, the westernmost, produced an east-side-down scarp, 5–14 m high where it cuts unit aic (131±1 ka) and as high as 19 m where mantled by the sheet of Inyo phreatic ejecta (unit pe) ~100 m northwest of South Inyo Crater. This fault strikes north-south for ~1 km southward from the west rim of that crater, then bends to a strike of S. 20º W. for another 1.5 km; along the latter reach it drops unit bar (88±5 ka) 3–10 m down to the east. Just north of South Inyo Crater, it bends northwestward and splays into a set of minor faults and fissures mapped at larger scale by Mastin (1991). Another north-striking fault drops the southeast rim of South Inyo Crater 13 m down to the east, and within 150 m east of this fault a parallel set of lesser faults outlines a pair of shallow graben. Additional extensional faults extend northward across the summit of Deer Mountain where another phreatic crater erupted during the Inyo episode of 1350 C.E. Some small fraction of the east-west extension here was probably promoted by southward propagation of the rhyolitic dike that drove the magmatic and phreatic eruptions of that year (Mastin and Pollard, 1988).

The *Dry Creek moraine faults* cut the blanket of late Pleistocene till (unit gdc), 2–5 km north of Dome 2861. The principal fault extends ~4 km northward from the Dry Creek Dome, striking N. 5º–15º W., displacing the till (MIS 2) as well as windows of units mnd and mor (66±2 ka) along a west-facing scarp typically 5–6 m high. At its south end, the fault cuts the Dry Creek Dome (unit rdc, 112±6 ka), atop which a graben-like trough may reflect vertical displacement as great as 10 m. About 1.5 km east of this fault, a set of three small north-striking normal faults likewise displaced the till and underlying unit mor (66±2 ka). Two of them produced west-facing scarps only a few meters high, whereas the easternmost of the three drops unit mor ~10 m, east-side-down. Although the set can be traced for ~1 km, and two of them cross Dry Creek, none propagated farther southward into the West Moat Coulee (unit rwm, ~150 ka).

The so-called *Earthquake Fault* is an open fissure that crosses Highway 203 just west of downtown Mammoth Lakes. Cutting dacite lava of unit d81 (99±7 ka), the fissure has long been highlighted as a tourist attraction and provided with its own carpark. A southern segment strikes N. 15º E. for ~900 m, then bends into a northern segment that strikes 5º W. for 600 m before ending in a set of three small splays just south of the base of Dome 2861. Its south end descends the flow front of unit d81 and disappears into landscaped rubble (till of unit gmm and scoria of unit mcl) at the site of Canyon Lodge. Width and depth vary along strike, but major parts of the open fissure are as deep as 15 m and as wide as 2 m. Vertical displacement is small or absent, and in any case hard to measure precisely. Benioff and Gutenberg (1939) estimated that relative elevation of the east rim could locally be ~0.5 m. On the south rim of Dome 2861, to the north of the fault termination, about ten vertical joints are eroded into gullies, but there is no ground breakage atop the dome, and we see no sign of a fracture continuous with the Earthquake Fault. Unlike Bailey (1989), we agree with Rinehart and Ross (1964) that the Earthquake Fault terminates just south of the dome.

The inferred *Sawmill Cutoff Fault* may extend 2 km northward from Shady Rest campground, striking N. 10º E. We think a poorly exposed fault may be required here to account for the eastern escarpments of units mkv (153±1 ka) and msc (155±28 ka), each more than 100 m high. The steep eastern scarps of these mafic phenocryst-poor lavas are unglaciated, were never subjected to stream erosion, and were unconstrained to the east when erupted. Apparent displacement may exceed 50 m, east-side-down, but probably diminishes toward the north end where part of unit msc banks against early postcaldera rhyolite (unit rer).

The *South Mammoth Mountain Fault* strikes northwest across the lower south slope of the edifice, displacing colluvium vertically by as much as 3 m, mountain-side-down. It can be mapped clearly for 1.7 km, and it might project an additional 1 km southeast to Horseshoe Lake (Hill and Prejean, 2005), but no surface displacement is discerned across the pumice-mantled slope of unit amp. The fault strikes principally across dacite lava of unit dsd (87±6 ka), although only thick colluvium that conceals the lava along the fault is demonstrably displaced. The southeastern end of the fault (as here mapped) is marked by weak fumarolic alteration and a small tree-kill area that reflects diffuse CO_2 discharge. The larger area of CO_2-induced tree kill at Horseshoe Lake (Farrar and others, 1995) is consistent with the possibility that the fault (or equivalent fracture) continues that far. The unusual strike and sense of displacement may reflect loading by the Mammoth Mountain edifice where it buries the caldera's topographic wall, which is, here, probably a steeply sloping contact between granitic bedrock and a pre-Mammoth Mountain apron of surficial debris (fig. 13).

The *McLeod Lake Fault* is similarly modest, striking north-south past the east side of that lake for ~1.5 km. Apparent vertical displacement of the granite basement, west-side-down, is only a few meters near and north of the

lake but may be ~10 m some 500 m south of the lake. Units aml and amp (97±1 ka) appear to be offset by little more than a meter. South of McLeod Lake, from Mammoth Crest to Fish Creek, we have been unable to verify the existence of several other north-striking faults portrayed by Bailey (1989) as cutting the granite (unit Kmo).

The *Chalets Fault*, ~250 m west of Mammoth Mountain Inn, strikes north or slightly east of north and vertically displaces pumice and till 4–9 m, east-side-down. It can be followed for ~700 m, but we were unable to verify its continuation south of Highway 203 as portrayed by Bailey (1989).

The *Mammoth Rock Fault*, a near-vertical fault, separates Paleozoic metasedimentary strata at Mammoth Rock from adjacent Mesozoic metavolcanic rocks. According to Rinehart and Ross (1964), the stratigraphic separation and thus the inferred displacement is 1.4 to 1.8 km, southwest side down. Although they inferred (and we concur) that all or most slip was pre-Cenozoic, the northwest end of the fault zone today controls weak fumarolic (H_2S-bearing) discharge and attendant alteration (Bailey, 1989).

The Chasm, a northwest-trending trough ~1.5 km long (fig. 12) that separates the steep northeast face of Mammoth Mountain's trachydacite summit ridge from the Face Lift planèze and Solitude Dome, was previously mapped as a fault (Bailey, 1989), inappropriately in our analysis. The elongate cleft was glacially excavated, facilitated by altered rocks at dome margins and by cornice-fed excess snow from the ridgecrest. The rhyodacites (units rmf, rce, rsq, and rss) are not present on the summit side of The Chasm, and the relative elevations of the four trachydacite units (dsd, ddu, dfl, and dsu) that do cross The Chasm (and are 20 m to 110 m lower on the northeast side) are consistent with simple downslope flow of the lavas, without fault displacement. Ice flowed away broadly to the north and northeast but preferentially to the northwest and east along the trough excavated between lava domes. With its floor today as high as 3,170 m, The Chasm was the main glacier headwall on Mammoth Mountain during the late Pleistocene, and it still retains snow slopes later each summer than anywhere else on the mountain.

Major Faults

The *Long Valley Caldera ring-fault zone* lies well inboard of the caldera's topographic walls (Hildreth, 2004; Bailey, 1989, cross-sections; Carle, 1988; Hill and others, 1985). Although it is everywhere deeply buried by postcaldera volcanic and sedimentary fill, the zone probably influenced eruption locations for Lookout Mountain (subunit rlm, ~690 ka), the Hot Creek flow (unit rhc, ~330 ka), and west-moat rhyolitic units rwm, rdc, and rmk (~150-100 ka). The zone is likely to be a family of nested faults and sheared breccia. Intense seismicity since 1980 along the caldera's south moat has been resolved into a 1-km-wide multifault shear zone outboard and several steeply inward-dipping fault planes just inboard of it (Prejean and others, 2002). Most seismicity is at depths of 3–9 km, and much of it is dextral, apparently reflecting reactivation of the ring-fault system by regional tectonic stresses (Riley and others, 2012) rather than by either magma intrusion or renewed normal-fault subsidence.

The ring-fault zone may not be as smoothly elliptical as commonly portrayed, particularly beneath the west moat, where subsidence may have utilized precaldera faults related to the left-stepping rangefront system. Offsets along that inherited en echelon fault system may have conveyed a jigsaw pattern to the western structural margin, which could, in turn, have influenced (1) the outboard dike that fed 100-ka rhyolite to the Deer Mountain vent; (2) the path of crystal-rich Long Valley subalkaline rhyolite that reached the northwest moat where it mixed with the 42–27-ka hybrid dacites (unit dnw) and the 1350 C.E. Inyo rhyolite (unit ric); and (3) ascent of deep thermal water that thence flows eastward in shallow aquifers to the active geothermal areas in south-central parts of the caldera.

Rangefront faults north and south of the caldera were not remapped as part of this investigation, but the Hartley Springs and Hilton Creek Faults (figs. 3, 4) are certainly important in having influenced intracaldera structural development in postcaldera time. Each is an important member of a family of rangefront faults, respectively north and south of the caldera, that represent Quaternary encroachment of Basin-and-Range extension (and locally transtension) into the Sierra Nevada microplate.

The *Hartley Springs Fault Zone* is a multistrand array ~10 km long that includes a steep east-facing scarp where it disappears into the northwest corner of the caldera. The family of anastomosing strands is ~2 km wide, trends ~N. 15–20° W., and includes a few large antithetic (west-side-down) faults that block out prominent granitic horsts (Bailey, 1989; Bursik and Sieh, 1989). Total relief across the fault zone is ~450 m, down to the east. The *Silver Lake Fault Zone*, ~6 km farther west, brings total basement relief across the rangefront fault system to ~750 m. The easternmost strand, which bounds a steep granitic scarp (unit Kjl) near Hartley Springs, locally drops the Bishop Tuff by 100–120 m, yielding an average vertical slip rate of ~0.15 m/kyr since 767 ka. Bursik and Sieh (1989) estimated ~30 m combined vertical offset for two strands (their F_1 and F_2) that cut a Tahoe moraine just northeast of June Lake; if the moraine represents MIS 6, the slip rate would be 0.23 m/kyr since 130 ka, or if MIS 4 (less likely), then ~0.4 m/kyr since ~70 ka. The Reversed Peak strand, 2 km northwest of June Lake, could also be considered part of the family; for that fault, Bursik and Sieh (1989) estimated 21 m vertical offset of a Tahoe moraine, which would give a slip rate of 0.16 m/kyr since 130 ka. Aggregate down-to-east displacement across the zone since the middle Pleistocene thus appears to be little more than 0.5 m/kyr (0.5 mm/yr). Bursik and others (2003) suggested that slip on the Hartley Springs Fault and southward propagation of the Inyo Dike (Eichelberger and others, 1984, 1985) may have exerted mutual influence in 1350 C.E.

The Hartley Springs Fault has no equivalent on the south wall of the caldera. Its buried extension beneath the west

moat may have influenced the several small young faults described there, but such structures terminate at the foot of the caldera wall buried by Mammoth Mountain. Faults portrayed by Bailey (1989) southward across granitic basement from Mammoth Crest to Fish Creek cannot be verified and, in our judgment, do not exist. The precaldera rangefront fault system had stepped left within the area of the subsequent caldera and did not continue south through the later site of Mammoth Mountain.

The *Hilton Creek Fault* extends S. 20° E. for ~18 km south of the caldera margin and is marked by a great east-facing bedrock scarp roughly 1,000 m high. Its displacement of Tioga (MIS 2) moraines by 15–26 m at McGee Creek (Berry, 1997) yields a vertical slip rate of at least 1 mm/yr for postglacial time. Along its northerly 6-km-long reach from McGee Creek to Convict Creek, its postglacial offset decreases, and its trace degrades into small scarplets of varied orientation in surficial deposits (Rinehart and Ross, 1964; Clark and Gillespie, 1981). Although minor ground cracking of colluvium by *M*6 earthquakes in May 1980 was mapped along its projection, both south and north of Convict Creek (Taylor and Bryant, 1980; Clark and others, 1982), we are unable to verify measurable fault displacements on various notional lineaments crossing the 330-ka Hot Creek Flow that were interpreted by Bailey (1989) as intracaldera splays of the Hilton Creek Fault. Both the Hartley Springs and Hilton Creek Faults certainly extended into basement rocks now buried beneath the caldera fill, but there is little evidence that their intracaldera segments, cut off by the caldera ring fault, have produced postcaldera surface displacements. Just outside the caldera, however, postcaldera slip on the Hilton Creek fault remained vigorous, helping to form the lowland basin now occupied by Lake Crowley and to downwarping the highstand strandline of Pleistocene Long Valley Lake south-southwestward toward the toe of the fault scarp.

On the north wall of the caldera, if the several lesser (non-range-bounding) faults mapped by Bailey (1989) in the Bald Mountain-McLaughlin Creek area were precaldera splays or extensions of the Hilton Creek Fault, then displacement had diminished greatly northward across the terrain that later became the caldera. Among the faults north of Bald Mountain, the largest scarp (up to 60 m high) is west-facing, and those (like the Hilton Creek Fault) that face east form scarps only 10–25 m high. Already in precaldera time, therefore, the two great rangefront en echelon faults died out or attenuated over the later site of the caldera, and between their dying ends was a 15-km left stepover, which, in postcaldera time, became the focus for eruption of the intracaldera Early rhyolite and for resurgent uplift. As Bailey (1989) reasoned, the stepover was probably the site of a northwest-sloping topographic ramp or warp in precaldera time.

Faults on the resurgent uplift. Both the Hilton Creek and Hartley Springs Faults strike N. 20º W. where they approach the caldera, and strikes of faults that cut the resurgent uplift range between N. and N. 35º W., averaging about N. 20º W. The main extensional belt defined by these faults crosses the western half of the resurgent uplift and is neither medial nor apical; it is ~9 km long, strikes N. 20º W., and is centered within the left stepover that separates the dead ends of the great rangefront faults.

The eastern half of the resurgent uplift is far less faulted, but it has a few north-striking faults of modest displacement. Three such faults, all west-facing, are mapped near Little Hot Creek and Little Antelope Valley, where they influenced distribution of widespread hydrothermal alteration during the middle Pleistocene (Cleveland, 1962; Bailey, 1989; Sorey and others, 1991).

The resurgent uplift has none of the radial faults expected for a structural dome. The main belt of normal faults striking N. 20º W. across the uplift likely reflects structural inheritance controlled by the precaldera stepover rather than faulting in response to doming. Across the principal graben (Smokey Bear Flat) within the belt, displacement of 700-ka rhyolites yields an average vertical slip rate of ~0.25 mm/yr, and graben subsidence between outcrops of rhyolite unit rwm yields essentially the same rate for the last 150,000 years.

Where Dry Creek crosses Highway 395, the graben displaces mafic lavas of unit mcl (~175 ka) as well as rhyolite lava of unit rwm (~150 ka). Near the Casa Diablo geothermal plant, faults of the graben system cut mafic lavas of units mcl and unit bcd (125±2 ka). The intracaldera extensional faulting thus persisted here for at least half a million years after the final eruptions of Early rhyolite (unit rer, ~750–650 ka), which constitute nearly all exposures on the resurgent uplift.

Composition of Eruptive Products

Major- and trace-element data for all eruptive units mapped are given in appendix 1 and plotted in figures 15–20. Chemical data for several postcaldera Long Valley rhyolites were also published by Heumann and Davies (1997), Heumann (1999), and Heumann and others (2002), along with Nd, Sr, Pb and U-Th isotope data for many of them. For numerous mafic lavas, as mapped by Bailey (1989), chemical data and Nd, Sr, and Pb isotope data were published by Cousens (1996).

A conventional alkali-silica diagram (fig. 15) illustrates the contrast between the alkaline Mammoth Mountain rocks (100–50 ka) and the postcaldera subalkaline rhyolites (750–100 ka) that erupted from the residual Long Valley system a few kilometers to the east. Relative to postcaldera Long Valley rhyolites, eruptive products of Mammoth Mountain are less silicic but more alkalic; this generalization likewise applies to all precaldera and caldera-forming Long Valley rhyolites (fig. 4 of Hildreth, 2004). Figure 15*B* shows that, except for a few basalts, nearly all of the many peripheral eruptive units (230–8 ka) of the Mammoth system are likewise alkaline by the criteria of LeBas and others (1986). The most strikingly subalkaline exception is the Holocene basalt of Red Cones, youngest eruptive unit in the whole Mammoth system.

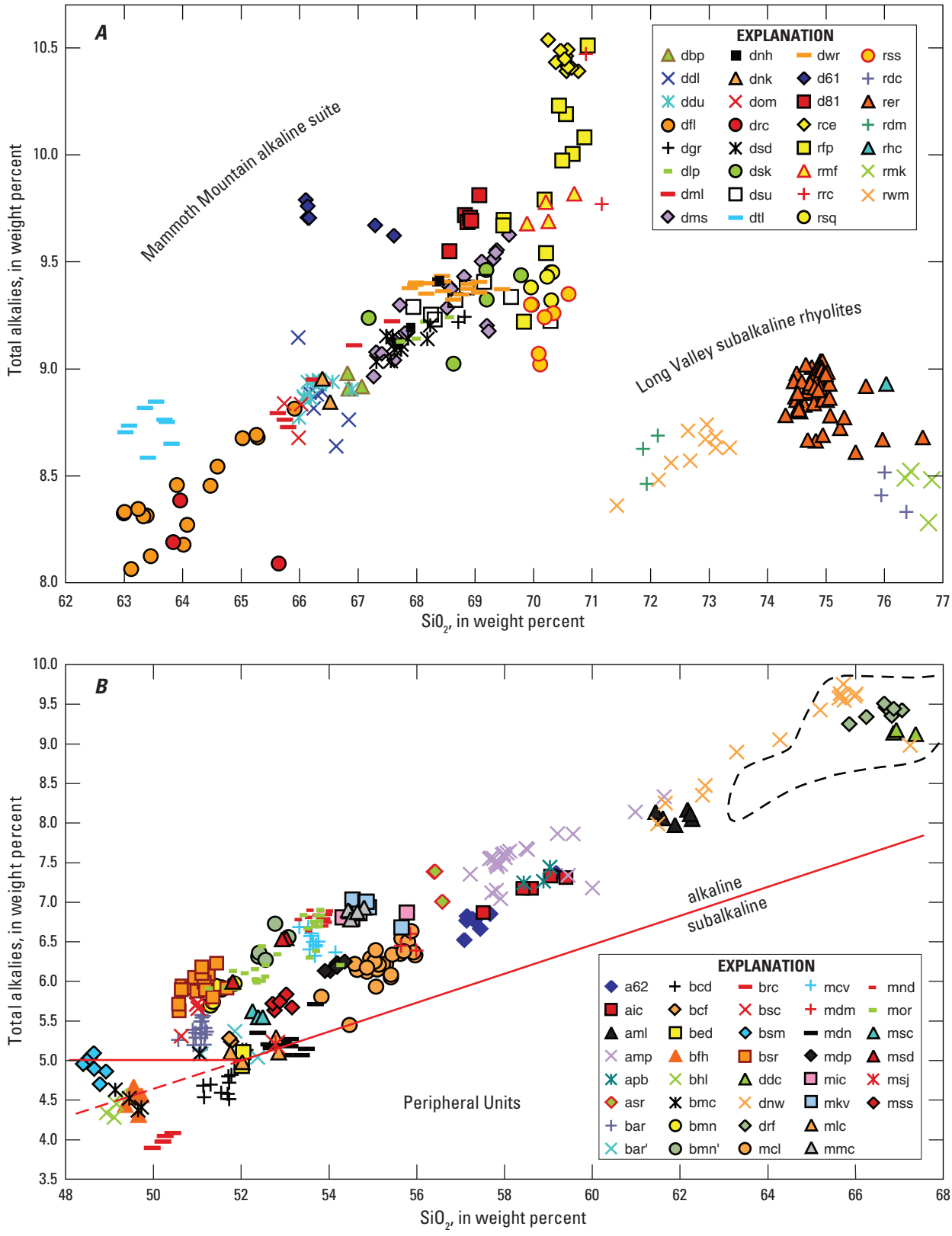

Figure 15. Total alkalies ($Na_2O + K_2O$) versus SiO_2 contents in weight percent for (*A*) Mammoth Mountain dome complex and (*B*) peripheral units of wider Mammoth magmatic system. Unit labels as in table 1, appendix, and Description of Map Units. Also plotted in panel *A* are data for six units of subalkaline Long Valley system, four of which erupted 150–100 ka, contemporaneous with Mammoth system. Alkaline/subalkaline boundary in panel *B* follows LeBas and others (1986). Dashed enclosure in panel *B* is field of Mammoth Mountain trachydacites (63–68 percent SiO_2) from panel A.

Figure 16 provides a compositional overview of the eruptive sequence documented, focal and peripheral, showing apparently unsystematic variation in SiO_2 content with eruption age since ~230 ka. It can be noted, however, that the five silicic andesite units (a62, aic, aml, amp, apb), all phenocryst-poor and widely scattered, erupted during the interval 140–90 ka, which overlaps both the final episode of Long Valley rhyolitic extrusions and initiation of Mammoth Mountain. The bulk of the silicic edifice was constructed in about 20 eruptive pulses between 90 ka and 60 ka. In contrast, eruption of mafic magmas (48–55 percent SiO_2) was fairly continuous over the interval 230–8 ka, with the possible exception of an eruptive lull at 60–30 ka, which coincided with termination of the silicic eruptive activity that had built the Mammoth Mountain edifice.

Figures 17–20 illustrate, for a large number of samples from all units of Mammoth Mountain and its periphery, the extent of compositional variation within each eruptive unit and the chemical grounds for correlating mutually isolated exposures of many such units. Figure 20 further compares compositions of the Mammoth system (largely late Pleistocene) with those of the many Neogene lavas preserved nearby.

Mammoth Mountain

The 25 eruptive units distinguished for Mammoth Mountain range continuously from 63 to 71 percent SiO_2 and from 3.6 to 5.1 percent K_2O (fig. 17*A*). Contents of MgO (0.2–1.7 percent), FeO* (1.4–4.7 percent), TiO_2 (0.30–1.04), and CaO (0.6–3.7 percent) all decrease fairly linearly with SiO_2 (figs. 17*B*, *C*). Broader, more scattered arrays are exhibited by Na_2O (4.5–5.7 percent), owing in part to hydration of generally glass-rich samples, and by Al_2O_3 (15–17 percent) and Ba (1,250–1,900 ppm), P_2O_5 (0.03–0.40 percent), and Zr (270–480 ppm), presumably owing, respectively, to heterogeneous distribution of feldspars, apatite, and zircon. Among the phenocryst-poorer rhyodacites alone, Ba ranges from 1,250 to

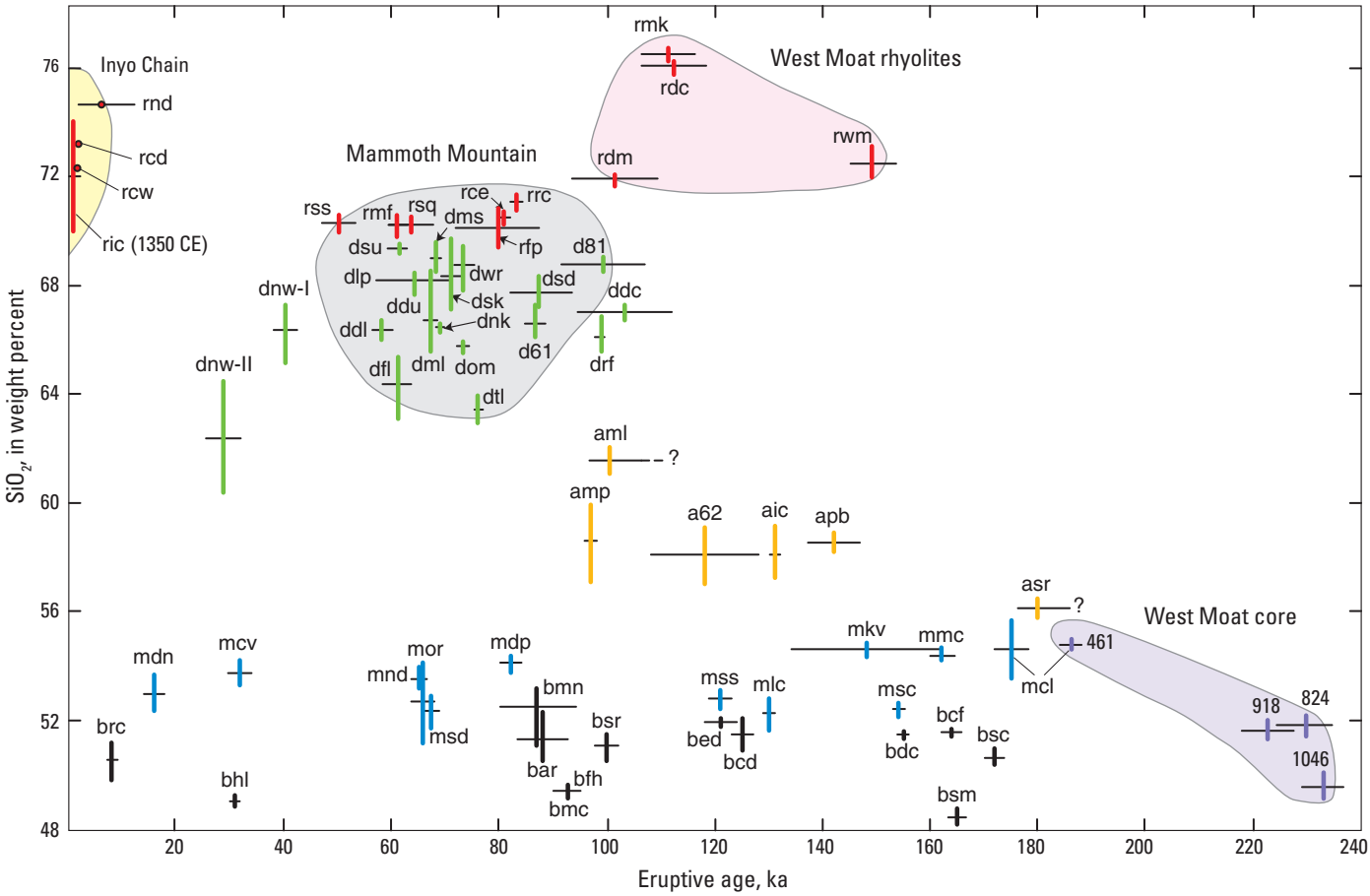

Figure 16. Plot of composition versus age for all dated units of the Mammoth system. Also plotted are Holocene Inyo chain and four subalkaline Long Valley rhyolites contemporaneous with alkaline Mammoth system. SiO_2 contents in weight percent. Unit labels as in text and table 1. Intraunit ranges in SiO_2 from appendix; error bars on ages express analytical precision from table 2. Five undated units in table 1 are not plotted but are probably all late Pleistocene: units dbp and dgr are constrained between 80 ka and 60 ka; unit mdm is older than 101 ka; mic is younger than 131 ka; and msj is older than 66 ka. Oldest four ages are core samples of lava flows from Inyo-4 drill hole (Eichelberger and others, 1985), identified by core depth, in feet; nowhere exposed at surface, samples represent Groups II, III, and IV of Vogel and others (1994).

1,620 ppm and Zr from 270 to 480 ppm (fig. 17*D*), evidently reflecting wide differences in degrees of sanidine and zircon retention in the crystal mush from which successive rhyodacitic melt batches were extracted. A Sr-Rb plot (fig. 17*E*) shows a moderately coherent trend dominated by plagioclase fractionation until reaching the rhyodacite range where sanidine retention (or removal) suppressed Rb enrichment in the most evolved melts. No systematic compositional trends with time are recognized among eruptive products of Mammoth Mountain, as more and less evolved units were emplaced both early and late during construction of the edifice (figs. 16, 17).

The longest arrays (1.5–2.9 percent SiO_2), although narrow, are shown by eruptive units dfl, dml, dms, and dwr. In contrast, units dlp, dsd, dtl, rce, rmf, rsq, and rss all exhibit tight arrays that extend through less than one percent SiO_2. Samples of units dbp, dom, ddl, and ddu overlap linearly within the limited SiO_2 range 65.7–67.1 percent, consistent with their stratigraphic stacking on the southeast side of the edifice. The steep Dome 2861 (unit d61) stands out among trachydacites in its enrichment in Ba and Zr (fig. 17*D*) and in its high Na content, which is reflected in its relative isolation on figure 15.The alkalic rhyodacites, poorer in phenocrysts than the trachydacites, tend to be compositionally bimodal (fig. 17); units rce, rfp, and rrc are richer in K and Nb than units rss and rsq but poorer in Ti, Fe, Mg, Ca, Sr, and P. Among the rhyodacites, unit rmf, slightly richer in phenocrysts and erupted at a different vent, is compositionally intermediate in some respects but unique in its low Fe and high Rb and Ba contents. Considering the Mammoth Mountain suite as a whole, there is remarkable compositional variety among the 25 silicic units that built a compact edifice over a lifetime of ~50,000 years, a variety (fig. 17) that presumably reflects both persistent mafic recharge and effective crystal-melt fractionation of its crystal-rich, multiphase phenocryst assemblage.

Mafic Periphery

Of the 38 late Pleistocene eruptive units peripheral to Mammoth Mountain, most are alkaline (fig. 15) by the IUGS criteria of LeBas and others (1986); six are transitional (units bcd–bed, bsm, mdn, mlc, and msj), and four are subalkaline olivine-rich basalts (units bfh–bmc, bhl, and Holocene brc). The six andesitic and three dacitic peripheral units are all unequivocally alkaline. The least silicic units (48.4–50.4 percent SiO_2) are bsm, bfh–bmc, bhl, and brc, the latter pair also being among the youngest basaltic units in the map area. The most magnesian units are bhl (9.9–10.5 percent MgO) and brc (8.1–8.3 percent MgO), and units bcd–bed, bfh–bmc, and bsm are next with 6–7 percent MgO. For clarity, plots of data for the many peripheral units are separated into three sets of figures, for units principally in the South Moat, West Moat, and San Joaquin drainage (figs. 18–20, respectively).

Tight compositional arrays are exhibited by units asr, bfh–bmc, bhl, brc, bsc, bsm, mcv, mdm, mdn, mdp, mkv–mmc, mlc, msc, and mss, each ranging less than one percent in SiO_2 content (figs. 18–20). The widest arrays (each ranging 2–3 percent in SiO_2) are shown by units aic, amp, mcl, and mor, all of which are phenocryst-poor, and by the contaminated hybrid dacite chain of unit dnw (60.4–67.3 percent SiO_2).

Many noteworthy points are illustrated in figures 18–20. All of the following concern the distribution, sequence, compositions, affinities, and distinctions among the 38 peripheral units of the Quaternary Mammoth system.

- Lava-flow aprons bcd, bfh, and mmc correlate well compositionally with their respective vent cones, units bed, bmc, and mkv, from which they are surficially separated by younger units.

- Spatially associated units mnd and mor and scoria from their inferred (but poorly exposed) vent complex, unit msd, together yield an overlapping continuous array.

- Units mss and mdp, directly superimposed on the canyon floor of the Middle Fork, yield tightly adjacent (but nonoverlapping) compositional groupings, centered respectively at 53 and 54 percent SiO_2 (fig. 20). Despite a measured age difference of ~40,000 years, the apparent chemical affinity of the units suggests location of the unknown vent for younger unit mdp somewhere not far from that of unit mss, which is exposed near Soda Springs Campground. Distinguishably different paleomagnetic directions (Hildreth and others, 2014) and Sr, Nd, and Pb isotope ratios (Cousens, 1996) confirm independence of the two units.

- Subunit bar' (51.1–52.4 percent SiO_2), which crops out in two areas within the primary apron of extensive phenocryst-rich unit bar (50.6–51.2 percent SiO_2), is a low-Mg, high-Al variant that shares similar concentrations of Ti, Fe, Ca, and Na and has only slightly lower K and P than unit bar. Although petrographically similar to most exposures of unit bar, the subunit carries slightly more plagioclase and only half as much olivine. It is inferred to be a late flow within the poorly exposed medial apron of bar flows.

- TiO_2 concentration generally exceeds 1.2 percent in all the mafic units (though not in the dacites), but it peaks at >2 percent in intermediate units mic and mkv–mmc, in the intermediate suite mor–mnd–msd, and in basaltic unit bsr, all of which are phenocryst-poor.

- Phenocryst-rich unit bhl is far more enriched in CaO (10.1–10.7 percent) than any other unit mapped here (fig. 18*B*). Carrying 5–7 percent clinopyroxene, 1–2 percent olivine, and 10–15 percent plagioclase, the unit is also the richest in MgO (9.9–10.5 percent) and

Sr, unusually rich in P, and relatively poor in Al. For its low SiO_2 content, the unit has moderate K_2O but unusually low Na_2O, accounting for its contrasting positions on figures 15*B* and 18*A*.

- Notably enriched in Al_2O_3 are units mlc (20.1–20.9 percent), bar' (19.1–19.9 percent), and mdn (18.6–19.5 percent). Each carries 15–20 percent plagioclase phenocrysts, somewhat more than other crystal-rich units like bcd, bfh, and bar but not greatly so. The latter three and most other mafic units here have peak Al_2O_3 values in the range 17.0–18.5 percent, while the andesites and dacites generally have still lower peak values. Noteworthy for its unusually low Al_2O_3 content is unit bhl (15.0–15.7 percent), probably owing to its abundance of clinopyroxene and olivine phenocrysts.

- Among the mafic units (49–55 percent SiO_2), a wide range in alkalinity, especially in K_2O, tends toward bimodality (figs. 15*B*, 18*A*, 19*A*). Scrutiny of the units composing the contrasting arrays apparent in those diagrams reveals no simple correlation with age or geographic distribution.

- Units ddc and drf, at 66–67 percent SiO_2 among the most evolved units peripheral to Mammoth Mountain (figs. 15*B*, 18, 19), are both crystal-poor trachydacites. Although their outcrops are now separated by >6 km on opposite sides of the Sierran divide, both appear to have erupted from vents later buried by the Mammoth Mountain edifice, and both yield radioisotopic ages of ~100 ka.

- Although most of the peripheral units have yielded compositional ranges of ≤1 percent SiO_2, several have ranges of ~2 percent (units a62, aic, bar, bmn, and mcl), and a few have ranges larger still (units mor 3.1 percent and amp 4.4 percent). Several trachydacites of the Mammoth Mountain edifice yielded comparably wide compositional ranges. The hybrid dacite chain of the northwest moat (unit dnw), with a range of 7 percent SiO_2, is the special case of a contamination series (as discussed in its unit description). Such ranges illustrate the importance of analyzing several samples from most units. Single analyses could misrepresent a unit, would miss evidence for fractionation or mixing trends within units, and might tempt unwarranted modelling of affinities between unrelated units.

- Sr, Nd, and Pb isotope ratios have been measured by others for 28 samples of the monogenetic peripheral units of the Mammoth system (Cousens, 1996; Bailey, 2004), representing eruptive units we can now identify as a62, aic, amp, bar, bcd, bfh, bhl, brc, bsr, drf, mcl, mcv, mdp, mor, and mss.

  Most samples cluster narrowly: $^{87}Sr/^{86}Sr$ 0.70613–0.70638; $^{143}Nd/^{144}Nd$ 0.51243–0.51259; and $^{206}Pb/^{204}Pb$ 19.16–19.27. Two $^{87}Sr/^{86}Sr$ values determined for Mammoth Mountain dacites (units d81 and rce) plot within the tight mafic cluster, as does a value for unit drf. Units bfh (0.70591), mss (0.70596), and bhl (0.7067) fall outside the $^{87}Sr/^{86}Sr$ cluster (although not outside for Nd or Pb). The only conspicuously anomalous outlier is the Holocene basalt of Red Cones (0.70516–0.70531 and 0.51277), unit brc, which is one of the few subalkaline peripheral units as well as one of the most primitive and the youngest.

  Although basement xenocrysts plagued early efforts to determine K-Ar ages of several of these units (Curry, 1971; Bailey and others, 1976; Mahood and others, 2010), Sr-Nd-Pb isotope data for nearby basement rocks show that upper-crustal contributions to mafic and dacitic products of the Mammoth system are small. For example, a metavolcanic schist of unit Mzmv near Agnew Meadows gave values of 0.72396 for $^{87}Sr/^{86}Sr$ and 18.94 for $^{206}Pb/^{204}Pb$. Metavolcanic rocks from the Ritter Range gave $^{87}Sr/^{86}Sr$ values that range from 0.7053 to 0.7264, most of them >0.709 (Kistler and Swanson, 1981). Metasedimentary rocks just south of Long Valley Caldera gave $^{87}Sr/^{86}Sr$ values that range from 0.7090 to 0.7250 (Goff and others, 1991). Granitoid plutons beneath the volcanic field have given $^{87}Sr/^{86}Sr$ values ranging from 0.70666 to 0.70987, and other nearby Sierran plutons range from ~0.707 to ~0.715 (Cousens, 1996; Bailey, 2004). The narrow isotopic ranges for products of the Mammoth system are incompatible with significant contributions from such basement rocks.

- Sampled only in the Inyo-4 corehole near Inyo Craters is a 170-m-thick stack of ~18 unexposed mafic lava flows that underlies ~150 m of flows correlated with units aic and mcl. All flows were analyzed chemically by Vogel and others (1994), and Sr, Nd, and Pb isotope ratios were determined for many by Cousens (1996). The unexposed units (~190–230 ka; figs. 6, 16) were grouped chemically by Vogel as follows: Lower Group II is basaltic trachyandesite (54.6–55.6 percent SiO_2); Group III is basaltic trachyandesite (52.3–53.2 percent SiO_2); and Group IV is transitional basalt (50.1–50.9 percent SiO_2). Vogel's Group I is our unit aic, and his upper Group II is our unit mcl. Because his Group V is not in place (Vogel and others, 1994, p. 19,832) and thus lacks stratigraphic context, we ignored it.

Neogene Periphery

We do not attempt in this report to discuss in detail the many Neogene basaltic, andesitic, and dacitic units preserved around the periphery of the map area, on the rim of Long

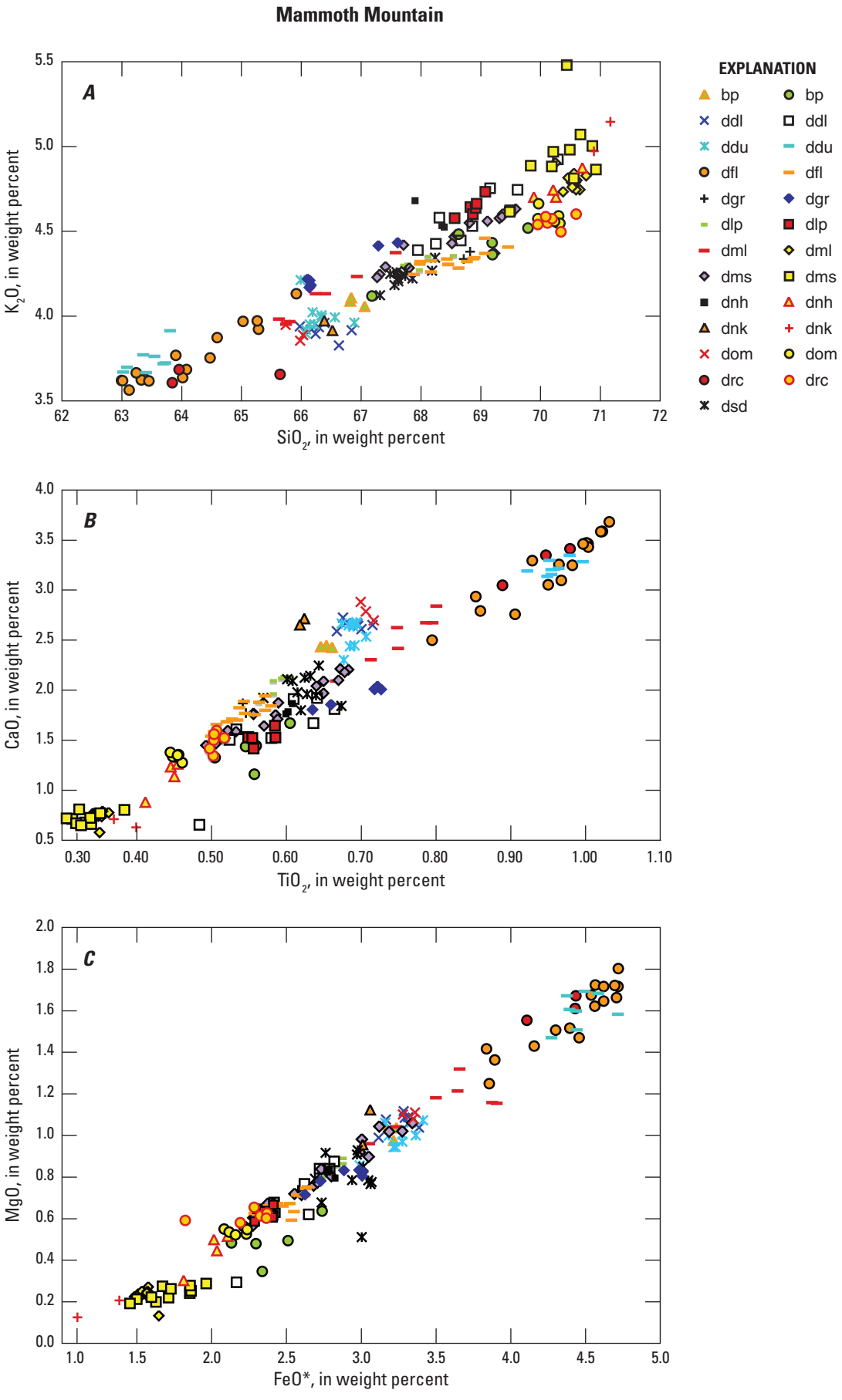
Mammoth Mountain
A
K_2O, in weight percent
SiO_2, in weight percent
B
CaO, in weight percent
TiO_2, in weight percent
C
MgO, in weight percent
FeO*, in weight percent
EXPLANATION
bp
ddl
ddu
dfl
dgr
dlp
dml
dms
dnh
dnk
dom
drc
dsd

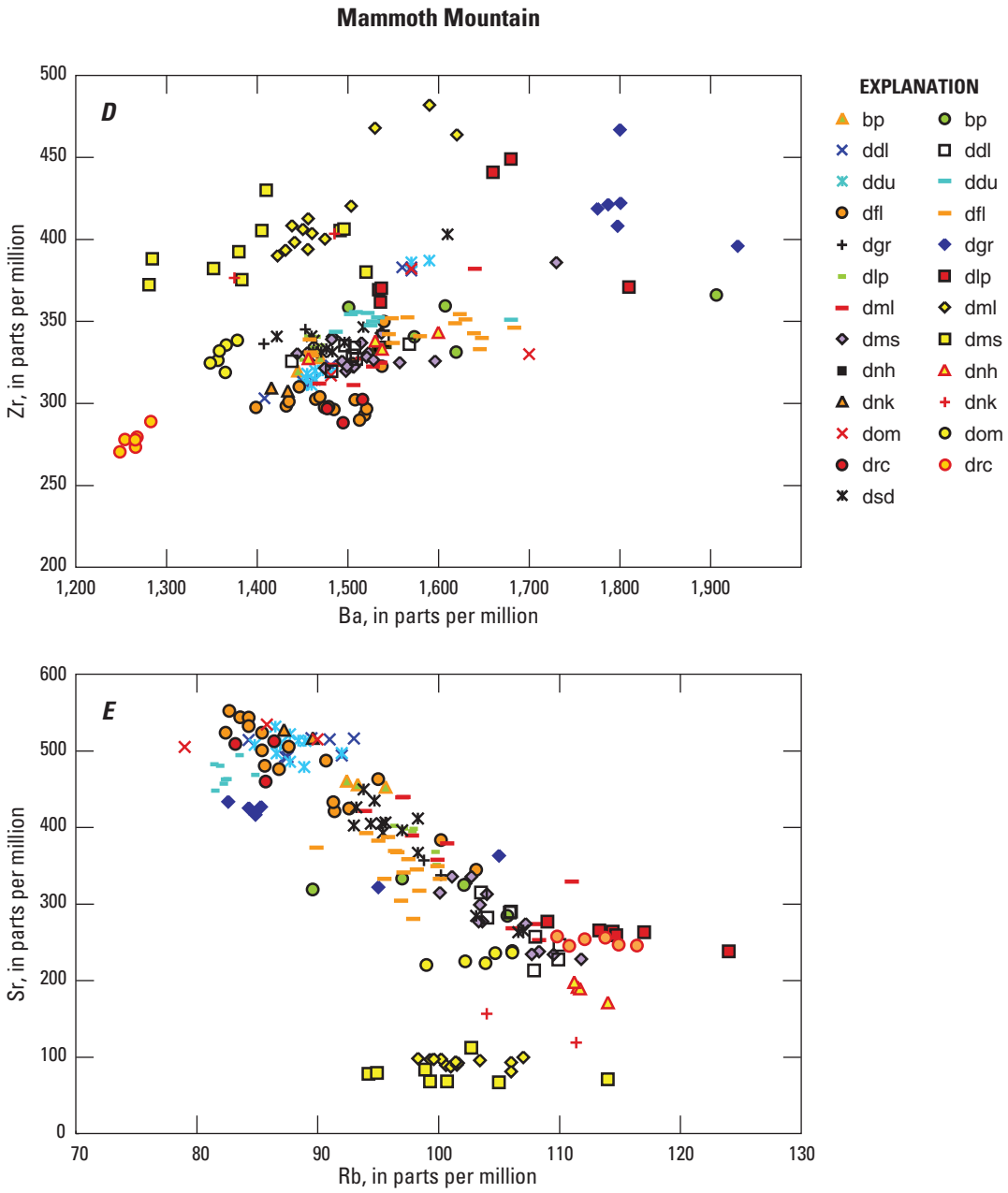

Figure 17. Compositional plots for Mammoth Mountain. *A*, K_2O versus SiO_2; *B*, CaO versus TiO_2; *C*, MgO versus FeO* (total iron calculated as FeO); D, Zr versus Ba; *E*, Sr versus Rb. Data for all samples in appendix.

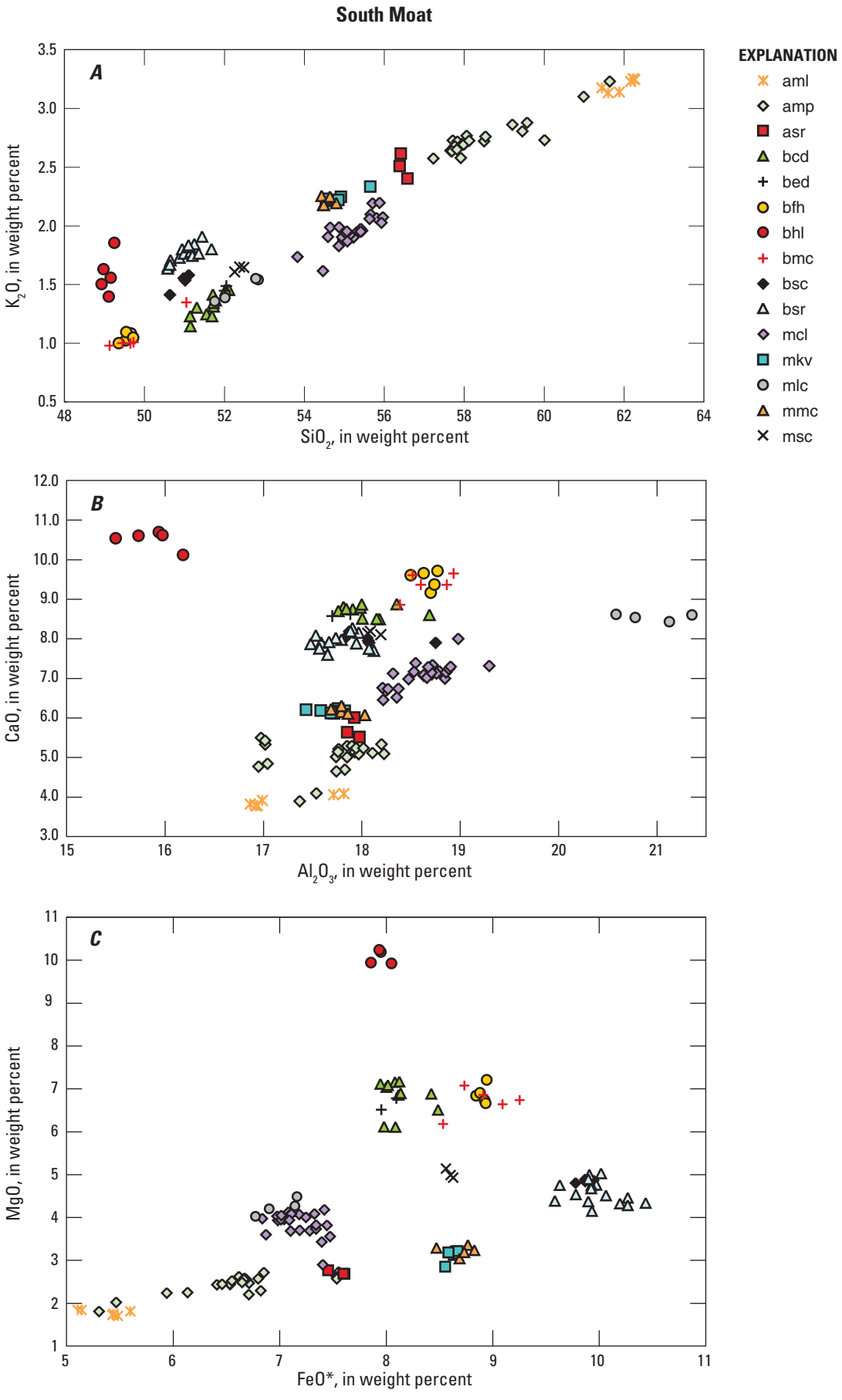
South Moat
A
B
C
EXPLANATION
aml
amp
asr
bcd
bed
bfh
bhl
bmc
bsc
bsr
mcl
mkv
mlc
mmc
msc
K2O, in weight percent
SiO2, in weight percent
CaO, in weight percent
Al2O3, in weight percent
MgO, in weight percent
FeO*, in weight percent

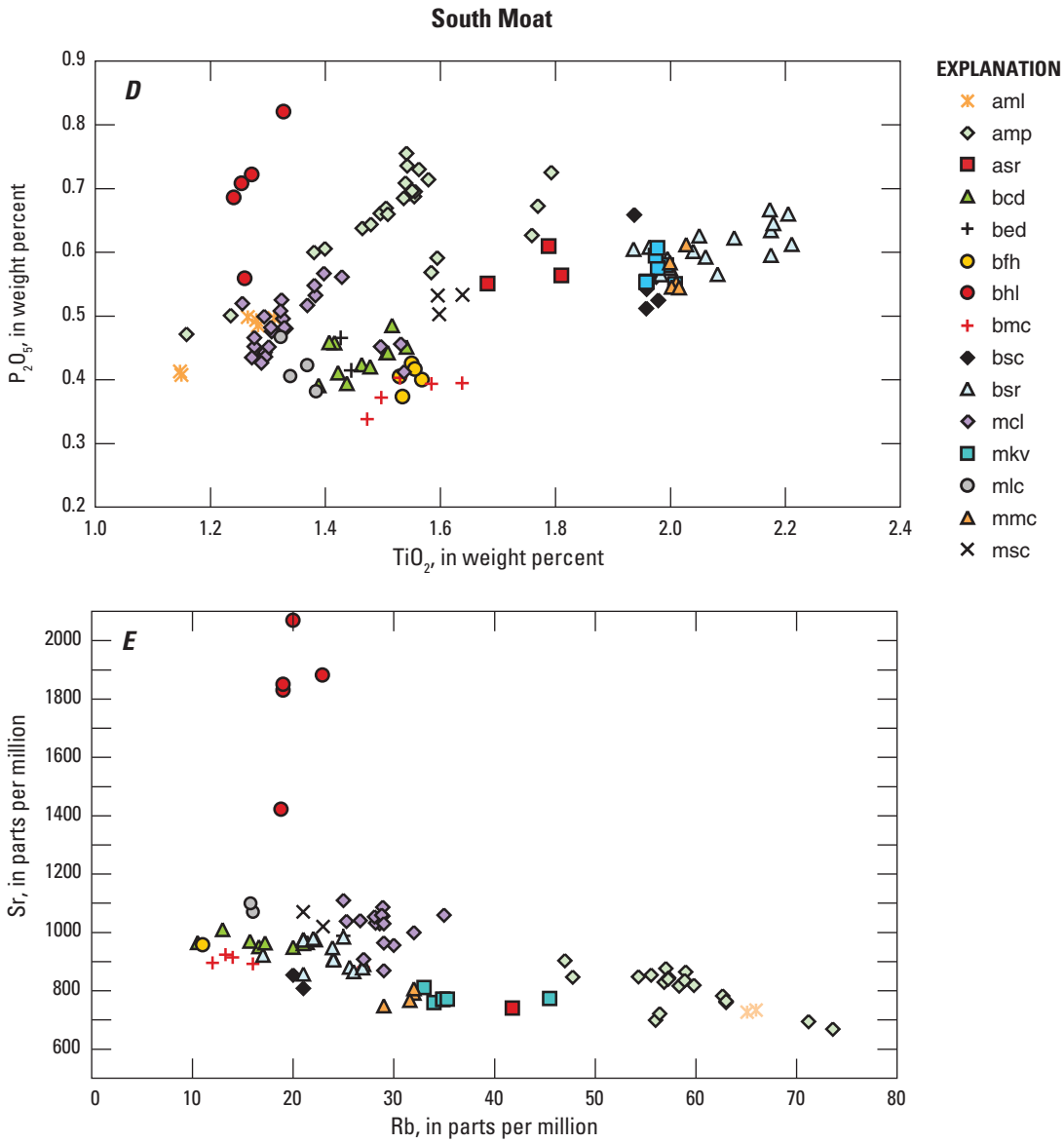

Figure 18. Compositional plots for peripheral units of Mammoth magmatic system that crop out along south moat of Long Valley Caldera and in Lakes Basin. *A*, K_2O versus SiO_2; B, CaO versus Al_2O_3; *C*, MgO versus FeO*; *D*, P_2O_5 versus TiO_2; *E*, Sr versus Rb. Data in appendix.

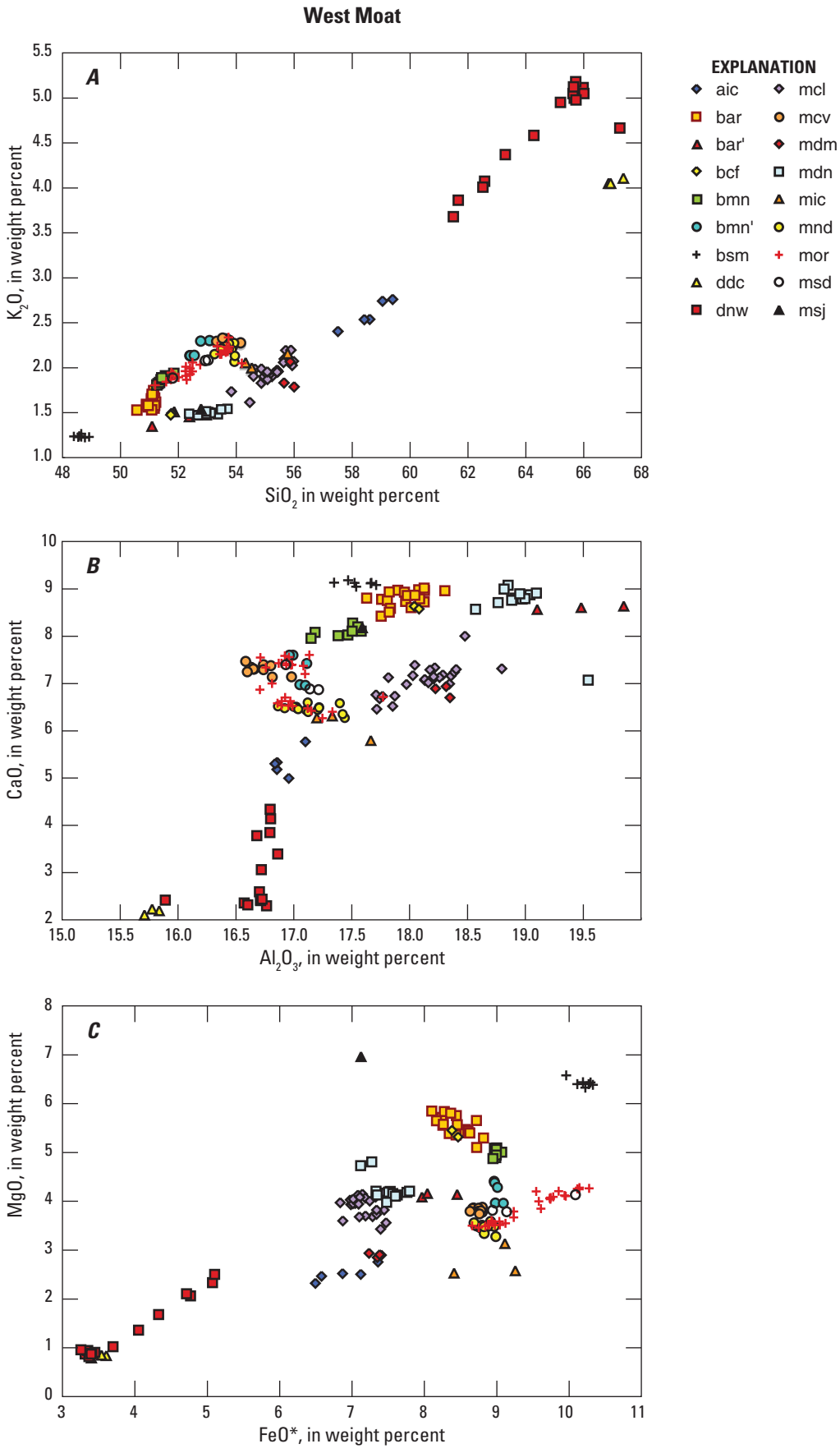
West Moat
A
B
C
EXPLANATION
aic
bar
bar'
bcf
bmn
bmn'
bsm
ddc
dnw
mcl
mcv
mdm
mdn
mic
mnd
mor
msd
msj
K2O, in weight percent
SiO2 in weight percent
CaO, in weight percent
Al2O3, in weight percent
MgO, in weight percent
FeO*, in weight percent

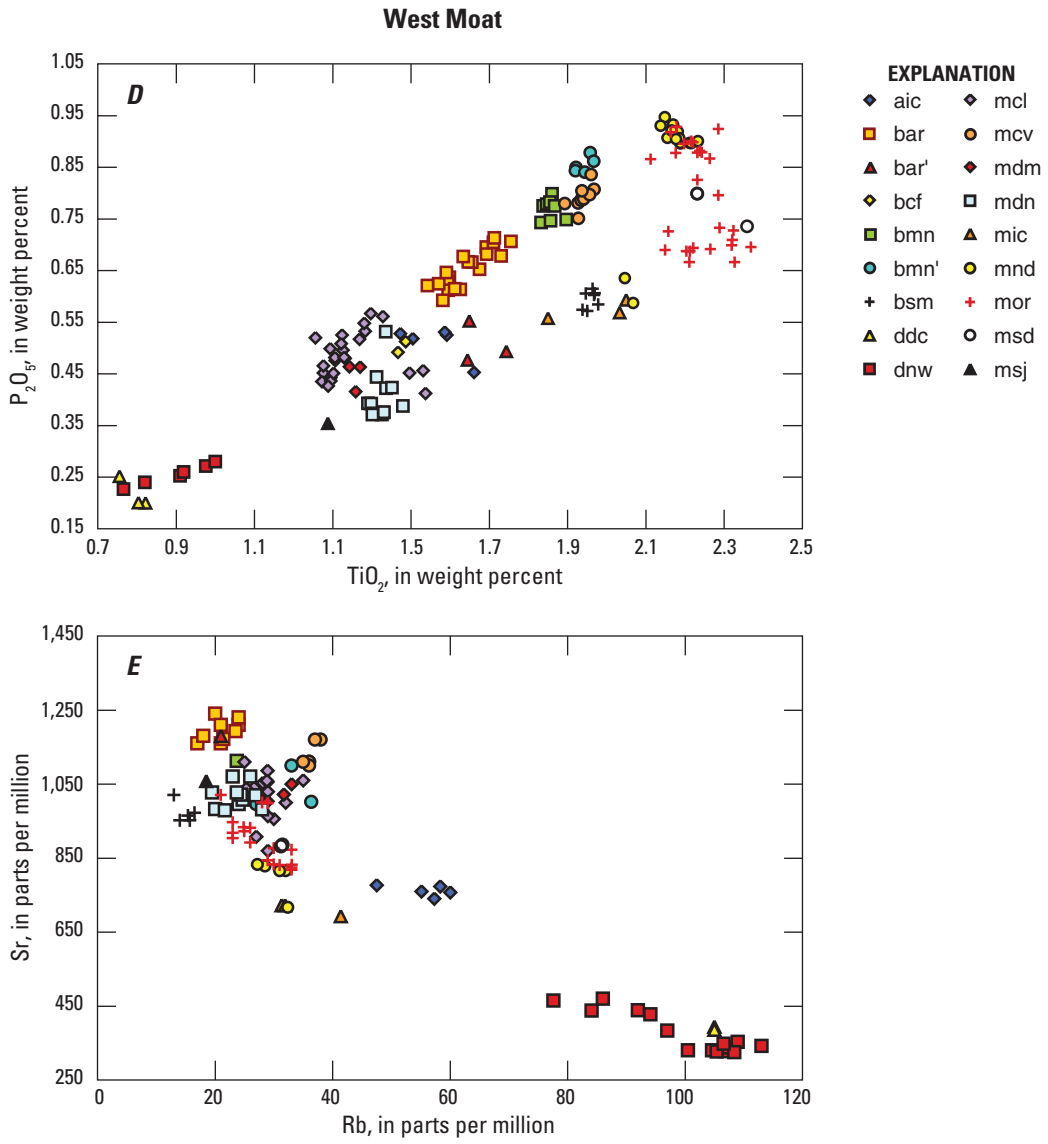

Figure 19. Compositional plots for peripheral units of Mammoth magmatic system that crop out along west moat of Long Valley Caldera. *A*, K_2O versus SiO_2; *B*, CaO versus Al_2O_3; *C*, MgO versus FeO*; *D*, P_2O_5 versus TiO_2; *E*, Sr versus Rb. Data in appendix.

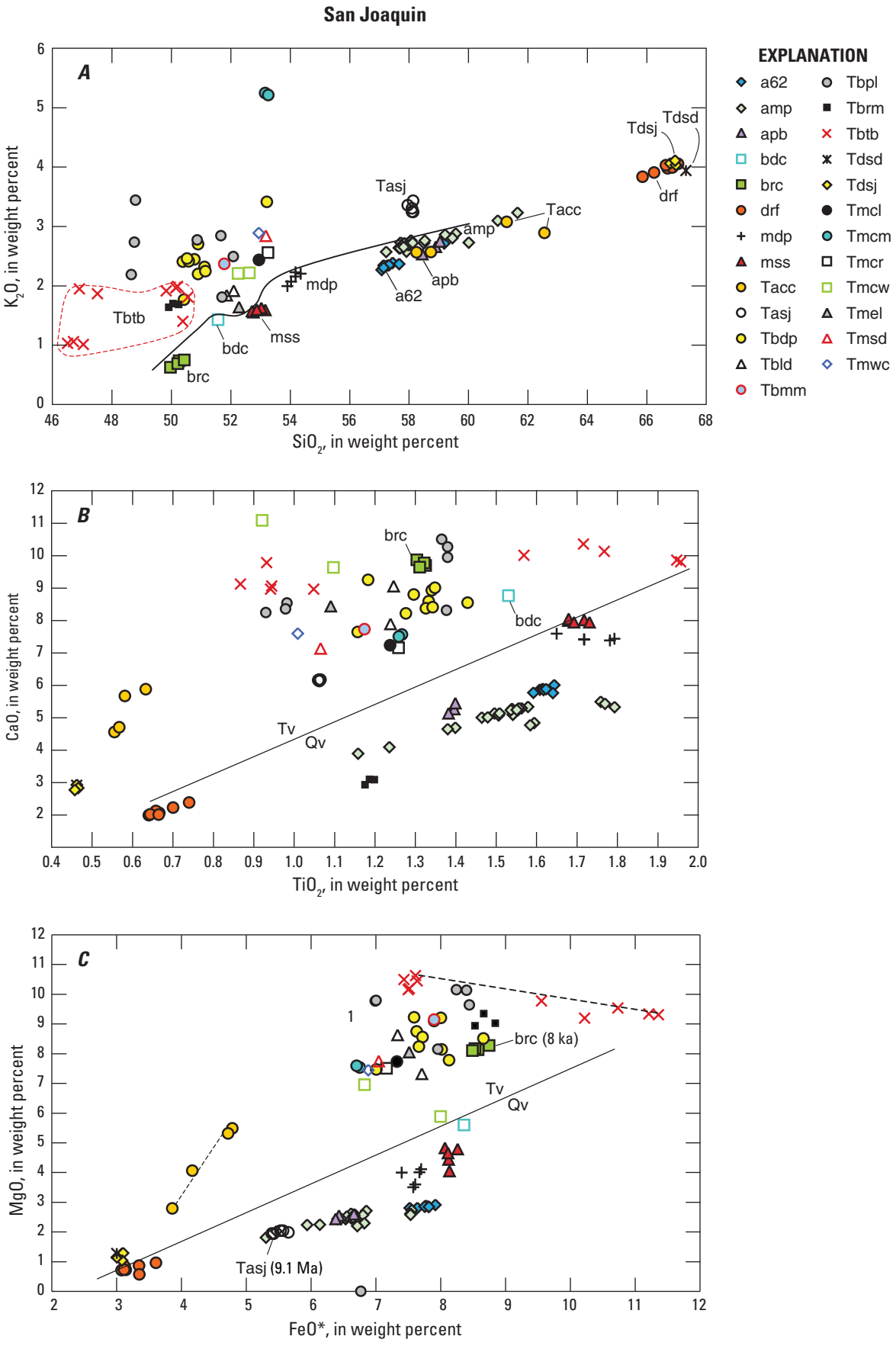
San Joaquin
A
K_2O, in weight percent
SiO_2, in weight percent
Tbtb
bdc
mss
brc
mdp
a62
apb
amp
Tasj
Tacc
Tdsj
Tdsd
drf
B
CaO, in weight percent
TiO_2, in weight percent
brc
bdc
Tv
Qv
C
MgO, in weight percent
FeO*, in weight percent
1
brc (8 ka)
Tv
Qv
Tasj (9.1 Ma)
EXPLANATION
a62
amp
apb
bdc
brc
drf
mdp
mss
Tacc
Tasj
Tbdp
Tbld
Tbmm
Tbpl
Tbrm
Tbtb
Tdsd
Tdsj
Tmcl
Tmcm
Tmcr
Tmcw
Tmel
Tmsd
Tmwc

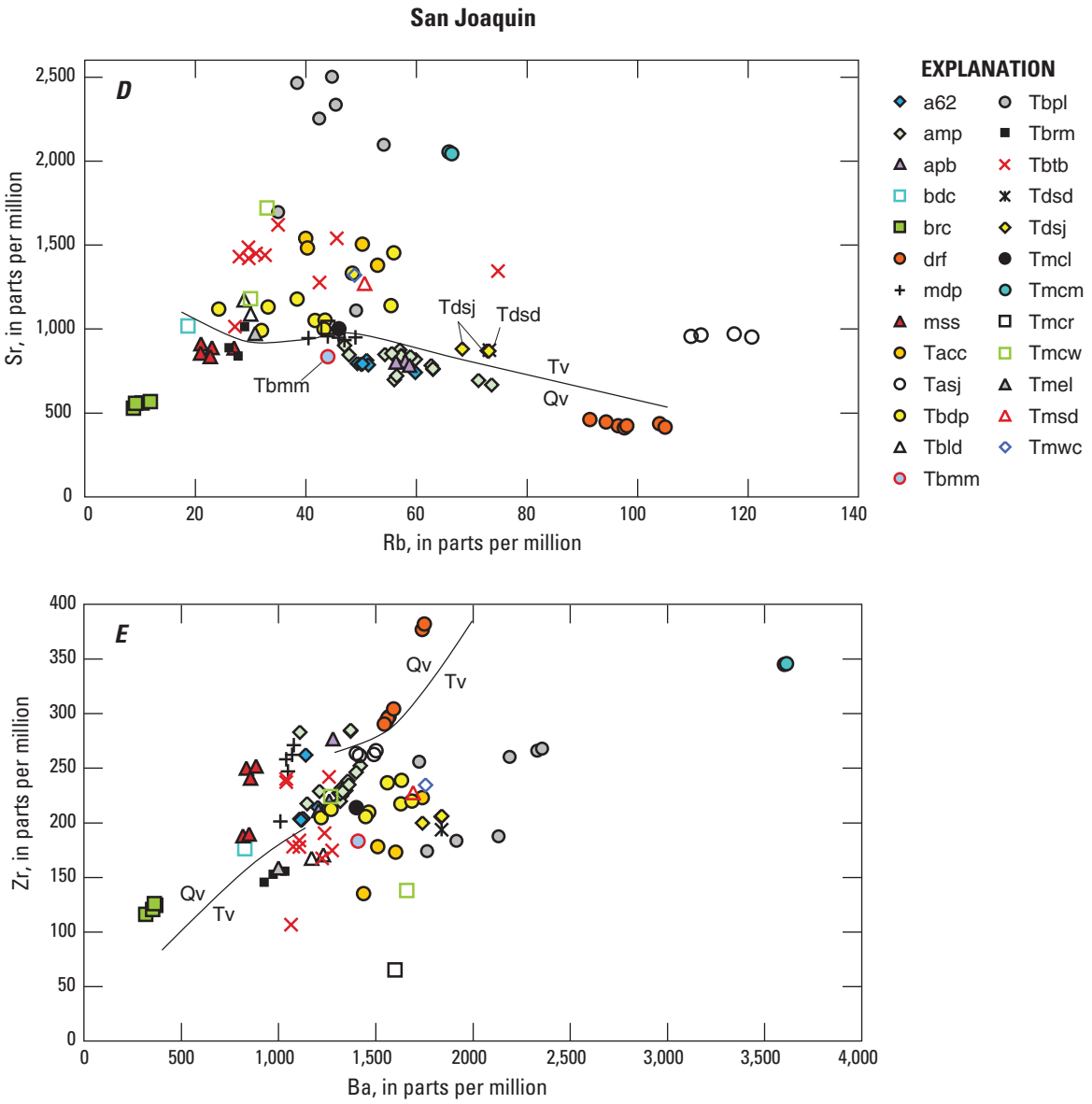

Figure 20. Compositional plots for eight peripheral units of Mammoth magmatic system that crop out along Middle Fork of San Joaquin River drainage system, along with data for 17 Tertiary units nearby. *A*, K_2O versus SiO_2; *B*, CaO versus TiO_2; *C*, MgO versus FeO; *D*, Sr versus Rb; *E*, Zr versus Ba. Data for all samples given in appendix. Dividing lines in each panel separate Tertiary (Tv) from Quaternary (Qv) volcanic units; a few exceptions are labelled. Dashed lines in panel C indicate compositional arrays of units Tacc and Tbtb, as discussed in text. Of four analyses for unit Tasj, two are samples from the map area and two are from near Millerton Lake (fig. 2), 80 km downstream.

Valley Caldera and within the Middle Fork San Joaquin drainage system. Their eruptive volume was at least five times greater than that of the entire late Pleistocene Mammoth system, and most of them erupted during the Pliocene. However, most of such pre-Quaternary eruptive products have been eroded away. No mafic or intermediate unit is known to have erupted between the end of the Pliocene and ~230 ka. We anticipate that ongoing work will comprehensively compare the many precaldera eruptive units north and east of the caldera with the westerly units described here (see Description of Map Units). Because Pliocene units Tacc, Tbtb, and Tmcw were previously mapped as Quaternary (Bailey, 1989), however, it seems necessary to comment here on their ages and compositions. We also summarize results of our search within the Middle Fork drainage basin for the unknown source vents of units Tbtb, Tmcw, and mdp.

The pair of glaciated domes combined as unit Tacc (fig. 10) on the granitic rim high above Crater Creek is compositionally bimodal (fig. 20). Although both are phenocryst-poor and similarly contaminated with granite-derived xenocrysts, the southwest dome has 58.3–58.7 percent SiO_2 and the northeast dome 61.3–62.6 percent. They differ likewise in Fe, Mg, and Ca contents, but what confirms their affinity is their similar and unusually low concentrations of TiO_2 (~0.6 percent) and P_2O_5 (~0.3 percent). The southwest dome yielded a $^{40}Ar/^{39}Ar$ age of 4.29±0.20 Ma.

The basalt of The Buttresses (unit Tbtb) is a severely glaciated stack of many lava flows preserved as five discrete remnants that span an elevation range of 470 m on the west wall of the Middle Fork canyon. As the largest remnant still extends down to river level, they appear to represent a conformable set of flows that once filled the canyon to a depth as great as 500 m. A columnar flow resting on granite gave a $^{40}Ar/^{39}Ar$ age of 3,754±7 ka, consistent with its reversed paleomagnetic polarity. Although all the flows examined are rich in olivine and clinopyroxene, the stack is compositionally bimodal, and the two compositions are interlayered in all sectors. Five flows sampled contain 46.5–47.5 percent SiO_2 and lack plagioclase phenocrysts; five other flows have 49.8–50.6 percent SiO_2 and carry a few percent plagioclase. Remarkably, Mg and Al increase systematically with SiO_2 while Fe, Ti, and P decrease steeply and Ca modestly within the 10-sample array (fig. 20). Preservation of the base of the Tbtb stack on granitic basement at river level indicates that the floor of this south-flowing reach of the Middle Fork canyon had already attained its present depth in the Pliocene. Pleistocene glaciation widened but did not deepen the canyon here.

Across the river and 2 km farther downstream along the east wall, a remnant pair of columnar lava flows (unit Tmcw) resembles some flows of unit Tbtb in carrying subordinate plagioclase and abundant olivine and clinopyroxene. The unit yields a reversed paleomagnetic direction similar to that of Tbtb. Nonetheless, the flows are more silicic (52.3–52.6 percent SiO_2) and far less magnesian than any flows of unit Tbtb (fig. 20). They probably represent a Pliocene eruptive episode independent of that of unit Tbtb, but vents have been located for neither unit.

In trying (unsuccessfully) to locate vents for units Tbtb and Tmcw (and for late Pleistocene unit mdp), we sampled nine more mafic remnants along the Middle Fork canyon (units Tasj, Tbdp, Tbld, Tbpl, Tmcl, Tmcm, Tmel, Tmsd, and Tmwc), for six of which we recognize vents. As none of the nine units provided satisfactory chemical or petrographic matches, the search was extended farther up-canyon, to Agnew Pass and Clark Lakes north of the map area, equally unsuccessfully. A rewarding result of the search for source vents, nonetheless, was finding that unit Tasj, which underlies unit Tacc on the Crater Creek rim, is compositionally and petrographically identical (fig. 20) to the intracanyon andesite of Kennedy Table (fig. 2), 80 km downstream along the San Joaquin River canyon (Huber, 1981). Distal and proximal outcrops both yield $^{40}Ar/^{39}Ar$ ages ~9.2 Ma.

Three more Pliocene mafic-lava remnants, units Tbmm, Tbrm, and Tmcr, also plotted in figure 20, rest on Mesozoic basement along the rim of Lakes Basin. They neither correlate with each other nor with Pliocene units recognized elsewhere, and source vents have not been located for any of them. Unit Tbmm is the type locality of the Mammoth Reverse Subchron (Doell and others, 1966).

The Tertiary samples plotted in figure 20 include three plugs high on the west wall of the Middle Fork drainage. That these units, Tmcl, Tmel, and Tmwc (all west of the map area; see fig. 3), had been reduced to nothing but massive vent-filling lavas draws attention to the severity of Pleistocene glacial erosion on the east flank of the Ritter Range (figs. 3, 4). Such upland erosion highlights even more strongly the contrasting evidence from unit Tbtb that the floor of this granitic segment of the Middle Fork had been cut to its present depth already in the Pliocene.

Of the eight late Pleistocene peripheral units along the Middle Fork (fig. 20), all are alkaline except the Holocene basalt of Red Cones (unit brc). The Neogene units plotted in figure 20 are similar to the Pleistocene alkaline units in total alkali contents, but almost all are more potassic (fig. 20*A*) as well as richer in Ca, Mg, Sr, and Ba (figs. 20*B–E*). At 5.2 percent K_2O, olivine-rich Pliocene unit Tmcm is shoshonitic (fig. 20*A*); and in common with unit Tmcm, unit Tbpl is unusually rich in Sr (fig. 20*D*).

Discussion

Were it not for its contiguity with Long Valley Caldera, the Mammoth volcanic field might long ago have been recognized as an independent magmatic system. Like the larger Lassen Volcanic Center in the Cascade arc (Clynne and Muffler, 2010), it consists of a central cluster of phenocryst-rich dacite lava domes surrounded by a contemporaneous array of mafic volcanoes in an extensional tectonic setting. The Long Valley system had erupted ~850 km^3 of rhyolite

magma, all of it subalkaline and most of it phenocryst-poor. In contrast, eruptive products of the Mammoth system are two orders of magnitude less voluminous and almost entirely alkaline. All of its silicic products are phenocryst-rich and none are rhyolitic.

Mammoth System Versus Long Valley System

The Long Valley vent array was 30 km across, and for nearly 2 million years (2.2–0.3 Ma) it erupted nothing but rhyolite, centrally or peripherally. Its large silicic magma reservoir evidently prevented eruption of the mafic magma inferred to have sustained it thermally; mafic enclaves have been found in only three of ~100 rhyolitic eruptive units. In contrast, the vent array of the Mammoth system is predominantly mafic and 10 by 20 km wide; its central trachydacite edifice is only 5 km across and carries abundant relatively mafic enclaves and xenocrysts. The footprint of the Mammoth vent array is compactly circumscribed, extending west from the caldera's ring-fault zone to the San Joaquin River and north-south from Deadman Creek to Pumice Butte. Beyond the limits of the well-defined Mammoth system, the nearest Quaternary mafic vents are in Mono Basin (at June Lake and Black Point) and 85 km southeast near Big Pine.

Inception of Mammoth mafic volcanism at 233±4 ka culminated the 2-million-year-long west-southwestward migration of the mantle-derived focus of deep crustal intrusion that had successively energized the rhyolitic systems manifest as Glass Mountain, the Bishop Tuff, and the early postcaldera rhyolite. Growth of the Mammoth system sustained that trend, yielding a secular drift of the melting anomaly toward 240º at a long-term average rate of ~15 m/kyr from Glass Mountain to Mammoth Mountain.

The Mammoth Mountain edifice and almost all of the 38 monogenetic peripheral units vented outside (west or southwest of) the caldera's ring-fault zone. However, proximity to the ring-fault zone of a few of the mafic vents (units bed, mdm, mkv; possibly also bsm and msc) inspires the attractive hypothesis that their intrusive counterparts (165–120 ka) reenergized part of the crystallizing Long Valley reservoir to yield eruption of the four subalkaline rhyolite lavas in the west moat at 150–100 ka (units rwm, rdc, rmk, and rdm). Moreover, glass and mineral Rb-Sr isochrons for these four rhyolites suggest a feldspar fractionation episode at 257±39 ka (Heumann and others, 2002); a ^{230}Th-^{238}U mineral isochron gives an age of 236±1 ka for rhyolitic unit rdm (Heumann and others, 2002), similar to the weighted mean (^{230}Th/^{238}U) model age of the main zircon population in that unit (Reid and others, 1997). These mineral-crystallization ages are 100–150 kyr older than eruption ages of the four west moat rhyolites, but they are essentially synchronous with initiation of the adjacent Mammoth system at 233±4 ka. Outside of the west moat, there have been no Long Valley eruptions since ~330 ka, and those between ~570 ka and 330 ka had been rhyolites of small volume.

A few of the Mammoth peripheral monogenetic vents are within the west moat, their locations thus conceivably influenced by proximity to a buried segment of the rangefront (basement-hosted) Hartley Springs Fault Zone that foundered with the 767-ka caldera. Most of the 38 peripheral units, however, vented in the Sierra Nevada, or high on the caldera wall, or beneath the Mammoth Mountain edifice. The footprint they define is broadly scattered, ovoid in plan, nonlinear, and (in contrast to the Holocene Inyo alignment) clearly not controlled by the rangefront fault zone. In any case, the rangefront fault zone terminated beneath what later became the caldera's west moat, never having extended as far south as the site of Mammoth Mountain and, instead, stepped left ~15 km across the later site of the caldera, resuming as the range-bounding Hilton Creek Fault south of the caldera margin (fig. 3).

In contrast to the wide mafic array, the Mammoth Mountain trachydacite edifice is focussed over a structural singularity (fig. 5). It banks against Long Valley caldera's steep topographic wall; it overlies the near-vertical regional contact that separates Paleozoic metasedimentary from Mezozoic metavolcanic sections; it overlies the margins of one or more Cretaceous granitoid plutons that intrude the pre-Cenozoic sections; and it overlies a segment of the near-vertical Sierra Crest Shear Zone System (fig. 5). Reflecting the field of mantle-derived magma ascent, the peripheral array of monogenetic vents is much broader than this structural nexus, but the intracrustal site of the Mammoth Mountain silicic magma body that developed at its core was probably localized by this convergence of older structures.

Rhyolitic Versus Trachydacitic Culminations

Why does the edifice that extruded piecemeal from a silicic magma body at the center of the Mammoth monogenetic volcanic field consist predominantly of crystal-rich trachydacite? Why does it lack the rhyolite characteristic of Long Valley, Mono Craters, Coso, and many more Neogene and Quaternary volcanic fields in the extensional Basin and Range Province? In common with many such fields, the Mammoth volcanic field tends toward compositional bimodality (fig. 16), but the modes here are 48–55 percent and 64–70 percent SiO_2, not basalt and rhyolite. The few silicic andesites (units a62, aic, aml, amp, apb) that occupy the gap between modes (fig. 16) are all phenocryst-poor, thus presumed to have been melt batches that separated from crystal-richer basaltic representatives of the mafic mode. Of the 25 silicic units exposed on the silicic edifice, 19 are crystal-rich trachydacites (64–69 percent SiO_2) and six are alkalic rhyodacites (70–71 percent SiO_2) that carry only half as many phenocrysts. Six times between ~85 and 50 ka, melt-enriched fractions separated from trachydacitic mush as small rhyodacite batches that were buoyant and voluminous enough to erupt. Most of the trachydacite extrusions carry relatively mafic blebs and enclaves and scattered

clinopyroxene crystals likely to represent persistent mafic recharge of a recurrently stirred crystal-rich reservoir. As crystal-depleted extracts from the top of the reservoir, the rhyodacites lack evidence of such mafic cargo.

Products of the Pliocene volcanic field (~4.0–2.6 Ma) that preceded the Long Valley rhyolitic episode are well exposed around the caldera rim (Bailey, 1989, 2004). The data define an alkalic compositional array that is fairly continuous from 49 to 69 percent SiO_2. Like the late Quaternary Mammoth suite, however, rhyolites are absent, and most of the silicic units are crystal-rich hornblende-biotite-feldspar trachydacites. The extended Long Valley rhyolitic interval (2.2–0.3 Ma), which was accompanied by no mafic eruptions, was thus bracketed by the Pliocene and Mammoth eruptive intervals, when alkalic basalts and their intermediate alkalic derivatives were accompanied principally by phenocryst-rich trachydacites but no rhyolites.

What accounts for the contrast between the exclusively rhyolitic episode and the basalt-to-dacite episodes that temporally bracket it? It cannot be presumed that primitive magma input from the mantle remained mildly alkalic basalt throughout the entire 4-million-year-long eruptive history. It seems likely that the contrasting patterns of intracrustal magma evolution reflect far more intensive mantle melting during the rhyolite interval. This would have entailed higher-melt-fraction subalkaline basalts, elevated rates of basaltic intrusion into the crust, and concomitantly greater degrees of deep-crustal partial melting, feeding back as an expanding barrier of mushy ductile crust that prevented further ascent of the basalts and thus intensified intracrustal melting. No mafic batches were erupted during the long rhyolitic interval, but mafic enclaves found in a few postcaldera rhyolitic lava flows are indeed subalkaline basalt in unit rer (~680 ka) and transitional basaltic andesite in unit rnc (~570 ka).

Simon and others (2007) inferred from U-Pb zircon ages and Pb-isotope ratios of phenocrysts and host glasses that, during the Glass Mountain through Bishop Tuff rhyolitic interval (2.2–0.76 Ma), the Long Valley system had undergone a broadly increasing rate of rhyolite production, decreasing magma residence times, declining crustal contributions, and an increasing proportion of mantle input. Such trends are unlikely to have reversed during the postcaldera eruption of ~100 km^3 of phenocryst-poor Early rhyolite (~750–650 ka), but the rhyolite eruption rate dropped drastically thereafter.

By contrast, during the low-flux dacite-culminating intervals, lower-melt-fraction alkalic basalts might ascend from the mantle in smaller batches, lodge at deeper crustal depths, induce less crustal melting, and produce derivative products dominated by fractionation and remelting of mafic intrusions. Smaller batches crystallize faster, and reduced contributions from dehydration melting of crustal wall rocks would limit the water contents of fractionating magmatic hybrids, favoring crystal-rich viscous intermediates rather than accumulation of water-enriched, low-temperature, low-crystallinity rhyolite. During the Mammoth episode and the much longer Pliocene episode of basalt-to-dacite eruptions, the volumetric eruption rate was an order of magnitude lower than during the extended Long Valley rhyolite interval (2,200–650 ka). Assuming similar rate ratios for fluxes of mantle-derived basalt, deep-crustal reservoirs should have remained relatively modest during the low-flux episodes, sporadically releasing small batches of dacite melt that could ascend to upper-crustal subvolcanic chambers where they could partially degas and crystallize extensively (Annen and others, 2006). Dacite and silicic andesite batches contemporaneous but peripheral to the Mammoth Mountain chamber evidently ascended to the surface with little interruption, erupting as crystal-poor units drf, ddc, aml, and amp. During the long high-flux interval between, deep-crustal melting was areally and volumetrically far more extensive, enabling the melting region to expand into the middle crust, inducing dehydration melting of hydrous protoliths, and releasing large batches of water-rich intermediate melt to shallow chambers where they could fractionate thick roof-zone layers of low-temperature crystal-poor rhyolite melt (Hildreth, 2004).

In summary, the 4-million-year-long magmatic history here is envisaged to include a 2-million-year-long episode of vigorous mantle upwelling and subalkaline basaltic magma production sandwiched by low-flux episodes of lower-melt-fraction alkalic basalt production. Derivatives of the main phase culminate in voluminous crystal-poor subalkaline rhyolite, whereas those of the less vigorous bracketing episodes culminate in crystal-rich trachydacite. The succession is not unlike that of oceanic hotspot volcanoes that move progressively across fixed melting columns, thus producing early and late alkalic episodes that sandwich far more voluminous tholeiitic shield stages. The GPS velocity of the Long Valley region (in a fixed North American reference frame) is 8–12 mm/yr northwestward (Oldow, 2003), in contrast to the southwesterly drift of the rhyolite focus and thus in complete conflict with the model of plate migration over a fixed melting column. Here, it is the mantle melting anomaly itself that waxed and then waned.

During the Pliocene, the basaltic flux was widely distributed but moderate, culminating in a field of trachydacite domes scattered from Crater Creek to San Joaquin Mountain, Bald Mountain, and Laurel Mountain, and probably spanning the later site of Long Valley Caldera. The mantle-derived flux intensified and focussed more locally by 2.2 Ma, first beneath Glass Mountain, then migrated west-southwest at ~15 mm/yr beneath the sites of Long Valley and the Early rhyolite, and finally diminished after ~650 ka. How regional redistribution of intraplate extension may have led to a refocusing of intense mantle upwelling ~20 km north, beneath subalkaline rhyolitic Mono Craters around 60 ka, is a speculation we need not address here. Adjacent to the southwest margin of the Early rhyolite, however, and on the trend of the secular migration of the magmatic focus, a relocated but diminished and more distributed flux of mantle magma ascent initiated the alkaline Mammoth basalt-to-dacite system by 230 ka.

Mammoth System Magma Reservoir

Although the vent field for Mammoth Mountain and its 38 peripheral units covers nearly 90 km^2, the total eruptive volume is small. The poorly constrained total eruptive volume for the peripheral array is between 7 and 12 km^3, the most voluminous units being mcl, amp, bar, bfh, and mormnd. The scattered peripheral vent array can be compared to the present-day midcrustal distribution of scattered long period (LP) seismicity, which extends ~10 km east-west from beneath Mammoth Mountain to the Middle Fork at depths of 10–18 km (Pitt and others, 2002; Hill and Prejean, 2005). The numerous LP earthquakes are likely to represent injection of basaltic dikes and ascent of CO_2-rich fluids derived from them. Beneath the LP array, at lower-crustal depths of 19–31 km, a few ascending swarms of brittle-failure earthquakes (2006–2009) were likewise interpreted (Shelly and Hill, 2011) as slip induced in otherwise ductile crust by pressurized fluids. Only a few dozen times in the 230,000-year-long Mammoth episode did magmatic dikes attain the surface and feed monogenetic eruptions, but ascent of magma-derived CO_2-rich hydrous fluids along fractures may be much more common. An 11-month-long earthquake swarm beneath Mammoth Mountain in 1989 (Hill and others, 1990) produced a vertical planar distribution of hypocenters at 6–9 km depth that was interpreted as fracture-bound fluid injection, potentially related to deeper dike intrusion beneath the brittle crust (Hill and Prejean, 2005). The several tree-kill sites peripheral to the edifice (figs. 5, 14), caused by elevated CO_2 emission, was first observed in 1990.

Mammoth Mountain itself, despite uncertainties about glacial losses and depth of its concealed base, erupted no more than 4±1 km^3 of silicic lavas and pyroclastics (including the two off-edifice domes d61 and d81). The consistent similarity of eruptive products at Mammoth Mountain—their high crystal content, multiphase mineralogy, and continuous range of bulk composition—throughout a 50,000-year active lifetime suggests a stably located, relatively simple magma reservoir. Vents on the edifice are confined within a footprint only ~2 km^2 in area, and most vents fall along a northwesterly trend (fig. 8) that crudely approximates that of the near-vertical bedding and foliation of the basement (fig. 5). The narrowly elongate vent corridor on the edifice may reflect northwest elongation of the silicic magma reservoir, as influenced by the basement structure, which might likewise favor a vertically prolate chamber and disfavor sill emplacement. The widespread occurrence in the trachydacites of well-distributed relatively mafic cargo—enclaves, blebs, streaks, plagioclase-clinopyroxene clots—attests to persistent mafic recharge and convective stirring within a compact unitary chamber. Nonetheless, over the course of a multiepisode 50,000-year eruptive history, it should be expected that small intrusive masses, rinds, and dikes would crystallize, probably coexisting transiently with active pods of crystal mush that wax and wane in crystallinity, sporadically erupt, and less often fractionate melt-enriched rhyodacitic lenses.

The $^{87}Sr/^{86}Sr$ values for Mammoth Mountain trachydacites (units d81 and rce), along with that for peripheral crystal-poor trachydacite unit drf, are virtually the same (0.7063±0.0001) as for most units of the contemporaneous mafic periphery, suggesting comagmatic descent (whether by direct fractionation or by also entailing partial remelting of forerunning crustal mafic intrusions). Sr-Nd-Pb isotope data for nearby basement rocks confirm that upper-crustal contributions to mafic and dacitic products of the Mammoth system are small. For example, a metavolcanic schist of unit Mzmv just northwest of Mammoth Mountain gave 0.72396 for $^{87}Sr/^{86}Sr$. Granitoid plutons beneath the Mammoth volcanic field have given $^{87}Sr/^{86}Sr$ values ranging from 0.70666 to 0.70987, and other nearby plutons in the eastern Sierra range from ~0.707 to ~0.715 (Cousens, 1996; Bailey, 2004).

Although the silicic magma reservoir beneath Mammoth Mountain may well have crystallized by ~50 ka, abundant geophysical evidence shows that mantle-derived mafic magma still intrudes the crust beneath the Mammoth volcanic field today, as it has since ~230 ka. The eruption ages summarized in figure 16 show that time intervals between eruptions here have rarely been as long as 10,000 years. The most recent eruption was ~8,000 years ago.

Mammoth Mountain When Active

The silicic edifice itself was intermittently active for several tens of thousands of years but has been quiescent since ~50 ka. Late Pleistocene glaciers mantled the entire edifice, quarried substantial fractions of its many domes and coulees, and removed almost all of its pyroclastic apron. Despite the glacial erosion, however, the 5-km-wide footprint of the lava-dome complex has been reduced only marginally, and its ~1 km of relief is unlikely to have been reduced by more than 100 m. What can be inferred about the volcano when it was active?

Historically active dome complexes comparable to Mammoth Mountain include Soufrière Hills, Unzen, Santiaguito, Augustine, and Mount St. Helens (Druitt and Kokelaar, 2002; Hoshizumi and others, 1999; Nakada and others, 1999; Harris and others, 2003; Waitt and Begét, 2009; Hopson, 2008; Clynne and others, 2008). Although each differs from Mammoth Mountain in particular characteristics, all were constructed by repeated extrusion of phenocryst-rich domes and derivative thick lobes and tongues of viscous lava. Bulk compositions of the crystal-rich domes and coulees range from silicic andesite to rhyodacite (58–71 percent SiO_2), overlapping those of Mammoth Mountain (63–71 percent SiO_2). All are amphibole-bearing, and all produced aprons of pyroclastic-flow deposits, principally from block-and-ash flows generated by gravitational collapse of oversteepened parts of growing lava domes and coulees. There can be little doubt that such aprons widely surrounded Mammoth Mountain, too, and that the fragmental deposits were glacially stripped during the late Pleistocene. Pumice-rich pyroclastic flows and

falls generated by column collapse (though common at Mount St. Helens) are generally subordinate at these volcanoes and likewise at Mammoth Mountain, where only one such eruptive unit (rfp) has been preserved.

As at Mammoth Mountain, most of the extrusions that built each edifice issued from either a central vent or a fairly compact vent complex. Patterns include tight clusters of interfering domes at summit vents (Augustine, Soufrière Hills), vent alignments 1–3 km long (Mammoth, Santiaguito), near-summit dome clusters (Fugendake cone at Unzen), and scatterings of flank domes 1–3 km outboard of a summit cluster (Augustine, St. Helens, Mammoth). Like the pair of off-edifice domes at Mammoth Mountain, two large middle-Holocene domes grew 4 km east of the compositionally similar and contemporaneous Fugendake edifice at Unzen.

At various stages of development, most of the comparative volcanoes named above were marked by craters or sector-collapse amphitheaters, which were commonly refilled by younger domes, but no evidence for such features survives at Mammoth Mountain. Neither are the tops of conduits or dikes exposed beneath the lavas of Mammoth Mountain, but studies at comparative volcanoes suggest that conduits for comparable viscous domes were 30–70 m in diameter, flaring to 100–250 m near the surface. Pulses of dome extrusion at the historically observed comparators were commonly punctuated by vulcanian explosions of short duration that produced ash plumes that rose several kilometers and modest density currents that extended a few kilometers radially, but no pyroclastic deposits from such events have survived glacial scour at Mammoth Mountain.

Millennium-long sequences of silicic dome extrusions are sometimes interrupted by central eruption of relatively mafic (or andesitic) magma (Unzen, St. Helens), but the last such penetration at the site of the silicic Mammoth edifice was by the voluminous unit amp at ~97 ka. Nonetheless, ubiquity of mafic enclaves in the silicic lavas of Mammoth Mountain and of most of its comparators provides evidence of frequent recharge and convective redistribution within crystallizing/fractionating/mixing upper-crustal magma chambers.

Extrusive episodes at these volcanoes have been shown to represent contrasting timescales. At one extreme, ~20 episodes of dome growth took place in six years in the crater of Mount St. Helens (1980–1986); following the first three, small domes were destroyed explosively. Similarly, at Soufrière Hills pulses of dome growth and partial collapse (1995–2012) have been numerous. At Unzen, in 1991–1995, a complex dacite dome produced 13 flow lobes in four years, each lobe advancing 1–10 m/day for several months. A typical lobe there is 350 m long, 250 m wide, and 50–100 m thick, smaller than most (but not all) at Mammoth Mountain. As each lobe cooled and stalled at Unzen, a new piggyback lobe sometimes formed over the vent. If successive flow units at Mammoth Mountain had extruded so quickly, they could be expected to have identical paleomagnetic directions (contrary to our measurements).

At Santiaguito, eight extrusive episodes since 1922 have produced lava lobes and flows 0.5–7 km long, and at Augustine, seven extrusive events have taken place since 1812. On such decadal timescales, paleomagnetic directions of successive lavas might be distinguishable or even describe a coherent secular path among dome fragments that survive, but in blocky silicic lavas the measurements might seldom be precise enough to confirm such patterns.

The eruptive history of Mount St. Helens since ~28 ka (Mullineaux, 1996; Clynne and others, 2008) may offer the closest analogue for the episodic extrusive record at Mammoth Mountain. Several eruptive stages, each a few thousand years long, were separated by dormant intervals that also lasted for thousands of years. During the past 4,000 years, the detailed stratigraphic record at Mount St. Helens indicates numerous eruptive events with a millennial to centennial (and sometimes decadal) frequency. Extrusion of dacite domes at Mount St. Helens was more commonly accompanied by pumice-rich eruption columns than at Mammoth Mountain, but the unsystematic timescales and the millennial episodes of dormancy appear to have been similar at both volcanoes.

Volcano Hazards

Since 1980, seismicity, deformation, CO_2 discharge, and changes in local hydrothermal systems have stimulated scientific and societal concern in the Mammoth Lakes area, prompting intensive and continuous monitoring by scientists of the Volcano Hazards Program of the U.S. Geological Survey (USGS). The unrest and monitoring have been interpreted and summarized by Hill and others (2002), Hill and Prejean (2005), and Hill (2006). Several Fact Sheets were prepared to interpret the ongoing processes for the general public (Sorey and others, 2000; Hill and others, 1997, 2014; Farrar and others, 2007). The USGS California Volcano Observatory Web site provides background, maps, images, monitoring data, and frequent updates for Long Valley and Mammoth Mountain (http://volcanoes.usgs.gov/observatories/calvo/).

The Mammoth Mountain trachydacitic system erupted many times during a 50,000-year-long interval (100 ka to 50 ka) but not at all during the last 50,000 years, suggesting that it is moribund. The dozens of basaltic and intermediate vent sites (~230 ka to ~8 ka) peripheral to Mammoth Mountain, however, outline a 10-by-20-km footprint for the mantle-derived magmatic flux that was intrinsic to generating the Mammoth Mountain silicic anomaly at its center. If the 1989 seismic swarm directly beneath the Mammoth Mountain edifice represented mafic dike emplacement at 7–9 km depth (Hill and others, 1990), and if the ensuing thousands of brittle-failure earthquakes that extended from 6 km to as shallow as 1 km below the summit represented propagation of a pressure front of magmatic fluid through a pre-existing fracture network (Prejean and others, 2003; Hill and Prejean, 2005), then this supports our inference that the trachydacitic magma reservoir had indeed solidified during the past 50,000 years. Moreover, it is implicit that the source of the ongoing CO_2 discharge is mafic magma, not silicic.

Midcrustal seismicity and CO_2 discharge under and around the Mammoth Mountain edifice persist in 2014, providing convincing evidence for mafic magma storage deep beneath the footprint today. In addition to abundant shallow brittle-failure seismicity (Prejean and others, 2003) under and within the edifice, numerous long-period (LP) earthquakes take place at depths of 10–18 km beneath the mafic vent array, from Mammoth Mountain to Red Cones and Devils Postpile (Pitt and Hill, 1994; Hill, 1996; Pitt and others, 2002; Foulger and others, 2003; Hill and Prejean, 2005). The area underlain by the LP array is marked by an extraordinary conductive heat-flow anomaly (3.75 heat-flow units in a 250-m hole drilled in granitic unit Kmo near Devils Postpile; Lachenbruch and others, 1976b), and it coincides with an extracaldera salient in the gravity low (Carle, 1988) that extends from Mammoth Mountain to Pumice Butte and Devils Postpile, an area uniformly underlain by the same Cretaceous granite.

All the evidence thus suggests that the next eruption on or near Mammoth Mountain should be of mafic magma, which has here typically produced scoria cones and derivative lava flows. Examples close to the edifice include the Red Cones (unit brc) eruption of ~8 ka and several more vent cones—near Deadman Pass (unit mdn, ~17 ka), Crater Flat (mcv, ~33 ka), Minaret Summit (bar, ~90 ka), and Mammoth Crest (bmc, ~92 ka). The vent cones for units mcl (~175 ka) and mkv (~153 ka) are directly adjacent to densely developed parts of Mammoth Lakes township, as is the Mammoth Knolls rhyolitic edifice (rmk, 100 ka). A new mafic eruption in the area from Red Cones to Pumice Butte is unlikely to do more than ignite a forest fire and rain fine ash on downwind settlements, but a recurrence in the Lakes Basin or around the eastern half of Mammoth Mountain could cause severe damage to property and the local economy. An eruption in the bed of the Middle Fork (like unit mss, ~121 ka) or an intracanyon lava flow (like units drf, amp, and mdp; 100–80 ka) would disrupt and temporarily impound the river, probably resulting in flooding, both locally and downstream.

Table 3 summarizes the measured lengths of some lava flows in the Mammoth Lakes region. Several mafic lavas flowed through what are now developed areas, and a few extended as far as 10 km or more. The aprons of mafic flows have typically been only ~1 km wide, but units amp, bar, bfh, bsr, and mor broadened to ~2 km locally. The rhyolitic and dacitic lava flows are generally shorter, thicker, and slower moving, but their broader hazard results from associated pyroclastic currents, not from the lava flows themselves.

The Mono Craters domes and their southern extension, the Inyo chain (figs. 2–4), represent a more clear and present threat of eruption, as reviewed by Hildreth (2004). Magmatic components of the late Holocene hybrid Inyo chain have compositional affinities with both the Mono domes and 100-ka rhyolite domes in the west moat of Long Valley Caldera, but they are unrelated (compositionally, spatially, or structurally) to Mammoth Mountain, which shut down ~50,000 years before the first Inyo eruption. The greater Mammoth vent system has a broad footprint that widely straddles the Sierran rangecrest, and the Inyo chain is a narrow linear vent array along the rangefront fault system. It can be inferred that the most likely eruptive recurrence of the Mono-Inyo system would be yet another rhyolite extrusion (with preceding pyroclastic outbursts) along the same alignment. Because a dozen or more such rhyolite eruptions have taken place there in the last 3,000 years, another in our time should not be unanticipated.

Kaye and others (2008) reported that a January 2006 face-to-face survey of employers and employees in the business and tourism sectors at Mammoth Lakes demonstrated only a low to moderate level of volcanic-hazards awareness, despite the long-term engagement of USGS personnel with the community and local authorities. Kaye and others (2009) went on to compare impacts of a dacite extrusion at Mammoth Mountain and a rhyolite extrusion at the south end of the Inyo chain, laying emphasis on effects of pyroclastic density currents associated with dome collapse. Impacts modelled by Kaye and others (2009) are, of course, far greater on and around heavily developed Mammoth Mountain than for an Inyo eruption. Deposits of such currents emplaced in 1350 C.E. extend several kilometers from the Inyo domes, and heavy pumice falls were regionwide (Miller, 1985). For Mammoth Mountain, most or all of its 24 identified extrusions were certainly accompanied by dispersal of pyroclastic ejecta, but nearly all evidence for this has been stripped by glacial erosion.

In the very unlikely event of a revival of dacitic magmatism at Mammoth Mountain, extrusion of another lava dome would probably generate pyroclastic density currents that could overrun parts of the residential, downtown, and ski areas. Timely evacuation would be wise and, no doubt, controversial. Recurrence of an eruption plume like that which deposited pumice-fall unit rfp (~80 ka) might again mantle the township with a few meters of pumiceous fallout.

The most certain things that can be said, realistically, about volcanic hazards here are (1) that a future dome extrusion on Mammoth Mountain is exceedingly unlikely; (2) that a basaltic scoria and lava-flow eruption is of greater likelihood but threatens rather limited downwind and downslope swaths with slow-paced devastation; and (3) that a Mono-Inyo rhyolite eruption is virtually inevitable on a millennial timescale and would impact areas with important highways but few habitations.

Introduction to Description of Map Units

The trachydacite complex of Mammoth Mountain and the array of contemporaneous mafic volcanoes in its periphery form a discrete magmatic system that is thermally and compositionally independent of the adjacent subalkaline Long Valley system (Hildreth, 2004). The Mammoth system first

erupted about 230 ka, last erupted about 8 ka, and remains restless and potentially active. Magmas of the Mammoth system extruded through Mesozoic plutonic rocks of the Sierra Nevada composite batholith as well as through extensive remnants of prebatholithic metasedimentary wall rocks and synbatholithic metavolcanic rocks (Bailey, 1989, 2004). All of the many mafic and silicic vents of the Mammoth system are west or southwest of the concealed structural boundary of Long Valley Caldera; none lie inboard of the caldera's buried ring-fault zone, and only one Mammoth-related vent appears to lie within that zone. Mammoth Mountain has sometimes been called part of the Mono-Inyo volcanic chain, but we regard that assignment inappropriate and misleading. Although the rhyolitic Inyo alignment (which is directed by the range-front fault system) trends toward Mammoth Mountain, the basalt-to-dacite Mammoth vent array is scattered, nonlinear, far broader, and much older. The 10 by 20 km footprint of the Mammoth vent array essentially ignores existence of Long Valley Caldera and the Mono-Inyo alignment. Moreover, the Mammoth Mountain dacite dome complex ended its period of eruptive activity (100–50 ka) well before the principal Holocene interval of Mono-Inyo rhyolitic volcanism.

Here we describe 63 map units that compose the Mammoth basalt-to-rhyodacite system, along with numerous other rock units that crop out within the map area—including 8 rhyolitic units of the Long Valley system, 4 units of the Holocene Inyo Chain, and 32 Tertiary volcanic units. Of the 63 Mammoth units, 17 are phenocryst-rich trachydacite lavas of the main edifice, two are similar trachydacite lava domes (units d61 and d81) that erupted at vents just north of the edifice, and 6 are edifice-based alkalic rhyodacites that carry fewer phenocrysts. Units of the Mammoth system peripheral to the edifice include 13 basalts, 16 mafic andesites, 6 silicic andesites, and 3 distinctly different dacites. All units are listed in table 1.

Usually we prefer to keep volcanic-rock nomenclature simple by basing it entirely on SiO_2 contents: basalt has 47–52 percent SiO_2, basaltic andesite 52–57 percent, andesite 57–63 percent, dacite 63–68 percent, rhyodacite 68–72 percent, and rhyolite more than 72 percent SiO_2. Because the Mammoth suite straddles the alkaline/subalkaline boundary of LeBas and others (1986), however, we largely adopt their nomenclature in the unit descriptions below. Of the basaltic units, some are subalkaline basalts and others are trachybasalts; all more silicic units of the Mammoth suite are alkaline—basaltic trachyandesites, trachyandesites, and trachydacites. Because the six most evolved map units erupted at the Mammoth Mountain edifice have fewer phenocrysts and higher silica contents (70–71 percent) than the volumetricaly dominant trachydacites (63–69 percent), we distinguish them as alkalic rhyodacites. Rhyolites of the Long Valley system are subalkaline, and products of the Inyo chain are complex hybrids.

In the unit descriptions, we abbreviate names of the common volcanic phenocrysts clinopyroxene and orthopyroxene as cpx and opx, respectively. *Phenocrysts* are defined here as 0.5 mm and larger; *microphenocrysts* (mph) as 0.1 to 0.4 mm; and *microlites* smaller still. The modifier *phenocryst-rich* means that a rock has ≥12 percent crystals larger than 0.4 mm; *phenocryst-poor* signifies ≤5 percent; *aphyric* means what it says—none. Rocks containing 6 to 12 percent phenocrysts we typically characterize as moderately porphyritic or of moderate phenocryst content. Because crystal sizes range widely for each species within most thin sections (and more so within map units), we give estimates of combined abundance of phenocrysts and microphenocrysts for each species in each unit, followed parenthetically by the size range measured in thin section for each—from microphenocrysts (>0.1 mm) to the largest crystal observed. [For example, 7–10 percent plagioclase (mph to 4 mm); 2–3 percent olivine (mph to 1.5 mm); and sparse Fe-Ti-oxide mph]. *Antecrysts* are cognate crystals out of equilibrium with their eruptive igneous host but inferred to have been inherited from an earlier stage of the same (thermally or compositionally) evolving magma system. *Xenocrysts* are crystals foreign to the system.

Most of the volcanic map units described here are newly defined, although equivalents of several were defined by Bailey (1989). Each is an eruptive unit derived from a single vent or dike-fed alignment of vents. Some are simple flow units, but many consist of scoria cones and one or several lava flows that have chemical and mineralogical coherence. Most units of the Mammoth Mountain edifice are lava domes, some of which also issued thick coulees 1–2 km long. Each map unit was delineated by field mapping on foot and its integrity confirmed, challenged, or revised by chemical, paleomagnetic, and microscopic work in the laboratory. Definition of a few units required iterative acquisition of field and lab data over a period of years, providing a firm basis for subdividing, lumping, or correlating somewhat heterogeneous packages of lavas. Most units have narrow compositional ranges, but some show zoning or heterogeneity spanning ranges of a few percent SiO_2.

SiO_2 contents reported in the description of each volcanic unit are based on major-element analyses (appendix) normalized on an anhydrous basis, determined by x-ray fluorescence methods in the U.S. Geological Survey laboratory at Lakewood, Colorado, supervised by J.E. Taggart, or in the Washington State University GeoAnalytical Laboratory, supervised by J.A. Wolff and R.M. Conrey. FeO* is total iron calculated as FeO.

Geographic names cited in the text are located on the geologic map, on map figures 2–5, and on some photo-figures. Many place names are informal but have long been used locally by the Town of Mammoth Lakes and the Mammoth Mountain Ski Area. Measurements are metric, as are elevations (except along north fringe of our map where contours are available only in feet). Grid references to site locations mentioned in the text are given to 100 m using the Universal Transverse Mercator (UTM) grid, zone 11 (North American datum of 1927), which is shown on U.S. Geological Survey topographic maps of the area. The first three digits are easting, and the second three are northing. For example, the summit of Mammoth Mountain is approximated as 208/665, 20.8 km east, 66.5 km north. Occasionally, a fourth digit is added for

precision to 10 m. The U.S. Geological Survey 7.5-minute quadrangles (1:24,000) on which the map is based are Bloody Mtn., Convict Lake, Crestview, Crystal Crag, Dexter Canyon, June Lake, Mammoth Mtn., Old Mammoth, and Whitmore Hot Sprs, all in California.

The basaltic trachyandesite of June Lake (unit mjl), which is described here and depicted on the map of Bailey (1989), lies just north of our map area near June Lake (fig. 3). Three more units of basaltic trachyandesite (Tmcl, Tmel, Tmwc), deemed significant to volcanic investigations in the San Joaquin River drainage system, are plugs that lie just west of our map (fig. 3).

For three mafic eruptive complexes, pyroclastic vent cones and lava-flow aprons are physically separated by erosion or younger deposits. Vent-cone units bed, bmc, and mkv are correlated with lava-flow units bcd, bfh, and mmc, respectively. Although several lines of evidence support the correlations, we retain independent designations to avoid the appearance of dismissing uncertainties explained in the unit descriptions.

Ages are estimated for all units, on the basis of mutual stratigraphic positions, numerous new $^{40}Ar/^{39}Ar$ age determinations, and relationship to glacial erosion and deposits. In unit descriptions, ages not credited to other sources were determined in this study (table 2). The radioisotopic age determinations were made in the U.S. Geological Survey geochronology laboratory at Menlo Park, California, supervised by A.T. Calvert, following methods described in Calvert and Lanphere (2006) and Muffler and others (2011).

Apart from the pre-Cenozoic basement rocks (not fully remapped by us), most units mapped are Pliocene or Quaternary. The Pliocene-Pleistocene boundary has recently been redefined at 2.588 Ma (Gibbard and others, 2009). Boundaries between early, middle, and late Pleistocene are widely agreed to be ~780 ka and ~126 ka (Gradstein and others, 2004). The formally defined boundary between the Pleistocene and Holocene is not very useful here, even as modified to 11.7 ka (Walker and others, 2009), because deglaciation took place several thousand years earlier.

DESCRIPTION OF MAP UNITS

SURFICIAL DEPOSITS

Surficial deposits are subordinate for the purposes of this volcanological map. They are mapped principally where such deposits form discrete landforms or are extensive enough to prevent inference of underlying rocks. Talus and colluvium are commonly omitted where subjacent volcanic units are identifiable or inferable with confidence. Surficial deposits are depicted extensively on the geologic map of Bailey (1989), and some are discussed in detail by Kesseli (1941a, b), Curry (1968, 1971) and Lipshie (1974).

pe **Phreatic ejecta (late Holocene)**—Poorly sorted fines-rich debris ejected in steam explosions from Inyo Craters in 1350 C.E. and, at uncertain times, from crater clusters west of Inyo Craters (Mastin, 1991) and from small craters beneath Chair 11 at northwest toe of Mammoth Mountain. Ejecta blankets extend 50–300 m radially from lesser craters but as far as 1 km northeastward from three principal Inyo Craters, which erupted in continuous sequence from north to south—Summit Crater (on Deer Mountain), North Inyo Crater, then South Inyo Crater (Mastin, 1991). Deposits are typically a few meters thick proximally but as thick as 13 m on east rim of South Inyo Crater and >20 m on walls of North Inyo Crater. Around Inyo Craters, ballistic ejecta are as big as 70 cm and up to 1 m around Summit Crater. Most block-sized fragments are crystal-poor mafic lavas (largely from unit aic) around South and North Inyo Craters. On floor of North Inyo Crater, sparse crystal-rich basaltic boulders are as big as 50 cm and granitoids are as big as 2.5 m, both presumed to have been entrained from unexposed underlying till. Around Summit Crater, white biotite rhyolite (from unit rdm) provided both ejected blocks and much of the cream to buff deposit matrix. Smaller and less abundant fragments from Inyo Craters include Early rhyolite tuff and lava (from unit rer) as well as granitoids and metavolcanics (both probably from subsurface gravels or till); Mastin (1991) tabulated lithologic proportions of finer ejecta. Ejecta around Summit Crater (3–10 m thick) likewise include granitoids and mafic lavas (crystal-poor and crystal-rich) but no fragments of oxidized crystal-poor mafic agglutinate from nearby unit mdm. Where exposed on crater walls, deposits are crudely stratified in meter-scale plane-parallel beds that show no evidence of erosion between successive eruptive pulses. Phreatic deposits around the three principal craters rest directly upon the pumice-fall deposits of the magmatic Inyo eruptions; because alignment of the phreatic craters extends that of the magmatic vents (unit ric), all are inferred to have resulted from southward propagation of a rhyolite dike (Miller, 1985; Eichelberger and others, 1984, 1985, 1988).

The West Crater and Middle Crater clusters of Mastin (1991) lie 0.5–1 km west of the three principal craters and, although undated, likewise erupted soon after the 1350 C.E. Inyo pumice falls, upon which their phreatic ejecta blankets rest. Ejected blocks include granitoids, metavolcanics, and Pliocene mafic lavas (all probably from till) as well as crystal-poor and crystal-rich Quaternary mafic lavas. Predominance of crystal-poor mafic lavas in the ejecta blanket, many meters thick, around the Middle Crater cluster suggests presence of buried lava flows like those exposed in South Inyo Crater (unit aic).

Phreatic ejecta beneath Chair 11, ~200–400 m southwest of Main Lodge in Mammoth Mountain Ski Area, issued from a contiguous pair of small craters (Bailey, 1989) now bulldozed for ski runs and a reservoir. Where undisturbed, deposit is >10 m thick, thinning to ~1 m within 100 m laterally. It directly underlies 1350 C.E. Inyo pumice falls (fig. 13) and rests on a layer of white crystal-poor rhyolitic ash (2–4 cm thick), which is thought to have erupted at Mono Craters. The poorly sorted, unconsolidated phreatic deposit consists of medium-gray mud that encloses subangular-to-subrounded matrix-supported clasts—exclusively of Mammoth Mountain lavas. Where deposit is ~1 m thick, clasts are 1–35 cm across; where deposit is proximally thickest, clasts are as big as 1 m and many are in mutual contact. Internally, deposit has modest porosity (especially around big clasts) that facilitated interstitial steam flux, which produced irregular lenses and patches of red, orange, and yellow alteration of matrix mud. Swelling clays impart

puffy texture to pale gray dried external surfaces. Matrix and clasts are thought to represent underlying till and colluvium remobilized by phreatic blasts.

Additional phreatic craters were depicted 500–700 m north of Lincoln Peak on northeast slope of Mammoth Mountain (three craters by Bailey [1989], four by Huber and Rinehart [1965a]), but our repeated scrutiny has identified neither explosive fragmental deposits nor thermal or fluid alteration effects. The sites have been groomed for several ski runs, but undisturbed areas between such runs consist only of rhyolitic unit rce, derivative regolith and colluvium, and limited patches of till

p **Pumice deposits (late Holocene)—**Pumice falls, local proximal pyroclastic-flow deposits, and derivative reworked deposits, all resulting from Inyo Chain eruptions of unit ric. Shown only where thick enough (≥2 m) to obscure underlying rocks sufficiently to prevent inference of their extent. Deposited by series of subplinian eruptions in 1350 C.E. (Millar and others, 2006). Within western half of map area, pumice mantle was originally ubiquitous, combined product of two successive outbursts from Deadman Creek vent and a third from Glass Creek vent (Miller, 1985; Nawotniak and Bursik, 2010; see unit ric). Deposits are unconsolidated and consist of pale-gray to cream, biotite-plagioclase rhyolite pumice lapilli, along with crystal-vitric ash and minor accidental lithic fragments. Combined primary thickness as great as 10 m near vents, 8 m on White Wing Mountain, and ~1 m near Mammoth Mountain and Devils Postpile. Widely sloughed from slopes and redeposited in areas of low local relief

rg **Rock glacier deposits (Holocene)—**Lobate masses of coarse angular debris that originated as talus, became impregnated with interstitial ice, and flowed glacier-like downslope (Wahrhaftig and Cox, 1959). Of many such masses nearby in the Sierra Nevada (Kesseli, 1941a; Rinehart and Ross, 1964; Millar and Westfall, 2008), typically on north-facing scarps that shed copious blocky rockfall debris, two are mapped here, east of Mammoth Rock, where each extends ~1.5 km north from headwalls of Mesozoic granodiorite (unit Krv). Both consist mostly of angular to subangular granodiorite blocks—commonly up to 1 m and as big as 5 m. Eastern deposit is forested and apparently inactive (rg'); it overlaps Tioga-age moraines, which (unlike these rock glaciers) contain abundant blocks of metavolcanic rocks in addition to granodiorite. Western deposit is more barren but divisible into two parts: (1) a lower subdued apron that supports scattered trees, has lost its flow morphology by collapse into chaotic jumbles that overlap Tioga moraines, and has probably been long inactive (rg'); and (2) an active upper lobe (rg) that has barren rugged surface, arcuate transverse flow ridges and furrows, and steep flow front 60 m high that probably dates from the Little Ice Age (~1350–1850 C.E.). Surface of active segment slopes 20º and has 32º front; inactive surfaces of both rock glaciers slope ~10º and have subdued convex fronts. Unusually low elevations (2,500–2,700 m) make it unlikely that either originated as (or evolved from) a debris-mantled ice-cored glacier (see Clark and others, 1994). Debris mantle insulates interstitial ice, permitting its perennial survival and flowage at elevations well below regional equilibrium-line altitude (ELA) for true glaciers. Till (unit glb) subjacent to talus from degrading fronts of both rock-glacier deposits can be distinguished by presence of blocks of unit bhl (31±1 ka) derived from Lakes Basin

sd **Spring deposits (Holocene and late Pleistocene)—**Postglacial aprons of travertine, tufa, and siliceous sinter, principally at southwest end of Mammoth Meadow below Mammoth Rock and The Bluff. Low-relief, sparsely vegetated prairie capped by surficial spring deposits crops out over 250 by 300 m area that slopes ~3º eastward toward marshy flatland and golf course. Springs are apparently inactive recently. Surface is largely calcareous, along with patchy exposures of sinter best revealed in gullies 1–2 m deep. Both lithologies are porous, mostly soft and crumbly deposits rich in fossil plant fragments; sinter is typically white and vaguely stratified on gully walls; travertine generally pale gray or off-white; both erode to flakes and slabs. Deposits postdate and overlap till along prairie margins; they are overlain by thin alluvium encroaching from mouth of steep ravine to west, and they interfinger distally with subhorizontal silty pond and marsh deposits. An organics-rich dark-gray silt layer, 3.5 cm thick, exposed along shallow arroyo cut in deposit of spring carbonate and white silt (at UTM 032505/416520), yields an uncalibrated radiocarbon age of 1,640±20 ^{14}C yr B.P.

Isolated travertine deposits a few meters thick, ~250 m southwest of prairie just described, drape bedrock and colluvial slopes below Mammoth Rock. Hidden Lake, adjacent to spring-deposit prairie, is not a maar or volcanic crater but simply a shallow pond impounded by a minor berm of meadow mud and turf bound together by willows; no ejecta surround it.

Sinter deposits also crop out along fault zone north of Hot Creek, across from fish hatchery, where they overlie units ss and oal as well as rhyolite-rich colluvium. Deposits are irregular and porous or laminated and dense. About 2.5 km northwest of there, in lower Fumarole Valley (UTM 341/690), an eroded sinter deposit rich in silicified marsh vegetation crops out as slabby ledge ~5 m high. Crude layers are 5–40 cm thick; some layers preserve fibrous vegetation in upright growth positions. At northwest end of ledge, intercalated layers of rhyolite-rich sandstone suggest proximity of paleoshoreline of Pleistocene Long Valley Lake (at elevation 2,170 m)

al **Alluvium, undivided (Holocene and late Pleistocene)—**Unconsolidated, water-transported mud, sand, gravel, and bouldery debris deposited in or adjacent to active, ephemeral, or recently abandoned streams; includes local marsh and pond deposits

fan **Alluvial fan deposits (Holocene and late Pleistocene)—**Sheets of boulder-bearing gravelly detritus deposited intermittently below mouths of steep gulches that drain southern wall of Long Valley Caldera east of Laurel Creek. Merges uphill into talus cones and distally into lower-gradient alluvium of various ages (mostly oal). Deposition of fans has continued since caldera formation at 767 ka and remains potentially active at times of torrential runoff or major rockfall, but exposed surfaces are dominated by late Pleistocene detritus. East of map area, numerous similar fans along east and northeast margins of Long Valley postdate, overrun, and widely obscure highstand strandlines of Long Valley Lake that were cut in later part of middle Pleistocene

oal **Older alluvium (late and middle Pleistocene)—**Stream deposits of various ages now undergoing erosion and dissection; largely unconsolidated. Includes glacial outwash, terrace gravels, and low-relief distal reaches of some alluvial-fan deposits. In northeast and southeast areas of map, unit is subdivided (where exposure permits) into successively younger (inset) stages—$oal_{1,2,3}$. Their absolute ages are poorly constrained, but all are inferred to be middle or late Pleistocene, MIS 6 or younger. Alluviated lowlands are commonly veneered by aeolian material rich in sand and pumice, still subject to recurrent reworking, that widely conceals subjacent alluvium.

Postcaldera sources of unit oal within map area include the following: (1) north moat, collecting contributions from Clark and Alpers Canyons, Glass Creek, and northwest moat via Deadman Creek; (2) Dry Creek, which flowed vigorously during Pleistocene, draining Mammoth Mountain and west moat; (3) “Powerline Canyon” (UTM 370/760), draining northeast sector of resurgent uplift; (4) Little Hot Creek, draining east sector of resurgent uplift; (5) Mammoth Creek/Hot Creek, which drains glaciated terrain east and southeast of Mammoth Mountain; (6) Sherwin and Laurel Creeks, which drain caldera’s southern wall and south moat; (7) Convict Creek and Tobacco Flat, which drain glacial deposits at Sierran front, feeding alluvial apron between Hot Creek flow and Lake Crowley. Contrasting alluvial clast assemblages reflect different basement rocks, volcanic units, and glacial deposits exposed in each sector.

Alluvium of all ages (units al and oal) transported by Little Hot Creek and “Powerline Canyon” is almost exclusively phenocryst-poor rhyolite because only Early rhyolite (unit rer) crops out in their drainage systems.

Wide swath of older alluvium extending from Laurel Creek to Convict Creek is late Pleistocene glacial outwash, supplemented by slopewash near rangefront. Exposures are as thick as 10 m in quarries north and west of Mammoth airport, where fluvial beds are 0.1–1 m thick and include subordinate pebble-rich matrix-supported debris-flow deposits and lenses of silt and sand. Rounded pebbles, cobbles, and sparse boulders are predominantly granitic and metasedimentary but include sparse dacites from Mammoth Mountain, rare clasts of (west moat) biotite rhyolite, and sparse basalts, among which are clasts from units bfh (92±2 ka) and bcd (125±2 ka). These gravels overlie units bfh, bsr, and mlc (130±1 ka). Lack of Early rhyolite (unit rer) clasts indicates stream transport

was from west, principally from Laurel and Sherwin Creeks, with little contribution from north. Farther east, oal from Laurel Creek merges with Tioga-age outwash from Convict Creek, which consists of metasedimentary, granitic, and carbonate clasts and lacks clasts of Quaternary volcanic rocks.

East of Convict Creek, 1-km-wide, gently sloping gravel bench (designated oal_1; 2,140–2,180 m elevation) consists of glacial outwash (>40 m thick) associated with high lateral moraine of Convict Creek (see unit gud) assigned to Tahoe glaciation by Sharp (1969) and now inferred to have been deposited during MIS 6. Pebble-cobble stream gravel in abandoned quarry (UTM 400/648), 1.3 km south of Whitmore Hot Springs, consists predominantly of metasedimentary clasts accompanied by sparse granitoids and lacks clasts of Quaternary volcanic rocks. Adjacent fan draining Tobacco Flat, designated oal_3, though morphologically younger, has same clast asemblage and shares same morainal source but is probably of Tioga age (MIS 2).

Swath of older alluvium (oal_1) that extends 8 km east from Arcularius Ranch along north moat of caldera is thicker than 12 m in quarry at UTM 362/785. Includes abundant pebbles and cobbles of metasedimentary, granitic, and metavolcanic rocks, phenocryst-poor mafic lavas, and Early rhyolite (unit rer; ~700 ka), plus common clasts of unit rnc (~500 ka), along with sparser clasts of Pliocene dacites, and Pliocene olivine basalts. Lack of dacite clasts from Mammoth Mountain or clasts of nearby unit bar (~90 ka) suggests that this extensive outwash sheet dates from MIS 6. Most alluvium along north moat underlies lava flows of unit bar (~90 ka). Inset swaths designated oal_2 carry same clast assemblage but may date from MIS 2. Gravels and pebbly sands in quarry (UTM 403/717), 400 m south of Cashbaugh Ranch, are as thick as 8 m. Pebbles, cobbles, and rare boulders enclosed in sand-silt matrix were deposited in thin to thick beds, some clast-supported but mostly matrix-supported. Predominant clasts are hornblende-biotite (west moat) rhyolite, Sierran metasediments, and phenocryst-poor basalt, along with sparser olivine-plagioclase basalt, Early rhyolite, granites, metavolcanics, and sandstone. Few clasts are larger than 5 cm, except scoriaceous basalts, which range up to 12 cm. Site is directly east of resurgent uplift and close to Mammoth Creek/Hot Creek, the latter being the principal contributor of its gravels. On quarry floor, gravels rest on tan sand and white stratified lake silt as well as primary pumice-fall deposit of unit rfp (70.4% SiO_2; 80±8 ka), here as thick as 91 cm. Gravel sheet carrying same clast suite extends 200 m north and 1 km south of Cashbaugh Ranch buildings, capping bluffs of sandstone and siltstone.

Coarse oal gravels at Dry Creek Sand Flat (UTM 303/762) are exposed to a depth of ~7 m where incised by an intermittent Holocene alluvial wash. Most clasts are Early rhyolite (unit rer), locally derived and subangular to subrounded. Well-rounded pebbles and cobbles are predominantly crystal-poor mafic lavas and scoria but include crystal-rich mafic lavas, Mammoth Mountain trachydacite, and rare granodiorite. Chemical analyses of mafic clasts confirm contributions from units mcl (175±3 ka), mnd (66±2 ka), and mdn (16–17 ka). Derivation of clasts from west moat along course of intermittent Dry Creek, which seldom flows vigorously today, suggests transport during Last Glacial Maximum (MIS 2). Presence of rhyolite and basalt boulders as large as 1–3 m suggests intermittent flood flow down late Pleistocene Dry Creek, which incised narrow 50-m-deep gorge through dense rhyolite of subunit rlm just downstream from Dry Creek Sand Flat

pal **Precaldera alluvium (early Pleistocene)—**Fluvial gravels that crop out just north of Long Valley Caldera in a belt that extends ~3 km from west of lower Alpers Canyon to upper Clark Canyon. Largely unconsolidated but locally cemented, the clast-supported gravels are seriate from pebbles to boulders and have a gritty matrix of coarse sand; some exposures are crudely stratified and gently dipping. Most clasts are rounded or subrounded, many are 20–50 cm across, and some are 1–2 m. Predominant clast types are varied metasedimentary rocks and various mafic lavas, while granitoids, quartzite, and hornblende-biotite dacite are also common; subordinate are clasts of phenocryst-poor felsite and welded tuff of unit Trac. Clasts of nearby Bishop Tuff (unit rbt, 767±2 ka) are absent. Gravels here represent oldest stream deposits exposed in map area, directly underlying Bishop Tuff and resting principally on Pliocene basalts and locally on units

Jbs and Trac. Clasts are of northerly derivation and not outwash from Sierran sources. A local scattering of 1–2 m boulders (UTM 299/802), interpreted by Bailey (1989) as Sherwin Till, is more likely a lag of deflated stream gravel, as it lies 5 km east of range-front till deposits (unit gst), and its clast assemblage is far more varied than the till near Crestview. Erosion of the pal gravel sheet, widely 50–70 m thick, facilitated headward retreat of overlying cliffs of Bishop Tuff along Alpers and Clark Canyons, producing deep embayments lined by scarps of welded tuff. Gravels probably represent main course of precaldera Owens River, which extended southeast across later site of caldera to Owens Gorge, where river had cut deep canyon in granodioritic basement rocks long before emplacement of Bishop Tuff

av **Rockfall avalanche deposits (Holocene and late Pleistocene)**—Sheets or tongues of monolithologic rubble fallen from steep scarps. Principal example here is apron of debris that wraps around east base of Dome 2861 (unit d61) and extends into 1-km-long tongues at northeastern and southeastern toes of dome. Unstratified monolithologic deposits consist of pale gray dacite blocks, some tinted pinkish and mostly angular, typically 10–50 cm across but rarely as big as 2 m, in a gritty pale gray matrix, which is nonindurated and seriate from gravel to fine sand. Blocks weather tan, and most are dense or finely vesicular, and glassy, partly glassy, or devitrified. Where southeast tongue overlaps till of unit gmm, it lacks the black and brick-red vitrophyre blocks (from Mammoth Mountain sources) predominant in the till. Northeast apron banks against Dry Creek Dome (unit rdc), exhibits subdued hummocks with 10–20 m relief, and appears to be modified and truncated by lateral moraine of late Pleistocene Dry Creek glacier. Roadcut in northeast apron is exceptionally matrix-rich and conceivably exposes a pyroclastic facies of unit d61, but no prismatic blocks or thermal effects of blocks on matrix were observed. Deposits were probably emplaced piecemeal from steep-sided dome over extended time interval.

Lesser rockfall deposits mapped on southwest wall of caldera near Mammoth Rock consist of angular blocks of granitoids and metavolcanics. Such deposits grade into piecemeal talus slopes, which we largely ignore on this map. A small rockfall avalanche from steep flow front of one of the unit dnw coulees emplaced a narrow blocky deposit that armors right-bank terrace of Deadman Creek for 200 m eastward (UTM 237/7775); many blocks exceed 1 m, but there is no equivalent deposit on left-bank terrace. Another avalanche mass, ~100 m wide, fell from east scarp of unit bmc and lodged just southwest of Crystal Lake

s **Surficial deposits, undivided (Holocene and late Pleistocene)—**Generally combinations of glacial, fluvial, pond, aeolian, and reworked fallout deposits or locally mixed accumulations of till, talus, protalus, or other colluvium. Widely omitted; mapped principally where such deposits form discrete landforms or are extensive enough to prevent inference of underlying rocks. Bulldozed ski runs on Mammoth Mountain combine debris that had naturally been colluvium, till (unit gmm), aeolian sand, and Inyo pumice falls (unit p).

Numerous pits, typically 2–4 m deep and 10–30 m across, excavated by Mammoth Mountain Ski Area to control storm and snowmelt runoff, currently entrap slurries that consist principally of sand and silt flushed from loose surficial debris and carry sparse dispersed clasts of Inyo pumice or Mammoth Mountain lavas and pumice. In low-relief areas around toe of Mammoth Mountain and on benches and swales higher on the edifice, such excavations commonly expose older slurry deposits beneath layers of 1350 C.E. Inyo fallout. Such diamicts could be misinterpreted as small pyroclastic-flow deposits. Sparse clasts in such diamicts are principally subangular to subrounded dense fragments (mostly 1–10 cm across) of texturally varied lavas, along with subordinate pumice, all exclusively trachydacites and alkalic rhyodacites of Mammoth Mountain. In most pits, pumiceous and hydrothermally altered clasts are sparse or absent, and sand-silt matrix is fresh and nonindurated.

In a few pits beneath 1350 C.E. fallout, there is also a massive sandy layer (30–112 cm thick), probably aeolian, that carries sparse pumice granules and sparser lapilli (as big as 4 cm) of Mammoth Mountain biotite-bearing rhyodacite pumice (like those of unit rfp). Such tan to orange-brown layers of massive sand overlie coarser diamicts thought to

be ground moraine. Sieve analyses at four sites yield median diameters (Md) that range 0.2–0.4 mm (medium sand) with 4–11 wt% silt and only 4–10 wt% coarser than 2 mm. A charcoal lens within a 45-cm-thick sand layer excavated at UTM 200/687 (near Chair 11) gave an age of 1,970±20 ^{14}C yr B.P. Charcoal layer that separates 112-cm-thick layer of massive sand from an underlying paleosol developed on diamict (probably till) at UTM 192/683 (along Reds Lake Road) gave 4,130±25 ^{14}C yr B.P. (fig. 13).

Along resurgent graben system that cuts Early rhyolite (unit rer), several shallow depressions crossed by Highway 395 contain multicomponent surficial deposits (unit **s**) eroded into small ridges with 10–20 m of local relief. Exposure is poor, owing to aeolian veneer, Inyo pumice falls, and near-absence of Holocene streamflow. At north end where graben is crossed by course of ephemeral Dry Creek, such ridges reveal small exposures of Pleistocene gravel (UTM 275/749 and 282/745) that includes cobbles of crystal-poor mafic lavas, hornblende-biotite rhyolite, and trachydacite of Mammoth Mountain, indicating late Pleistocene transport from west moat. Near junction of Sawmill Cutoff with Highway 395 (UTM 280/740), another 15-m-high ridge has scattered clasts of nearby units mcl and rer as well as sparser clasts of metasedimentary and granitic rocks that probably originated at west wall of caldera. As indicated by their clast contents and volcanic units they bank against, these depression-filling deposits are younger than 66±2 ka and their relief owes to late Pleistocene streamflow. A few kilometers farther south, Smokey Bear Flat (UTM 290/730) is a large flat-floored depression surrounded by Early rhyolite; lacking relief and streamflow, its depth of fill is unknown and its floor is covered by aeolian deposits, Inyo pumice, and rhyolitic pea gravel. At south end of graben, another depression (UTM 303/683; west of geothermal plant) includes a 10-m-high east-west ridge of surficial fill incised by Highway 395; in addition to pebbles of local units rer and bcd (125±2 ka), fill has sparse clasts of granitic unit Kmo and common clasts of hornblende-biotite rhyolite (100–150 ka).

eb **Explosion breccia deposit of Bailey (late Pleistocene)**—Unconsolidated heterogeneous assemblage of erratic blocks atop low-relief crest of granitic ridge 3044 (Hemlock Ridge; fig. 7), which buttresses west flank of Mammoth Mountain. Along most of 600-m-long crest of ridge, rocks exposed through Inyo pumice cover are exclusively loose clasts of porphyritic granite (unit Kmo), rounded to subangular, pebbles seriate to 2-m boulders, plucked and redistributed from local bedrock by ice. Limited to a 50-m-long strip (~20 m wide) on southwest slope of saddle along crest, however, abundant granite boulders are joined by blocks of crystal-poor mafic lavas, biotite rhyodacite, and various felsite and vitrophyre clasts containing hornblende, biotite, and feldspars—each clast type as big as 30–75 cm. Seven chemically analyzed clasts are identified as Mammoth Mountain rhyodacites and trachydacites and andesite of Mammoth Pass (unit amp). Interpreted tentatively as accidental ballistic ejecta from a (phreatic?) outburst on Mammoth Mountain; unit was probably more widely distributed but survived glacial scour only in saddle.

South of our map area, Bailey (1989) also assigned to this unit comparable lithic assemblages sparsely scattered on upland surfaces; those atop the Pliocene erosion surfaces of Mammoth Crest and Red Mountain, however, are not ejecta from Mammoth Mountain but are, instead, clasts of rhyolite, dacite, and basalt derived from a precaldera volcanic highland on the later site of Long Valley Caldera.

lmd **Diamict of lower Mammoth Creek (late Pleistocene)—**Unconsolidated, unstratified, poorly sorted deposit ~10 m thick that makes up hill 2200+, just south of Mammoth Creek, ~1 km east-southeast of Casa Diablo geothermal plant. Hill is 400 m long, 200 m wide, and poorly exposed; though possibly matrix-dominant, many large blocks protrude from sideslopes in clusters. Hilltop is veneered with fine sandy-pebbly aeolian sediment, through which very few blocks are exposed. Counts of clasts larger than ~10 cm (n=300) yield 43% phenocryst-poor mafic lavas, 14% phenocryst-rich mafic lavas, 28% hornblende-biotite-feldspar rhyolite, 2% phenocryst-poor Early rhyolite (unit rer), 4% dacites of Mammoth Mountain, 8% Mesozoic metavolcanics, 1% granitoids, and <1% schistose metasedimentary rocks. Clasts 10–50 cm across are abundant and those 50–200 cm across are not uncommon; many are rounded to subrounded, but numerous blocks of mafic lava (whether massive or scoriaceous, crystal-rich or crystal-poor) are

subangular to angular. Blocks of mafic lava in the deposit are correlated chemically with units mkv, mmc, bcd, bsr, and possibly asr—all within the local drainage area and none farther than 6 km from the deposit. Occurrence of clasts of youngest local units (bsr, bcd; both ≤125 ka) shows deposit is not MIS 6 Casa Diablo Till (unit gcd), nor derived therefrom. Deposit is neither alluvium nor till, though subordinate rounded cobbles may have been entrained from such deposits. Probably some kind of mass-flow deposit, but it entrained little or no material from nearby moraines, which are rich in granitoids, metavolcanics, and Mammoth Mountain trachydacites. Overlies unit bfh (92±2 ka)

ss **Sandstone of Long Valley Lake (middle Pleistocene)—**Littoral apron of well-indurated sandstone, grit, and pebble conglomerate that sloped gently eastward and northeastward into former Long Valley Lake (Mayo, 1934b; Rinehart and Ross, 1964; Bailey, 1989). Unit crops out over ~18 km^2 north and west of Hot Creek and also covers ~9 km^2 east of the Hot Creek flow (unit rhc) beyond our map area. Strata range from laminae to beds as thick as 30 cm; most are planar or broadly low-angle lenticular but locally cross-bedded or deltaic. They are silica-cemented, seldom carbonate-cemented. Sorting is moderate to good, but average grain size of alternating layers ranges widely from medium sand to pebble gravel. Subordinate layers of fine sand and silt are more common distally and conglomeratic layers abundant proximally. Within map area, sediment was derived predominantly from phenocryst-poor Early rhyolite (unit rer); accordingly, pebbles and sand grains are glassy, devitrified, or pumiceous rhyolite plus minor derivative feldspar and biotite (and locally quartz, presumably from Sierran sources). Many rhyolitic clasts are angular or subangular, reflecting nearby provenance. East of Hot Creek flow, Sierran sources provide a greater contribution of sand and gravel of granitic and metasedimentary origin. Exposed thickness of unit is as great as 25 m, but drill holes north and east of Hot Creek flow penetrated >300 m of lake sediments, a significant but unquantified fraction of which is sandstone and rhyolite-pebble conglomerate (Smith and Rex, 1977; Sorey and others, 1978; Lewis, 1975; Fournier, 1989). Overlies and interfingers distally with ash-rich, fine-grained, diatom-and-ostracod-bearing lacustrine silt and siltstone. Interfingers proximally with pumiceous lava-flow breccias of unit rer and in distal drillholes with pyroclastic facies of Early rhyolite (subunit rtav) beneath caldera's southeast moat. Deposition presumed to have begun in early postcaldera time (~760–650 ka) and persisted until well after 330-ka emplacement of Hot Creek flow, which both overlies and is overlain by sandstone strata. Sandstone surrounds (and locally coats) ledge of unit mcl (179.5±2.4 ka) near Casa Diablo geothermal plant. At slightly lower elevation ~1.2 km southeast of that ledge, no sandstone or other lake sediment overlies extensive lava flow of unit bsc (172±2 ka), suggesting withdrawal of lake in that time interval. Unit is widely overlain and concealed by aprons of late Pleistocene alluvium (unit oal). Sandstone is overlain by subaerial pumice fall of unit rfp (80±8 ka) near Cashbaugh Ranch

st **Siltstone of Long Valley Lake (middle Pleistocene)—**Fine-grained lacustrine basin facies of Pleistocene Long Valley Lake (Mayo, 1934b; Rinehart and Ross, 1964; Bailey, 1989). White to pale gray silt, clay, and fine sand is horizontally layered, laminated to thin bedded, and weakly indurated. Puffy surface crusts decimeters thick, promoted by swelling clays, typically conceal well-bedded deposits. Unit is exposed discontinuously over ~60 km^2 area, largely in Long Valley lowland east of map area but also in dissected terrain between Hot Creek and Little Hot Creek. Exposures are generally 10–20 m thick, their upper surfaces armored by sandstone or veneers of pebbly alluvium. Drill holes north and east of Hot Creek flow penetrated >300 m of lake sediments, a significant but unquantified fraction of which is siltstone (Smith and Rex, 1977; Sorey and others, 1978; Lewis, 1975; Fournier, 1989). Large proportion of the fine sediment is derived from rhyolitic ash of unit rer. Unit contains widely dispersed diatoms and ostracods, as well as common tan layers 1–3 cm thick that consist almost entirely of ostracod shells and thin white laminae of nearly pure diatomite. Intercalated tephra layers 1–30 mm thick are also widely exposed. Unit is overlain by littoral sandstone/conglomerate facies of Long Valley Lake (unit ss) and is interbedded with it at a few exposures (more extensively so in subsurface); also overlain by units oal and al. Hot Creek and Owens River have cut broad shallow floodplains on the siltstone unit, which there widely floors marshes, wet

meadows, and alkali flats. Where preserved on hillocks in Long Valley, the primary top surface of siltstone is generally near 2,100 m elevation; in reentrant between Hot Creek and Little Hot Creek, however, sandstone/siltstone contact climbs to 2,150 m. Lake Crowley is not a remnant of the Pleistocene lake but a reservoir created by completion of Long Valley Dam in 1941

GLACIAL DEPOSITS

Late Pleistocene glacial deposits are here divided into four lithologic assemblages that reflect provenance and a fifth undifferentiated catch-all that includes moraines peripheral to the study area, poorly exposed deposits, and patchy remnants. All or nearly all are thought to be products of the last Pleistocene glacial episode (Marine Isotope Stage 2; MIS 2), conventionally called the Tioga glaciation in eastern Sierra Nevada (Blackwelder, 1931). A few modest distal moraines near Laurel and Sherwin Creeks were assigned older ages by Bailey (1989), but it seems prudent to leave them undifferentiated until surface exposure dating can confirm pre-Tioga ages. The 40-odd nested moraines north and south of Mammoth Creek, including the most distal, contain basaltic blocks of unit bhl (31±1 ka), so they are clearly not of MIS 4 age or older. No evidence is recognized here for MIS 4 or "early Wisconsin" glacial deposits (historically assigned to "Tahoe glaciation"). Elsewhere in the eastern Sierra Nevada, many deposits long called Tahoe Till (Blackwelder, 1931) have been shown by surface exposure dating (Phillips and others, 1996, 2009; Rood and others, 2011) to be pre-Wisconsin, deposited at 165–130 ka (during MIS 6). Useful discussions and illustrations of glacial deposits in and near the map area were provided by Kesseli (1941b) and Rinehart and Ross (1964).

Tioga advances ranged between 28 and 15 ka (Phillips and others, 1996, 2009); retreat from Last Glacial Maximum positions began by 19 ka (Rood and others, 2011); and glaciers had retreated to the Sierran crest by 15–14.5 ka (Clark and Gillespie, 1997). Recess Peak moraines (bracketed between 14.2 and 13.1 ka; Clark and Gillespie, 1997; Gillespie and Zehfuss, 2004), which occur in Sierran cirques higher than 3,300 m, are not present within the map area, as only a few summits reach such an elevation. Nor are there locally any Little Ice Age cirque moraines (roughly 1350–1850 C.E.), although some are present at higher elevations elsewhere in the Sierra. Nor has evidence been found in the Sierra for glacial deposits of Younger Dryas age (12.9–11.5 ka; Gillespie and Clark, 2011) nor of early Holocene age.

Degraded glacial deposits of MIS 6, locally called Casa Diablo Till (Curry, 1968, 1971), are preserved on both sides of Mammoth Creek, 1–2 km outboard of the most distal Tioga-age moraines. Sherwin Till, older than the 767-ka Bishop Tuff and probably deposited during MIS 22, crops out northwest and southeast of Long Valley Caldera.

gcc **Till of Cold Water Canyon (late Pleistocene)—**Glacial deposit dominated by clasts of metavolcanic rocks (unit Mzmv) transported northwestward down Cold Water Canyon to Lake Mary and Panorama Dome. During major ice advances, such material merged with and medially mixed with granite-dominant debris (units glb and gcd) quarried by ice from Mammoth Crest. Clast counts at Panorama Dome (n=450) give 80–90% metavolcanics, 10–20% unit bhl (31±1 ka), and <3% small granitoids; around Lake Mary, metavolcanic clasts exceed 95%, and in Cold Water Canyon, they approach 100%. By contrast, adjacent till of unit glb near Twin Lakes outlet is granitoid-dominant and has common clasts of Mammoth Mountain dacites as well as subordinate clasts of units Mzmv and bhl. Deposit contains many 2–3 m boulders and represents final glacial advance along Cold Water and upper Mammoth Creeks; ice followed a deep narrow canyon from cirque headwalls at elevations as high as 3,350 m (11,000 ft). Overlies units bhl, ddl, ddu, dom, and dtl; younger than all contiguous units except al and sd. Banks against, overlies, and locally grades into unit glb, deposited contemporaneously during MIS 2

gdc **Till of Dry Creek (late Pleistocene)—**Lobe of glacial till as wide as 3 km that extends along both sides of Dry Creek from base of Mammoth Mountain to sharp terminus 8 km northeast. Marked by few prominent moraines, hummocky sheet appears to reflect ablation of dead ice of a debris-laden piedmont lobe. West margin obscured by Inyo pumice-fall

deposit (unit p) related to unit ric (1350 C.E.). Clasts in till near Dry Creek are predominantly basaltic but include abundant trachydacite from Mammoth Mountain (100–50 ka). Clast count (n=374) in Scenic Loop roadcut (UTM 259/743) gave 51% crystal-poor mafic lavas, 20% Mammoth Mountain lavas, ~8% each of units ddc, bar, and bmn, and 4% hornblende-biotite rhyolite. Along fault scarp 1.5 km farther west (UTM 245/738), clast count (n=175) gave 53% crystal-poor mafic lavas, 12% Mammoth Mountain lavas, 18% ddc, 13% bar, 4% bmn, and no rhyolite. Few stones are larger than 1 m. Lack of basement clasts shows that ice came from Mammoth Mountain, not from caldera's southwest wall. Deposit overlies units d61 (87±2 ka) and mor (66±2 ka); till is younger than all contiguous units except Inyo pumice fall and phreatic ejecta of 1350 C.E. Deposited during MIS 2

glb **Till derived from Lakes Basin (late Pleistocene)—**Set of 40-odd nested morainal ridges and associated ground moraine that extends 6 km eastward from outlet of Mammoth Lakes Basin to area of Sherwin Creek campground, where its most distal end moraine is breached by Mammoth Creek. Till was deposited during MIS 2 by a broad piedmont glacier that terminated ~1.5 km short of the Casa Diablo moraines of MIS 6 (unit gcd). Some morainal ridges are as high as 40–50 m, and numerous drill holes adjacent to such ridges penetrated 10–90 m of till (fig. 6). Moraine surfaces are boulder-rich, sharp-crested, and little weathered. Boulders are dominantly granitoids but include metavolcanics, mafic lavas, Mammoth Mountain dacites, and rare metasedimentary rocks. Source of ice-transported debris was principally Lakes Basin with lesser but important contributions from south slope of Mammoth Mountain and granodiorite and metavolcanic debris from rangefront scarp south and east of Mammoth Rock. North of Mammoth Creek, stones in till are 80–90% porphyritic granite (unit Kmo) as big as 5 m, ~5% crystal-rich basalt of unit bhl (31±1 ka) as big as 3 m, and 3–5% metavolcanics, also as big as 3 m; sparser constituents are stones from big-feldspar basaltic unit bmc, crystal-poor scoria and lava clasts of units mcl and amp, fine-grained granitoids, and rare hornblende-biotite rhyolites. Northernmost moraines are poor in metavolcanics and carry only sparse Mammoth Mountain dacites, but both of these clast groups are present in inner moraines close to Mammoth Creek. South of Mammoth Creek, granodiorite stones (unit Krv) derived from south wall commonly outnumber porphyritic granites (unit Kmo) derived from Lakes Basin; in southernmost moraines granodiorite typically dominates, but metavolcanics are also abundant and are locally dominant; sparser constituents are boulders of units bhl, amp, and various Mammoth Mountain dacites. Few clasts of unit bmc are present south of Mammoth Creek. Innermost moraines south of Mammoth Creek are poor in Mammoth Mountain dacite but relatively enriched in porphyritic granite; during recession, shrinking axial ice from Lakes Basin flowed principally through a Twin Lakes outlet trough already deeply incised through several Mammoth Mountain dacite units. Whether entire nested moraine set represents Last Glacial Maximum and its recessional stillstands awaits testing by surface-exposure dating; presence of clasts of unit bhl (31±1 ka) in all moraines on both sides of Mammoth Creek as far east as confluence of Sherwin Creek nonetheless proves that all were deposited during MIS 2, not in early or middle Wisconsin time. Deposits overlie units amp (97±1 ka), bhl (31±1 ka), ddl (58±2 ka), dtl (76±1 ka), asr, bsr, and mcl

gmm **Till derived from Mammoth Mountain (late Pleistocene)—**Two tongues of glacial till that extend eastward from sources exclusively on Mammoth Mountain. One extends 3 km from northeast base of Mammoth Mountain into downtown Mammoth Lakes; second extends 3 km along valley between Dragons Back and Lincoln Peak as far as Juniper Ridge. Linking the tongues, till west of Camp High Sierra grades up steep east-facing scarp of Timber Ridge into colluvium rich in rhyodacite of unit rce. Sandy-gravelly fines-poor matrix dominates and encloses boulders and smaller stones that are nearly all (>99%) Mammoth Mountain dacites and rhyodacites (100–50 ka), accompanied by sparse mafic lavas and rare metavolcanic and granitoid clasts. Stones range from subrounded to subangular, and many are 10–50 cm across but rarely 1–2 m. In contrast to granitoid boulders, ice transport of Mammoth Mountain dacites tended to re-fracture rather than round them. Major outcrop area in residential neighborhood that extends from Canyon Lodge to downtown is an irregular terrain of hills and short ridges with 15–30 m

local relief; abundance of small moraines and weak development of lateral moraines may reflect short runout of glaciers and overloading of ice by debris from numerous brecciated silicic lava domes. A few elongate moraines, all east-trending, include Juniper Ridge, ridges just east of The Village, a ridge just north of Forest Trail, and another along valley 1 km south of Lincoln Peak (Gold Hill ski run); the last is actually a medial moraine (without laterals) squeezed between convergent ice sheets that draped slopes of Dragons Back and Lincoln Peak. Although they were deposited in large part contemporaneously, distal till of unit gmm overlies till of unit glb along an abrupt contact, from which we infer that ice advancing down Mammoth Mountain outlasted retreat of the Lakes Basin glacier from distal lowlands. Their contrasting compositions are readily compared on adjacent moraines of Juniper Ridge (gmm) and Lone Tree Hill (glb). Northern tongue was previously interpreted as deposit of a debris-avalanche from Lincoln Peak (Bailey, 1989), but it lacks hummocks, megablocks, and composite blocks; its varied Mammoth Mountain clasts (64.0–70.5% SiO_2; n=12), moreover, are not derived principally from Lincoln Peak, which in any case lacks evidence for an amphitheater or other avalanche scar. Volume of 3-km^2 northern tongue of unit gmm (~0.1 km^3) alone exceeds that of Lincoln Peak (unit dlp). Very sparse boulders of mafic lava in unit gmm are correlated chemically with units bhl (31±1 ka), aml, amp, and mcl. Deposits overlie units d81, dtl, rce, rss, glb, scoria cone mcl, and bank against units mkv, bsm, mcl, and rmk. Overlain by rockfall avalanche deposits from Dome 2861 (unit av) and by Inyo pumice-fall deposits (unit p; 1350 C.E.). Deposited during MIS 2

gud **Undivided glacial deposits (late and middle Pleistocene)—**Moraines at Sherwin, Laurel, and Convict Creeks, moraines buried by Holocene pumice-fall deposits in caldera's west moat, and discontinuous till remnants near Middle Fork San Joaquin River canyon, are largely or entirely of Tioga age—broadly of last major glacial episode during MIS 2. Several distal lobes of Sherwin, Laurel, and Convict Creek moraine complexes may be pre-Tioga (fig. 21), as suggested by Rinehart and Ross (1964), Sharp (1969), and Bailey (1989), but this is unproven. Scattered patches of till along ice-scoured Middle Fork canyon and ground moraine west of Mammoth Pass consist largely of locally derived material. Speculation by Fullerton (1986) about middle Pleistocene glaciation near Reds Meadow was based on a K-Ar age far too old for intracanyon lava of Devils Postpile (unit mdp), now dated at 82±1 ka. Main occurrences of unit gud are the following.

Till of west moat. Glacial deposits in caldera's west moat, poorly exposed beneath late Holocene pumice-fall deposits (unit p), form several buried moraines between Crater Flat and Deadman Creek. Scattered erratic blocks and sparse gully exposures through pumice cover indicate that clasts from Mammoth Mountain are uncommon, granitoid clasts are abundant, and clasts of metamorphic rocks, Pliocene lavas, and units ddc, bar, and bmn are all ubiquitous but subordinate. Dacite erratics from Mammoth Mountain on divide northeast of Minaret Summit (UTM 188/695) provide evidence that some late Pleistocene ice flowed north-northwestward from edifice along ridgecrest, as well as northward toward Dry Creek.

Till of Convict Creek. Main components are (1) north-trending lobate complex, 2 km wide and 3 km long, constructed of many nested loop and lateral moraines, and (2) older northeast-trending double-crested lateral moraine, 3 km long and >300 m high; both were characterized in detail by Sharp (1969) and not restudied by us. Sharp (1969) reviewed several previous interpretations of moraine-emplacement sequence and concluded that entire lobate complex (plus set of seven lateral moraines just east of Convict Lake and north-trending lateral moraine along east side of Convict Creek) are all of Tioga age (MIS 2). Sharp (1969) showed the enormous northeast-trending lateral moraine to be older and, by regional comparison, inferred it to be of Tahoe (early Wisconsin) age, but he suggested that it might conceal still older buried till. Surface exposure dating (Phillips and others, 2009) has shown many eastern Sierra Nevada moraines long called Tahoe to have been deposited 165–130 ka (MIS 6). Stones are predominantly metasedimentary and granodioritic, along with subordinate metavolcanics.

Till of Laurel Creek. Moraine complex, ~3 km long and as wide as 1.5 km, that extends north from canyon of Laurel Creek to caldera floor near Sherwin Creek Road;

characterized by Rinehart and Ross (1964) and not restudied in detail by us. Treeless Laurel Creek moraines contain subordinate granodioritic debris but consist predominantly of metasedimentary material, in contrast to adjacent Sherwin Creek moraines, which are densely forested (see fig. 36 of Rinehart and Ross, 1964) and consist almost exclusively of granodiorite till, suggesting lithologic or edaphic control of vegetation. A sharp-crested lateral-terminal moraine loop that closes at ~2,560 m elevation is generally thought to be of Tioga age (MIS 2). Older lateral moraines that extend ~1 km farther north and 300 m lower (fig. 21) are morphologically more subdued though lithologically similar; their termini at 2,260–2,300 m are similar in elevation to Casa Diablo Till (unit gcd) of Mammoth Creek, only 2–4 km north, suggesting that they too could have been deposited during MIS 6 (or alternatively during early MIS 2). Prominent alluvial fans issuing from these distal moraines may in part be comparably old.

Till of Sherwin Creek. Massive apron, 3 km wide, of unusually coarse till that emerges from two rangefront canyons and extends ~3 km farther northward on both sides of Sherwin Creek to caldera floor near Sherwin Creek Campground. At least 200 m thick, complex deposit includes a few modest longitudinal ridges distally but lacks high lateral moraines typical of most canyon-mouth glacial deposits in eastern Sierra Nevada. Till consists almost entirely of granodiorite (from unit Krv) derived from steep canyon walls; abundant boulders armoring deposit are commonly as big as 2–5 m. Jointed bedrock of narrow cirque-canyons so overloaded glaciers with coarse debris that glacier rheology (and morphology of resulting deposit) approached those typical of rock glaciers, as noted by Kesseli (1941b) and Rinehart and Ross (1964). At northeast extremity of deposit, two morainal ridges, each ~40 m high, diverge ~700 m beyond main lobe; although emplaced before massive main lobe, neither appears definitively older on basis of boulder weathering or soil development. Nonetheless, they could be either early MIS 2 lateral moraines that predated overloading of ice that led to construction of the massive rock-glacier-like lobe atop them or, alternatively, they could represent MIS 4 or 6. Eastern distal ridge of Sherwin Creek moraine complex (UTM 301/650) is relatively unforested (unlike other Sherwin Creek glacial deposits); although armored by granodiorite boulders like rest of complex, its matrix contains abundant pebbles and cobbles of metasedimentary rocks, which apparently inhibited forest development as on adjacent Laurel Creek moraines (see fig. 36 of Rinehart and Ross, 1964). Like distal Laurel Creek moraines, it probably predates main advance of LGM (fig. 21). Excepting this anomalous northeasternmost moraine, distal till of Sherwin Creek laps against units bsr (99±1 ka) and amp (97±1 ka), showing that voluminous Sherwin moraines were deposited in late Pleistocene (not during MIS 6)

gcd **Casa Diablo Till (latest middle Pleistocene)—**Subdued glacial deposits preserved in two swaths—a northerly one along and north of Sawmill Road and a southeasterly one that extends across Highway 203 and Mammoth Creek. Sawmill Road swath extends 3 km eastward from near Shady Rest Park, locally includes a low moraine crest, and is exposed to thicknesses as great as 20 m. Boulder counts (n=328) yield 80% granitoids, 9% metavolcanics, and 11% mafic lavas; abundant granitoids are 0.5–2.5 m in diameter; metavolcanics are typically 10–40 cm but as big as 1 m; mafic lavas are typically 10–80 cm, massive or vesicular, and of low to moderate phenocryst content. Southeast swath, which extends 1.2 km southeastward, is lithologically different, and its thickness exceeds 30 m at Mammoth Creek. Boulder counts (n=836) on a prominent knoll 120 m north of Highway 203 (UTM 300/675) gave 27% granitoids, 56% metavolcanics, 16.5% mafic lavas, and two clasts of hornblende-biotite-feldspar rhyolite. A second site (n=183) on a ridgetop 200 m south of Highway 203 (UTM 301/6715) gave only 5% granitoids, 10% mafic lavas, and 85% metavolcanics. At both southeasterly sites, average clast size is somewhat smaller than in Sawmill swath: granitoids are typically 10–50 cm and rarely up to 2 m; metavolcanics typically 5–50 cm but up to 1 m; and mafic lavas 5–50 cm. Clasts of Mammoth Mountain dacites (100–50 ka) are absent at all sites. The two swaths were probably distal lateral moraines of a single 10-km-long valley glacier that descended from accumulation areas in and near present-day Mammoth Lakes Basin; there is no need to appeal to Ritter Range sources. Right-lateral moraine was supplied predominantly

Figure 21. Bare moraines of Laurel Creek and forested moraines of Sherwin Creek. View southwest from Sherwin Creek Road toward south wall of Long Valley Caldera. Green swath at left is Laurel Creek. Rangefront scarp, here as high as 1,200 m, is largely granodiorite (unit Krv), though reddish rocks along right skyline are pre-batholith Mesozoic metavolcanic rocks along Solitude surface. Predominant material in Sherwin moraines is granodiorite but in Laurel moraines is Paleozoic metasedimentary rocks of Morrison pendant; both high moraines (y, younger) are thought to have achieved present morphology in Tioga glaciation (Marine Isotope Stage [MIS] 2). Lower pair of bare distal moraines in center middle ground (o, older), however, may have formed in MIS 6; they appear to be paired lateral moraines deposited by a glacier with a trajectory intermediate between those of their higher successors. Clasts in low moraine at left are mostly metasedimentary; those in low moraine at right are mixed, uniquely reflecting combined granodiorite and metasedimentary provenance. Basaltic flow front, ~8 m high, on sagebrush flat at right is unit bsr (99±1 ka; 103.5±1.4 ka).

by metavolcanic terrain south and east of Lake Mary; left-lateral moraine mainly by granitic headwall sources between Lake George and Minaret Summit (now partly covered by Mammoth Mountain). Sawmill swath overlies units rer, asr, mcl, mkv, and mmc (160±2 ka); overlain by units bcd (125±2 ka) and bsr (99±1 ka). Southeast swath overlies unit mmc and is overlain by units bcd and bsr. Weathering of granitoid boulders is more advanced than on nearby late Pleistocene moraines. Boulders of mafic lava in Casa Diablo Till are correlated chemically with units bsc (172±2 ka), mkv (153±1 ka), mmc (160±2 ka), msc (154±2 ka), mcl (175±3 ka), and aic (156±15 ka). Unit bsc today crops out only distally relative to gcd glacial deposits. Rare rhyolite clasts in till are probably from unit rwm (~150 ka). Casa Diablo glacial advance took place during MIS 6. Former speculations on possibly older ages for this till were based on K-Ar ages (far too old) for xenocryst-bearing mafic lavas that sandwich Casa Diablo Till and for Mammoth Mountain biotite that carries excess Ar

gst **Sherwin Till (late early Pleistocene)—**Boulder-rich glacial diamict that crops out near Crestview and (southeast of map area) at Rock Creek, Sherwin Hill, and Owens Gorge (Blackwelder, 1931; Putnam, 1960; Sharp, 1968; Bailey, 1989). Not present at Sherwin Creek (see unit gud, above). Moraine ridges are not preserved, but till is as thick as 200 m near Rock Creek and 60 m northwest of Crestview. Till is poorly sorted and unstratified, containing sandy-silty matrix and stones that are everywhere dominantly Sierran granitoids. Metasedimentary clasts are sparse, and, north of caldera, clasts of Pliocene mafic lavas are common. In till northwest of Crestview, many granitic clasts are 0.5–3 m across, mafic lava clasts are generally 5–40 cm, and sparse cobbles of hornblende-biotite-plagioclase dacite probably came from June Mountain. Many granitic stones are grussy, far more deeply weathered than in other tills in map area. Till sheet extends farther out from Sierran rangefront than that of any younger glaciation. Remnant on west rim of Alpers Canyon, shown as till by Bailey (1989), is probably lag of coarse stream gravel (unit pal). Unit overlies Mesozoic granitoids and Tertiary mafic lavas. Overlain directly by Bishop Tuff (767±2 ka), both north and southeast of caldera. Age 50–70 ky older than Bishop Tuff was inferred from weathering of till beneath ignimbrite (Gillespie and Zehfuss, 2004), suggesting correlation of Sherwin glacial advance with MIS 22

PRE-CENOZOIC BASEMENT ROCKS

[Listed in order of increasing age]

Kmo **Mono Creek Granite (Late Cretaceous)—**One of several extensive plutons of megacrystic granite emplaced during terminal stages of 140-million-year-long accumulation of Sierra Nevada composite batholith (Bateman, 1992a, b). Elongate pluton extends >50 km northwest from Pine Creek to Minaret Summit and, within map area, forms Mammoth Crest and underlies parts of Mammoth Mountain and valley of Middle Fork San Joaquin River. Light-colored granite carries several percent alkali-feldspar megacrysts (1–3 cm) in medium-grained (1–5 mm) groundmass. Ranges of mineral contents: 20–35% total alkali feldspar; 20–40% quartz; 30–50% plagioclase; ~5% biotite; and trace amphibole (Rinehart and Ross, 1964; Huber and Rinehart, 1965a; Bateman, 1992a); mafic enclaves uncommon. Foliation is generally inconspicuous except along Rosy Finch Shear Zone (Tikoff and Saint Blanquat, 1997), a steeply foliated belt that encompasses both pluton margin and its metavolcanic wall rocks; zone strikes beneath Mammoth Mountain and is well exposed south of Lake George. Pluton intrudes unit Mzmv and, south of map area, units Pzms and Krv

Krv **Round Valley Peak Granodiorite (Late Cretaceous)—**Three discrete plutons, lithologically similar, were assigned to this unit (Rinehart and Ross, 1964; Bateman, 1992a, b). Two are in map area, whereas third and largest intrudes Mount Morrison Pendant (Pzms) along Rock Creek farther southeast (Bateman, 1965; 1992b). Within map area, western pluton extends 15 km southeast from Mammoth Rock and forms a northwest-elongate mass 3–5 km wide that separates wall-rock units Pzms and Mzmv. Eastern pluton, only 3 km wide and equant in plan view, intrudes Pzms sequence on Long Valley Caldera rim north of Laurel Mountain. Homogeneous and equigranular, rocks have average grain size of 1–2 mm, and euhedral hornblende and biotite are evenly distributed. Mineral contents: 20–35% quartz; 15– 25% alkali feldspar; 45–60% plagioclase; 5–15% biotite; and 1–5% hornblende (Rinehart and Ross, 1964; Bateman, 1992a). Mafic enclaves are not abundant but are far more common than in nearby granitic unit Kmo.

Subunit Krv' represents dikes of leucogranite (70% SiO_2) inferred to have issued from the western Krv pluton. One cuts Pzms strata at ~2,575 m elevation just north of Mammoth Rock, and another cuts unit Mzmv at 3,100 m on the crest of Red Mountain. Each is 20–25 m wide and crops out along strike for ~250 m. Both are coarse grained and carry only sparse mafic crystals

Kjl **Granite of June Lake (Late Cretaceous)—**Elongate granitic pluton that forms White Wing Mountain at northwest rim of Long Valley Caldera and extends at least 13 km northwest through June Lake to Grant Lake. Medium-grained hornblende-biotite granite is not strongly porphyritic but contains scattered alkali-feldspar megacrysts—seldom

bigger than 1 cm. Ranges of mineral contents (Kistler, 1966): 11–25% quartz; 22–42% alkali feldspar; 27–55% plagioclase; 5–12% biotite; and 1–6% hornblende. Formerly correlated with Late Triassic megacrystic pluton of Wheeler Crest by Huber and Rinehart (1965a) and Kistler (1966), but reassigned to Cretaceous by Bateman (1992a). Two isolated exposures that intrude Paleozoic metasedimentary rocks along caldera wall east and northeast of Deadman Pass are apparently correlative; quite felsic and medium-to-fine-grained, they have ~74% SiO_2, carry only ~10% mafic minerals, and contain aplitic masses and dikes and locally thick quartz veins. Third and southernmost plutonic outcrop along west wall of caldera, ~2.5 km southeast of Deadman Pass, is different (see unit Mzgd)

Jbs **Granite of Big Springs (Jurassic?)—**One or more plutons that crop out along north margin of Long Valley Caldera, east and west of Big Springs and north and east of Crestview. Exposures locally extend 2–3 km north of caldera margin. Rocks are medium-grained and range from biotite leucogranite to hornblende-biotite granodiorite. Correlated tenuously with faraway Leucogranite of Casa Diablo Mountain (Rinehart and Ross, 1957) by Bateman (1992a), who cited a U-Pb age of 161 Ma for that pluton; unit was described as "quartz monzonite of Big Springs" by Rinehart and Ross (1964), who had mapped both plutons. Exposures north and east of Crestview are more mafic than those near Big Springs, containing 25–30% mafic and accessory minerals. Intrudes unit Pzms

Mzgd **Granodiorite northeast of Minaret Summit (Mesozoic)—**Cliffy exposure of mafic granodiorite, ~1 km long, on west wall of Long Valley Caldera 2 km northeast of Minaret Summit and just northwest of unit bar scoria cone. Medium-grained equigranular rock carries 25–30% mafic and accessory minerals, including anhedral biotite and hornblende-biotite aggregates. Intrudes unit Pzms, includes abundant wall-rock fragments, and injects aplite dikes (1–2 m thick) into metasedimentary host rocks. Pluton is cut, in turn, by two porphyritic granitic dikes (74% SiO_2), each 5–10 m thick, which trend east-northeast and carry quartz and feldspar phenocrysts (1–10 mm) in dark-gray, finely crystalline matrix laced locally by epidote veinlets. A similar porphyritic granitoid dike, 2 km north-northwest of Deadman Pass (UTM 165/754), is 5–15 m thick, strikes ~25° NW, and intrudes vertically foliated unit Pzms for ~150 m; arbitrarily assigned to unit Mzgd, it may or may not be correlative. Unit was correlated improbably by Huber and Rinehart (1965a) and Bailey (1989) with Late Triassic Granite of Lee Vining Canyon (Kistler, 1966; Bateman, 1992a), which has only 2–7% mafic minerals. Main southern outcrop overlain by Pliocene basaltic unit Tbdp. Age unknown but certainly Mesozoic

Mzmv **Metavolcanic rocks of Ritter Range pendant (Mesozoic)—**Heterogeneous assemblage of subaerial (and sparser subaqueous) arc-volcanic rocks of Triassic through Cretaceous age, moderately metamorphosed during intrusion by plutons of Sierra Nevada batholith in Cretaceous. Thicker than 10 km, assemblage was deposited as felsic ignimbrites, varied pyroclastic and volcaniclastic deposits, andesite-dacite lava flows, and subordinate shallow-water sedimentary intercalations (mostly tuffaceous), as described by Rinehart and Ross (1964) and Huber and Rinehart (1965a); see summary by Bateman (1992a, p. 10–13). Deformed during Cretaceous plutonism, sequence now forms steeply west-dipping homoclinal section that extends west to Ritter Range and strikes northwest from south of Mammoth Rock through Minaret Summit, west of caldera rim. Within map area, intruded by major Late Cretaceous plutons Kmo and Krv

Pzms **Metasedimentary rocks of Mount Morrison pendant (Paleozoic)—**Deep-water continental-slope and submarine-fan sedimentary deposits of Cambrian through Permian age, moderately metamorphosed during intrusion by plutons of Sierra Nevada batholith in Mesozoic. Assemblage thicker than 7 km consists of calc-silicate and siliceous hornfels, argillite, chert, limestone and marble, siltstone, sandstone, and quartzite, as mapped and described by Rinehart and Ross (1964), Stevens and Greene (1999), and Greene and Stevens (2002). Sequence was coeval with shallow-water continental-shelf and platform deposits now exposed in White-Inyo Mountains to southeast. Assemblage makes up much of south wall of Long Valley caldera; components of it also crop out on west and north walls (Bailey, 1989) and have been penetrated in drill holes deep beneath caldera floor

TERTIARY VOLCANIC ROCKS

[Listed alphabetically by unit label]

A few Miocene and numerous Pliocene volcanic units crop out beneath or around the periphery of the Mammoth Mountain volcanic field, principally around the rim of Long Valley Caldera and on valley walls of the Middle Fork San Joaquin River.

Tacc **Trachyandesite of Crater Creek (Pliocene)**—Pair of glacially eroded knobs of phenocryst-poor andesite (58.3–62.6% SiO_2) on east rim of Crater Creek canyon, 2 km north of Pumice Butte (fig. 10). Centered ~1 km apart, both knobs are elongate northeast-southwest. Larger northeast knob is 600 m long with 90 m relief, whereas southwest knob is 300 m long with 50 m relief. Both consist of pale-to-medium-gray massive lava, locally mottled, that weathers tan or pale pink and disintegrates into chaotic talus of blocks, plates, and slabs that reflect crude flow foliation. Rocks are nearly aphyric but contain hornblende needles (0.2–2 mm long), some with swallowtail morphology; trace amounts of olivine (0.5–1 mm), opx (0.5–1 mm), and cpx (2–4 mm long, some in clusters) are present. Both knobs also contain common xenocrysts of 1-mm quartz, singly or in clusters, with reaction rims; less common are composite xenocrysts of quartz and cloudy feldspar; free feldspar crystals (1–4 mm) are rare and probably also xenocrystic. Lack of exposure in saddle between knobs leaves unresolved whether they are separate domes or eroded parts of a once-continuous coulee. Two analyses of northeast knob yield 61.3–62.6% SiO_2 whereas two of southwest knob yield 58.3–58.7% SiO_2, suggesting separate domes; the four analyses, however, define linear compositional arrays for most elements. Steep north face of southwest knob exhibits near-vertical jointing, but lack of oxidation, ejecta, or breccia provides no suggestion of vent features. Unit rests on Mesozoic granite and lavas of unit Tasj (9.164±0.017 Ma). $^{40}Ar/^{39}Ar$ age: 4.29±0.20 Ma (G.A. Mahood, unpublished data, 2010)

Taec **Trachyandesite east of Crestview (Pliocene)—**One or more phenocryst-poor lava flows (57.1% SiO_2) exposed for ~600 m along both walls of distal reach of southeast-draining gulch at southwest toe of Dome 8325 (unit Td83), ~1 km east-northeast of Crestview. Crops out as massive, block-jointed ledges typically 3 m high, with locally exposed relief as great as ~8 m. Phenocrysts: None. Sparse olivine microphenocrysts (0.1–0.4 mm), many iddingsitized; rare feldspar xenocrysts broken, sieved, and resorbed. Banks against unit Td83 (3.42±0.08 Ma). Overlain by flows of units Tb84 and Tmcv. Source vent buried; may be an early product of Cone 8478. Undated

Tasj **Trachyandesite of San Joaquin River (Miocene)—**Glaciated phenocryst-rich lava flows (58.0–58.1% SiO_2) and subjacent intrusive mass that extend for ~1.1 km along east wall and rim of Middle Fork canyon, north and west of Pumice Butte and ~7 km southwest of Mammoth Mountain. On plateau near rim, as high as 2,820 m, massive lavas are ice-scoured into smooth swells, nubbins, and ledges, their surfaces typically polygonally jointed, locally columnar, and widely glassy or partly so. Cliffy outcrop is as thick as 250 m at its north end where it fills a reentrant in the granitic canyon wall, there displaying glassy chunky structure with local tiers of short irregular columns; lower half is probably intrusive. Phenocrysts: 15–20% plagioclase (0.5–2.5 mm); ~1% cpx (0.5–2 mm); <1% olivine (0.2–1mm); and scattered Fe-Ti oxide mph. Unit intrudes and rests on Mesozoic granite (unit Kmo). Overlain by units Tacc (4.29±0.20 Ma) and a62. $^{40}Ar/^{39}Ar$ age: 9,164±17 ka. A trachyandesite lava flow as thick as 75–85 m at Kennedy Table near Millerton Lake Reservoir (Huber, 1981; Bateman and Busacca, 1982) on San Joaquin River (fig. 2), 66–85 km downstream and 2,400 m lower in elevation, is mineralogically and chemically similar and yields a $^{40}Ar/^{39}Ar$ age of 9,192±15 ka

Taww **Trachyandesite north of White Wing Camp (Pliocene)—**Phenocryst-poor lava flows (59.0–59.7% SiO_2) that form southeast-facing caldera-wall scarp east of Glass Creek flow and ~700 m north of White Wing Camp. Unit crops out in a few ledges and buttresses for ~1 km along 80-m-high scarp. Ledges suggest presence of several flows, but mantle of pumiceous scree from 1350 C.E. Inyo ejecta obscures most of unit. Unit may be thicker than 80 m, but upland slope above scarp rim is covered by Inyo

ejecta. Outcrops are flow-foliated, nonvesicular, slabby or irregularly block-jointed, and pale gray, weathering orange-brown or gray-brown. Phenocrysts: 1–3% olivine (0.5–2.5 mm); sparser cpx (0.5–1 mm); and 1–2% microphenocrystic plagioclase laths, rarely longer than 0.5 mm. Overlies unit Tmwo (3,153±26 ka) near Glass Creek. Overlain on caldera rim by unit Tmcv. K-Ar age: 2,950±90 ka for outcrop at UTM 241/790 (Mankinen and others, 1986)

Tbbs **Basalt east of Big Springs (Miocene)—**Phenocryst-poor mafic lava flows (49.8–51.9% SiO_2) preserved as 500-m-wide remnant south of uppermost Owens River, midway between Big Springs and Arcularius Ranch. Deeply weathered rock disintegrates into dark gray corestones with crumbly brown rinds. Unit has ~40 m relief on south wall of river gorge, but base is not exposed there. Poorly exposed remnant of vent cone, 1.2 km north-northwest of Big Springs, includes oxidized scoria bombs as big as 30 cm. Contains only sparse olivine mph, contrasting with phenocryst-rich Pliocene mafic lava flows to east and west. Banks against granite of unit Jbs; overlain by units Trac (~11.7 Ma) and rer. Undated

Tbdp **Trachybasalt of Deadman Pass (Pliocene)—**Stack of numerous mafic lava flows on San Joaquin Ridge between Minaret Summit and Deadman Pass (figs. 3, 4, 7). Samples analyzed range in SiO_2 from 50.4 to 53.2%. Flows are subset of sequence that continues along ridge beyond map area, altogether for 12 km northwest as far as Clark Lakes and Agnew Pass (Huber and Rinehart, 1965a; Chaudet, 1986; Bailey, 1989, 2004). Within map area, at least 30 flows range in thickness from ~3 m to >70 m, supporting benches and cliffs widely frost-riven into slabby ledges. Cliffs, 200 m high, ~1 km east of Deadman Pass, expose stack of ~20 thin rubbly flows, capped by a few flows 15–40 m thick. Entire sequence is as thick as 300 m on east-facing caldera wall and as thick as 450 m where it filled a paleotributary of Middle Fork on southwest-facing side of San Joaquin Ridge, ~1 km south of Deadman Pass (fig. 9). Dark gray in fresh interiors, most exposures are weathered and resinous; whether massive or vesicular, slabs and hackly blocks typically carry orange-brown weathering rinds 1–2 cm thick. Unit includes degraded scoria cone ~250 m wide, on west rim of main ridge (UTM 182/715); cone consists of brick-red lapilli and sparse bombs in palagonitized coarse ash matrix, arranged in decimeter-to-meter-scale fall layers that dip 15º–20ºW or NW; east half of cone is covered by surficial debris. Flows contain 5–15% olivine (0.5–2 mm, commonly altered); some (generally thicker) flows also have 1–5% cpx (1–5 mm) and abundant Fe–Ti oxide mph; but none carry plagioclase phenocrysts. Zeolites and veinlets of silica and carbonate are common. Overlies pre-Cenozoic basement rocks. Overlain by Pliocene trachydacite pyroclastic deposits of units Tdpd and Tdsj (Bailey, 1989, 2004; Bailey and others, 1990). K-Ar age: 3.15±0.1 Ma (Dalrymple, 1964a; recalculated by ^{40}K decay constants of Steiger and Jäger, 1977) for flow at east rim of stack. $^{40}Ar/^{39}Ar$ ages: 3,700±12 ka for lowest flow in channel-filling stack (UTM 170/719) just east of Agnew Meadows; 3,277±7 ka for top flow of stack, on caldera rim (UTM 191/720) ~2 km east and 400 m higher

Tbld **Trachybasalt south of Lost Dog Lake (Pliocene)—**Two glaciated remnants of olivine-rich basalt (51.9–52.1% SiO_2) 0.6–1.3 km south of Lost Dog Lake and ~7 km west of Mammoth Mountain summit. North remnant is east-trending lava ridge, 100 m wide, 350 m long, and as thick as 20 m at its eastern scarp. South remnant is 200 x 400 m across and likewise thickest at its eastern scarp, which exposes 10 m of massive lava atop 10 m of agglutinated red scoria fall and a lower 10 m slope concealed by its own blocky talus. Vent complex, centered on south remnant, consists predominantly of agglutinated red scoria lapilli but includes scoria bombs as big as 30 cm and angular lava fragments up to 40 cm. Lava flows are dense, massive, and dark gray, weathering orange-brown or pale gray-brown; rock splits on irregular fractures into angular blocks on scarps and on sets of parallel hairline fractures into plates and flakes on ice-scoured ridgetop surfaces. Weathering rinds are commonly 1–1.5 cm thick. Phenocrysts: 5–7% olivine (0.1–1.2 mm); no plagioclase or pyroxene phenocrysts; Fe-Ti oxides limited to finely crystalline groundmass. Also contains sparse quartz xenocrysts as big as 5 mm and scattered anhedral feldspar xenocrysts (1–4 mm). Compositionally unrelated to nearby basalt of The Buttresses (unit btb). Rests on Mesozoic granite. $^{40}Ar/^{39}Ar$ age: 3,353±31 ka

Tbmm **Trachybasalt of Mammoth Mine (Pliocene)—**Olivine-rich basaltic lava flow (51.8% SiO_2; 9.1% MgO) preserved as 300-m-wide remnant, high on northwest nose of Red Mountain, ~1 km northeast of Lake Mary and 400 m southwest of Mammoth Rock. Single flow, inset along gently inclined paleoswale cut in Mesozoic metavolcanic rocks, wedges out southeastward but is as thick as 80 m at its northwest limit on sidewall cliff of glacially excavated outlet of Lakes Basin. A gulch cut into basalt surface by a successor stream trends northwestward, apparently parallel to the paleochannel filled by the lava flow. Cliff-forming lava breaks into meter-scale massive blocks and slabs that form long steep talus. Source vent unknown. Unit is type locality of Mammoth Reversed-Polarity Subchron of the Gauss Normal-Polarity Chron (Doell and others, 1966). Phenocrysts: 7–10% olivine (mph to 2.5 mm); plagioclase, pyroxene, and oxides limited to groundmass, which is holocrystalline. K-Ar age: 3.15±0.1 Ma (Dalrymple, 1964a; Doell and others, 1966; recalculated by ^{40}K decay constants of Steiger and Jäger, 1977). Four small basalt remnants, 1–2 km southeast along southwest rim of Red Mountain, first correlated by Rinehart and Ross (1964) with unit Tbmm, are compositionally different and are here assigned to unit Tbrm

Tbpl **Trachybasalt east of Pond Lily Lake (Pliocene)—**Glaciated stack of phenocryst-rich lava flows (48.8–51.7% SiO_2) that extends 2 km along east wall of Middle Fork San Joaquin River canyon as far as nose above its convergence with Fish Creek, ~10 km south-southwest of Mammoth Mountain. Above exposed base at rim of 2,100-m shelf traversed by Pacific Crest Trail, ledgy stack is as thick as 300 m. About ten ledges crop out in particular sections, and total number of flows is ~20. Massive zones are 5–15 m thick, slabby or hackly, locally vesicular, and commonly polygonally jointed to columnar; one flow at north limit of outcrop is ~30 m thick. Flows are dark gray, weathering pale gray to tan and typically having 1-cm-thick weathering rinds. Within stack of flows, two unstratified intervals of coarsely blocky, oxidized autobreccia are each ~20 m thick; most blocks are nonvesicular, suggesting fragmentation during downslope flow rather than proximity to vent. Vent location unknown, but attitudes of flows and breccia sheets and interflow unconformities indicate flow directions toward west and southwest, not southward along Middle Fork canyon. Phenocrysts: all flows examined have 5–10% olivine (0.3–1.5 mm); most contain 1–5% cpx (0.1–2 mm, commonly in clusters); plagioclase is limited to groundmass and rare xenocrysts (as big as 3 mm); rimmed quartz xenocrysts (also up to 3 mm) are not uncommon. Samples analyzed are unusually rich in Sr (fig. 20*D*). Unit rests directly on Mesozoic granite (unit Kmo). Overlain by unit rbt (767±1 ka). Undated

Tbrm **Basalt of Red Mountain (Pliocene)—**Glaciated remnants of single flow of olivine-rich basalt (49.9–50.3% SiO_2) aligned along southwest rim of Pliocene erosion surface just east of Lake Mary. Four remnants, each 15–25 m thick, extend linearly but discontinuously for ~1 km, banked against Red Mountain sidewall of Lakes Basin, along and just below scarp rim, apparently channeled by what was then a shallow paleovalley. Base of remnants is ~100 m higher than that of compositionally different Pliocene basaltic unit Tbmm, which lies ~1 km northwest. Compared to unit Tbmm, unit is richer in Fe, Ca, and Sr and poorer in SiO_2, K_2O, P, Ba, Rb, and Zr. Remnants form dark gray ledges, slabby or block-jointed, and mostly massive but locally retaining upper vesicular facies. Phenocrysts: 8–10% olivine (mph to 3 mm); common Fe-Ti-oxide mph. Unit rests exclusively on Mesozoic metavolcanic basement. Undated

Tbtb **Basalt of The Buttresses (Pliocene)—**Stack of severely glaciated phenocryst-rich lava flows (46.5–50.6% SiO_2) that form stairstep benches just west of Middle Fork San Joaquin River, southwest of Devils Postpile. Main remnant is ~1 km wide and extends 2 km north-south; consists of several flows, individually 15–40 m thick, altogether at least 100 m thick, but draping granitic basement to produce local relief of ~170 m. A 300-m-long columnar outlier lies south of King Creek at southwest surviving limit of unit. Three more outlying remnants, ~1 km west of main one, extend to elevation of 2,750 m, ~470 m higher than base of unit along Middle Fork. Several ledge-forming flows have tiers of bold vertical columns, typically 30–80 cm wide and locally as tall as 10 m; elsewhere flows are block-jointed, or intricately hackly jointed with spacings of 10–30 cm, or

locally exhibit crude variously oriented columns. Except for rubbly breccia zones locally exposed, flows are massive, nonvesicular, and (though phenocryst-rich) have aphanitic crystalline groundmass. Rocks are dark gray, weathering gray-brown; weathered surfaces are speckled by crystals (1–3 mm) of olivine and cpx (or clusters thereof) that stand out in relief. Along 300-m-long reach of Middle Fork that begins 400 m south of Devils Postpile, unit Tbtb drapes steep west-bank granite wall all the way to riverside, indicating that river has here simply re-incised its pre-basalt channel and cut no deeper during entire Pleistocene. Above river and elsewhere, zones of interflow autobreccia as thick as 8 m are conspicuous; angular dense clasts and subrounded vesicular clasts coexist within clast-supported pale-gray matrix of unstratified coarse ash; yellow-orange alteration is superficial, confined to fracture films and patchy domains in ash-rich breccia, not penetrative into lava blocks. There is no explosively ejected facies nor evidence for a vent here or elsewhere; vent is inferred to have been far upstream, north or northwest of map area. Phenocrysts: some flows contain 2–3% plagioclase (0.5–1.5 mm, rarely to 3 mm); 7–10% olivine (1–3 mm); and 10–12% cpx (1–2.5 mm), commonly in clusters. Other flows contain no plagioclase phenocrysts but have 5–10% each of olivine and cpx (both as big as 3 mm), including abundant cpx clusters, in olivine-rich groundmass. Contains sparse quartz xenocrysts as big as 6 mm. Sites in north-central and King Creek sectors of unit yield same (reversed) paleomagnetic direction (Hildreth and others, 2014). Rests exclusively on Mesozoic granite. $^{40}Ar/^{39}Ar$ age: 3,754±7 ka

Tb84 **Trachybasalt and basaltic trachyandesite of Cone 8478 (Pliocene)—**Stack of varied mafic lava flows (49.0–55.5% SiO_2) above northwest wall of Long Valley caldera, north and east of Crestview. Vent complex at Cone 8478 is centered 1.5 km north of Crestview. Total exposed relief and apparent thickness ~300 m. Several flows, 5–20 m thick and irregularly block-jointed, are exposed discontinuously as ledges and buttresses through thick mantle of Inyo pumice fall. Interflow breccias zones, 1–5 m thick, are exposed only in roadcuts. Most exposures are massive, only locally vesicular, and pale to medium gray, weathering gray-brown or orange-brown, commonly with rinds 1–2 cm thick. Summit of Cone 8478 exposes coarse scoria and agglutinate, black to brick red, interlayered with dense sheets of fountain-fed lava. Phenocrysts: 5–7% olivine (0.3–3 mm); 1–4% cpx (0.5–2.5 mm); sparse Fe-Ti oxide mph. Different flows range widely in content (1–7%) of plagioclase (0.5–2.5 mm), some of it phenocrystic, much of it antecrystic, broken, or resorbed. Some flows also contain xenocrysts of quartz and feldspar and small cognate microdiorite inclusions; disequilibrium cargo may account for wide chemical range of unit. Overlies granitic unit Jbs and phenocryst-poor lava flows of unit Taec, which in turn banks against dacite Dome 8325 (unit Td83; 3.42±0.1 Ma). Overlain by units gst, rbt (767±2 ka), Tmcv, and coarse ejecta of 1350 C.E. Inyo eruptions. $^{40}Ar/^{39}Ar$ age: 3,436±44 ka

Tdlm **Trachydacite of Laurel Mountain (Pliocene)—**Phenocryst-poor lava-flow remnant (63.0% SiO_2) at 2,900 m on high rim of Long Valley Caldera, 2 km west of Convict Lake and 2 km northeast of summit of Laurel Mountain. Frost-wedged, massive to flow-foliated lava is largely devitrified and splits slabby. Remnant is only ~120 m wide and 50 m thick. Phenocrysts: <1% plagioclase (0.3–1 mm), rare opx (0.2–1.5 mm), and ~5% opacitized hornblende (0.2–2 mm long). Crystalline groundmass contains abundant plagioclase-lath mph and sparse Fe-Ti oxide mph. Overlies several meters of alluvium rich in metasedimentary and granitoid cobbles that rests in turn on Devonian quartz sandstone (Greene and Stevens, 2002). No evidence for vent recognized. Lava was emplaced on a precaldera surface of only moderate relief. Its isolated presence on south rim suggests that a precaldera dacite dome field could have extended across present site of Long Valley Caldera, continuous with numerous Pliocene dacites on north and northwest rims. $^{40}Ar/^{39}Ar$ age: 3,600±43 ka

Tdpd **Trachydacite pyroclastic-density-current deposit of Deadman Pass (Pliocene)—**Stratified assemblage of phenocryst-rich pumiceous pyroclastic-flow and surge deposits rich in accidental lithic fragments; best exposed along northeast face of San Joaquin Ridge between Dome 3321 and Deadman Pass. Equivalent in part to "lower pyroclastic member" of Bailey and others (1990). Interpreted here as vent-opening explosive phase of

eruption that ended with extrusion of Dome 3321 (unit Tdsd), just east of which pyroclastic assemblage exposes its maximum thickness of ~150 m and is eroded into spires and fluted cliffs. Thins to ~30 m at Deadman Pass, 2 km southeast. Dominant lithology of thick cliff sections is white nonwelded ignimbrite, indurated by weak silicification and crudely stratified by varied abundances of lithics. Massive lithic-poor intervals are as thick as 10 m, separated by numerous lithic-richer layers 0.5–3 m thick and an interval of thin-bedded fall and surge deposits, together ~7 m thick (see fig. 5 of Bailey and others, 1990). Most layers are ash-dominant, carrying abundant pumice (1–5 cm) and highly varied contents (5–30%) of lithics (<1 to 30 cm). In some layers, most lithics are comagmatic trachydacite lava; others carry abundant clasts of metasedimentary, basaltic, and granitoid rocks derived from basement through which tuff vented explosively. Despite dozens of varied layers and high-energy emplacement, no significant unconformities are exposed. Uppermost 20–30 m of proximal section (near base of Dome 3321) consists of ash-rich coarse breccia in layers as thick as 5 m, dominated by angular basement clasts commonly 20–40 cm across and rarely >1 m. Unit is observed to rest only on metasedimentary rocks (unit Pzms), but plutonic, hypabyssal, and basaltic rocks are inferred to be concealed nearby, possibly beneath dome 3321. Not directly dated but probably same age as inferred vent-filling lava dome, 2.8-Ma unit Tdsd.

Diamicton at Deadman Pass (Bailey and others, 1990) is deflated colluvial lag residual from this pyroclastic unit; much of ash and pumice has been stripped from top few meters, concentrating coarse lithics in wind-scoured ridgecrest saddle. Clast suite is same as within intact pyroclastic assemblage north of pass: Felsic and mafic granitoids > metapelite, hornfels, and quartzite > porphyritic Mesozoic dike rocks; only ~5% each of clasts are Pliocene basalt (as big as 70 cm) and (juvenile) Pliocene trachydacite (as big as 25 cm). No metavolcanic clasts from Ritter Range or upper Middle Fork are present. Most blocks larger than 1 m are granitoids or quartzite. Most clasts are angular or subangular except some subrounded grussy granitoids

Tdsd **Trachydacite of Dome 3321 (Pliocene)—**Phenocryst-rich lava dome (67.3% SiO_2) on crest of San Joaquin Ridge 2 km northwest of Deadman Pass. Equivalent to "South Dome" of Bailey and others (1990), 500-by-700-m dome is partly covered by dacitic pyroclastic deposits but has ~120 m relief on its steeply exposed east face. Exposures are coarsely block-jointed, finely crystalline or vitrophyric, medium to dark gray, weathering brown with oxidized dark-brown rinds on joint faces; lower parts of east face are strongly flow foliated. Phenocrysts: 25–30% plagioclase (mph to 2.5 mm), 5–7% biotite (mph to 2 mm), ~1% hornblende (0.5–2 mm), and traces of opx and Fe-Ti oxide mph. Dome lava overlies trachydacitic pyroclastic complex (unit Tdpd), which is probably its own vent-opening eruptive phase that, in turn, rests on unit Pzms. Dome is partly surrounded and overlapped by trachydacitic block-and-ash-flow deposits (unit Tdsj), which were in part derived from Two Teats dome (1 km northwest) but in part produced during fitful extrusion of Dome 3321 itself. K-Ar age: ~2.8±0.1 Ma (Curry, 1966)

Tdsj **Trachydacite block-and-ash-flow deposits of San Joaquin Ridge (Pliocene)—**Phenocryst-rich block-and-ash-flow deposits (66.8–67.0% SiO_2) that cap San Joaquin Ridge (Sierran drainage divide) as 700-m-wide ridgecrest swath extending 3 km southeast from Dome 3321 (unit Tdsd). As thick here as 120 m, unit is equivalent to "upper pyroclastic member" of Bailey and others (1990). Clasts are almost exclusively juvenile dacite shed during extrusive dome growth, in contrast to underlying "lower pyroclastic member" of those authors (our unit Tdpd), which is rich in basement clasts excavated during explosive reaming of vent later filled by dome lava. Clasts are angular to subrounded, mostly glassy, and dense or weakly vesicular; many are prismatically jointed. Clast sizes are seriate from ashy matrix to meter-scale blocks, a few as large as 5 m. On wind-scoured ridgecrest, deposit is widely deflated, concentrating coarse blocks on surface, which, with thick colluvium, obscures any internal stratification in the deposit. Bailey and others (1990) reported similar deposits surrounding lithologically similar trachydacite domes (San Joaquin Mountain and Two Teats) farther northwest, beyond our map area; what fractions of such deposits had issued from each of those and from Dome 3321 has not been determined. Phenocrysts: ~25% plagioclase (mph to 4 mm), 5–7%

biotite (mph to 1.5 mm), ~1% hornblende (0.5–1 mm), and traces of opx and Fe-Ti oxide mph. Overlies units Tbdp (~3.28 Ma), Tdpd, and Pzms. Not directly dated but probably equivalent in age to inferred source lava dome, 2.8-Ma unit Tdsd

Tdud **Trachydacite complex of upper Deadman Creek (Pliocene)—**Phenocryst-rich pyroclastic vent complex with two lava domes centered on knoll 3025 between headwaters forks of Deadman Creek. Tuff (stippled) crops out over rugged area of 0.3 km^2 with >300 m of relief. Domes, which erupted through and overlap tuff complex, have maximum dimensions of 350 m and 600 m and relief of 150 m and 300 m, respectively. Lavas are glassy or finely crystalline, massive to finely vesicular, flow foliated, block jointed, and generally pale to medium gray, weathering tan to orange-brown. Tuff is massive to chaotic, locally crudely stratified, is nonwelded but widely indurated by silicification, and carries abundant dacitic and basement lithics and abundant punky dacitic pumice; generally white, it weathers tan or yellow, hackly, pitted, or cavernous, and erodes into spires and hoodoos. Tuff lithology is unlike that of pyroclastic units Tdpd or Tdsj ~1 km south. Tuff is cut by dikes and irregular intrusive masses of crystal-rich hornblende-biotite-plagioclase trachydacite (67.4–70.7% SiO_2), which are presumed comagmatic. Both domes have 20-25% plagioclase (1–4 mm), 5–7% biotite (mph to 1.5 mm), trace hornblende (mph to 12 mm), and trace Fe-Ti oxide mph. Larger dome (68.5% SiO_2) contains common ovoid inclusions (5–20 mm) of similar micropumiceous feldspar-rich dacite in which mafic phenocrysts are smaller and generally oxidized. Smaller southwest dome has 67.9% SiO_2. Domes and tuff all erupted through and rest upon (or steeply against) unit Pzms. Undated but presumed Pliocene in common with several other trachydacite domes nearby

Tdww **Trachydacite of White Wing Mountain (Pliocene)—**Phenocryst-rich lava dome (66.8% SiO_2) and associated fragmental deposits that cap western quarter of White Wing Mountain, which consists predominantly of Mesozoic granite and forms steep northwestern segment of Long Valley Caldera wall. Glaciated dome is 1 by 1.5 km in area and has 100–200 m of relief, much of it blanketed by 1350 C.E. Inyo pumice-fall deposits. Summit of White Wing Mountain (peak 3051), which stands 50 m higher than any exposure of dacite lava, consists almost entirely of fragments of same dacite, angular to subrounded, many as big as 1–2 m, that form a deflated lag deposit that armors summit and its west ridge. Rare blocks of granite suggest deposit could have been glacially transported from adjacent dome. However, remnant deposits of similar angular dacite blocks down at 2,660–2,775 m elevation on south ridge of White Wing Mountain lack basement clasts and include fragments of hydrothermally altered dacite, suggesting emplacement as explosively driven fragmental flows. Blocks and dome lava are glassy or finely crystalline, dense to finely vesicular, and flow foliated. Phenocrysts: 25–30% plagioclase (1–6 mm); 6–8% biotite (mph to 1.5 mm); ~1% hornblende (0.3–1 mm); traces of quartz (0.5–1.5 mm) and Fe-Ti oxide mph. Overlies granitic unit Kjl. K-Ar age: 2.6±0.4 Ma (Jenny Metz, analyst; reported by Chaudet, 1986)

Td65 **Trachydacite of Dome 2965 (Pliocene)—**Phenocryst-rich lava dome (64.4% SiO_2) just southwest of White Wing Mountain on divide between headwaters of Glass and Deadman Creeks. Subcircular in plan view, dome is ~1.3 km in diameter and has as much as 350 m of relief. Outcrops are limited, as lower slopes of dome are brush-covered, but crest and south ridge are largely bare, covered by coarsely blocky to platy scree. Although dome was locally glaciated and is lapped on west by till deposits, material exposed consists mostly of glassy to finely crystalline, pale-gray blocks and slabs that weather tan to orange-brown. Phenocrysts: ~30% plagioclase (1–5 mm); 6–8% biotite (mph to 1.5 mm); 1–2% hornblende (0.5–3 mm); traces of opx (mph to 1 mm) and Fe-Ti oxide mph. Base not exposed, but unit is inferred to intrude and overlie granitic and metasedimentary basement rocks. Undated but may be similar in age to lithologically similar lava dome, adjacent unit Tdww

Td78 **Trachydacite of Dome 7835 (Pliocene)—**Small dome of phenocryst-rich dacite (65.2% SiO_2) 500 m east of lithologically similar large Dome 8325 (unit Td83) on northwest wall of Long Valley Caldera. Poorly exposed, ~1 km northwest of Big Springs, domelet is 200 by 300 m in plan view and has maximum exposed relief of ~35 m. Unit is nonvesicular, pale gray, weathers tan and punky, and disintegrates into irregular angular blocks.

Phenocrysts: 5–7% biotite (0.2–2 mm); 3–4% amphibole prisms (1–4 mm long); feldspar present only as mph; tiny Fe–Ti oxides only in groundmass. Overlies units Pzms and mafic granodiorite assigned to unit Jbs. Overlain by unit rbt (767 ka). Undated

Td83 **Trachydacite of Dome 8325 (Pliocene)—**Phenocryst-rich dacite dome (66.0–66.5% SiO_2) on northwest wall of Long Valley Caldera ~1 km northeast of Crestview. Dome is ~1 km in diameter, has 280 m of exposed relief, and is heavily mantled by colluvium and Inyo fall-out except near windscoured summit. Massive lava is strongly flow foliated, splits slabby, and is pervasively pink. Phenocrysts: 5–8% biotite (mph to 2.5 mm); 3–5% hornblende (mph to 1.5 mm, rims commonly opacitized); trace cpx (mph to 1.2 mm); ~1% plagioclase (0.2–1.5 mm, rims commonly resorbed). Partly glassy groundmass rich in mph and microlites. Overlies Mesozoic granodiorite. Banked against it are units Taec, Tb84, rbt (767±1 ka), and mor (66±2 ka). K-Ar age: 3.42±0.08 Ma (Metz, 1987)

Tmcl **Basaltic trachyandesite west of Cabin Lake (Pliocene?)—**Olivine-rich mafic plug (52.9% SiO_2) that intrudes Mesozoic metavolcanic basement at elevation 2,920 m on south wall of Shadow Creek (UTM 099/731), 300 m west of Cabin Lake, 700 m east of Ediza Lake, and 3.7 km east of summit of Mount Ritter (west of map area; see fig. 3). Ovoid in plan, plug is 25 x 35 m across and has no relief above gently sloping surface of glacially scoured host rock. Rock is nonvesicular and dark gray, weathering tan to orange-brown. Generally displays irregular joint blocks 10–50 cm across, but steep joints and flow lamination locally parallel contact. No ejecta or agglutinate preserved. Phenocrysts: 8–10% olivine (0.5–1.5 mm). No xenoliths seen. No outflow equivalents known to be preserved. Undated

Tmcm **Basaltic trachyandesite south of Upper Crater Meadow (Pliocene)—**Remnants of single glaciated olivine-rich lava flow (53.2% SiO_2; 7.5% MgO; 5.25% K_2O) on both rims of a gorge tributary to Crater Creek (UTM 190/608), ~600 m south of Upper Crater Meadow. Rim ledges are 1–4 m thick and overlain by thin till deposits and Inyo pumice. Phenocrysts: ~7% olivine (0.5–2 mm), many with tiny spinel inclusions; also contains sparse quartz xenocrysts with reaction rims. Holocrystalline groundmass, rich in flow-aligned plagioclase-lath mph, also carries abundant olivine mph and rare Fe-Ti oxides (both ~0.1 mm). Rests on and armors 20-m-thick remnant of massive white grus exposed on gorge walls where grus grades down into fresh Mesozoic granite. Unit is unusually rich in Sr (2,050 ppm) and Ba (3,600 ppm) (fig. 20). $^{40}Ar/^{39}Ar$ age: 3,363±15 ka

Tmcr **Basaltic trachyandesite of Mammoth Crest (Pliocene)—**Olivine-rich mafic lava flow remnant (53.3% SiO_2, 7.5% MgO) preserved as hill 3228 atop Mammoth Crest, ~1 km southwest of Crystal Crag. Remnant of single flow, resting on Cretaceous granite, is 250 by 400 m in plan view and only ~25 m thick. Ice-scoured, finely crystalline, massive lava is frost-riven into whaleback pile of slabs. Phenocrysts: ~7% olivine (mph to 2 mm); common Fe-Ti oxide mph. Source vent unknown. Lower MgO content than olivine-rich 3.15-Ma basalt (unit Tbmm) at Mammoth Mine, base of which lies 300 m lower in elevation and 3.5 km northeast across Lakes Basin, but the two are lithologically and petrographically similar. Undated

Tmcv **Basaltic trachyandesite of Crestview (Pliocene)—**Olivine-rich lava flows notably enriched in K and P (53.1–54.9% SiO_2; ~4.5% K_2O; ~0.85% P_2O_5) that crop out discontinuously on scarps east, north, and west of confluence of Glass and Deadman Creeks. South-facing scarp 600 m southeast of Crestview is stack of flows ~40 m thick that rests on Mesozoic granodiorite. On steep nose 500 m northwest of Crestview, unit is ~60 m thick. Along rim of southeast-facing scarp 1–2 km southwest of Crestview, unit may be single flow; its exposure there is at least 10–30 m thick, but its upland slope continuing northwest above rim is wholly concealed by 1350 C.E. Inyo ejecta. Exposures are block-jointed and massive to sparsely vesicular. Phenocrysts: 7–10% olivine (mostly 0.2–3 mm; locally hopper-shaped crystals as big as 4–7 mm); sparse cpx (0.3–1 mm); sparse plagioclase-lath mph; and cpx-plagioclase microdioritic inclusions. Also carries quartz and feldspar xenocrysts. Overlies Mesozoic granodiorite and units Taww (2,950±90 ka), Tmwo (3,153±26 ka), Taec, and Tb84. Overlain by Sherwin Till (unit gst). Relative elevations of three main outcrop strips suggest a westerly source vent, now concealed. Undated

Tmcw **Basaltic trachyandesite west of Crater Creek (Pliocene)—**Glacially eroded remnant of two moderately porphyritic lava flows (52.3–52.6% SiO_2) that form 200-by-300-m

steep-sided bench banked against granitic canyon sidewall, 2 km west of Red Cones and 1.5 km south of Rainbow Falls. Remnant consists of two similar lava flows, lower one 15–20 m thick and upper one 8–10 m thick. Basal colonnade of lower flow has slender vertical columns 2–12 m high and 25–70 cm thick, resting directly on granite. Upper flow has irregular vertical joints, and both have hackly entablatures and locally inclined or subhorizontal columns. Both have gray-brown or orange-brown weathering rinds, extensive patches of colorful lichens, sparse vesicles filled with secondary minerals, and sparse veinlets of silica. Phenocrysts: 1–3% plagioclase (0.5–1.5 mm), generally corroded or tinted pale soapy green; 5–8% apple-green olivine and black cpx (both 0.5–3 mm), commonly clustered and many with alteration rims. In contact only with Mesozoic granite. Petrographically similar to basalt of The Buttresses (unit Tbtb), 2 km upstream, which, despite its more mafic composition, shares with unit Tmcw a similar (reversed) paleomagnetic direction (Hildreth and others, 2014). Undated but presumed to be similar in age to lava flows of unit Tbtb

Tmel **Basaltic trachyandesite of Emerald Lake (Pliocene?)—**Moderately porphyritic mafic plug (52.3% SiO_2) that intrudes Mesozoic metavolcanic basement at east shore of Emerald Lake (UTM 095/774), near John Muir Trail ~1 km east of Thousand Island Lake in headwaters of Middle Fork (west of map area; see fig. 3). Glacially scoured remnant is 30 by 70 m across and has only 15 m of relief. Rock is nonvesicular and dark gray, weathering pale gray to brown; generally hackly or chunk-jointed, it locally displays inclined columns. West end of plug has 3-m-thick, flow-foliated rind in which vertical laminae parallel conduit margin against wall rock. No ejecta or agglutinate preserved. Phenocrysts: 5–8% olivine (1–3 mm) and 1–2% cpx (1 mm). No outflow equivalents known to be preserved. Undated

Tmsd **Basaltic trachyandesite south of Deer Creek (Pliocene?)—**Moderately porphyritic lava flows (53.2% SiO_2) that cap high divide between upper Deer Creek and Fish Creek canyon. Stack of flows is ~150 m thick where exposed on cirque headwall at head of Deer Creek. Glaciated unit extends 2 km west from vent remnant at hill 3206, which lies 5 km east of Pumice Butte and 9 km south of Mammoth Mountain. Upland surface of unit is blocky colluvial rubble with a few ledgy exposures. Phenocrysts: 5–7% olivine (0.2–3 mm); trace cpx but no feldspar. Overlies Mesozoic granite (unit Kmo). Undated

Tmwc **Basaltic trachyandesite west of Castle Lake (Pliocene?)—**Mafic plug and adhering remnants of lava and agglutinated scoria (52.9% SiO_2) that form Crag 10640 (3,243 m) on crest of southeast arm of Volcanic Ridge, 600 m west of Castle Lake and 9.5 km northwest of Mammoth Mountain summit (UTM 1236/7121). Unit is west of map area; see fig. 3. Glaciated remnant forms column atop pedestal, together ~25 m high, ~15 m wide at top, and ~25 m wide at base, which is surrounded by apron of mafic scree. Blocks of massive lava and scoria bombs are both as big as 50 cm. Fragments of metavolcanic basement rocks are common in both agglutinate and homogenized lava. Phenocrysts: ~7% olivine (0.2–1.2 mm), many with tiny spinel inclusions. No plagioclase or cpx phenocrysts. Rare tiny oxides in finely crystalline groundmass. Rests on deformed Mesozoic metavolcanic rocks (Huber and Rinehart, 1965a). No remnants of outflow lavas known to be preserved. Undated

Tmwo **Basaltic trachyandesite west and east of Obsidian flow (Pliocene)—**Phenocryst-rich lava flows and agglutinate (53.1-54.5% SiO_2) that crop out as glaciated near-vent remnants just west of Obsidian flow (unit ric) and along walls of Glass Creek from beneath Obsidian flow for ~1.3 km eastward. Three proximal remnants form north-south alignment only 200 m long, each only 30–70 m in maximum dimension. Northern remnant is largest, a 15-m-high steep pile of brick-red agglutinated spatter and scoria with ejecta as large as 30 cm; this is invaded by thin dikes and on its north and west walls by irregular masses of dark-gray block-jointed lava. Middle remnant is 6-m-high ledge of coarsely block-jointed massive lava ~30 m long. Southern remnant is another ledge of similar lava ~70 m long, somewhat more vesicular and strewn with glacial erratics and Inyo ejecta. Lavas are locally streaky but generally dense and massive or weakly flow-foliated, their surfaces weathering dark brown to orange brown. Outcrops on walls of Glass Creek are irregularly block-jointed ledges as thick as 10 m, but exposure is limited by Inyo ejecta and

derivative scree; ledges suggest possibility of more than one flow. Drill holes beneath and adjacent to Obsidian flow (Eichelberger and others, 1985) penetrated 250–350 m of unexposed mafic lavas sandwiched between till and granitic basement; unit Tmwo represents at least upper part of mafic section. Phenocrysts: 3–7% olivine (0.2–1 mm), iddingsite rims common; 1–4% plagioclase (0.3–1 mm long, mostly laths); 1–3% cpx (0.5–1.5 mm), many in clusters; also carries sparse quartz xenocrysts. Finely crystalline groundmass is rich in tiny plagioclase laths and clusters of pyroxene mph. Distal exposure on south wall of Glass Creek is least evolved chemically and poorest in phenocrysts, with plagioclase limited to microphenocrysts. Base not exposed, but inferred to rest on Mesozoic granite (exposed nearby). Overlain by units Taww (2,950±90 ka), Tmcv, and gst, which is in turn overlain by unit rbt. Fresh condition of lava led Putnam (1949) to infer Pleistocene age, but unit was called Pliocene by Bailey (1989). $^{40}Ar/^{39}Ar$ age: 3,153±26 ka

Tmww **Basaltic trachyandesite of White Wing Mountain (Pliocene?)—**Moderately porphyritic scoria cone, agglutinate, and subordinate lava (52.3–52.4% SiO_2) preserved as two remnants on southwest ridge of White Wing Mountain. Major remnant is 300 by 500 m across, extending downslope just south of summit from elevation 2,990 m to 2,830 m. Massive lava exposed at base is pale gray, weathers orange-brown, splits slabby, and contains vesicle sheets. Principal outcrops are cliffs, 30–50 m high, of crudely stratified ejecta, tack-welded to moderately agglutinated. Ejecta are dominantly lapilli but seriate from coarse ash to 30 cm, enclosing scattered scoria bombs as big as 50–200 cm. Most clasts are vesicular scoria, but many are dense juvenile fragments. Cliffy pyroclastic section is black below but grades upward to brick-red, then orange-brown with yellow palagonitic matrix locally. Major ridge-capping remnant erodes craggy; huge agglutinate blocks were ice-transported into a hollow 250 m east. Smaller remnant, down ridge at elevation 2,700 m, is only 100 m across and consists of ledges of scoria lapilli and tack-welded agglutinate. Phenocrysts: 5–8% olivine (mostly mph but a few as big as 1.5 mm), and rare cpx (<1 mm). Overlies granitic unit Kjl. Undated

Trac **Rhyolite tuff of Alpers Canyon (Miocene)—**Phenocryst-rich rhyolitic ignimbrite exposed on north and south walls of uppermost Owens River at its confluence with Alpers Canyon. Outcrops are densely welded, crystal-rich, poor in fiamme, and contain only sparse lithic fragments (1–5 cm). Lithics are mostly mafic and rhyolitic lavas, crystal-poor to crystal-rich, and rare hornblende dacite. Tuff is pale gray (almost white) but weathers tan to orange-brown or dark gray-brown; irregularly block-jointed, many outcrops are crumbly or cavernously weathered, and some erode into knobs and spires. Unit is 60–90 m thick on canyon walls, but base is not exposed where thickest. Rare outcrop of silicified nonwelded tuff contains abundant fragments (2–10 mm) of crystal-poor pumice. Source unknown, but Bailey (1989) reported additional remnants 9–20 km to northeast. Once a regional outflow sheet, surviving remnants are small and scattered. Phenocrysts: 15–20% each of sanidine and quartz (many broken); 1–2% each of biotite and plagioclase; sparse Fe-Ti oxide mph; quartz and feldspars mostly 0.5–3 mm, biotite 0.1–1 mm; oxides ≤0.4 mm. Easily distinguished from Bishop Tuff (unit rbt), which contains abundant pumice lapilli and fiamme. Overlies Mesozoic granodiorite and phenocryst-poor Miocene basalt (unit Tbbs). Overlain north of Owens River canyon by coarse gravel (unit pal), which lacks clasts of nearby Bishop Tuff (767±2 ka). Lithic-free whole-rock composition 71.5% SiO_2. K-Ar age: 11.7±0.1 Ma (Huber, 1981; Bailey, 1989)

QUATERNARY VOLCANIC ROCKS

[Listed alphabetically by 3-letter unit label]

a62 **Trachyandesite of Cone 2962 (late Pleistocene)**—Scoria cone and adjacent lava-flow apron (57.1–59.2% SiO_2) on divide between Deer and Crater Creeks, 7 km south of Mammoth Mountain. Cone is 160 m high, ~1 km wide, elongate northeast, and is centered 2 km northeast of Pumice Butte (fig. 10). From its southwest toe emerges a 1-km-wide apron of blocky lava flows that extends 3 km southwest to rim of San Joaquin River canyon. Vent-proximal half of apron is plateau where lavas were lightly ice-scoured and striated but remain block-jointed and vesicular. Southwest-sloping distal half of apron, however,

was ice-free and remains ruggedly blocky, glassy, and scoriaceous (although weathered and frost-damaged). Longitudinal troughs between flow ridges and knolls provide 10–20 m local relief, and several stairstep flow fronts are 10–15 m high. At San Joaquin River canyon rim, apron drapes granitic wall, exposing at least ten flows in a steeply dipping stack as thick as 200 m. Scoria cone is poorly exposed except on its nonglaciated summit flat, around margins of which arcuate ridges of coarse red scoria (loose or tack-welded) appear to be rim remnants of a filled crater; scoria bombs there are as big as 70 cm. True summit is a 10-m-high pile, ~25 m in diameter, of frost-shattered lava blocks, massive to vesicular, that was a knob-like extrusion; its southeast margin adjoins a stack of red scoria bombs, some >1 m in diameter. Lower slopes of cone locally expose glaciated ledges of massive platy lava. Phenocrysts: bombs and lapilli on cone and lava flows alike are crystal-poor, containing ≤1% plagioclase (0.5–1.5 mm), still sparser olivine mph, and trace cpx (mph to 1 mm). Scoria cone overlies Mesozoic granite and basaltic lava flows of unit bdc (155±2 ka); lava-flow apron overies units Tasj and rbt and banks around Pumice Butte (unit apb; 142±5 ka). $^{40}Ar/^{39}Ar$ age: 118±10 ka (Mahood and others, 2010)

aic **Trachyandesite of Inyo Craters (late middle Pleistocene)—**Stack of at least five phenocryst-poor lava flows (57.5–59.4% SiO_2) exposed on walls of South Inyo Crater (at south toe of Deer Mountain) and along south-striking fault scarp for ~1 km south from crater. Flows are thin and rubbly, but their (modestly vesicular) more massive interior zones support ledges 3–6 m thick. All have sparse plagioclase and still sparser olivine and cpx (both ≤1 mm), and some carry rare feldspar and quartz xenocrysts as large as 10 mm. Relations on crater walls suggest flow direction was toward northeast. Base not exposed, but a set of at least five (compositionally correlative) flows, each 5–13 m thick, was cored by Inyo-4 slant drill hole at slant depths of ~21–62 m (fig. 6), where they overlie a contrasting set of basaltic trachyandesite lavas (see unit mcl) and cinders (Eichelberger and others, 1988; Vogel and others, 1994). In drill hole DC-1 (Sorey and others, 1978), located at UTM 259/781 (fig. 8), ~6 km northeast of South Inyo Crater, a 15-m lava flow of unit aic was penetrated at depth of ~90–105 m (fig. 6), beneath flows of units mcv, mor, and another flow compositionally indistinguishable from unit bsr (99±1 ka). Flows compositionally correlative with unit aic have not been identified elsewhere.

Flows exposed on crater wall are directly covered by 8–12 m of red mafic pyroclastic strata (unit mic), suggesting presence of an unexposed vent nearby; these in turn are overlain by ~1 m of Inyo pumice fall (1350 C.E.), atop which lies as much as 13 m of phreatic ejecta (unit pe) that extends to crater rim and was explosively emplaced at end of 1350 C.E. eruptive sequence (Mastin, 1991). Three flows drilled at top, middle, and bottom of stack exposed on crater wall gave nearly identical paleomagnetic directions (Mankinen and others, 1986). Absence of rhyolitic ejecta or float from nearby Deer Mountain intercalated between lava flows (or within or beneath subjacent pile of mafic lavas cored by Inyo-4 strongly suggests that unit aic is older than Deer Mountain (unit rdm; 101±8 ka). Vogel and others (1994) gave $^{40}Ar/^{39}Ar$ ages of 151±17 ka and 161±14 ka for two flows in the uppermost set of lava flows in Inyo-4 core, flows chemically similar to those exposed on crater walls, for which we obtained a $^{40}Ar/^{39}Ar$ age of 131±1 ka

aml **Trachyandesite of McLeod Lake (late Pleistocene)—**Phenocryst-poor lava flow (61.5–62.3% SiO_2) exposed as narrow sliver along north-striking fault 40 m east of McLeod Lake (also variously rendered McCloud or McClowd, but named for U.S. Forest Service Ranger Malcolm McLeod), ~1 km south of southern toe of Mammoth Mountain. Crops out as 1-m-high ledge of black massive aphanitic lava, locally weakly vesicular and partly glassy; block-jointed or locally slabby; weathers tan and carries pink films along joint planes. Unit banked against Mesozoic granite (unit Kmo), and both are severely glacially eroded; more remnants of lava may be buried by glacial deposits or beneath lake. Phenocrysts: 1–2% plagioclase (0.5–2 mm); 1–2% amphibole (0.1–1.3 mm long; rare opx microphenocrysts (in clots with oxides and plagioclase); and sparse Fe-Ti-oxide microphenocrysts (0.1–0.4 mm). At bottom of 98-m-deep drill hole (HSL-1; fig. 6) near Horseshoe Lake carpark, scoria lapilli (oxidized, not rounded) of a 10-m-thick stratified fall deposit (rich also in granitoid and metavolcanic lithic lapilli) are compositionally

similar to lava of unit aml; scoria fall directly underlies a 15-m-thick trachydacite lava flow similar to unit dsd, which is in turn overlain by 73-m-thick stack of 7–10 phenocryst-poor vesicular lava flows of unit amp (97±1 ka). It can be inferred that unit aml predates all or much of Mammoth Mountain and that its vent lay within a few kilometers of Horseshoe Lake. In water well 30M (fig. 6), 2 km southeast of downtown Mammoth Lakes, a 15-m-thick lava flow of unit aml was penetrated at a depth of 45–60 m, where overlain by a thin flow of unit amp and ~35 m of late Pleistocene till (unit glb, which extends to surface). Lava of unit aml thus flowed as far east as Sherwin Creek, but none is exposed farther east nor recognized in other south moat drill holes. Undated

amp **Trachyandesite of Mammoth Pass (late Pleistocene)—**Aprons of phenocryst-poor lava flows (57.2–61.6% SiO_2) that erupted on high divide north of Mammoth Pass at vent later covered by construction of Mammoth Mountain. Flows emerge from beneath south toe of Mammoth Mountain edifice and turn both east and west, extending 9 km east to terminus near Sherwin Creek Campground and at least 7 km southwest where remnants survive on both sides of lower Crater Creek. Entire western apron is glacially scoured from Mammoth Pass down to Sotcher Lake, Reds Meadow, and Boundary and Crater Creeks. Lavas of eastern tongue have been more severely eroded and widely concealed by late Pleistocene till, although windows are exposed along Mammoth Creek, and a 1-km-wide blocky terminal lobe just beyond distal moraines of unit glb is virtually uneroded. Lavas form glaciated ribs, nubbins, and ledges, block-jointed or slabby, rarely platy, and typically massive and aphanitic with pale-gray mottling; locally oxidized, especially in healed flow-breccia zones. Vesicular zones are widely stripped. Thickest exposures are typically massive with vertical joints, irregularly prismatic. On west slope, belt between 2,750 and 2,850 m elevation was glacially eroded into west-trending noses, each sculpted from a single lava flow, each having 10–25 m local relief, and scoured free of till and all but sparse erratics. Thickest exposures are 30 m near upper Twin Lakes, 100 m near Horseshoe Lake, and >140 m along Boundary Creek where at least 5 cliffy flows are exposed, each 10–30 m thick. Drill hole HSL-1 (fig. 6), near Horseshoe Lake, penetrated 7–10 flows in a total thickness of 73 m of unit amp, which rests at depth on an unexposed trachydacite lava flow of typical Mammoth Mountain lithology. On north-facing scarp of Hill 2938 (high point of unit), a glacially excavated trough at south toe of Mammoth Mountain exposes a pair of 8-m-thick platy lava flows of unit amp; minor scoriaceous lava-flow rubble is present but no ejected scoria exposed. Vent is inferred to have been farther north, subsequently covered by Mammoth Mountain trachydacite pile. Vents shown by Bailey (1989) at hill 2938 and Sherwin Creek Campground do not exist. Phenocrysts: typically ~1% plagioclase (0.5–1.5, rarely as big as 3 mm), uncommonly in clots; traces of olivine and cpx (both ≤1 mm); sparse Fe-Ti-oxide mph (0.1–0.3 mm); rare plagioclase antecrysts (3–5 mm). Among many flows, plagioclase content ranges from almost none to as much as 3%. Groundmass is grainier, slightly coarser than in subjacent unit drf, with which unit can easily be confused, especially where unit is locally platy and mottled. Olivine crystals, where oxidized light to dark brown, can resemble opx prisms of unit drf, but olivine is generally equant, not elongate.

Unit overlies Mesozoic granite, Bishop Tuff (unit rbt; 767±2 ka), unit drf (98±1 ka) near western limit, and unit bsr (99±1 ka) at eastern limit. Overlies unit aml in drilholes at Horseshoe Lake and southeast of downtown Mammoth Lakes (fig. 6). Overlain by unit mdp (82±1 ka) near Sotcher Lake, by units dbp, dnh, and bhl near Twin Lakes, and widely overlain by late Pleistocene till (unit glb). Flows of unit amp emerge from beneath base of South Summit Dome (unit dsd; 87±6 ka) at drainage divide, but they overlie an unexposed trachydacite lava flow in drill hole HSL-1 (fig. 6). Southwest distal remnants overlie unit drf and fill paleochannels cut in granite. Steep slope extending 2 km north of Boundary Creek at 2,500–2,600 m elevation reflects draping and concealment of previously glaciated granitic canyon sidewall by flows of unit amp. Low-relief belt along western slope at 2,700–2,750 m is poorly exposed, as is southwest corner of apron where lavas bank against Bishop Tuff; both areas are mantled by Inyo pumice and ground moraine. Sites sampled near Reds Meadow and in Valentine Reserve Ecological Study Area on Mammoth Creek yield similar paleomagnetic directions (Mankinen

and others, 1986; Hildreth and others, 2014). $^{40}Ar/^{39}Ar$ ages: 97±1 ka (table 2); 81±1 ka (Mahood and others, 2010); K-Ar age: 86±10 ka (Mankinen and others, 1986)

apb **Trachyandesite of Pumice Butte (middle Pleistocene)—**Scoria cone and moderately porphyritic lava flows (58.4–59.0% SiO_2) atop plateau between canyons of Fish Creek and San Joaquin River, 6 km east of their confluence and 8 km south-southwest of Mammoth Mountain (fig. 10). Pumice Butte scoria cone, ~750 m wide and 150 m high, stood above Pleistocene ice and is only moderately eroded, its slopes strewn with red and black sloughing scoria. Lava flows form a stubby lobe at north toe of cone and a narrow tongue that extends southwestward from midway up west slope. Lavas are glacially scoured, coarsely blocky, partly glassy, and massive or vesicular. Summit preserves a low-relief dish-like crater, largely filled; below its northwest and east rims are steep faces, 20–30 m high, of coarse red scoria—some loose but mostly tack-welded. Scoria bombs are as big as 1 m. Phenocrysts: 2–3% plagioclase (0.5–3.5 mm; mostly ≤1 mm); ~1% olivine (mostly mph but rarely as big as 1.5 mm); ~1% cpx (mph, some clustered with plagioclase and (or) oxides); trace Fe-Ti-oxide mph. In thin section, glassy groundmass is choked with microlites and plagioclase-lath mph. Overlies Mesozoic granite (unit Kmo) and Bishop Tuff (unit rbt; 767±2 ka). Overlain by lava flows of unit a62 (118±10 ka) from nearby scoria cone 2962. $^{40}Ar/^{39}Ar$ age: 142±5 ka (Mahood and others, 2010)

asr **Trachyandesite of Shady Rest Campground (middle Pleistocene)—**Phenocryst-poor lava flow (56.4–56.6% SiO_2) exposed poorly for ~400 m along southeast toe of Knolls Vista (hill 2517), from elevation ~2,375 m at road near campground entrance to as high as ~2,410 m. Subrounded to angular joint blocks are finely vesicular to massive and weakly flow-foliated. Phenocrysts: Almost aphyric; <1% plagioclase (0.5–1.3 mm), rare cpx (0.1–0.8 mm), anhedral plagioclase antecrysts (~4 mm), and tiny rare Fe-Ti oxides. Partly glassy groundmass rich in plagioclase laths. Base not exposed. Overlain by units mcl (175±3 ka), bsr (99±1 ka), and till of units gcd and glb. Slope is lightly strewn with unit gcd erratics that include abundant granitoids but no dacites from Mammoth Mountain. In water well 30M (fig. 6), 3 km south of Knolls Vista, a 17-m-thick flow of unit asr was penetrated at 143–160 m depth, directly beneath flows of unit mcl but atop uncorrelated (and nowhere exposed) mafic lavas (51.5–53.2% SiO_2) at 160–195 m depth. Undated

bar **Trachybasalt of Arcularius Ranch (late Pleistocene)—**Scoria cone (fig. 7) and extensive phenocryst-rich lava flows (50.6–52.4% SiO_2) that erupted on southwest wall of Long Valley Caldera, 2 km northeast of Minaret Summit and 4 km north of summit of Mammoth Mountain. Lava flows covered much of caldera's southwest moat, next poured 13 km northeastward between Deer Mountain and West Moat Coulee (unit rwm), wrapped west side of Lookout Mountain, then turned eastward at north wall of caldera near Big Springs, and extended additional 10 km along north moat to terminus along Owens River (fig. 9). Scoria cone, 160 m high and 700 m wide, consists of lapilli and bombs as big as 70 cm, mostly oxidized, generally loose but locally agglutinated. Stratified cinders at least 12 m thick exposed along gulch just south of cone are palagonitized and capped by a unit bar lava-flow remnant ~10 m thick; bombs in fall deposit include common representatives of phenocryst-poorer unit bmn as well as predominant phenocryst-rich bombs of unit bar. Cone banks high against wall of precaldera basement and, though degraded, was not devastated by late Pleistocene glaciation. Proximal lava-flow apron and windows through till south of Crater Flat are glacially scoured, but exposures west, north, and east of Lookout Mountain lie outside the glacial limit and thus remain ruggedly scoriaceous, even craggy. Wherever exposed, individual flows are 3–10 m thick, both proximally and along north moat, where two (virtually identical) flows extend together almost to ultimate terminus. Block joints are common, and crudely prismatic joints locally mark vesicular surfaces. Phenocrysts: 15–25% plagioclase (1–7 mm, rarely to 10 mm); 2–5% olivine (0.5–2 mm, rarely to 3 mm), commonly in clusters; cpx (0.5–2.5 mm) is sparse proximally and rare distally. Scoria bombs on cone contain scattered silicic xenoliths (1–5 cm), some partially melted, probably of metavolcanic basement. Overlies units bcf, bmn (87±7 ka), and ddc (103±9 ka). Overlain by units mcv, mnd, mor (66±2 ka), and gdc. Locally uplifted on roof of large dacite dome, unit d61 (87±2 ka). Subunit bar' includes this uplifted fragment as well as a medial exposure west of Lookout

Mountain; compositionally, lavas at the two sites are identical (n=3), but they differ slightly from rest of unit bar (n=17) in being somewhat richer in Al and slightly poorer in Mg, K, and P. Subunit bar' is inferred to be a single flow, slightly poorer in olivine (1–2%) and a bit richer in plagioclase (20–25%), much of which is more sieve textured than in associated flows of bar. Six sites drilled, proximally, medially, and distally, all yield similar paleomagnetic directions for bar and bar' (Mankinen and others, 1986; Hildreth and others, 2014). K-Ar ages: 108±12 ka (distal at Big Springs) and 95±13 ka (proximal) (Mankinen and others, 1986). $^{40}Ar/^{39}Ar$ ages: 88±5 ka (quarry north of MMSA Main Lodge) and 94±9 ka (toe of scoria cone) (Mahood and others, 2010)

bcd **Basalt of Casa Diablo Hot Springs (late Pleistocene)—**Apron of phenocryst-rich lava flows (51.1–52.1% SiO_2) that emerges from beneath younger unit bsr ~1 km east of Shady Rest Park and extends 3.5 km southeastward to its terminus just south of Mammoth Creek and Highway 395. Forms a 1-km-wide expanse that spans cloverleaf junction of Highways 203 and 395 and adjoins geothermal plant at former site of Casa Diablo Hot Springs. Near plant, lava apron is cut and moderately displaced by faults of the resurgent graben system. Source vent is probably spatter cone 2580+ (unit bed; 121±3 ka) just west of Dome 2861 (unit d61; 87±2 ka); cone agglutinate of unit bed is similar to unit bcd petrographically and in major- and trace-element composition, but paleomagnetic directions differ. Apron outcrops are gently rolling scoriaceous surfaces or (where stream-incised) block-jointed ledges, commonly crudely columnar; nearly all exposures are vesicular except at lowest levels exposed along arroyos. No exposure is thicker than 15 m. Phenocrysts: 7–12% plagioclase (0.5–7 mm); 5–8% olivine (0.5–2.5 mm); 1–2% cpx (1–2.5 mm); Fe-Ti oxides limited to crystalline groundmass. Overlies units mmc and gcd. Overlain by units bfh (92±2 ka) and bsr (99±1 ka). Crops out only beyond limit of late Pleistocene till. $^{40}Ar/^{39}Ar$ age: 125±2 ka

bcf **Trachybasalt south of Crater Flat (middle Pleistocene)—**Spatter cone 2545, consisting of phenocryst-poor agglutinate (51.7–51.8% SiO_2), 500 m south of Crater Flat and 5 km north of summit of Mammoth Mountain. Low cone is glacially scoured, 500 m wide, and only 40 m high. Mantled by late Holocene Inyo pumice-fall deposit, cone is poorly exposed, cropping out only as brick-red ledges of dense agglutinate on south slope, a few reaches along shallow draw at southeast toe of cone, and one massive lava ledge just southeast of that draw. Phenocrysts: ~1% plagioclase (0.5–4 mm); traces of olivine and cpx mph (both 0.1–0.2 mm); Fe-Ti oxides limited to finely crystalline groundmass; also contains sparse quartz and feldspar xenocrysts with reaction rims. Base not exposed. Overlain by units bmn (87±7 ka) and bar (88±5 ka). $^{40}Ar/^{39}Ar$ age: 164±2 ka

bdc **Trachybasalt west of Deer Creek (middle Pleistocene)—**Moderately porphyritic lava flows (51.6% SiO_2) that crop out as a pair of 10-m-high benches that extend for ~1 km along southeast toe of Cone 2962, just west of Deer Creek. Fresh angular joint blocks are massive, nonvesicular, and moderately ice-scoured. Contains 3–5% olivine (0.5–1 mm) and 8–10% plagioclase (mostly 0.5–1 mm but as big as 4 mm). Not related to Pliocene mafic center 3206, 2–4 km east (Bailey, 1989), which consists of weathered lava flows of cpx-olivine basaltic trachyandesite (unit Tmsd) that lacks plagioclase phenocrysts. Veneer of till obscures contact with closely underlying granite of unit Kmo. Unit is directly overlain by scoria Cone 2962 (unit a62; 118±10 ka). $^{40}Ar/^{39}Ar$ age: 155±2 ka

bed **Basalt east of Dry Creek (late Pleistocene)—**Poorly exposed, glacially eroded, phenocryst-rich spatter cone (52.0–52.1% SiO_2) between Dry Creek and Dome 2861. Cone 2580+ is ~500 m wide, ~50 m high, and moderately degraded, with a subdued crater open to north. Ejecta are almost entirely hidden by late Holocene Inyo pumice-fall deposit, and cone is also strewn with glacial erratics of unit ddc and trachydacites of Mammoth Mountain. Lone significant outcrop is on east rim of summit where ledges of oxidized agglutinate are 1–2 m thick and enclose thin dark-gray massive lenses. Most is tack-welded with oxidized lapilli and bombs still discernible, but this facies grades abruptly into massive domains, somewhat homogenized though still streaky. No lava flows associated with cone are exposed proximally, but flows of unit bcd (125±2 ka), ~8 km east-southeast, are chemically and petrographically identical; although paleomagnetic directions differ, this may reflect mobility of cone agglutinate. Phenocrysts: 7–10% plagioclase (1–5 mm);

5% olivine (1–2 mm); 1–2% cpx (1–3 mm); Fe-Ti oxides limited to crystalline groundmass. Base not exposed; unit is in exposed contact with no other except till. $^{40}Ar/^{39}Ar$ age: 121±3 ka (Mahood and others, 2010)

bfh **Basalt of Fish Hatchery (late Pleistocene)—**Apron of phenocryst-rich lava flows (49.4–49.7% SiO_2) that emerges from beneath younger unit bsr ~1.5 km south of Casa Diablo geothermal plant and extends 5.5 km east along south side of Mammoth and Hot Creeks to its terminus against rhyolitic Hot Creek flow (unit rhc). Flow surfaces are rough and scoriaceous, marked by polygonally jointed or block-jointed swells, tumuli, and crags. All exposures lie beyond limits of late Pleistocene till and Casa Diablo Till. Parts of southwest sector are covered by marsh deposits and postglacial alluvium of Laurel Creek. Near Fish Hatchery, lava flow is both underlain and overlain by Pleistocene alluvium (unit oal). Source vent is Mammoth Crest scoria cone (unit bmc), which is compositionally, petrographically, and paleomagnetically identical. Phenocrysts: 5–10% plagioclase (1–15 mm); 1–3% olivine (0.5–2 mm); and sparse to common cpx (1–8 mm); unusually large feldspar crystals are diagnostic of unit. Overlies units bcd (125±2 ka), mlc (130±1 ka) and bsc (172±2 ka), and banks against rhyolitic Hot Creek flow (333±2 ka). Overlain by unit bsr (99±1 ka) and diamict unit lmd. In MLGRAP-2 drill core (fig. 6; downtown Mammoth Lakes), 40 m of unit bfh directly underlies late Pleistocene till (unit glb) and rests on 17 m of alluvial and glacial deposits (probably unit gcd), which in turn overlies unit mcl (175±3 ka). $^{40}Ar/^{39}Ar$ age: 92.4±2.4 ka (cf. 92.7±2.4 ka for source scoria cone, unit bmc)

bhl **Basalt of Horseshoe Lake (late Pleistocene)—**Phenocryst-rich lava flows (48.9–49.3% SiO_2) that floor 1-km-wide shelf between Lake Mary and Horseshoe Lake in Mammoth Lakes Basin. Thickest exposure of severely eroded unit is ~60 m on glacially excavated cliffs overlooking Twin Lakes. Ice-scoured ledges and swells are block-jointed to slabby, locally flow-foliated, and typically massive but slightly to moderately vesicular in places; some lava outcrops adjacent to lake are heterogeneously streaky, as if fountain-fed. Glacially ravaged source vent was at site of Horseshoe Lake and is partly preserved on its east peninsula where a remnant of block-jointed lava caps and thus preserved a proximal scoria-fall deposit. Primary basaltic ejecta are mostly 5–25 cm, but a few are as big as 50–80 cm, and some have oxidized rinds. A smaller exposure on northeast rim of lake (UTM 032189/416440) likewise consists of scoria fall armored by a lava remnant. Elsewhere, southeast and east shores of lake are strewn with scoria and angular vesicular blocks of bhl lava, all ice mobilized and mixed with granitic erratics (many as big as 1–3 m) and sparser erratics of unit amp. Stratified surficial deposit that dips into lake at its southwest corner is largely a scree cone of scoria lapilli that washed down the cirque wall from unit bmc scoria cone atop Mammoth Crest. Phenocrysts in unit bhl: 10–15% plagioclase (0.5–5 mm); 5–7% cpx (1–3.5 mm); and 1–2% olivine (1–2.5 mm). Lava flows are notably rich in Mg and Ca but relatively poor in Al. Overlies units dbp and amp (97±1 ka). Overlain only by late Pleistocene till. Clasts of unit bhl are present in all late Pleistocene moraines of unit glb on both sides of Mammoth Creek. $^{40}Ar/^{39}Ar$ age: 31±1 ka

bmc **Basalt of Mammoth Crest (late Pleistocene)—**Eroded scoria cone (49.5–51.1% SiO_2) preserved as 1-km-long remnant, 500 m wide, atop north end of Mammoth Crest, an arête on main regional drainage divide, 1 km west of Crystal Crag. Upper half of cone remnant consists of stratified scoria, mostly brick-red but locally black, that dips radially and includes a few tack-welded layers; lapilli dominate but bombs as big as 1.5 m are common along crest. Gutted crater is enlarged and modified by erosion. Lower half of 120-m-thick unit consists of stratified agglutinate and fountain-fed lavas in layers 1–5 m thick that drape granite rim of arête; centrally these thicken downslope eastward to fill a paleoswale, where they are now eroded into a 40–50 m-high ledgy cliff. Massive cliff section is hackly or block-jointed but grades up into stratified agglutinate at its 3,100-m rim. Directly downslope from toe of cliff, at ~3,000 m, a bench-forming outlier of partly glassy massive lava is 70 m long, 25 m wide, and >8 m thick on its steep downslope face, which lies only ~55 m above Crystal Lake; outlier is in place, as shown by its intact jointing, consistently north-trending glacial striae, and paleomagnetic direction identical

to cliff above. A second outlier, 150 m southwest of Crystal Lake, is a chaotic slide mass (unit av on map). Lava evidently flowed down floor of Lakes Basin, from which it was subsequently stripped by glacial erosion, and extended 18 km to terminus near Hot Creek Fish Hatchery, where unit bfh is chemically, petrographically, paleomagnetically, and geochronologically identical. It is inferred that Lakes Basin contained little or no ice at time of eruption. Nonetheless, it seems required that stripping of unit bmc/bfh from most of Lakes Basin took place before emplacement of unit bhl (31±1 ka), which survives on the basin floor. This inference suggests that bmc/bfh lavas were removed during the interval 90–30 ka, presumably during MIS 4, by cirque glaciation within Lakes Basin. Scoriae reworked from the cone postglacially form a 5-m-thick stratified deposit of well-rounded lapilli (1–10 cm) at southwest shore of Horseshoe Lake. Lowest 1.5 m of this reworked section dips 25º NE into lake, and its clasts are less rounded than those higher in deposit, where wave reworking continues during seasonal highstands. Section represents a scree fan of sloughed cinders, in which many lapilli layers are separated by thin partings of buff ash.

Phenocrysts: Unit ranges from moderately to highly porphyritic; 8–15% plagioclase (1–22 mm, mostly 3–10 mm); 1–2% olivine (0.5–3 mm, plus sparse crystals as long as 8 mm); and sparse cpx (1 mm). Also contains olivine clusters of as many as 20 grains, rare olivine-plagioclase intergrowths, sparse xenocrysts of feldspar and quartz, and scattered granitoid xenoliths (1–15 cm), both rounded and angular. Scoria cone rests on Mesozoic granite and contacts no other volcanic unit. $^{40}Ar/^{39}Ar$ age: 105±7 ka (Mahood and others, 2010); 92.7±2.4 ka (cf. 92.4±2.4 ka for distal lava flow of unit bfh)

bmn **Trachybasalt northeast of Minaret Summit (late Pleistocene)—**Apron of modestly porphyritic lava flows (51.3–53.1% SiO_2) that extends for 2.8 km northeast from basin east of Minaret Summit; exposed discontinuously (through thick mantle of late Holocene Inyo pumice). Source vent is scoria cone 2 km northeast of Minaret Summit, same cone that later produced lavas of phenocryst-rich unit bar. Proximal scoria-fall deposit at south base of cone, 12 m thick where dissected by stream, includes ballistic bombs, 10–70 cm across and dense to scoriaceous, that are predominantly of bar type but commonly also of bmn petrography and composition. Lava apron, ~1 km wide, is everywhere glacially scoured and crops out as jointed ledges and platy floors of shallow draws; only distally is it eroded into cliffs and noses with 15–20 m relief. Southwesternmost proximal lava exposure (UTM 1993/6998) is compositionally most evolved part of unit (52.4–53.1% SiO_2, designated subunit bmn') and carries about half as many phenocrysts as the rest. Phenocrysts in most of unit: 3–5% plagioclase (1–3 mm, rarely 4–8 mm); 0.5–3% olivine (0.5–2 mm), and rare Fe-Ti-oxide mph (0.1–0.2 mm); cpx is absent or rare, found only in clots with plagioclase. Overlies unit ddc (103±9 ka). Overlain by unit bar (88±5 ka), late Pleistocene till, and 1350 C.E. Inyo pumice-fall deposit. Proximal, medial, and distal drill sites yield similar paleomagnetic directions (Mankinen and others, 1986; Hildreth and others, 2014). $^{40}Ar/^{39}Ar$ age: 87±7 ka (Mahood and others, 2010)

brc **Basalt of Red Cones (Holocene)—**Pair of scoria cones, agglutinate, and associated apron of subalkaline basaltic lava flows (49.9–51.2% SiO_2; 7.9–8.3% MgO; 0.6–0.8% K_2O), centered 3–4 km southwest of southern toe of Mammoth Mountain (fig. 10). Each cone is ~120 m high, 500 m wide, and consists of loose brick-red scoria and lesser spatter; lapilli dominate and bombs as big as 50 cm are uncommon. Scoria fall extends northeastward, thinning to a few cm within 2 km. Cone summits are 700 m apart, defining a north-northeasterly trend that strikes toward summit of Mammoth Mountain. Each has a small breached crater; that of northern cone opens southwest and that of southern cone northwest. Both breaches funnel into fans of agglutinate and thin fountain-fed lava flows, and these in turn merge into a 1.2-km^2 lava-flow field that steeply drapes the canyon wall for ~1 km west, thence extends 1.5 km southward to an uneroded terminus. Surface of lava apron is rubbly and scoriaceous, marked by ridges, steps, knobs, and swales that impart 3–8 m of local relief. Apron lavas are numerous and thin, 1–2 m thick proximally and 3–6 m distally; massive interior zones, which are typically <1 m thick, are only rarely exposed. Magma volume erupted is ~0.01 km^3, approximately equally divided between lavas and fragmental deposits. Unit has lowest alkali content in entire volcanic field.

Phenocrysts: 5–12% plagioclase (0.5–3 mm, rarely to 6 mm) seriate to groundmass laths; 5–8% olivine (0.5–2 mm, rarely 3 mm); cpx phenocrysts (0.5–1 mm) rare but cpx mph common. Also present are spinel inclusions in olivine, free titanomagnetite microphenocrysts, and sparse corroded plagioclase antecrysts. Xenocrysts and lithic ejecta derived from granitoids are common. Overlies Mesozoic granite (unit Kmo). Age: ~8 ka, from ^{14}C data for small charcoal fragments in sediments a few centimeters beneath ashfall at site 4.5 km northeast of Red Cones (Deming, 2002; Browne and others, 2010)

bsc **Trachybasalt of Sherwin Creek Road (middle Pleistocene)—**Low-relief sheet of phenocryst-poor lava (50.6–51.1% SiO_2) that extends 2 km eastward in two tongues near junction of Sherwin Creek Road with Highway 395, south of Mammoth Creek. Rolling surface is marked by low block-jointed swells and is highly vesicular. Unit is only patchily exposed, nowhere stream-incised, and widely mantled by sagebrush, aeolian sand, and marsh deposits. Phenocrysts: <1% plagioclase (0.5–1 mm, rarely up to 3 mm), many resorbed and corroded; rare olivine (mostly 0.1–0.3 mm; rarely 0.5–1 mm). Also contains sparse quartz and feldspar xenocrysts. Base not exposed. Overlain by units mlc (130±1 ka) and bfh (92±2 ka) as well as by alluvial, aeolian, and marsh deposits. Source vent unknown, buried by younger units far to west. Despite distal elevation as low as 2,170 m, lava flow was not inundated by Long Valley Lake. In water well 30M (fig. 6), 2 km southeast of downtown Mammoth Lakes, a 15-m-thick lava flow of unit bsc was penetrated at 92–107 m depth, where it directly overlies unit mcl (175±3 ka) and underlies ~30 m of glacial and alluvial deposits (inferred to be unit gcd). Clasts of unit in exposures of Casa Diablo Till (unit gcd) demonstrate an age greater than that of MIS 6. $^{40}Ar/^{39}Ar$ age: 172±2 ka

bsm **Basalt of Sawmill Cutoff (middle Pleistocene)—**Poorly exposed phenocryst-poor subalkaline lava flows (48.4–48.9% SiO_2, 10.3% FeO*, 6.4% MgO, 1.2% K_2O) that make up 1-km-wide steep ridge that extends 1.3 km eastward from beneath overlying margin of West Moat Coulee (unit rwm), 3–4 km north of Mammoth Lakes business district. Also includes an exposure on south slope of Knolls Vista and two isolated low-relief exposures north and south of Dry Creek near southwest foot of Lookout Mountain, all correlated on basis of petrography and distinctive chemical composition. Exposures are block-jointed, massive, only locally vesicular or vuggy, and have fine-grained groundmass. Unit is presumed to include several flows, at least on ridge where >90 m thick, but mantle of Inyo pumice and colluvium obscures almost all outcrops. Eastern nose of ridge abuts Early rhyolite (unit rer), but steepness of its north and south slopes is enigmatic. Glacial confinement of its low-viscosity lava flows during MIS 6 is conceivable, but till deposits are absent and exposure is too poor to provide evidence.

Phenocrysts: sparse plagioclase (1–2 mm, plus rare shattered megacrysts as big as 10 mm); sparser olivine (0.5–1 mm, rarely 3 mm, some in clots with plagioclase); rare cpx (1–3 mm); and rare plagioclase antecrysts, rounded and corroded. Also contains sparse quartz and feldspar xenocrysts. Unit banks against unit rer (~700 ka here) and overlies unit mcl (175±3 ka). Overlain by units rwm (~150 ka) and mkv (153±1 ka). $^{40}Ar/^{39}Ar$ age: 165±2 ka

bsr **Trachybasalt of Shady Rest (late Pleistocene)—**Apron of phenocryst-poor lava flows (50.6–51.7% SiO_2) that emerges from beneath late Pleistocene till at Shady Rest Campground and extends 5.5 km southeast to its terminus along and north of Laurel Creek (fig. 21). Apron has rolling surface marked by swells, ridges, and scattered tumuli; as thick as 8–12 m along its eastern flow front and medially where incised by Mammoth Creek. Exposures are generally vesicular and block-jointed except in a few places that are deeply incised where massive and slabby. Phenocrysts: 1–3% plagioclase (0.5–2 mm, rarely 3–4 mm); <1% olivine (0.5–1.5 mm; mostly mph); and traces of cpx (<1 mm) and Fe-Ti oxides (0.1–0.5 mm). North-central flow lobe that terminates just south of Sawmill Road is chemically identical but carries slightly more phenocrysts—3–5% plagioclase (1–4 mm), ~1% olivine (1 mm), and scattered cpx (1–2 mm). Small granitic xenoliths and derivative xenocrysts are sparse but widespread. Rare gabbroic intergrowths of olivine, cpx, and plagioclase as big as 10 mm are also present. Unit contains more and larger plagioclase and olivine than comparably phenocryst-poor unit amp near their mutual

contact east of Sherwin Creek Campground. Flows are notably rich in Fe and Ti. Overlies units asr, mmc, bcd, bfh, and Casa Diablo Till (gcd). Overlain by unit amp (97±1 ka) and by late Pleistocene till (unit glb). Source vent is buried somewhere to west, beneath either Mammoth Mountain or glacial deposits. In drill hole DC-1 (fig. 6; Sorey and others, 1978), located at UTM 259/781 (fig. 8), ~12 km north of Shady Rest Campground, a 20-m-thick lava flow compositionally and petrographically identical to unit bsr occurs beneath a flow of unit mor (66±2 ka) and atop a flow of unit aic (131±1 ka); if indeed coerupted with exposed unit bsr, this flow took a separate path, down west moat from a presumed vent near present site of Mammoth Mountain. Three sites sampled—proximal, medial, and distal—yield virtually identical paleomagnetic directions (Mankinen and others, 1986; Hildreth and others, 2014). $^{40}Ar/^{39}Ar$ ages: 99±1 ka (Mahood and others, 2010); 103.5±1.4 ka (table 2). K-Ar age: 64±14 ka (Mankinen and others, 1986). Overlies unit bfh (~bmc), which provided separate ages of 92.4±2.4 ka and 92.7±2.4 ka. Age conflict between units bfh and bsr is unresolved

dbp **Trachydacite of Bottomless Pit (late Pleistocene)—**Phenocryst-rich coulee (66.8–67.1% SiO_2) as thick as 160 m that forms east-facing bluff that rises above middle of the three Twin Lakes at southeast toe of Mammoth Mountain (fig. 22). Name derives from erosional tunnel, a rocky sloping passageway that descends through flow from high rim to talus at foot of bluff. Tunnel is flanked by several open chutes nearby, all eroded into bluff rim parallel to near-vertical northwest-striking flow foliation and jointing. Elsewhere, unit is block-jointed and glacially scoured into rounded knobs and buttresses. Flow is pervasively oxidized, atypically strongly so for Mammoth Mountain; crops out pale pinkish brown to reddish brown or locally tan with streaks and layers of black vitrophyre. Phenocrysts: 10–15% feldspar (0.5–6.5 mm); 3–4% hornblende (1–2 mm, rarely as long as 10 mm); 1–3% biotite (mph to 2 mm); common Fe-Ti-oxide mph, mostly in clots with feldspar. Overlies units dnh (64.5±0.8 ka), dsd (87±6 ka) and amp (97±1 ka). Overlain by units ddl (58±2 ka), ddu, and bhl (31±1 ka). Undated

ddc **Trachydacite of Dry Creek (late Pleistocene)—**Moderately porphyritic lava flow (66.9–67.4% SiO_2) that crops out in a north-northwest-trending belt 2.5 km long in upper Dry Creek basin, west of Dome 2861. As thick as 40–50 m, flow was everywhere glacially eroded into ridges, knobs, bluffs, and ledges; its width of exposure is only ~1 km because it was overrun by younger lavas. Exposures range from glassy to finely devitrified with pale-gray mottling, and from massive and block-jointed to (more widely) flow-foliated and thinly platy; platy jointing is commonly ramped or even near-vertical. Phenocrysts: 3–5% plagioclase (≤1 mm, rarely to 2 mm), a minority coarsely sieved internally; ≤1% opx (0.5–1 mm); and abundant Fe-Ti oxide mph (0.1–0.3 mm). Not coarsely porphyritic like hornblende-biotite trachydacites of units d61, d81, and Mammoth Mountain. Source vent buried by younger units to south or southwest, probably beneath Mammoth Mountain. Base not exposed, but may bank around base of unit d81 (99±7 ka). Overlain by units bar (88±5 ka) and bmn (87±7 ka). K-Ar age: 103±9 ka (Mankinen and others, 1986)

ddl **Trachydacite of lower Dragons Back (late Pleistocene)—**Phenocryst-rich coulee (66.0–66.8% SiO_2) as thick as 180 m that caps distal 600 m of Dragons Back, southeast ridge of Mammoth Mountain (fig. 22). Flow forms steep east-facing bluff above Twin Lakes as well as north- and south-facing scarps of ridge itself. Narrow ridgetop plateau is capped by blocky to craggy unglaciated vitrophyre that survived as cleaver above adjacent late Pleistocene glaciers. Eroded scarps are block-jointed ledges and buttresses of dense vitrophyre with locally pronounced flow foliation; blocks typically have thin brown scoriaceous rinds while freshly broken surfaces are sheer, black, and shiny. Where ddl flow overlaps oxidized unit dbp, it locally exposes a 10-m-thick massive red-brown lower zone that grades down into oxidized basal breccia, both of which pinch out toward eastern cliff. At north foot of steep Dragons Back ridge, chemically identical lava forms a glaciated shelf 30 m wide and 80 m long (UTM 225/659), which is block jointed on top but platy to slabby on its 15-m-high north-facing scarp, with oxidized flow breccia at base of flow. Glacial excavation of Twin Lakes Basin separated Dragons Back segment from its eastward extension, which survives as till-mantled Panorama Dome

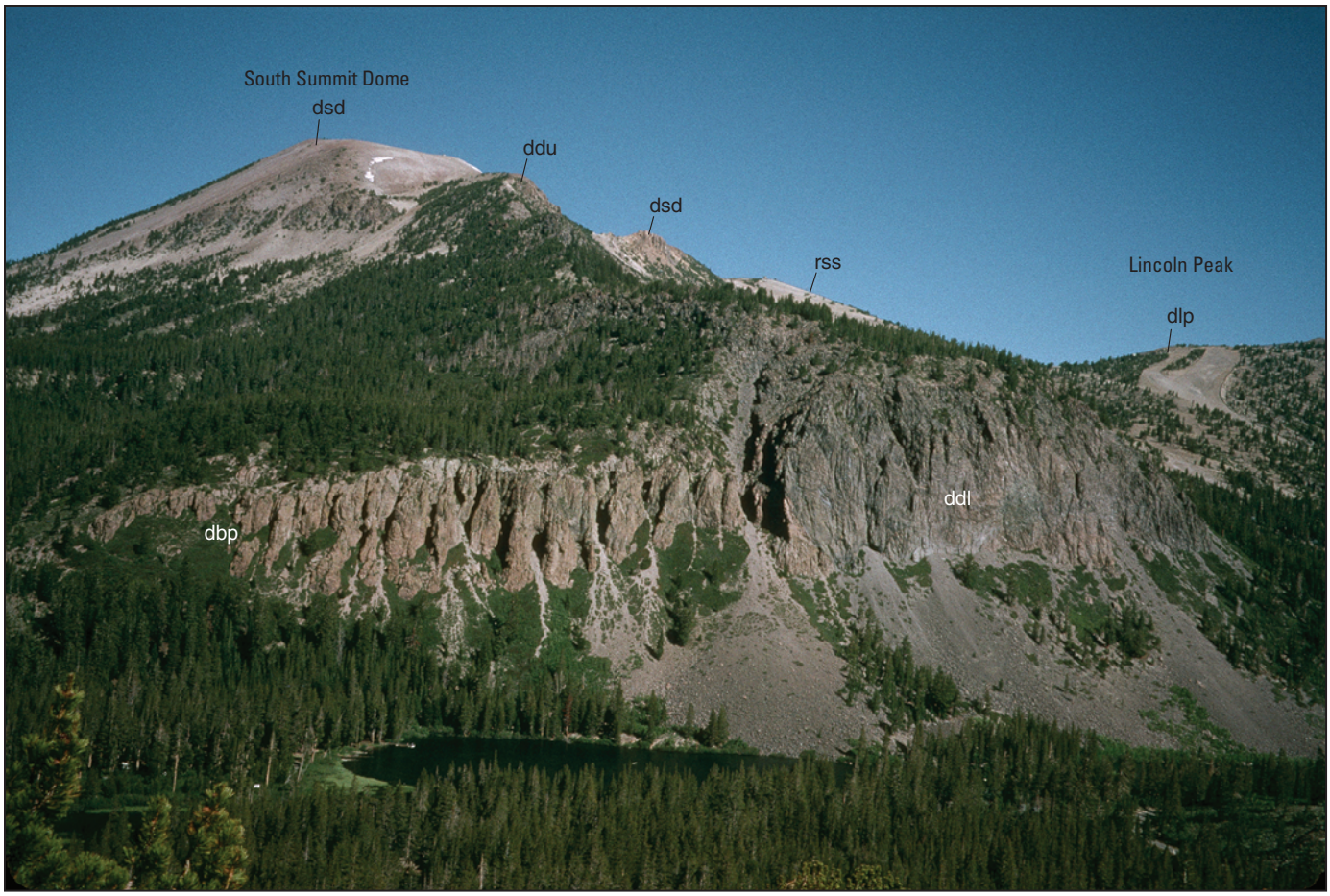

Figure 22. Southeast side of Mammoth Mountain above glaciated trough floored by Twin Lakes. Pervasively oxidized Bottomless Pit flow (unit dbp) is overrun by lower Dragons Back flow (unit ddl), which is, here, as thick as 180 m. Scree-mantled South Summit Dome (unit dsd), one of largest units on edifice, is widely altered hydrothermally.

(2,723 m on top); this segment crops out only in roadcuts on Lake Mary Road (2,640 to 2,660 m), where exposures are block jointed to slabby, moderately flow-foliated vitrophyre and felsite, widely iron-stained along partings. Phenocrysts: 10–15% feldspar (0.5–10 mm), 3–5% hornblende (1–5 mm); 1–2% biotite (mph to 1.5 mm); trace pyroxene mph; common Fe-Ti oxide mph; also contains oxide-amphibole-feldspar clots and cpx-oxide-feldspar clots. Overlies units dbp, dom (73±1 ka), and dtl (76±1 ka). Overlain by unit ddu. Paleomagnetic direction differs from those of unit dbp below and unit ddl above. $^{40}Ar/^{39}Ar$ age: 58±2 ka (Mahood and others, 2010)

ddu **Trachydacite of upper Dragons Back (late Pleistocene)—** Phenocryst-rich coulee (66.0–66.9% SiO_2) as thick as 160 m that caps uppermost 1-km-long segment of cleaver called Dragons Back, southeast of Mammoth Mountain summit; flow extends along ridgecrest from ~3,270 m down to eroded flow front at ~2,960 m. Much of crest is pale gray or iron-stained, crumbly vitrophyre or partly devitrified lava, but blocky remnants of massive dark gray vitrophyre, some of it vesicular, survive locally; flow foliation is locally conspicuous and many blocks retain thin brown scoriaceous crusts. Ice-scoured buttresses on north slope of flow are slabby to platy near base of unit. An erosional outlier <100 m wide that forms nubbin 3120+ (UTM 210/669), ~700 m north of upper end of Dragons Back and ~400 m northeast of Mammoth Mountain summit, is a precise match compositionally. Distal remnants also crop out through till on northeast side of Panorama Dome and in vicinity of 2,610-m switchback on Old Mammoth Road (UTM 240/652). Phenocrysts: 12–15% feldspar (0.5–7 mm); ~5% hornblende (1–5 mm, rarely 10 mm long); 1–2% biotite (mph to 1.5 mm); sparse Fe-Ti oxides; also contains common clots of

all combinations of these phases. Overlies units dsd (87±6 ka), dbp, and ddl (58±2 ka). Chemically almost identical to subjacent flow unit ddl but consistently slightly richer in Al (n=17 analyses; ddl and ddu together). Undated

dfl **Trachydacite of Face Lift (late Pleistocene)—**Phenocryst-rich lava flows (63.0–65.9% SiO_2) that extend from north face of Mammoth Mountain summit for ~1.5 km northward beneath unit rmf on Face Lift planèze (fig. 12) and bank against unit dms of McCoy Station plateau. Base not exposed but has as much as 80 m of relief along east margin, 50 m along west margin, and ~60 m at foot of summit scarp along The Chasm. Generally hackly or block jointed; flow foliation locally pronounced. Everywhere glacially eroded, but exposures are mostly glassy; oxidation and iron-staining along joint planes only modest and local. Phenocrysts: 15–20% feldspar (0.5–5 mm); 5–7% biotite plus amphibole in varied but subequal amounts (each as big as 2.5 mm); 1–2% pyroxene (0.3–2 mm); common Fe-Ti oxide mph. Also carries mafic blebs, oxide-pyroxene clots, feldspar clusters, and sparse angular xenoliths of pale-gray or tan, moderately porphyritic felsite (1–4 mm). Apparently extruded beneath summit or where The Chasm was eroded (fig. 12). Several dfl flows underlie unit rmf (61±1.5 ka) along both flanks of Face Lift planèze. Proximally, unit underlies summit-capping unit dsu (61.4±2 ka); distally, it banks against both sides of unit dms (68±1 ka) as well as apparently against unit dnk (60.4±1.2 ka). Several adjacent units here yield eruptive ages that are similar, but unit dfl is distinctive among them in being chemically less evolved and richer in pyroxene. Unit is similar in composition and paleomagnetic direction to unit drc, which crops out to south, on opposite side of Mammoth Mountain. $^{40}Ar/^{39}Ar$ age: 61±3 ka

dgr **Trachydacite of Gold Rush Express (late Pleistocene)—**Ice-scoured remnant of phenocryst-rich lava dome (68.7–68.8% SiO_2) that forms north-trending ridge 350 m long and only 150 m wide, just west of Lincoln Peak. Flat summit of ridge is current terminus of Gold Rush Express (Chair 10); lava nose that descends to north has ~100 m relief. Ridgecrest consists of pale-to-dark gray vitrophyre, block-jointed and flow-foliated; nose below to north is partly devitrified, widely oxidized, and strongly flow-laminated. Phenocrysts: 15–20% feldspar (0.5–4 mm, many atypically small for Mammoth Mountain); 5–6% biotite (mph to 2 mm); sparse hornblende (≤1 mm); ≤1% pyroxene (0.2–0.7 mm); common Fe-Ti oxide mph. Although slightly more evolved, this unit is chemically similar to Lincoln Peak (unit dlp); however, it contains far less hornblende and has a paleomagnetic direction distinct from that of adjacent Lincoln Peak. Contact relations with units dlp (64±7 ka) and rce (80±1 ka) are obscured by colluvium, but dgr is probably younger than rce and older than dlp. Undated.

Preserved atop dgr dome (UTM 217/670) is a 50-m-long remnant of poorly sorted, unstratified diamict 6–7 m thick. Enclosed in sandy matrix are angular clasts of phenocryst-rich dacite (typical of Mammoth Mountain) seriate in size from granules to blocks as big as 50–80 cm. Absence of thermal effects and prismatic jointing, along with contrasting textures among blocks (fresh vs altered; vesicular vs dense; glassy vs devitrified), suggests deposit is glacial or colluvial, not pyroclastic. One large block analyzed is petrographically and chemically indistinguishable from unit dsd (87±6 ka), which crops out ~1 km uphill

dlp **Trachydacite of Lincoln Peak (late Pleistocene)—**Phenocryst-rich Dome 3079 (67.7–68.5% SiO_2) centered 1.5 km northeast of Mammoth Mountain summit (fig. 1). In plan view, glaciated lava dome is 500 by 700 m, elongate to east-northeast. Steep north face has 160 m of relief and east face as much as 220 m; south and west slopes are gentler. Many exposures are black to medium-gray vitrophyre that splits blocky to slabby. Flow foliation conspicuous and nearly ubiquitous; common for pale gray or reddish brown layers to interleave with dark glassier ones. Eastern cliffs dominated by buttresses of shiny black vitrophyre; northern cliff includes such vitrophyre but also has medium-gray partly devitrified domains that weather dull gray and, locally, flow-laminated domains that split into thin plates with tan and pink films. Phenocrysts: 15–20% feldspar (0.5–8 mm, few >5 mm); 2–4% biotite (mph to 1.5 mm); 1–3% hornblende (mph to 2.5 mm); trace cpx (0.4–0.8 mm); common Fe-Ti oxide mph. Flow-foliated rocks of summit and nearby southeast spur (UTM 222/672) are physically disturbed, as inferred from anomalous

paleomagnetic vectors; after partial cooling, upper crags were probably heaved and rotated by renewed inflation of dome. Overlies units rce (80±1 ka) and probably banks against unit dgr. Unit rsq (63.7±4 ka) banks against south toe of Lincoln Peak dome. $^{40}Ar/^{39}Ar$ age: 64±7 ka

dml **Trachydacite of Main Lodge Coulee (late Pleistocene)—**Phenocryst-rich coulee (65.6–68.6% SiO_2) that emerges from beneath unit dms at 2,900 m elevation and extends 1 km northward to an eroded flow front at 2,710 m, just east of MMSA Main Lodge. Outcrops of glaciated flow are patchy because of heavy mantle of till and colluvium, but relief of at least 50 m is exposed along east margin. Exposures are weakly to moderately flow-foliated vitrophyre, medium gray to black with subordinate layers vesicular, sheared, or weathered reddish brown; splits slabby but more commonly coarsely blocky; weathered outcrops crumbly. Where bulldozed for ski runs, pale gray or pinkish gray devitrified interior facies is locally exposed. Phenocrysts: 12–20% feldspar (mph to 5 mm); 2–4% biotite (mph to 2.5 mm); 1–4% hornblende (mph to 2 mm; ~1% pyroxene (0.5–2.5 mm); common Fe-Ti oxide mph. Also contains rare 1–3 mm inclusions of intergrown feldspar and black pyroxene. Base not exposed. Overlain by unit dms (68±1 ka). $^{40}Ar/^{39}Ar$ age: 67±1 ka (Mahood and others, 2010)

dms **Trachydacite of McCoy Station (late Pleistocene)—**Phenocryst-rich coulee (68.5–69.6% SiO_2) that emerges from beneath sloping apron of unit rmf and extends ~1 km northward, forming plateau site of McCoy Station (fig. 7) and distal lobe farther downslope atop unit dml. Although thinned substantially by glacial erosion, flow is still as thick as 60 m on northeast-facing scarp of plateau. Farther north, unit pinches out as a few deeply scoured remnants exposed patchily through till, colluvium, and Inyo pumice covering surface of underlying dml coulee. Moderately to strongly flow-foliated vitrophyre; dense black glassy layers alternate with pale gray partly devitrified layers and lenses, some lithophysal or spherulitic; glassy parts often disintegrate crumbly where weathered. Phenocrysts: 10–12% feldspar (0.5–5 mm); 2–5% biotite (mph to 3 mm); ~1% opx (mph to 2 mm); sparse hornblende (0.3–1 mm; rarely as long as 3 mm); common Fe-Ti oxide mph; also carries sparse mafic blebs and common pyroxene-oxide-feldspar clots. Composition significantly more silicic than adjacent units dfl and dml. Overlies unit dml (67±1 ka); overlain by units dfl (61±3 ka) and rmf (61±1.5 ka). $^{40}Ar/^{39}Ar$ age: 68±1 ka (Mahood and others, 2010)

dnh **Trachydacite north of Horseshoe Lake (late Pleistocene)—**Two phenocryst-rich lava flows (67.9–68.4% SiO_2) in poorly exposed window between units amp and dbp, ~700 m north of Horseshoe Lake. Widely covered by colluvium, unit crops out as minor southeast-trending rib ~500 m long and ~150 m wide, expressed mainly as two 10-m-high glaciated ledges (at elevations 2,760 and 2,860 m) that probably represent two southeast-sloping lava flows. Both ledges are block-jointed vitrophyre, black to pale gray or locally oxidized. Phenocrysts: 12–15% feldspar (0.5–5 mm); 2–3% biotite (mph to 3 mm); 0.5–2% hornblende (mph to 1.2 mm); ~1% opx (mph to 2.5 mm); common Fe-Ti oxide mph. Also carries sparse mafic blebs. Paleomagnetic directions of both flows are apparently excursional, contrasting with those for units dsd, dbp, and others nearby (Hildreth and others, 2014). Lower ledge contains abundant gray fine-grained enclaves (56.7% SiO_2), 1–20 cm across and variously rounded, angular, or crenulate; they carry fewer crystals than host lava but their crystal cargo consists of same species plus common cpx. Base of unit not exposed but inferred to bank against unit amp (97±1 ka). Overlain by unit dbp. $^{40}Ar/^{39}Ar$ age: 64.5±0.8 ka

dnk **Trachydacite of North Knob (late Pleistocene)—**Phenocryst-rich lava dome (66.4–66.5% SiO_2) centered 450 m west of McCoy Station at midslope on north flank of Mammoth Mountain (fig. 7). Terminus of Broadway Express (Chair 1) is on summit of dome (3,016 m). Dome exposure is altogether 700 m in diameter and includes 400-m-long ice-scoured rib separated by scree chute just west of main knob; relief is ~200 m on steep north slope of dome. Outcrops are mostly medium-gray vitrophyre, massive or flow-foliated, and widely oxidized reddish brown (especially upper parts); extensive domains are partly devitrified (owing to glacial removal of original glassy carapace), and southeast slope is hydrothermally altered. Phenocrysts: 12–15% feldspar (0.5–8 mm); 3–5% biotite

(mph to 2 mm, rarely to 5 mm); 2–3% hornblende (mph to 2 mm); common Fe-Ti oxide mph. Also carries plagioclase clusters and biotite-oxide-feldspar clots. Almost surrounded by surficial deposits but probably older than unit dfl along its east margin. Northerly paleomagnetic declination and moderate (40°) inclination differ from steep northwesterly directions of flow sequence that built adjacent Face Lift planèze (units dml, dms, dfl, rmf, and dsu). $^{40}Ar/^{39}Ar$ age: 60.4±1.2 ka

dnw **Trachydacites of northwest moat (late Pleistocene)—**Five discrete nonglaciated extrusions of related but variably contaminated magma (60.4–67.3% SiO_2) in northwest moat of Long Valley Caldera, 9 km north of Mammoth Mountain; their vents are aligned roughly northwest-southeast along a 2.5-km-long trend. From northwest to southeast, the five are generally more voluminous and more contaminated. All are glassy but choked with microlites and carry 15–20% crystals larger than 0.5 mm—phenocrysts, antecrysts, and xenocrysts. All have abundant biotite and sparser amphibole (both mph to 1.5 mm), both euhedral but ranging from fresh to opacitized. All contain rounded quartz (1–3 mm), many of them embayed. Intergrown clots (1–4 mm) of cpx, Fe-Ti oxides, and plagioclase (all generally mph) are common in all five. Free cpx (and rare opx) euhedra (mph to 1 mm) are probably disaggregated from such clots. Feldspars (1–25 mm) dominate all assemblages, include both sanidine and plagioclase, and are mostly sieved and partly resorbed; some have clear overgrown rims, and some were in advanced stages of dissolution when eruptively quenched. Subordinate plagioclase populations (0.5–3 mm) are euhedral. Sparse mafic blebs and enclaves are crystal-poor but olivine-bearing, and some enclose sieved feldspars from host dacite. From north to south, the five subunits mapped are:

1. Small coulee (65.7% SiO_2), 20–30 m thick, that crops out 500 m long and 400 m wide below snout of 1350 C.E. Glass Creek flow (unit ric), which conceals its vent at caldera wall. Coulee is glassy and rugged, its knolls and ridges consisting of joint blocks with rough scoriaceous surfaces; rich in hornblende, biotite, and plagioclase, but few phenocrysts >5 mm. Contains mafic blebs as big as 1 mm; larger enclaves were sought but none found.

2. Small steep-sided dome (66.0% SiO_2), nearly circular in plan, intrudes east margin of subunit 1 near base of caldera wall. Dome is 250 m in diameter, 50 m high, largely glassy, coarsely blocky, and little eroded. Rocks are mostly massive, with scattered irrregular vugs and a few internal shear planes of oxidized breccia; some blocks have scoriaceous surfaces. Contains abundant feldspar (both plagioclase and sanidine; mostly 1–3 mm, fewer 6–10 mm); Carries sparse cpx+olivine+plagioclase-bearing mafic enclaves (1–10 cm), but fewer than in subunits to southeast.

3. Adjacent to subunits 1 and 2, knob 2430 caps a coulee that spread radially from a vent marked by a steep dome 30 m high. Knobby lobate coulee is 750 by 1000 m wide and has relief of 20–80 m, greatest at its eastward-descending lobe. This subunit, too, is glassy and block jointed but, in addition, is strongly flow foliated, its foliation ramping radially upward toward coulee margins. Crystal cargo is like that of subunit 2, including abundant biotite, but its mafic enclaves are more abundant, mostly 1–5 cm across, and irregularly distributed; a sampled enclave has 56.4% SiO_2. Vent dome and adjacent southeast surface of coulee differ from rest of subunit in containing abundant and conspicuous large feldspar crystals (10–25 mm). At 67.3% SiO_2, vent dome is most silicic part of unit dnw sampled; subjacent coulee has 65.2–65.7% SiO_2 (n=5).

4. Fourth in line is a bilobate lava flow (62.5–64.3% SiO_2—strongly hybridized) that spread radially from its apparent vent at knob 2400+. Sections of its chilled carapace were dragged and spread by its then still-mobile interior to produce a labyrinth of rifted troughs on its surface; such fissures are typically 10–15 m wide, as deep as 10 m, and extend for several hundred meters. Flow surface is glassy and coarsely blocky, and northeast flow front is 25–30 m high. Surfaces of blocks are commonly scoriaceous and oxidized, though smooth on walls of fissures. Contains abundant plagioclase and sanidine crystals (mostly 5–15 mm but overall 1–25 mm), many equant but some elongate or broken; also a varied cargo of biotite, hornblende, opx, cpx, rounded or wormy quartz, cpx-olivine-oxide-plagioclase clots, and rare olivine xenocrysts. Also contains

abundant mafic enclaves (1–10 cm), typically fine-grained, phenocryst-poor, olivine-bearing, and oxidized.

5. Most voluminous, most contaminated (60.4–61.7% SiO_2), and southeasternmost of the five subunits is a major coulee, 1–1.5 km wide, that flowed 2 km northeastward from its vent. Its surface is a rough craggy plateau that descends gently northeastward to a steep lobate flow front as high as 20 m, which overlies lava field of unit mcv (~33 ka). Rugged block-jointed ridges and swells on its surface have 3–8 m of local relief. Like subunit 4, flow surface has rifted troughs, fewer and smaller than on its neighbor, variously oriented, 100–200 m long, their floors 5–12 m wide and their walls 3–7 m high. Nearly all outcrops are black crystal-rich vitrophyre carrying scattered irregular vesicles; block surfaces are commonly scoriaceous and oxidized brown. Contains same crystal cargo as accompanying subunits, including abundant plagioclase and sanidine as big as 25 mm; coexisting quartz and magnesian olivine; opacitized biotite and hornblende; numerous rounded, embayed, or strongly sieved crystals; microdioritic inclusions; and abundant mafic enclaves (1–10 cm). Xenoliths of granitic and metamorphic rocks are also present (Rinehart and Ross, 1964; Bailey, 2004). Vent for coulee, near its southwest limit, is marked by tack-welded to dense agglutinate and lineated rolls of extrusive lava.

Unit dnw overlies units bar, mnd, and mcv; probably also rests on Mesozoic granite and Pliocene mafic lavas, both of which crop out within a few hundred meters of north margins of dnw. Overlain by Inyo pumice-fall deposit and rhyolitic Glass Creek flow (both 1350 C.E.). $^{40}Ar/^{39}Ar$ ages (sanidine from each subunit): (1) 40±1 ka; (2) 42±1 ka; (3) 40±1 ka; (4) 30±1 ka; (5) 27±1 ka (1–2 from table 2; 3–5 from Mahood and others, 2010)

dom **Trachydacite of Old Mammoth (late Pleistocene)—**Most distal and topographically lowest of four dacite coulees east of Twin Lakes that step down eastward toward Old Mammoth district. Phenocryst-rich flow (65.7–66.0% SiO_2) emerges from under till and unit ddu near 2,570 m elevation along Old Mammoth Road grade and extends ~1 km eastward as flat-topped till-strewn bench to its eroded terminus at steep east-facing bluff above Mammoth Meadow (fig. 23). Glacially scoured flow is at least 90 m thick as exposed on north, east, and south scarps, locally called The Bluff. Rock is predominantly flow-foliated vitrophyre, patchily oxidized, with some layers and domains partly devitrified (especially on deeply scoured rim of The Bluff). Phenocrysts: 10–12% feldspar (0.5–10 mm); 3–5% hornblende (mph to 2 mm); 1–2% biotite (mph to 2 mm); common Fe-Ti oxide mph. Base not exposed, but south margin banks against pre-Cenozoic rocks. Overlain by units ddu and ddl (58±2 ka). $^{40}Ar/^{39}Ar$ age: 73±1 ka

drc **Trachydacite of upper Reds Creek (late Pleistocene)—**Phenocryst-rich lava flow (63.8–65.7% SiO_2) on upper southwest slope of Mammoth Mountain; exposed as 250-m-wide swath ~600 m long that descends steeply from beneath summit dome (unit dsu) at ~3,260 m to an eroded flow front at 3,040 m on west wall of Reds Creek. Rock is flow-foliated and block-jointed vitrophyre, black to medium gray; only locally vesicular or oxidized. Uppermost outcrops are ribs and ledges widely concealed by scree; distal outcrops are steep rugged cliffs that weather dark brown. Phenocrysts: 15% feldspar (0.5–7 mm); 3–5% hornblende (mph to 2 mm, rarely to 3.5 mm); ~1% biotite (mph to 1.5 mm); ~1% pyroxene (mph to 2.5 mm); common Fe-Ti oxide mph. Also carries mafic blebs, oxide+cpx±plagioclase clots, and brick-red dacitic autoliths. Base not well exposed but fresh drc overlies adjacent unit dsd (87±6 ka), which is acid-altered at and near contact. Also overlies units dwr (73±2 ka) and dsk (71±1.5 ka), but is overlain by unit dsu (61.4±2 ka). Unit is similar in composition and paleomagnetic direction to unit dfl (61±3 ka), which crops out to north, on opposite flank of Mammoth Mountain. Undated

drf **Trachydacite of Rainbow Falls (late Pleistocene)—**Phenocryst-poor coulee (65.7–67.1% SiO_2) that extends from near Reds Meadow for 6 km southward along or near course of Middle Fork San Joaquin River. Severely glaciated flow is 30–40 m thick in north and as thick as 80 m in south; its surviving width is ~600 m but was originally more expansive and may have extended much farther downstream. Unit fills paleochannels cut in Mesozoic granite, and it supports two prominent waterfalls along Middle Fork (the eponymous fall being 30 m high). Striking meander of Middle Fork, 250 m in amplitude and ~800 m

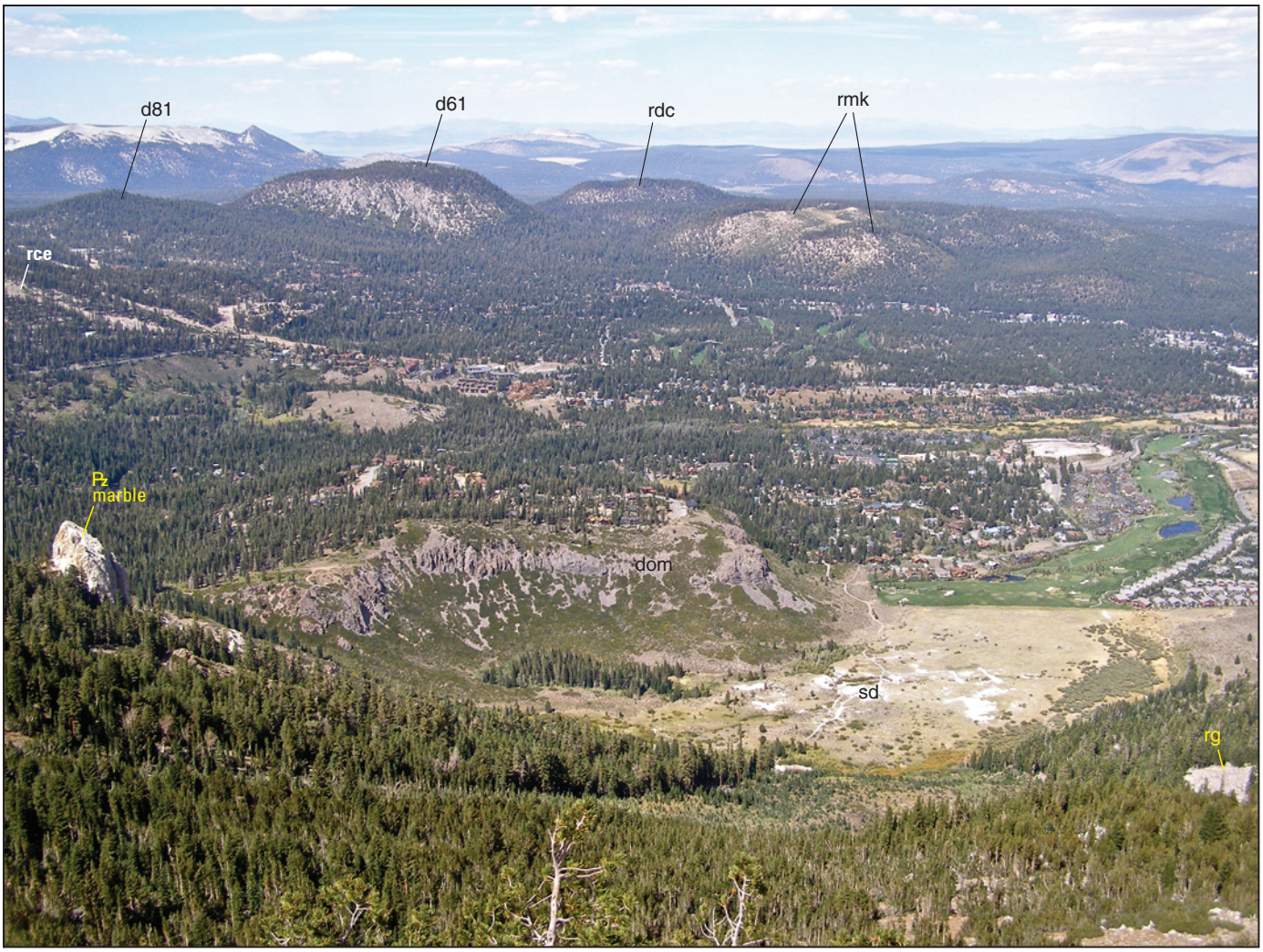

Figure 23. Town of Mammoth Lakes and four adjacent late Pleistocene (~110–87 ka) lava domes: Units d81 and d61 consist of Mammoth Mountain trachydacite, whereas units rdc and rmk are Long Valley high-silica rhyolite. Background scarp is northwest wall of Long Valley Caldera, in the west moat of which the four domes erupted. In left foreground, Mammoth Rock is white spire of Paleozoic marble. Near center is 90-m-high scarp (called The Bluff), which is easternmost coulee of Mammoth Mountain trachydacite (73-ka unit dom). Avalanche scar in lower foreground; toe of rock glacier (unit rg) at lower right. Barren part of Mammoth Meadow in center-right foreground is covered in part by postglacial travertine and sinter (unit sd). View northward from Solitude surface on Red Mountain.

upstream from Rainbow Falls, produced channel entrenched in dacite and abandonment of shallower channel along west edge of unit that had temporarily accommodated overflow when intracanyon dacite lava flow displaced river. Where exposed atop granite, basal zone includes vertical prismatic joints that locally form slender polygonal columns 3–8 m high, overlain by abrupt transition to platy interior of flow (fig. 24). Surface is rolling terrain of ice-scoured hillocks, ridges, ribs, and ledges. Some outcrops are massive, block-jointed, hackly, chunky, or slabby, but most are strongly flow-foliated and thinly platy. A few glassy domains survive, notably basal vitrophyre zones locally, but most exposures are devitrified, aphanitic, pale gray, and commonly mottled. Phenocrysts: 1–3% plagioclase (mostly 0.5–1 mm; some slender laths as long as 3 mm); rare biotite (mph to 1 mm); sparse opx (0.3–1 mm; either equant or prismatic); trace Fe-Ti oxides (0.1–0.3 mm); with or without sparse hornblende needles (mph to 2 mm long, some with rounded resorbed ends), unevenly distributed. Also contains pale gray, tan-weathering sugary enclaves (1–30 mm), some vesicular and either angular or rounded; in thin section, enclaves are meshwork of slender plagioclase and hornblende prisms, studded with tiny equant pyroxenes and oxides. Unit overlies Mesozoic granite (unit Kmo)

Figure 24. Trachydacite of Rainbow Falls, ~1 km downstream from Devils Postpile, showing abrupt change from columnar base (which rests on granite) to platy interior, which is characteristic of most outcrops. Glacially scoured intracanyon flow, here only ~12 m thick, is elsewhere as thick as 80 m and is preserved for ~6 km along Middle Fork San Joaquin canyon. Phenocryst-poor lava flow erupted at 98±1 ka.

and banks against unit Tbtb (3,754±7 ka). Overlain by units mdp (82±1 ka) and amp (97±1 ka). Contact of massive unit amp atop platy unit drf is well exposed on south wall of gorge just below Rainbow Falls. $^{40}Ar/^{39}Ar$ ages: 98±1 ka (Mahood and others, 2010); 98.8±0.6 ka (table 2)

dsd **Trachydacite of South Summit Dome (late Pleistocene)—**Phenocryst-rich lava dome (67.3–68.4% SiO_2) that forms 500-m-wide plateau just south of summit dome (unit dsu) and most of south slope of Mammoth Mountain (figs. 1, 22)—from 3,320 m down to 2,900 m. One of most extensive on edifice, unit also crops out as altered arete 3180+ (500 m east of summit) and in windows through till as low as 2,860 m in valley north of Dragons Back. Long south slope is mantled by thick colluvium, and steep northeast face is widely draped by till. Upper slopes, northeast arete 3180+, and Reds Creek area are extensively acid altered (cream-white to yellow) and locally also oxidized brick red. Alteration facilitated glacial excavation of northwest-trending trough (The Chasm, which is not a fault zone) along base of steep northeast face of Mammoth Mountain. Deep erosion has exposed varied lithologies, ranging from devitrified through pale-gray or black vitrophyre and from massive to weakly or strongly flow foliated. Best outcrops are block-jointed ledges. Phenocrysts: 10–15% feldspar (0.5–7 mm); 3–5% biotite (mph to 2.5 mm); 2–5% hornblende (mph to needles as long as 10 mm); sparse pyroxene (mph to 2.5 mm);

common Fe-Ti oxide mph; also has mafic blebs, pyroxene-oxide-plagioclase clots, and clots as big as 20 mm of oxides, amphibole, biotite, and feldspars in varied proportions. Overlies units rrc (83±1 ka) and amp (97±1 ka). Overlain by units dbp, ddu, drc, and dsu (61.4±2 ka). $^{40}Ar/^{39}Ar$ age (at south toe of unit): 87±6 ka.

In drill hole HSL-1 near Horseshoe Lake (fig. 6), a trachydacite flow ~15 m thick (nowhere exposed) is similar to unit dsd chemically and petrographically, but it underlies stack of thin flows of unit amp, which predates dsd. It may be the oldest trachydacite known on Mammoth Mountain

dsk **Trachydacite of Skyline Dome (late Pleistocene)—**Phenocryst-rich lava dome (67.2–69.8% SiO_2), ~700 m wide, on crest of Mammoth Mountain (fig. 7) just southeast of Scottys Dome (unit dwr). On precipitous north rim is conspicuous terminal of Chair 23; north-face has more than 200 m exposure, its toe concealed by talus. Unit is block-jointed or slabby, and flow foliation is subdued (relative to lavas of adjacent domes). Upper part of unit is widely acid-altered, its surfaces cream-white, yellow, or rusty reddish brown, but interiors of some thick slabs are pale to medium gray and fairly fresh. Lower part of north face is fresher, eroding into coarsely block-jointed ledges. Erosional outlier, similar in composition and paleomagnetic declination, forms ice-scoured rib at 3,100 m elevation (UTM 204/672), 600 m north of summit and 270 m lower; northwest-trending rib, ~80 m wide and 250 m long with <20 m local relief, consists of flow-foliated black and reddish-brown vitrophyre with a slabby devitrified domain exposed at its lower end. Phenocrysts: 12–15% feldspar (0.5–5 mm); 3–5% biotite (mph to 1.5 mm); sparse Fe-Ti oxide mph; trace pyroxene (0.3–0.8 mm); also contains biotite-oxide-feldspar clots and rare clusters of pyroxene. Overlies unit dwr (73±2 ka). Overlain by units drc and dsu (61.4±2 ka). $^{40}Ar/^{39}Ar$ age: 71±1.5 ka

dsu **Trachydacite of Mammoth Mountain summit (late Pleistocene)—**Phenocryst-rich summit dome (68.0–69.6% SiO_2) of Mammoth Mountain (elevation 3,369 m; figs. 1, 7). Ice-scoured dome-flow complex extends ~700 m along crest and has ~150 m of relief. A large but uncertain fraction has been glacially stripped. Summit is site of café, interpretive center, and terminus of góndola that ascends from north toe of edifice. Most exposures are ledges and cliffs of flow-foliated vitrophyre, black to pale gray, widely exhibiting reddish brown films on joint surfaces. Cliffs also expose shear zones of flow breccia as thick as 10 m. Much of upper surface and south slope are acid altered, whereas freshest rocks are cliffs at southeast end of unit and a strongly flow-foliated lava flow along its northwest rim. An outlying remnant, only ~300 m long and 50 m wide, banks against unit rmf along upper east side of glaciated Face Lift planèze, where it is youngest unit preserved. Phenocrysts: 10–15% feldspar (0.5–7 mm); 3–5% biotite (mph to 2.5 mm); 1–2% hornblende (mph to 2.5 mm); sparse pyroxene (0.3–1 mm); sparse Fe-Ti oxide mph; also carries mafic blebs, biotite-oxide-feldspar clots, hornblende-feldspar clots, and angular biotite-felsite xenoliths (1–15 cm). Intrudes and overlies unit dsd (87±6 ka. Overlies units drc, dfl (61±3 ka) and rmf (61±1.5 ka); apparently banks against unit dsk (71±1.5 ka). $^{40}Ar/^{39}Ar$ age: 61.4±2 ka

dtl **Trachydacite of Twin Lakes outlet (late Pleistocene)—**Phenocryst-rich lava flow of low-silica trachydacite (63.0–64.0% SiO_2) that extends ~1 km eastward from Twin Lakes outlet bridge. Crops out as a 50-m-high ledge above Lake Mary Road just north of outlet and extends downstream along both banks of Mammoth Creek, supporting a scenic waterfall at 2,550 m. Elsewhere extensively covered by glacial deposits, unit is also exposed in 2,530-m roadcut on Old Mammoth Road (240/6575) and as three small windows at 2,760–2,810 m on floor of till-mantled valley north of Dragons Back. Everywhere glaciated, outcrops are partly glassy or widely devitrified, block-jointed or slabby, patchily oxidized, variously massive, vuggy, or weakly vesicular, with flow foliation typically poorly developed. Phenocrysts: 15–25% feldspar (0.5–7 mm); 3–5% hornblende (0.5–7 mm); 3–5% biotite (mph to 1.5 mm); 1–2% pyroxene (mph to 2 mm); common Fe-Ti-oxide mph. Also contains mafic blebs, fine-grained cpx-oxide-plagioclase clots, intergrowths of plagioclase and hornblende (1–2 cm), and finely porous, fine-grained inclusions (1–25 mm, rounded to angular) that carry mph of plagioclase, hornblende, biotite, and pyroxene—all typically ≤0.5 mm. Base not exposed but probably overlies

unit amp (97±1 ka). Inferred to be overlain by nearby units dbp and ddl (58±2 ka), but all contacts are covered by surficial deposits. $^{40}Ar/^{39}Ar$ age: 76±1 ka

dwr **Trachydacite of White Bark Ridge (late Pleistocene)—**Phenocryst-rich lava dome-flow complex (67.9–69.5% SiO_2) that makes up entire west flank of Mammoth Mountain (fig. 7). Outcrop belt is ~1 km wide and extends ~2.5 km north-south, including White Bark Ridge (UTM 192/677), Scottys Dome (UTM 197/671), and southwest flank west of Reds Creek. Exposed up to 3,175 m atop steep-walled dome, down to 2,850 m on White Bark Ridge, and as low as 2,780 m at southwest extremity. From 2,800 m to 2,960 m, pumice-mantled southwest lobe consists of four ledges of block-jointed vitrophyre, which appear to be discrete (but compositionally similar) lava flows. Most outcrops are black to medium-gray vitrophyre, strongly to weakly flow-foliated, block-jointed or slabby, and only locally either vesicular or partly devitrified. Craggy rim of dome retains reddish-brown scoriaceous crusts and may have stood above ice; unit is everywhere else glacially eroded. Although unit consists of several physiographic components, no simple subdivision of sprawling complex can be made on basis of broadly similar compositional data; for example, TiO_2 (0.50–0.58%) and K_2O (4.25–4.46%) exhibit no systematic spatial pattern (n=15). Nonetheless, two extrusive episodes are indicated by paleomagnetic data: northern coulee and western flow lobe share modest inclination and northeasterly declination, whereas younger components (Scottys Dome and topmost coulee to southwest) share steep inclination and northerly declination (Hildreth and others, 2014).

Phenocrysts: 10–15% feldspar (0.5–6 mm); 3–5% biotite (mph to 2.3 mm); <1% hornblende (mph to 1.5 mm); sparse pyroxene (0.2–1 mm); sparse Fe-Ti oxide mph; also carries varied clots of these phases in all combinations. Overlies units rrc, amp (97±1 ka), and dsd (87±6 ka), and banks against Mesozoic granite (unit Kmo) at topographic wall of Long Valley Caldera, thereby enclosing 1-km-long hollow that now contains Reds Lake. Overlain by units drc and dsk (71±1.5 ka). $^{40}Ar/^{39}Ar$ ages: 79±12 ka for western flow lobe; 73±2 ka for top of Scottys Dome

d61 **Trachydacite of Dome 2861 (late Pleistocene)—**Large dome of phenocryst-rich lava (66.1–67.6% SiO_2) of Mammoth Mountain type centered 2 km northeast of toe of Mammoth Mountain edifice and 3 km northwest of Mammoth Lakes business district (fig. 23). Steep- sided dome is 1.5–2 km wide and >300 m high. Most exposures are flow-foliated and variously block-jointed, hackly, or slabby. Rolling unglaciated upper surface of dome remains glassy and micropumiceous, but steep faces have at least been frost riven, as much of their glassy carapace has been removed. Ten steep (55º) chutes are cut into upper 120 m of south face; because there is little catchment area above, their excavation along parallel vertical joints may have been accomplished by late Pleistocene frost action beneath a thin mantle of ice or nevé. Dome was called "Mammoth Shoulder dome" by Suemnicht and Varga (1988). Inappropriately called "Earthquake Dome" (for example, by Bailey, 1989) because that name associates dome with "Earthquake Fault" (a tourist attraction and open fissure), which cuts adjacent Dome 2781 (see unit d81) but not this one. Low-relief aprons adjacent to southeast and northeast toes of dome consist of monolithologic fragmental deposits derived from it, including angular to subrounded clasts (1–50 cm) enclosed in a dominant matrix of pale-gray fine-to-coarse ash; blocks are pale purplish-gray, tan-weathering, glassy, and finely to non- vesicular. Deposits are unstratified, tan-weathering, and at least 2–7 m thick. Hummocky surfaces suggest deposition as rockfall avalanches (unit av) from steep faces of dome, but a few increments may have originated as pyroclastic flows. Phenocrysts: 10–15% feldspar (0.5– 4 mm); 1–2% biotite (mostly mph but as big as 1.5 mm); 2–3% hornblende (mph to 3.5 mm); trace pyroxene (0.2–0.7 mm); common Fe-Ti-oxide mph. Roof of piston-like dome lifted a 500-m-long slab containing mafic lavas of units mcl (175±3 ka) and bar (88±5 ka). Dome appears to overlap adjacent dome (unit d81; 99±7 ka). $^{40}Ar/^{39}Ar$ age: 87±2 ka (Mahood and others, 2010)

d81 **Trachydacite of Dome 2781 (late Pleistocene)—**The "real" Earthquake Dome, a sprawling phenocryst-rich flow-dome complex (68.6–69.1% SiO_2) that lies between adjacent younger edifices of Dome 2861 (unit d61) and Mammoth Mountain. Gently sloping edifice is 2 by 2.5 km wide, has total relief of 180 m to north and 300 m to south, and

is centered 3.5 km northeast of Mammoth Mountain summit (fig. 23). Poorly exposed slopes are deeply mantled by colluvium and by 1350 C.E. Inyo pumice-fall deposit. Good exposures are present at summit, along west and southeast margins, and along open fissure nicknamed "Earthquake Fault" (Benioff and Gutenberg, 1939). Exposures are generally crumbly, thinly flow-foliated vitrophyre, black or locally oxidized, but include pale-gray, brown-weathering pumiceous carapace preserved near summit. Surface around summit consists of knolls of block-jointed and flow-foliated vitrophyre, commonly frost-riven but not glaciated. Moderately sloping morphology of edifice contrasts with cliffy form of adjacent Dome 2861, which is of similar (Mammoth Mountain type) lithology and slightly less silicic. Phenocrysts: 10–12% feldspar (0.5–4 mm); 2–3% biotite (mostly mph but as big as 1.5 mm); ≤1% hornblende (mph to 2 mm); sparse pyroxene (mph to 1 mm); common Fe-Ti-oxide mph. Overlies unit mcl scoria cone (175±3 ka). Overlain by units msd and d61 (87±2 ka). Margin of edifice is lapped or abutted by units ddc and rce, and by late Pleistocene till on its northwest (unit gdc) and southeast (unit gmm) sides. $^{40}Ar/^{39}Ar$ age: 99±7 ka. Oldest unit exposed having Mammoth Mountain lithology

mcl **Basaltic trachyandesite of Canyon Lodge (middle Pleistocene)—**Phenocryst-poor scoria cone and lava flows (53.8–55.9% SiO_2; n=22) that crop out at several isolated locations (fig. 9), correlated on basis of composition, petrography, stratigraphy, and paleomagnetism. Scoria cone, ~600 m wide, was bulldozed for chairlifts in front of Canyon Lodge; it consists predominantly of brick-red scoria lapilli in layers 10–100 cm thick, ranging from loose to tack-welded to moderately agglutinated. Sparse bombs are as big as 1.5 m, a few of which have dense unoxidized interiors. Most extensive lava outcrops are several block-jointed knolls and ledges, east and west of Highway 395 near its crossing of Dry Creek, 7–9 km from vent, where Inyo pumice-fall deposit obscures continuity among numerous local exposures. From Canyon Lodge cone, lavas flowed northeast along west moat prior to emplacement of rhyolite lavas there (units rwm, rdc, rmk). An intricately shattered slab of unit mcl lava, as thick as 25 m and 250 by 450 m in plan view, was uplifted on roof of Dome 2861 (unit d61) during its plug-like extrusion (86±2 ka) and now dips 25º–30º NNE. Lavas from the cone also flowed at least 8.5 km eastward along south moat, where unit is identified at depths of 110–190 m (beneath till in and near the town of Mammoth Lakes) in at least three water wells (fig. 6), as a ledge near southern base of Knolls Vista (UTM 265/6875), and as a faulted remnant that forms 10-m-high bench (UTM 319/678) ~300 m southeast of Casa Diablo geothermal plant. Near the geothermal plant, outcrop of unit mcl is surrounded and lapped by rhyolite-derived sandstone and pebble conglomerate (unit ss) of Pleistocene Long Valley Lake.

Lava exposures are generally massive or locally vesicular, block-jointed or hackly, rarely slabby, and commonly erode as ledges 3–7 m high. Scoria cone and Knolls Vista exposure were glaciated, and exposures beyond glacial limits are fairly degraded; many joint blocks have been rounded and stripped of primary scoriaceous carapace. Phenocrysts: Plagioclase (0.5–2 mm) content is 0.5–2% at most exposures and up to 5% in a few intercalated flows, which additionally carry sparse plagioclase crystals as long as 4 mm (many larger ones sieved or rounded) and feldspar xenocrysts as large as 10 mm with reaction rims. Olivine is sparse and tiny (0.1–0.7 mm), seldom in clusters. Cpx is typically absent but present rarely as microphenocrysts. Granitic xenoliths occur sparsely. Within compositional range of unit mcl (7.5-6.8% FeO*; 1.8-2.2% K_2O), phenocryst-poorer flows (or domains within them) tend to be slightly more evolved chemically. Overlain by units bsm (165±2 ka), rwm (~150 ka), mkv (153±1 ka), mor, mnd, and bar (in slab uplifted atop Dome 2861).

In south moat water wells (fig. 6), unit is also overlain by units amp, bcd, bsc, and gcd. Along south moat, unit is inferred older than units mmc and bfh. Drill hole SF66–31 on Sawmill Road [UTM 302/6765], ~1 km west of geothermal plant, is collared in unit bcd, which caps a 67-m-thick section of mafic lava flows; lowest flow is chemically and petrographically identified as unit mcl, which rests on ~9 m of crystal-rich ash that overlies Early rhyolite tuff (unit rer) hundreds of meters thick. In water well 30M, 2 km southeast of downtown Mammoth Lakes, a 27-m-thick section of two or three mcl lava flows penetrated at 110–137 m depth directly underlies unit bsc

(172±2 ka) and overlies unit asr. In Inyo-4 slant drill hole beneath South Inyo Crater (Eichelberger and others, 1988), unit mcl closely underlies unit aic (131±1 ka) at slant depths of ~70–245 m; several flows comprising upper ~75 m of Group II of Vogel and others (1994) are compositionally indistinguishable from unit mcl, and several more comprising the lower ~55 m of Group II are similar but not identical. In drill hole OIP-1 (UTM 237/749), ~1 km northeast of Deer Mountain, phenocryst-poor lava flows correlated chemically with unit mcl were penetrated at depths between 90 and 190 m, where they underlie one flow of unit mdn and another of unit bmn. At exposures southwest of Lookout Mountain, hilly local relief of 20–40 m, multiledge knolls, steep bluffs, and rhyolite remnant (unit rwm) atop 40-m-high knoll of unit mcl indicate that unit mcl is significantly eroded. Relief probably owes to combination of displacements on resurgent graben fault system and Pleistocene incision by Dry Creek drainage system, which issued from glacial limit only 2 km to west. $^{40}Ar/^{39}Ar$ ages: 175±3 ka (UTM 278/742); 172±2 ka (UTM 282/755); 179.5±2.4 ka (UTM 319/678). Inyo-4 core sample at slant depth of 461.5 ft (140.6 m), upper Group II, gave 186±2 ka. One $^{40}Ar/^{39}Ar$ age of 190±9 ka (UTM 281/757) was determined by Mahood and others (2010)

mcv **Basaltic trachyandesite south of Crestview (late Pleistocene)—**Scoria cone west of Crater Flat and lava flow field (53.3–54.2% SiO_2) that extends northward across Deadman Creek to terminus near Crestview highway maintenance station, 9 km from vent. Cone is 130 m high, 1 km wide, and heavily covered by Inyo pumice-fall deposit. Its unusually deep and steep-walled crater is breached and open to north. Outcrops on cone are limited to east and south rims, consisting of brick-red ejecta, both loose scoria and tack-welded stratified agglutinate. Coarse scoriae armoring crater rim are abundantly 30–50 cm and as big as 1 m. Lithic clasts among rim ejecta include a 5-m block of unit bar; Mesozoic metavolcanics; various mafic and felsic lavas (many probably from subjacent till); and abundant fragments (1–8 cm) of uncorrelated black, glassy, moderately porphyritic, hornblende-biotite-plagioclase rhyolite (72.1% SiO_2) that is somewhat more evolved than rhyolite of nearby Deer Mountain (unit rdm). One mcv lava flow crops out poorly along draw at south base of cone, but lava apron north of cone is wholly concealed by Inyo pumice. Lavas flowed northeast around Deer Mountain, beneath later sites of rhyolitic Deadman Creek flow (unit ric) and coulee of unit dnw, emerging from beneath latter ~7 km from vent cone. North of flow front of dnw coulee, unit mcv forms a low-relief sagebrush-covered lava flow field that extends 2–2.5 km northward to end against north wall of Long Valley Caldera. Its rough, little-eroded surface is marked by low swells and hillocks, a few crags, and scattered small tumuli. Lavas are generally block-jointed, vesicular, commonly scoriaceous and oxidized reddish brown, and seldom expose more massive internal zones. Phenocrysts: 1–2% plagioclase (0.5–2 mm); traces of olivine and cpx (each mostly mph but as big as 1 mm); much of cpx occurs in clots with plagioclase. Overlies units bar and mor. Overlain by unit dnw (27±1 ka), by Inyo pumice deposits (primary and reworked), and by alluvium of Deadman Creek. Drill hole DC-1 (fig. 6; Sorey and others, 1978), located at UTM 259/781, ~800 m northwest of Crestview roadside rest, penetrated to base of unit mcv at ~25 m depth, then successively downward through a 30-m-thick flow of unit mor (66±2 ka), a 20-m flow compositionally identical to unit bsr (99±1 ka), a 15-m flow of unit aic, and a 10-m uncorrelated phenocryst-poor flow, before passing into ~75 m of gravels and ashy sediments, and finally, at a depth of 191 m, into tuff and lava of Early rhyolite (unit rer; ~700 ka). $^{40}Ar/^{39}Ar$ ages of unit mcv: 31±2 ka (Mahood and others, 2010); 33.8±1 ka (table 2)

mdm **Basaltic trachyandesite of Deer Mountain (late or middle Pleistocene)—**Poorly exposed scoria cone (55.7–56.0% SiO_2) partly overlapped by northeast base of rhyolitic Deer Mountain dome in west moat of Long Valley Caldera. Exposures limited to loose scoria and tack-welded agglutinate, all brick-red, that form a ledge, 1–3 m high, around east to southeast rim of cone and to a 15-m-high stack of agglutinate ledges lower on east slope. Subdued crater, open to north, is filled and obscured by 1350 C.E. Inyo pumice-fall deposits (see units ric and p) and ensuing lithic ejecta (unit pe) from phreatic eruptions of nearby Inyo Craters. Abundant lithics here include granitoids, rhyolite of Deer Mountain, and varied mafic and silicic lavas (many from underlying gravels and till), but

they were ejected in 1350 C.E., not with mdm scoria. These late Holocene fall deposits blanket >90% of the mafic cone and obscure its contacts with contiguous rhyolite of Deer Mountain (unit rdm; 101±8 ka), which is probably younger. Cone is at least ~90 m high and ~400 m wide. Scoriae are oxidized, predominantly lapilli but as big as 30 cm, and almost aphyric, containing rare plagioclase (0.5–2 mm) and still rarer oxidized mafic mph. Crude layers are 20–100 cm thick; within coarser layers, dominant lapilli (1–6 cm) are accompanied by subordinate 10–15 cm scoriae and by rare spindle bombs. Compositions of scoria are unlike those of units mic and aic (131±1 ka) exposed in nearby South Inyo Crater; their relative ages are not established, but all three units appear to be older than unit rdm. Undated

mdn **Basaltic trachyandesite northeast of Deadman Pass (late Pleistocene)—**Glacially eroded remnants of phenocryst-rich scoria and agglutinate (52.4–53.7% SiO_2) surrounding each of three vents, aligned northwest-southeast partway up west wall of Long Valley Caldera, south of upper Deadman Creek and 1.5–2 km northeast of Deadman Pass. Northwest vent is shallow crater, 100 m across, surrounded by 300-m-wide ejecta ring of loose brick-red scoria. Ejecta are mostly lapilli but include finely to coarsely vesicular bombs, abundantly 20–50 cm, sparsely 1–2 m, and as big as 3.5 m; many large bombs have dense interiors. Two ledges of tack-welded to dense agglutinate crop out on eastern outer slope, 15–25 m below rim. Circular crater, heavily mantled by Inyo pumice-fall deposits, has 13 m relief on its southeast inner wall and at least twice that much on its north wall.

Middle exposure is a northeast-facing agglutinate cliff, 8–15 m high and ~200 m long. Lowest 1 m of exposure is brick-red agglutinate, dense but streaky, that grades up into ~10 m of massive gray fountain-fed lava, almost homogenized but locally displaying subtle flow foliation and carrying cream-white metavolcanic xenoliths (1–7 cm) that tend to be elongate and oriented along flow-foliation planes. Lava sheet and its foliation dip ~20º NE. Top 3 m of cliff is brick-red massive agglutinate with faint streaky or blobby structure patchily discernible. Sparse scoria bombs as big as 50 cm near cliff rim suggest that vent lies nearby, probably concealed by adjacent moraine that extends from Deadman Pass cirque on southwest and, in turn, by Inyo pumice-fall deposit.

Southeast exposure includes a 600-m-long ridge of lightly welded brick-red agglutinate and an adjacent steep-walled gorge, both walls of which expose denser agglutinate 50–80 m thick. Ridgecrest becomes narrow arête to northeast and consists mostly of tack-welded scoria lapilli sprinkled with sparse scoria blocks (20–70 cm) and spindle bombs up to 1 m. On gorge walls, deposit is dense red-brown agglutinate with a few thin lava ledges intercalated, some of which are block-jointed and dark gray. Wall sections grade down into dense fountain-fed lava near gorge floor. Narrow gorge through vent complex was probably cut glacially and later deepened by glacial outlet stream; its walls remain glacially striated, but stream now draining it is feeble and intermittent.

Products of all three vents are chemically and petrographically alike and presumed to have been erupted contemporaneously from a common dike; vents align along local rangefront scarp . A lone distal exposure crops out 2.8 km northeast of those vents as a water-smoothed lava ledge ~30 m long at 2,445 m elevation on floor of Deadman Creek (UTM 2115/7618); outflow lavas are elsewhere wholly concealed by surficial deposits. Products are not related to Cone 2652 (large scoria cone of phenocryst-poor unit mcv), toward which the mdn vent alignment roughly strikes.

Phenocrysts: 10–15% plagioclase (1–3 mm, rarely 4–5 mm); 1–3% olivine (0.5–1 mm); 1–2% cpx (0.5–2 mm); and common 5–10 mm intergrowths of 10–15 grains each of cpx and plagioclase (both 0.5–2 mm). Northwestern vent ejected metavolcanic xenoliths (1–4 cm, rarely to 8 cm), some partially melted; middle vent ejected partially melted xenoliths of both granitoids and silicic metavolcanics. Base not exposed but presumed to overlie Mesozoic granitic rocks and still older metamorphic rocks, both exposed nearby but covered locally by till, colluvium, and Inyo pumice-fall deposit. All three proximal exposures were overtopped and eroded by glacial ice and strewn with basement erratics. Scoria lapilli (1–6 cm), chemically and petrographically indistinguishable from unit mdn, are scattered atop Dome 2861, 6 km southeast of mdn vents. $^{40}Ar/^{39}Ar$ age: 16±2 ka.

The undated basaltic trachyandesite of June Lake (unit mjl), which lies on the range-front fault system 10 km north of unit mdn, is similar to it in composition, mineralogy, and unusually steep paleomagnetic direction (Hildreth and others, 2014). As both are overlain by MIS 2 glacial deposits, they may have erupted contemporaneously.

Blocky rubble, designated subunit mdn', banked against southwest base of Lookout Mountain (at UTM 03277/41769), consists exclusively of coarsely vesicular blocks of unit mdn, indistinguishable from near-vent outcrops chemically, petrographically, and in age ($^{40}Ar/^{39}Ar$ age: 16.9±1.3 ka). Angular clasts (10–300 cm) protrude from thick mantle of Inyo pumice-fall deposit over an area 65 m along slope (north-south) and 35 m upslope (east-west), forming a flat-topped bench ~10 m high. Of 140 clasts counted, all are of unit mdn lithology. In drill hole OIP-1 (fig. 6), ~1 km northeast of Deer Mountain, a 10-m-thick lava flow chemically and petrographically similar to unit mdn is topmost of seven mafic lava flows penetrated and is covered there by ~18 m of Inyo ejecta (unit pe) and glacial deposits. Material was apparently transported from caldera-wall vents, first as periglacial or englacial lava flows, subsequently as fragmental flows. Straight-line path north of Deer Mountain would be 7–8 km from vents to moraine limit and additional 2 km to rubble deposit banked against Lookout Mountain

mdp **Basaltic trachyandesite of Devils Postpile (late Pleistocene)—**Glacially eroded sheet of phenocryst-rich lava (53.9–54.4% SiO_2) preserved discontinuously along floor of Middle Fork San Joaquin River canyon in two major remnants and several small ones, distributed for 7 km downstream from near (upper) Soda Springs Campground. Vent location unknown, but unit is inferred to have erupted near or upstream from that campground, where scoria cone and dikes of subjacent unit mss are exposed. No dikes or near-vent features of unit mdp are recognized. Largest remnant measures 2 km north-south, ~1 km wide, and includes near its south end the spectacular columnar jointing that constitutes the Devils Postpile, which was designated a National Monument in 1911. At base of columnar cliff is a remarkable postglacial talus of fallen columns (fig. 11). Far more than half of original unit has been lost to erosion, as shown by 3.5-km-long gap between cliffy outcrops near Reds Meadow and small remnants southeast of Rainbow Falls. As with unit Tbtb, just downstream, river re-incised through intracanyon lava only to granitic floor of pre-lava channel, and no deeper. Ice-polished polygonal mosaic on bench at top of iconic columnar cliff is 50 m higher than basal colonnade at 2,295-m river level. Just east of that bench, however, glacially scoured top of flow extends up to elevation 2,405 m, 60 m higher than top of main colonnade and 110 m above flow base at riverside. At three additional locations, one 300 m north of Sotcher Lake and two on west side of river (opposite Pumice Flat and Devils Postpile Campgrounds), scoured top of flow is also at 2,400–2,410 m elevation. Vesicular lava and scoriaceous joint blocks on these glaciated surfaces suggest proximity to primary flow top. By coincidence, ~110-m original flow thickness is same as that of 1959 Kilauea Iki lava lake (Hawaii), which took 20–25 years to solidify fully and produced audible cracking as polygonal contraction joints advanced incrementally into thickening crust (Peck and Minakami, 1968; Ryan and Sammis, 1978).

Lava is widely striated and plucked, eroded into knolls, ridges, and sidewall benches; surviving exposures are nearly all massive and have only sparse scattered vesicles. Slender columns of Devils Postpile colonnade are 15–20 m high, polygonal, typically 0.5–1 m thick, and variously vertical, curved, inclined, or subhorizontal (Huber and Rinehart, 1965b); elsewhere in unit, sets of stouter or less regular columns are widespread, but hackly and block jointing is common, too. Partly glassy chunk jointing is present at riverside, and locally fanned or chevron sets of columns reflect localized control of cooling geometry by major fractures. Evidence for ice-contact emplacement has not been observed and would not be expected here at time of eruption. Some column faces exhibit wavy undulations and, although widely obscured by weathering and glacial scour, bands ("chisel marks") are present locally, representing incremental advance and stoppage as contraction fractures penetrated stepwise into solidifying interior (DeGraff and Aydin, 1987).

Phenocrysts: 7–10% plagioclase (0.5–4 mm); 2–3% olivine (0.5–1.5 mm), commonly clustered; and ~1% cpx (1–3 mm), both free and intergrown with plagioclase. Overlies

units amp, mss, and drf. Widely rests on and wedges out laterally against Mesozoic granite on both walls of canyon. At its northwesternmost outcrop, unit mdp lava rests on ~9 m of fluvial sand and gravel. $^{40}Ar/^{39}Ar$ ages: 82±1 ka (near Minaret Falls Campground; Mahood and others, 2010); 82±2 ka (distal downstream outlier at UTM 03121/41161; table 2). K-Ar age of 940±160 ka reported by Dalrymple (1964b) suggests either an abundance of excess Ar in the plagioclase fused or an error in decimal-place transcription

mic **Mafic pyroclastic deposit of Inyo Craters (Holocene or late Pleistocene)—**Vaguely stratified ash-rich fragmental deposit exposed on walls of South Inyo Crater (Rinehart and Huber, 1965). Those authors reported it on walls of North Inyo Crater as well, but, if present, it was scree-covered during our investigations. Weakly to moderately indurated deposit is slope-forming and widely scree-mantled, may be as thick as 8–12 m, and is best observed on east wall of South Inyo Crater. Gritty reddish-brown matrix is volumetrically dominant and appears to be seriate from sand grade through granules to lapilli. Among lapilli, scoriae are outnumbered by lithic fragments, which are mostly 1–8 cm but rarely as big as 25 cm. Commonest lithics are (in order of declining abundance) crystal-poor mafic lavas, rounded granitoids, crystal-rich mafic lavas, and porphyritic trachydacite; among the trachydacites, one clast analyzed chemically is identical to unit dwr on Mammoth Mountain, and was presumably entrained from till or alluvium. Scoriae—not necessarily juvenile—are black or brick red, mostly 3–6 cm across but as large as 20 cm, and crystal-poor, containing sparse olivine and plagioclase phenocrysts. Three scoriae analyzed have 54.3, 54.5, and 55.8% SiO_2; they are far less evolved and notably richer in FeO and TiO_2 than underlying lava flows of unit aic and are compositionally unlike any other unit exposed in map area. Unit may be a phreatic or phreatomagmatic deposit that entrained clasts from unexposed scoria layers as well as from till; nine layers of cinders were identified between mafic lava flows in top 306 m of nearby Inyo-4 core (Eichelberger and others, 1988). Deposit rests directly upon unit aic (131±1 ka). According to Mastin (1991), top 2 m of pyroclastic section is weathered and capped by a thin organic mat, which is in turn overlain by 1 cm of Mono Craters "tephra 2" of Wood (1977), then by >1 m of 1350 C.E. pumice-fall deposits (unit p) associated with Inyo Chain eruptions (unit ric), and finally by thick phreatic deposit ejected from Inyo Craters (unit pe). Undated

mjl **Basaltic trachyandesite of June Lake (late Pleistocene)—**Scoria cone and associated moderately porphyritic lava flows (53.5–54.1% SiO_2) just west of Mono Craters. Although cone is ~5 km north of our map area, it is described here because of its proximity, compositional similarity, and contemporaneity with mafic eruptive units of the Mammoth magmatic system. Cone is 700 m wide, 75 m high, and is centered 1 km northeast of June Lake (fig. 3). The cone has loose scoria on its slopes and scoria blocks as big as 1.2 m on top, but most exposures are brick-red agglutinate, largely tack welded, and some are dense enough to maintain glacial striae. Entire cone is till covered, best exposure being 30-m-high wall of stratified agglutinate inside breached and eroded crater, which is open to north. Lava-flow field forked into two lobes, one terminating 3 km north of vent, another flowing 4 km northeast, where ponding produced a rootless secondary vent that built a 30-m-high craggy pile of coarse red agglutinate, beyond which lava flowed an additional 7 km northward around east side of Aeolian Buttes to a broad flow-front terminus at southeast margin of Pumice Valley. Lava flows rafted away parts of cone, distributing them atop both lobes as far as 3 km from vent as piles of red scoria and agglutinate that simulate rootless vents and might readily be confused as such. Lavas are massive and weakly vesicular internally but scoriaceous and blocky on unglaciated surfaces. Distal apron has scattered tumuli, some of which burst to produce rootless spatter mounds as high as 5 m; distal flow front is 2.5 km wide, commonly 5–15 m high, and block-jointed to rubbly. Cone and proximal 2 km of lava-flow field are overlain by Tioga Till (MIS 2); most of main tongue and distal 600 m of north lobe are unglaciated. Phenocrysts: 5–10% plagioclase (0.5–4 mm); 1–2% olivine (0.5–1 mm); trace cpx (0.5-1 mm). Plagioclase content may increase distally, although cone and lava lobes show little range in chemical composition. Lava flows locally contain abundant granitic xenoliths and derivative xenocrysts. Lavas bank against 767-ka Bishop Tuff and overlie pre-Tioga glacial deposits variously named or subdivided by others (Putnam, 1949; Bailey, 1989, 2004; Bursik

and Gillespie, 1993). Overlain by Tioga Till, by rhyolitic South Coulee of Mono Craters (~2 ka), and by pumice deposits from Holocene vents at Mono Craters. Several $^{40}Ar/^{39}Ar$ age experiments have failed to yield interpretable plateaus or isochrons; data suggest a very late Pleistocene age, conceivably intra-Tioga.

The 17-ka basaltic trachyandesite northeast of Deadman Pass (unit mdn), which lies 10 km south of the June Lake cone, is similar to it in composition, mineralogy, and unusually steep paleomagnetic direction (Hildreth and others, 2014). As both units are overlain by MIS 2 glacial deposits, they may have erupted contemporaneously

mkv **Basaltic trachyandesite of Knolls Vista (middle Pleistocene)—**Phenocryst-poor agglutinate and fountain-fed lava flows (54.5–54.9% SiO_2) that make up 1.3-km-long northeast-trending ridge, ~100 m high, that lies just east of Mammoth Knolls and just north of Mammoth Lakes business district. Cone 2517 at southwest end of ridge best preserves evidence of spatter-vent complex. Ledges poorly exposed on colluvium-mantled slopes suggest stacks of several lava flows, each 3–10 m thick. Sparse scoriaceous ejecta loose on slopes are finely to coarsely vesicular, mostly 20–40 cm but as large as 1 m. Summit of ridge is eroded into small nubbins and ledges of dense lava typically 2–3 m thick that are locally flow-foliated and widely exhibit streaky texture inherited from spatter-fed origin. Some ridgetop lavas have scoriaceous surfaces; others grade into brick-red agglutinate, which ranges from tack-welded to moderately welded lenticulite. Ridge-forming products are compositionally identical to lavas of unit mmc, 4 km southeast. Six poorly exposed block-jointed and hackly ledges on steep south slope of edifice are all phenocryst poor, but only the upper three belong to unit mkv; lower three are chemically identified as units bsm (165±2 ka), mcl (175±3 ka), and asr. Phenocrysts: <1% plagioclase (0.5–1.5 mm); <1% olivine mph (0.1–0.3 mm); rare cpx (0.5 mm); and sparse Fe-Ti oxide mph (0.1–0.4 mm). Foot of edifice is lapped by both Casa Diablo Till (unit gcd) and late Pleistocene till (units gmm and glb) and by lavas of unit bsr (99±1 ka). North margin of unit is apparently overlapped by unit msc (154±2 ka). Sites drilled atop cone yield excursional paleomagnetic direction (Mankinen and others, 1986; Hildreth and others, 2014). $^{40}Ar/^{39}Ar$ ages: 148±14 ka (Mahood and others, 2010); 153±1 ka (B. Turrin, unpublished data)

mlc **Basaltic trachyandesite of lower Laurel Creek (middle Pleistocene)—**Phenocryst-rich lava flow (51.8–52.9% SiO_2; 20.1–20.9% Al_2O_3) exposed only south of Mammoth Creek at rugged terminal flow front that runs ~1 km south-southwest from junction of Sherwin Creek Road and Highway 395. Exposure is only 500 m long (along eastward direction of flow). Outcrops include ridges, hillocks, and tumuli, heaved and tilted surfaces of which are fissured, pervasively vesicular, and marked by crude polygonal joints, many of which extend into columns 1–2 m long. Crops out only beyond ice limit of Tioga and Casa Diablo glaciations. Source vent unknown, buried by younger units to west. Phenocrysts: 10–15% plagioclase (mostly 0.5–1.5 mm; few as big as 3.5 mm); 2–3% olivine (0.5–2 mm); sparse cpx (1 mm). Lacks large plagioclase of adjacent unit bfh; contains fewer olivine and cpx than nearby unit bcd but more abundant and smaller plagioclase. Bulk lava flow is unusually rich in Al. Overlies unit bsc (172±2 ka). Overlain by unit bfh (92±2 ka). Also overlain by alluvium and marshy sump of (artificially diverted) Laurel Creek and by sandy aeolian deposits that are widely as thick as 1 m. $^{40}Ar/^{39}Ar$ age: 130±1 ka

mmc **Basaltic trachyandesite of Mammoth Creek (middle Pleistocene)—**Phenocryst-poor lava flow (54.4–54.8% SiO_2) exposed as 1-km-long window through younger units along floor and walls of shallow gulch tributary to Mammoth Creek and as 30-m-high hill between Highway 203 and Mammoth Creek. Only additional exposure is a small window through Casa Diablo Till 500 m farther north, just east of Sawmill Road. Crops out mostly as block-jointed ledges, massive below and vesicular to scoriaceous on or near flow surface. Phenocrysts: <1% plagioclase (0.5–2 mm); rare olivine (0.5 mm); trace cpx mph; and rare Fe-Ti-oxide mph (0.2–0.5 mm). Base not exposed. Overlain by units bcd, bsr, and Casa Diablo Till (gcd). $^{40}Ar/^{39}Ar$ age: 162±2 ka (Mahood and others, 2010); K-Ar age: 129±26 ka (Mankinen and others, 1986). Although paleomagnetic directions differ and overlap of radiometric ages is equivocal, this flow is chemically and petrographically identical to agglutinated products of unit mkv vent complex, 4 km northwest

mnd **Basaltic trachyandesite northwest of Dry Creek (late Pleistocene)—**Phenocryst-poor lava flows and agglutinate (53.3–54.0% SiO_2) exposed in six different places along 6-km-long belt northwest of Dry Creek; correlated chemically, petrographically, and stratigraphically. Largest patch is 1.3-km-wide unglaciated lobe that extends 1 km beyond limit of late Pleistocene till (unit gdc) to terminus 4 km northeast of Deer Mountain; margins and flow front are little modified and have 10–20 m relief. Surface is marked by several tumuli and rootless vents that fed ragged piles and ridges (3–5 m high) of oxidized tack-welded agglutinate, rich in scoria bombs. Second large exposure is 1-km-wide unglaciated steep-sided lobate bench, just north of Dry Creek and west of Highway 395, that rises steeply 40 m higher than both; probably fault-bounded as well as eroded by Pleistocene Dry Creek. In both unglaciated areas, most surfaces are rubbly and scoriaceous, whereas sparse outcrops of flow interiors are block-jointed and massive to weakly vesicular. Several lesser exposures to southwest are glaciated windows through blanket of till. Narrow sliver of oxidized tack-welded agglutinate at north end of west-facing fault scarp, 2 km northeast of Deer Mountain, is probably part of a rootless vent. Three southernmost outcrops are a cluster of discrete ice-scoured swells that rise above till blanket within 1 km west of rhyolitic Dry Creek Dome and only 100–400 m west of Dry Creek; each is ~100 m wide, has only a few meters of ledgy relief, and consists of streaky to flow-foliated, aphanitic lava. Sites drilled at several of the outcrops yield similar paleomagnetic directions (Hildreth and others, 2014). Phenocrysts: <1% plagioclase (0.5–1 mm); trace olivine mph (rarely as big as 0.5–1 mm). Also contains rare but widespread xenocrysts or antecrysts of rounded or corroded plagioclase (1–6 mm). Overlies units mcl (~175 ka) and bar (~95 ka). Overlain by units mor (66±2 ka), dnw, and gdc. Geothermal corehole PLV-2 (Benoit, 1984), collared in northernmost area of the unit, penetrated 169 m of mafic lavas (perhaps as many as 8 flows), which overlie at least 467 m of rhyolitic tuffs and lavas that extend to bottom of hole (fig. 6). Many distal samples of extensive flow field of unit mor are chemically and petrographically indistinguishable from those of unit mnd, whereas steep-sided, well-defined, proximal-to-medial part of mor, which directly overlies mnd, carries significantly more phenocrysts and has 1–2 percent less SiO_2 than unit mnd. Medial and distal sites drilled in unit mor and sites in unit mnd (both east and west of mor) all yield similar paleomagnetic directions (Hildreth and others, 2014). It is thus inferred that unit mnd represents early phase of more extensive (and chemically more varied) subsequent effusion of unit mor (66±2 ka), probably from same source vent (southwest of Dome 2861; see unit msd) and of virtually same age. Not independently dated

mor **Basaltic trachyandesite of Owens River Road (late Pleistocene)—**Phenocryst-poor lava flows (51.2–54.2% SiO_2) along and north of Dry Creek that condense west of Lookout Mountain into a single steep-sided coulee that is exposed continuously beyond till limit (unit gdc) near Dry Creek for 5.5 km to flow terminus at north wall of Long Valley Caldera along Deadman Creek. Coulee is 1 km wide in south, broadening distally to 2 km, and has steep lobate margins, commonly as high as 30 m. Full thickness exceeds 50 m at north toe of Lookout Mountain and along flow front at Deadman Creek, west of Big Springs. Unglaciated surface is rolling, hilly, and rubbly, marked by scoriaceous knobs, tumuli, and several rootless vents for craggy piles and fissure-fed ridges of red agglutinate and scoria. For 6 km southwest of glacial limit, unit is covered by till unit gdc and exposed only along and adjacent to a 5-m- high west-facing fault scarp north of rhyolitic Dry Creek Dome, where concealed unit is probably at least 1 km wide. Source vent appears to be poorly exposed scoria cone in saddle between Domes 2861 and 2781 (see unit msd). Phenocrysts: Unit ranges from almost aphyric through as much as 4–5% plagioclase, most commonly 0.5–2%. Plagioclase phenocrysts are mostly 0.5–3 mm but rarely 4–5 mm, though scattered antecrysts or xenocrysts as big as 10 mm are also present. Sparse olivine occurs mostly as microphenocrysts, rarely as big as 1 mm. Cpx is generally absent but rare microphenocrysts occur in trace amounts. Sparse Fe-Ti oxides are typically 0.1–0.3 mm, rarely 0.5 mm. Granitic xenoliths and derivative xenocrysts are uncommon but widespread. Glaciated or stream-worn exposures are massive or weakly flow-foliated and mostly block-jointed; little eroded surfaces are blocky or

rubbly, vesicular to scoriaceous, and block-jointed or hackly. Overlies units mnd, mcl, and bar (88±5 ka) and banks against Early rhyolite of Lookout Mountain (subunit rlm; 692±14 ka). Units mnd and mor overlap chemically and have indistinguishable paleomagnetic directions (see unit mnd). Unit mcv (31±2 ka) banks against northwest margin of unit mor. $^{40}Ar/^{39}Ar$ age: 66±2 ka (Mahood and others, 2010)

msc **Basaltic trachyandesite of Sawmill Cutoff (middle Pleistocene)—**Poorly exposed bench of phenocryst-poor lava flows (52.3–52.5% SiO_2) that extends 1.5 km north from Knolls Vista edifice (unit mkv) between Sawmill Cutoff Road and West Moat Coulee (unit rwm). Bench is 600 m wide and 100–140 m high; neither of two hillocks along its crest provides evidence of a vent. Exposure is inadequate to determine how many flows comprise section, which emerges eastward from beneath steep margin of overlying rhyolite coulee and is abruptly truncated by an inferred fault at a scarp with 50–100 m relief. Scattered outcrops are block-jointed ledges and knobs of vesicular or locally massive lava. Phenocrysts: 1–3% plagioclase (0.5–2 mm), both equant and laths (the latter seriate to microphenocrysts and groundmass); 1–2% olivine (0.3–1 mm); cpx microphenocrysts rare. More and larger plagioclase and olivine than in adjacent (chemically more evolved) unit mkv, which is abutted and apparently draped by msc lavas. Banks against postcaldera Early rhyolite (unit rer; 694±17 ka; Mankinen and others, 1986) as well as against unit mkv. Overlain by unit rwm (~150 ka). Clasts of unit msc are present in Casa Diablo Till (unit gcd) of MIS 6. $^{40}Ar/^{39}Ar$ age: 154±2 ka. K-Ar ages: 155±28 ka and 154±72 ka at two separate sites. Drilled at same two sites, unit has anomalously steep northerly paleomagnetic direction (Mankinen and others, 1986).

Scattered on surface of unit msc are sparse clasts of aphyric, hydrothermally altered Early rhyolite (unit rer; 1–25 cm), of hornblende-biotite-plagioclase vitrophyre (unit rmk; 4–13 cm), and of similarly crystal-rich rhyolitic pumice (unit rwm, as big as 12 cm). All were probably expelled during explosive phases of rhyolitic units rwm and rmk, both of which vented ~1.5 km southwest

msd **Basaltic trachyandesite scoria southeast of Dry Creek (late Pleistocene)**—Phenocryst-poor scoria (51.8–53.0% SiO_2) exposed poorly in 100-m-wide window at northwest end of saddle between Domes 2861 and 2781. Largely obscured by colluvium from adjacent domes; no stratified cinders or lava flows are exposed; instead, site is a scattering of scoria blocks and bombs as big as 50 cm, finely to coarsely vesicular, mostly dark gray but some oxidized brick- red. Phenocrysts: <1% plagioclase (0.5–5 mm; many probably xenocrysts) and trace of olivine (<1 mm). Base not exposed. Overlain by glacial erratics and by colluvial debris from both domes (units d61 and d81), which appear to be older. Chemically and petrographically similar to presumptively comagmatic units mnd and mor (66±2 ka), for which unit is inferred to mark source vent. Undated

msj **Basaltic andesite of Scenic Loop Road junction (late or middle Pleistocene)**—Poorly exposed, moderately porphyritic lava flow (52.8% SiO_2) that forms a pumice-mantled shelf (UTM 2785/754) adjacent to west lane of Highway 395, ~300 m north-northwest of its junction with Scenic Loop Road. Shelf, with only ~15 m relief, protrudes ~200 m eastward from beneath high bluff of unit mnd. A few weathered blocks of lava are exposed through pumice cover. Phenocrysts: ~3% olivine (0.5–1 mm, some with reaction rims); sparse plagioclase (1–4 mm); rare cpx mph. Compositionally and petrographically unique in map area, lava is transitional between subalkaline and alkaline fields; contains 7% MgO, only 5.2% alkalies, and low TiO_2 (1.29%). Overlain by unit mnd. Base not exposed. Undated

mss **Basaltic trachyandesite of upper Soda Springs (late Pleistocene)—**Phenocryst-poor lava flows (52.7–53.2% SiO_2) that erupted at severely eroded scoria cone exposed on west bank of Middle Fork San Joaquin River, opposite upper Soda Springs Campground. Riverbank exposure of stratified scoria is 8–25 m high, black to yellow-orange, thin-to-thick bedded, and includes three layers of dense agglutinate (each 2–3 m thick); scoria are predominantly lapilli but include blocks as big as 35 cm. Because at least half of cone has been eroded away by river, all layering dips 15–20º W; base of scoria is not exposed. Two vertical dikes, respectively <1 m and ~5 m thick, strike east-northeast and cut scoria section on riverbank; at rim, thicker southern dike grades into dense

agglutinate, which in turn grades into a thin lava flow. From cone, eroded remnants of lavas extend 300 m upstream and ~1 km downstream, preserved as a narrow ice-scoured strip (100–250 m wide) between Pacific Crest Trail and river. Lava flow surface is rolling glaciated plateau marked by knobs and ledges cut on a single downstream flow. Unit is as thick as 40 m near vent but thins (largely owing to erosion) to <10 m both upstream and downstream. Lavas and dikes are massive, hackly, chunky, or block-jointed. Phenocrysts: 1–3% plagioclase (1–3 mm) and <1% olivine (0.5–1 mm, rarely 2 mm). Some exposures ~400 m downstream from dikes carry as much as 5% plagioclase but are chemically indistinguishable from rest of unit. Cpx is absent (or extremely rare) in contrast to overlying unit mdp. Overlies Mesozoic granite (unit Kmo). Overlain by phenocryst-richer unit mdp (82±1 ka), which has certain compositional affinities (fig. 20) with lower-SiO_2 unit mss. Nonetheless, in addition to differences in age, chemistry, mineral content, and paleomagnetic direction, units mdp and mss differ in Pb, Nd, and Sr isotope ratios (Cousens, 1996); for example, $^{87}Sr/^{86}Sr = 0.70613$ and 0.70596, respectively. $^{40}Ar/^{39}Ar$ age: 121±2 ka

rbt **Bishop Tuff (middle Pleistocene)—**Rhyolitic ignimbrite, voluminous compositionally zoned pyroclastic unit (71–78% SiO_2), eruption of which permitted collapse of Long Valley caldera (Gilbert, 1938; Hildreth, 1979; Bailey, 1989; Wilson and Hildreth, 1997; Hildreth and Wilson, 2007). Variably welded outflow sheets crop out radially around caldera; concurrently erupted fall deposit is preserved patchily from Pacific Ocean to Nebraska. Intracaldera thickness beneath postcaldera volcanics and sediments exceeds 1 km, as recorded in many drill holes (McConnell and others, 1995). Total eruptive volume of equivalent magma estimated to have been 600–650 km^3 (Hildreth, 2004). Within map area, main outcrops are (1) nonwelded to densely welded outflow sheet along north wall of caldera; and (2) glaciated remnants along walls of Middle Fork San Joaquin River canyon—including nonwelded to sintered exposures east of Sotcher Lake, sintered to densely welded ledges southwest of Pumice Butte, and densely welded (vitric and devitrified) zones near Reds Meadow, Boundary Creek, Crater Creek, King Creek, and Fish Creek. Remnants are generally steep, and some welded zones are columnar jointed. More than 95 percent of the ignimbrite originally deposited along San Joaquin canyon has been removed by glacial and fluvial erosion. Thicknesses preserved generally increase downcanyon from ~160 m near Reds Meadow to ~195 m near King Creek and 230 m southwest of Pumice Butte. Unit is also exposed along north edge of map area where many outcrops range from sintered to densely welded; nonwelded base is exposed in Highway 395 roadcut at UTM 242/813. Accidental clasts of welded Bishop Tuff as big as 50 cm are locally abundant in intracaldera pyroclastic deposits (subunits rtav, rtcd) of early postcaldera rhyolite (unit rer), which had excavated them explosively from the caldera fill hundreds of meters deeper. Phenocrysts: total content zoned from ~1% to ~25%, including sanidine, quartz, plagioclase, biotite, allanite, Fe-Ti oxides, zircon, and (in late subunits) antecrysts of cpx and opx (Hildreth, 1979; Hildreth and Wilson, 2007). Rests on Mesozoic granitoids, Paleozoic metasedimentary rocks, glacial till (unit gst), alluvium (unit pal), and various Tertiary mafic and intermediate lavas. Overlain in map area by units a62, amp, apb, drf, and gud (and by many more outside map area and beneath caldera floor). $^{40}Ar/^{39}Ar$ age: 767±2 ka (Rivera and others, 2011)

rcd **Rhyolite of Cratered Dome (Holocene)—**Disrupted rhyolite minidome (73.2% SiO_2) on north bank of Glass Creek, 150 m north of Glass Creek flow (unit ric); extruded through Mesozoic granitoid at foot of Sierran escarpment on trace of Hartley Springs Fault. Dome is <150 m in diameter, and its craggy rim stands only 10–15 m above its external base. Most of dome center, however, is now a closed funnel-shaped crater 25–30 m deep and ~100 m wide at its rim. An annular terrace 5–10 m wide rings much of inner pit, ~10 m below its rim and ~18 m above its floor. Coarsely block-jointed flow-foliated rhyolite forms ragged narrow rim and steep inner walls of crater; foliation was mapped by Mayo and others (1936). Rock is glassy, micropumiceous, pale gray, and weathers tan to pale orange-brown; its groundmass is rich in microlites. Phenocrysts: 1–2% feldspar (mph to 1.5 mm), some in clusters; trace amounts of biotite, opx, cpx, and Fe-Ti oxides (all mph). Unit is chemically similar to evolved end of zoned array of phenocryst-poor member of

unit ric erupted in 1350 C.E. (Sampson and Cameron, 1987). Cratered Dome is older, however, as its floor and parts of its rim are covered by 1350 C.E. pumice-fall deposit. Apparent absence of tephra from nearby South Mono and Wilson Butte eruptions, each ~1.3 ka (Bursik and Sieh, 1989), suggests that cratering (if not necessarily eruption) of Cratered Dome postdates those events. Coarse ejecta around crater, dominated by a sheet that extends ~150 m south and southeast of rim, include granitoids, Mesozoic metavolcanic rocks, and mafic lavas as well as juvenile rhyolite. Some blocks are as big as 50 cm; abundance of rounded ones suggests (at least partial) derivation from underlying till. Rhyolite debris appears inadequate to account for crater volume, suggesting that magma withdrawal could have contributed to crater formation. Undated but apparently bracketed between 700 C.E. and 1350 C.E.

rce **Alkalic rhyodacite of Canyon Express (late Pleistocene)—**Moderately porphyritic lava-flow apron (70.3–70.8% SiO_2) that emerges from beneath unit rss west of Lincoln Peak and spreads northward for 2 km to foot of Dome 2781(unit d81) and eastward for 2.5 km to east-facing bluffs (Timber Ridge) southeast of Canyon Lodge. Upper terminus of Canyon Express (Chair 16) is built on this rhyodacite at 2,910 m elevation near northwest base of Lincoln Peak. Exposures include black to gray flow-foliated vitrophyre and extensive tracts of cream-white massive felsite; locally oxidized pink or weathered brown, especially along vuggy foliation planes. Some outcrops form bold ledges and nubbins; others are crumbly vitrophyre surfaces bulldozed smooth for ski runs. Unit everywhere glacially eroded, strewn with till and colluvium, and widely concealed by such deposits distally. Phenocrysts: 4–7% feldspar (0.5–3 mm); 1–2% biotite (mph to 2 mm); trace Fe-Ti-oxide mph. Also carries rare mafic blebs, feldspar clusters, and biotite-oxide-feldspar clots. Vent inferred to underlie unit rss at Solitude Dome. Consistently distinguished from nearby units rmf and rss by lower Fe and Sr contents and higher Nb, Zr, K, and Na. Overlies or banks against unit d81 (99±7 ka) and Canyon Lodge scoria cone (unit mcl; 175±3 ka). Overlain by units rsq (63.7±4 ka), rss (50±3 ka), dfl (61±3 ka), and dlp (64±7 ka). $^{40}Ar/^{39}Ar$ ages: 81±1 ka (Mahood and others, 2010); 80±1 ka (table 2)

rcw **Rhyolite of caldera wall (Holocene)—**Sparsely porphyritic rhyolite minidome (72.2% SiO_2) on northwest wall of Long Valley Caldera, <100 m west of southwestern snout of Glass Creek flow (unit ric). Tiny forested protrusion, only ~50 m wide and 20 m high, perched partway up wall at 2,440–2,460 m elevation, erupted through scree-mantled Mesozoic granite (unit Kjl) just west of trace of Hartley Springs Fault. Rock is pale gray, glassy, micropumiceous, and carries abundant microlites. Phenocrysts: 1–2% feldspar (mph to 1 mm), some in clusters; <1% biotite (mph to 1 mm); trace hornblende (mph to 1.5 mm long); trace cpx (mph to 0.7 mm long); trace tiny Fe-Ti-oxide mph; also contains rare mafic blebs as big as 5 mm that carry pyroxene and oxide mph. Unit is chemically similar to evolved end of zoned array of phenocryst-poor member of unit ric that erupted in 1350 C.E. (Sampson and Cameron, 1987). Age unknown, but mantle of Inyo tephra and absence of South Mono and Wilson Butte tephras appear to bracket its extrusion (like that of unit rcd) to between 700 and 1350 C.E. (Sampson, 1987; Sampson and Cameron, 1987)

rdc **Rhyolite of Dry Creek Dome (late Pleistocene)—**Phenocryst-rich steep-sided rhyolite lava dome (76.0–76.4% SiO_2) between West Moat Coulee (unit rwm) and Dry Creek, centered 6.5 km northeast of Mammoth Mountain summit (fig. 23). Dome is circular in plan, 1.2 km in diameter, and has as much as 240 m relief—greatest on its northwest side. Summit plateau, ~700 m wide, is marked by small rifts and knobs that provide 10–40 m of local relief. Unglaciated surface consists of cream-to-white, tan-weathering, micropumiceous carapace, locally block jointed. Phenocrysts: 10–15% feldspar (0.5–1.5 mm; plagioclase and sanidine); ~3% quartz (0.5–1.5 mm), many embayed; 2–3% biotite (0.1–1.5 mm); sparse hornblende (≤0.5 mm); trace amounts of Fe-Ti oxides, zircon, apatite, and allanite. Intrudes and overlies unit rwm. Late Pleistocene till (unit gdc) and avalanche deposits (unit av) from Dome 2861 (unit d61) bank against west toe of dome. K-Ar age: 110±11 ka (Mankinen and others, 1986). $^{40}Ar/^{39}Ar$ age: 112±6 ka (Heumann and others, 2002)

rdm **Rhyolite of Deer Mountain (late Pleistocene)—**Phenocryst-rich lava dome (71.9–72.1% SiO_2) centered 7.5 km north of Mammoth Mountain summit and 2.5 km inside northwest topographic wall of Long Valley Caldera. Steep-sided dome is nearly circular in

plan, 900 m in diameter, and ~180 m high. Exposures are largely of glassy, white, finely pumiceous carapace, but outcrops are limited to areas near summit and upper west slope of dome, owing to extensive cover by late Holocene phreatic ejecta from Inyo Craters; denser vitrophyre layers and lenses are present locally. North and South Inyo Craters lie at south toe of Deer Mountain, and two additional phreatic craters (roughly contemporaneous with them) were excavated through its summit and its lower north flank (Mastin, 1991). Total phenocrysts 25–35%. Contains 10–15% feldspar (both plagioclase and sanidine); 10–12% quartz (rounded and embayed, commonly broken, 0.2–4 mm); ~3% biotite (mph to 1.5 mm); ~1% hornblende (mph to 1.5 mm); trace tiny Fe-Ti-oxide mph. Also contains trace amounts of cpx, opx, zircon, allanite, apatite, and pyrrhotite (Mayo and others, 1936; Reid and others, 1997). Appears to overlap and partly cover adjacent, severely eroded, scoria cone of unit mdm. $^{40}Ar/^{39}Ar$ age: 101±8 ka (Heumann and others, 2002). K-Ar age: 115±3 ka (Mankinen and others, 1986)

rer **Early rhyolite of Bailey (middle Pleistocene)—**Aphyric to sparsely porphyritic lava flows, domes, and predominant pyroclastic deposits (74–75% SiO_2) that represent earliest episode of postcaldera volcanism in Long Valley Caldera. Erupted from several separate vents and exposed principally on resurgent uplift and Lookout Mountain, as depicted by Bailey (1989).

Vents mostly obscured by lavas that retain little primary morphology; several are indicated on map sheet by stars, and others are probably downfaulted beneath graben system and Fumarole Valley.

Drilling shows assemblage to be as thick as 622 m near center of its outcrop area; and even where deeply buried by younger units, wells prove it as thick as 537 m beneath west moat and >350 m beneath southeast moat. Volume roughly 100 km^3 (McConnell and others, 1995; Hildreth, 2004). Phenocrysts: 0–2%, including combinations (in various eruptive units) of plagioclase (0.5–1.5 mm), opx (0.2–0.7 mm), rare biotite (<1 mm), and traces of apatite, zircon, titanomagnetite, ilmenite, and pyrrhotite (Bailey, 1978). Relatively mafic enclaves and blebs (0.5–6 cm; 51–59% SiO_2) are very rare but found in four different lava flows of unit rer. Eight K-Ar ages, all for glass from obsidian flows, range from 751±16 ka to 652±14 ka (Mankinen and others, 1986). McConnell and others (1995) gave a $^{40}Ar/^{39}Ar$ plateau age of 675±9 ka for an obsidian, corroborating the K-Ar age of 680±29 ka for same lava flow. Areas of acid alteration and strong silicification are patterned on maps of Cleveland (1962) and Bailey (1989) and not repeated here

rlm **Lookout Mountain subunit** is a unique element of Early rhyolite, forming a discrete rhyolitic shield 3–4 km in diameter with as much as 340 m of relief that separates caldera's west moat from its north moat and is not deformed by resurgent uplift, lying just outboard of the resurgent structure. Extraordinarily for a rhyolitic volcano, edifice has shallow summit crater ~1 km wide. Outcrops along crater rim are predominantly obsidian that form a series of knolls and ridges separated by five shallow saddles and notches. Devitrified exposures are few, and pumiceous carapace facies is preserved on rim only locally, just east of northeast rim notch. Sparse felsite (exposed principally on east rim) is flow-foliated, pale gray or tan, and mostly dense, although locally vuggy or brecciated. Outer slopes of edifice are largely mantled by thick colluvium, but sparse exposures are mostly obsidian. Pumiceous carapace crops out locally on north slope and north lobe; pyroclastic deposits are rare on Lookout Mountain, which is armored by lava flows in all sectors. Southeast lava-flow lobe that extends 2 km beyond Dry Creek gorge is compositionally identical to edifice. All rhyolite facies on Lookout Mountain are aphyric; rare plagioclase microphenocrysts (<0.5 mm) are present locally, as are 0.5-mm aggregates of 0.1-mm crystals of orthopyroxene and plagioclase; mafic enclaves were sought but none found. Low-relief crater floor is wholly covered by colluvium, Inyo pumice, and forest litter. No explosion breccia is exposed that might account for crater. Edifice was not glaciated, crater floor is not gullied, and narrow rim notches are only weakly incised, rendering unlikely an erosional origin for crater. Creation of a summit depression by subsurface magma withdrawal or by construction of a peripheral ring of several discrete extrusions would be mechanisms extraordinary for a rhyolite volcano. A speculative possiblity is that effusion of the southeast lava lobe from a flank vent permitted summit subsidence.

K-Ar ages: 692±14 ka; 677±14 ka (Mankinen and others, 1986). $^{40}Ar/^{39}Ar$ age: 678±9 ka (Simon and others, 2014)

rtav **Tuff of Little Antelope Valley subunit** is a major component of Early rhyolite (partly equivalent to unit Qet of Bailey, 1989). Consists predominantly of white nonwelded high-silica-rhyolite ignimbrite, massive to vaguely stratified, but locally includes intervals a few meters thick in which thin pumice-fall and hybrid-fall layers (Wilson and Hildreth, 1998) are intercalated. Although widely obscured by colluvium, unit extends 9 km from Dry Creek Sand Flat nearly to Hot Creek, covering ~20 km^2 of map area. From map pattern and drillhole data, tuff is inferred to be present over a far greater subsurface area (in all directions), where buried by associated rhyolite lava flows (unit rer), by various mafic lava flows, and by lacustrine siltstones that were in large part reworked from it. Exposed tuff is widely 50–300 m thick, although few individual outcrops exceed 40 m. In several drill holes, tuff is ~150–560 m thick, but proportions of primary ignimbrite and reworked rhyolitic siltstone are seldom clear from core logs. Outcrops are white to cream, weakly to moderately indurated but locally case-hardened or pervasively silicified, and uncommonly medium-gray or green where altered. Exposures are nonwelded, but partial welding is reported in some cores (McConnell and others, 1995). Tuff is poorly sorted, ash-dominant, and rich in small pumice fragments— mostly 0.2–2 cm and rarely 3–10 cm. Where tuff is not massive, vague gradational layers, 3–150 cm thick, are defined by alternating pumice-poor and pumice-bearing intervals. Pumice lapilli and granules are concentrated into lenses or thin layers only locally. Locally exposed within otherwise massive tuff sections, however, are packages 1–2 m thick of thin (2–20 cm) planar beds rich in pumice granules separated by 1–2 cm laminae of medium ash. All pumice is aphyric or nearly so, containing only trace amounts of opx, biotite, and plagioclase. Lithic fragments are typically sparse to rare, and nearly all are cognate aphyric rhyolite lava, mostly glassy, and smaller than 2 cm; exceptions include rare (vent-proximal?) outcrops of massive ignimbrite that carry distributed rhyolitic lithics as large as 8 cm and of stratified ignimbrite containing clast-rich layers 1–2 m thick that are rich in 5–15 cm fragments of rhyolitic lava. Clasts of densely welded phenocryst-rich Bishop Tuff, 5–50 cm and subrounded to subangular, are sparsely distributed but locally abundant in nonwelded massive ignimbrite, evidently explosively excavated from intracaldera welded tuff several hundred meters below modern surface. Base of unit is nowhere exposed but is shown by drilling to rest on intracaldera Bishop Tuff in several wells. Tuff is overlain by rhyolite lava flows of units rer and rlm and by rhyolitic sandstone of Long Valley Lake (unit ss). Along eastern limits of its outcrop, near Clay Pit and Little Hot Creek, tuff is overlapped by and may grade into sedimentary pumice breccia and ash-grade lacustrine siltstone, both of exclusively rhyolitic derivation. Not directly dated, but bracketed by Bishop Tuff (767±2 ka) and an Early rhyolite obsidian flow (751±16 ka)

r68 **Pumice Cone 2368 subunit** is a vent knoll of nearly aphyric Early rhyolite (UTM 340/740) ~2 km north of Little Antelope Valley. Exposed cone is 800 m long, 450 m wide, elongate northeast, and has ~100 m maximum relief at its southwest end. Pumice clasts (74.7% SiO_2) are closely packed, mostly subangular, and seriate from granules to predominant lapilli, with subordinate blocks. Pumice is white, weathering tan, and frothy to finely vesicular with both equant and fibrous vesicles. Exposures lack interstitial ash and layering. Pumiceous carapace of flow-foliated lava is locally exposed on southwest rim and in excavation near summit. Most clasts are 1–5 cm (rarely 10 cm) along northeast ridge, but commonly 10–35 cm on pair of low knolls along crestal plateau; there, rare shattered pumice blocks were originally as large as 1 m. By contrast, few pumice clasts in surrounding unit rtav, which underlies the cone, are larger than 2 cm. Total phenocrysts <1%; plagioclase (0.2–0.7 mm), opx (0.3–0.6 mm long), biotite (0.2–0.5 mm), and trace Fe-Ti oxide mph (~0.1 mm). Undated but presumed to be in age range of Early rhyolite (unit rer)

rtcd **Tuff east of Casa Diablo subunit** is discrete exposure of Early rhyolite ignimbrite, 700 m by 2,000 m across, between Fumarole Valley and Casa Diablo geothermal plant. Total exposed relief ~150 m. Dominantly massive white ash, unit lacks obvious layering and carries sparse aphyric pumice clasts, few of which exceed 2 cm. Abundant lithic content

distinguishes unit from unit rtav, which is generally lithic-poor. Contains subangular to subrounded clasts (10–100 cm) of welded Bishop Tuff (unit rbt); abundant cognate clasts (1– 30 cm) of flow-foliated Early rhyolite lavas—felsitic, perlitic, and obsidian; and sparse blocks of Mesozoic metavolcanic rock (as big as 40 cm) and of grussy granodiorite (as big as 65 cm). All accidental lithics appear to be ejecta, not glacial erratics, although some may have come from Sherwin Till beneath intracaldera Bishop Tuff. Unit is thought to represent explosive opening phase of Early rhyolite eruption that produced obsidian flow that overlies its north margin. Tuff is also overlain by another Early rhyolite lava flow to its south. Tuff not directly dated, but obsidian flow interpreted as coeruptive gave K-Ar age of 688±14 ka (Mankinen and others, 1986)

rfp **Alkalic rhyodacite pumice fall of Highway 203 (late Pleistocene)—**Lapilli-fall deposits of well-inflated pumice (69.5–70.9% SiO_2) exposed in roadcuts north and east of Mammoth Mountain. Sparse, isolated exposures dominated by white pumice lapilli are 3–6 m thick. Excavation of complete section at location A (see below) provided evidence for several eruptive pulses and one substantial time break (fig. 25). (1) lapilli fall, 63 cm thick, complexly bedded; capped by a pyroclastic density-current deposit 20 cm thick. (2) Lapilli fall, 77 cm thick, with grain-size fluctuations indicating six eruptive pulses; capped by a 14-cm-thick paleosol that contains colluvial blocks of lava-flow unit d81. (3) Lapilli fall, >4 m thick, divisible into 35-cm basal fall, 12-cm-thick dark-colored fall layer with ~30% lithic fragments, and >367-cm pumice fall that is crudely inversely graded, vaguely stratified, and far coarser than any layers below. Base of section rests on ~0.5 m of crudely stratified colluvium, which, in turn, overlies pumiceous lava carapace of unit d81 dome. Most pumice clasts are 1–5 cm across, although small fraction in top unit are 10–29 cm; most are pale gray or white to buff, oxidized pale pink only in cores of large clasts. Lithic fragments, which make up 2–3% of total deposit, are predominantly phenocryst-rich trachydacite and common but subordinate alkalic rhyodacite of Mammoth Mountain; clast counts yield 94% Mammoth Mountain lavas, 4% mafic lavas, and 2% metavolcanics (n=321). Most lithics are <1 to 8 cm across, rarely 9–16 cm. Phenocrysts: 4–6% plagioclase and sanidine (0.5–3 mm); 1–2% biotite mph; sparse tiny Fe-Ti oxide mph.

Outcrops are too small to show on geologic map. Principal locations are: (A) roadcut on eastward salient of Highway 203 at elevation 2,545 m (UTM 2405/69135; best complete section; fig. 25); (B) three roadcuts along north side of Highway 203 at elevations 2,560 m (UTM 2393/6892), 2,665 m (UTM 223/686), and 2,683 m (UTM 220/687); (C) roadcut on north side of Forest Trail (residential street) at elevation 2,480 m, ~350 m west of Highway 203 (UTM 248/688); (D) disturbed (possibly transported) pumice lapilli strewn around abandoned former maintenance yard (UTM 295/675) at 2,295 m along north side of Highway 203, ~1 km east of its junction with Meridian Boulevard; and (E) primary pumice fall (fig. 25), weakly inversely graded, as thick as 91 cm, on floor of old gravel quarry (UTM 403/717) ~300 m south of Cashbaugh Ranch buildings; here, 19 km east of source vent, deposit underlies ~8 m of unit oal, and its white pumice weathers buff-yellow and ranges in grain size from 0.2 to 4 cm. (Another pumice-fall deposit atop roadcut on northbound side of Highway 395 [UTM 2727/7668; assigned to this unit by Bailey, 1989; his unit rmp] is 1350 C.E. Inyo fallout). Vent is certainly on Mammoth Mountain edifice, probably beneath Solitude Dome, along with that for unit rce, lavas of which are chemically and mineralogically similar to unit rfp pumice lapilli. $^{40}Ar/^{39}Ar$ ages: 80±8 ka (table 2); 88±6 ka, 91±2 ka (Mahood and others, 2010)

rhc **Rhyolite of Hot Creek flow (middle Pleistocene)—**Phenocryst-poor coulee (76.0–76.2% SiO_2), as wide as 2.5 km and 5 km long, in south moat of Long Valley Caldera. Equivalent to part of unit Qmrh of Bailey (1989). Erupted at subaerial vent west of Whitmore Hot Springs, coulee flowed northward where much of it invaded Pleistocene Long Valley Lake (Mayo, 1934b; Bailey and others, 1976), producing widespread flow breccia and perlite. Steep-sided coulee has 100 m of relief proximally, and its upper surface is hilly and craggy, but distal exposures have low relief and are partly lapped by lake sediments (unit ss). Lithologically, rhyolite is flow-foliated and variously includes black vitrophyre, gray to pink felsite, coarsely pumiceous carapace, pale gray perlite, and flow breccia. Strongly oxidized and hydrothermally altered exposures are common along Hot

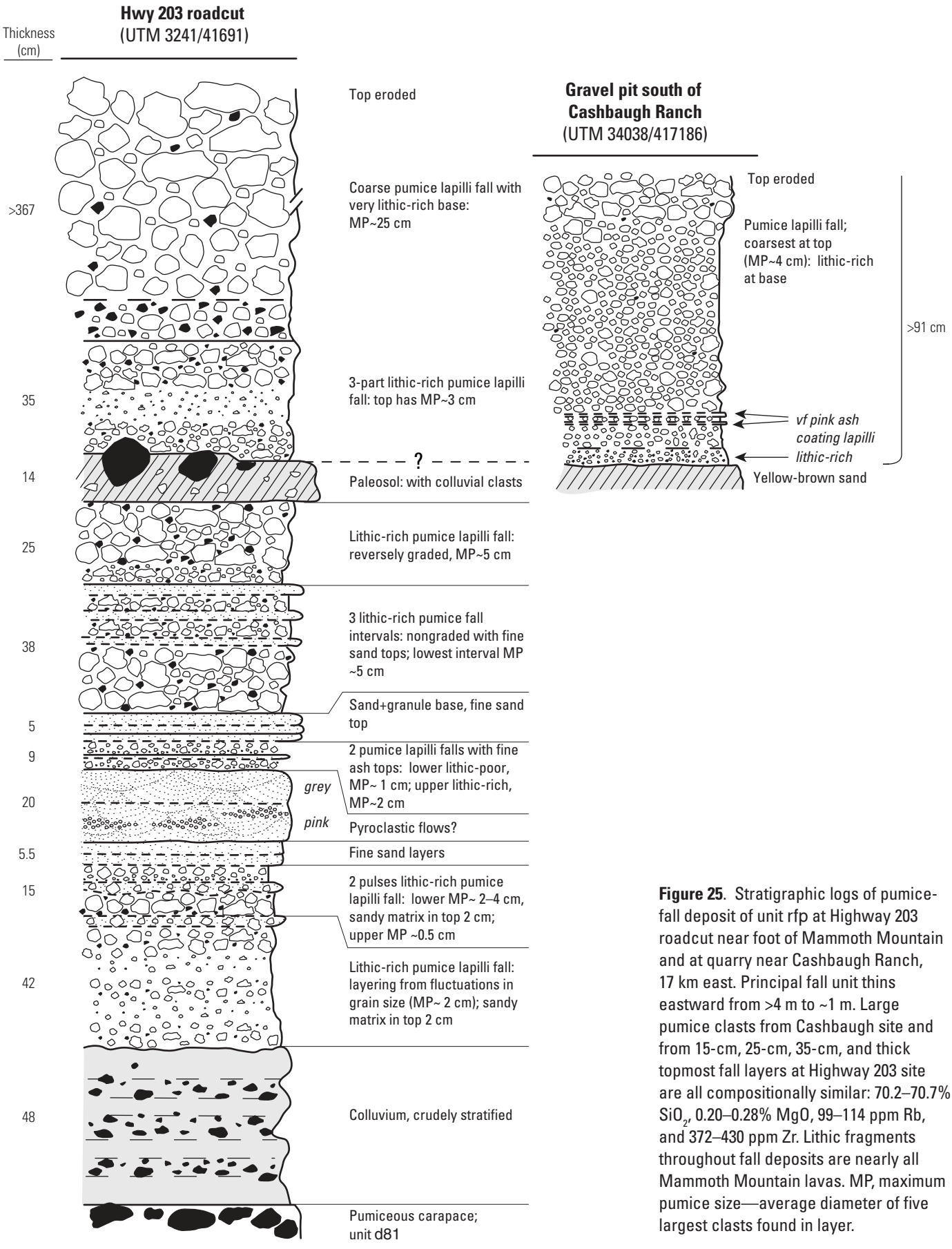

Figure 25. Stratigraphic logs of pumice-fall deposit of unit rfp at Highway 203 roadcut near foot of Mammoth Mountain and at quarry near Cashbaugh Ranch, 17 km east. Principal fall unit thins eastward from >4 m to ~1 m. Large pumice clasts from Cashbaugh site and from 15-cm, 25-cm, 35-cm, and thick topmost fall layers at Highway 203 site are all compositionally similar: 70.2–70.7% SiO_2, 0.20–0.28% MgO, 99–114 ppm Rb, and 372–430 ppm Zr. Lithic fragments throughout fall deposits are nearly all Mammoth Mountain lavas. MP, maximum pumice size—average diameter of five largest clasts found in layer.

Creek gorge, which incises coulee distally and remains present-day site of boiling pools, geysers, and fumaroles (Farrar and others, 2007). Phenocrysts: ~1% total, of which about half is plagioclase (0.5–1.5 mm), along with trace amounts of sanidine, biotite, and cpx, as well as microphenocrysts of Fe-Ti oxides, zircon, and apatite. Base not exposed, but drill hole CH-10B penetrated lake sediments beneath north-distal part of lava flow at a depth of 60 m. Overlain by rhyolitic sandstone and pebble conglomerate of Pleistocene Long Valley Lake (unit ss). Basalt of Fish Hatchery (unit bfh; 92±2 ka) and late Pleistocene alluvium (unit oal) bank against unit rhc coulee. K-Ar age (for glass): 288±31 ka (Mankinen and others, 1986). U-Pb age for zircon ~300 ka (J.A. Vazquez, unpublished data). $^{40}Ar/^{39}Ar$ age for sanidine: 333±2 ka (Simon and others, 2014).

Subunit rhc' represents two small knolls of brecciated high-silica rhyolite that crop out near the Hot Creek coulee and are compositionally identical to it. (1) Knob 2122 (UTM 394/714), on north side of Antelope Springs Road southwest of Cashbaugh Ranch, is 4-m-high mound, 25-m-wide, of unstratified all-rhyolite breccia (76.2% SiO_2) ~1.3 km north of apparent terminus of main coulee. Breccia may have avalanched across shallow lake or mudflat from advancing flow front. Alternatively, because outcrop is surrounded by lake silt, it could be an exposure of the coulee itself if its distal 1.3 km reach is now sediment-covered. (2) A small knoll (UTM 401/6615) next to carpark at Whitmore Hot Springs, 100 m east of margin of Hot Creek coulee, is similar rhyolite breccia (76.1% SiO_2) mixed with lake sediment. Exposure is ~20 m wide and has only 2–3 m of relief. Because it is unlikely that such tiny masses are independent extrusions, we attribute them to the Hot Creek eruptive episode

ric **Rhyolite and rhyodacite of Inyo chain (1350 C.E.)—**Compositionally complex lava flows and pumiceous ejecta (70–74% SiO_2) that erupted from a dike-fed, 5-km-long, north-south chain of three separate vents (Miller, 1985) in late summer of 1350 C.E. (Millar and others, 2006). (1) Southern vent released ~0.05 km^3 of magma as pyroclastic flows (>10 m thick proximally), which extend as far as 6 km from vent, as well as a similar volume as pumiceous fall deposits distributed in two narrow sequential lobes that extend >20 km northeast and >25 km south-southwest. These were followed by extrusion of ~0.13 km^3 of lava as **Deadman Creek flow**, pancake-shaped, weakly lobate flow on south bank of Deadman Creek, ~1 km inside northwest topographic wall of Long Valley Caldera. Barren, rugged, sprawling flow is nearly circular in plan, 1.3 km in diameter, and has flow fronts as high as 40 m and total relief of 170 m. Pyroclastic-flow deposits near Deadman Creek flow have poorly sorted, tan matrix of fine-to-coarse ash that carries scattered clasts, mostly lapilli but commonly 10–20 cm across, of wide textural variety, ranging from pumiceous to finely microvesicular to dense black vitrophyre.

(2) Northern vent was second to erupt, releasing ~0.02 km^3 of magma as a narrow lobe of pumiceous fallout that extends >25 km northeast, followed by thin proximal pyroclastic flows. These were followed by extrusion of ~0.17 km^3 of lava as **Obsidian flow**, just north of Glass Creek at foot of Sierran rangefront fault scarp. Rugged barren lava flow is 1.5 by 1.8 km across, and its steep margins are 30–50 m high, thickening to more than 100 m centrally. Because emplaced on a slope, its total exposed relief reaches ~190 m. Its conduit lava remains as wide as 33 m where intersected by drilling at a depth of ~500 m (Eichelberger and others, 1984, 1985).

(3) Last of three magmatic vents to open was high on topographic rim of Long Valley Caldera, ~1.5 km south of vent for Obsidian flow and 3.5 km north of that for Deadman Creek flow. It released ~0.1 km^3 of pumiceous fallout, as thick as 10 m proximally, that extends more than 190 km southward, by far most widespread and voluminous explosive product of 1350 C.E. sequence ("Tephra 1" of Wood, 1977; Miller, 1985). Along crest of White Wing Mountain (fig. 26), where fallout is 8 m thick, 2–4 km southwest of Glass Creek vent, tree-ring study of numerous trees killed by the eruption yielded an eruption age of 1350 C.E. (Millar and others, 2006). This outburst was followed by remobilized flows of pumiceous proximal ejecta (Miller, 1985), which are poorly exposed for several kilometers eastward along Glass Creek, and finally by extrusion of ~0.1 km^3 of lava as rugged, blocky **Glass Creek flow** (fig. 26). From its vent on caldera rim, this 700-to-900-m-wide flow spread ~500 m northward (to a steep northerly flow-front as

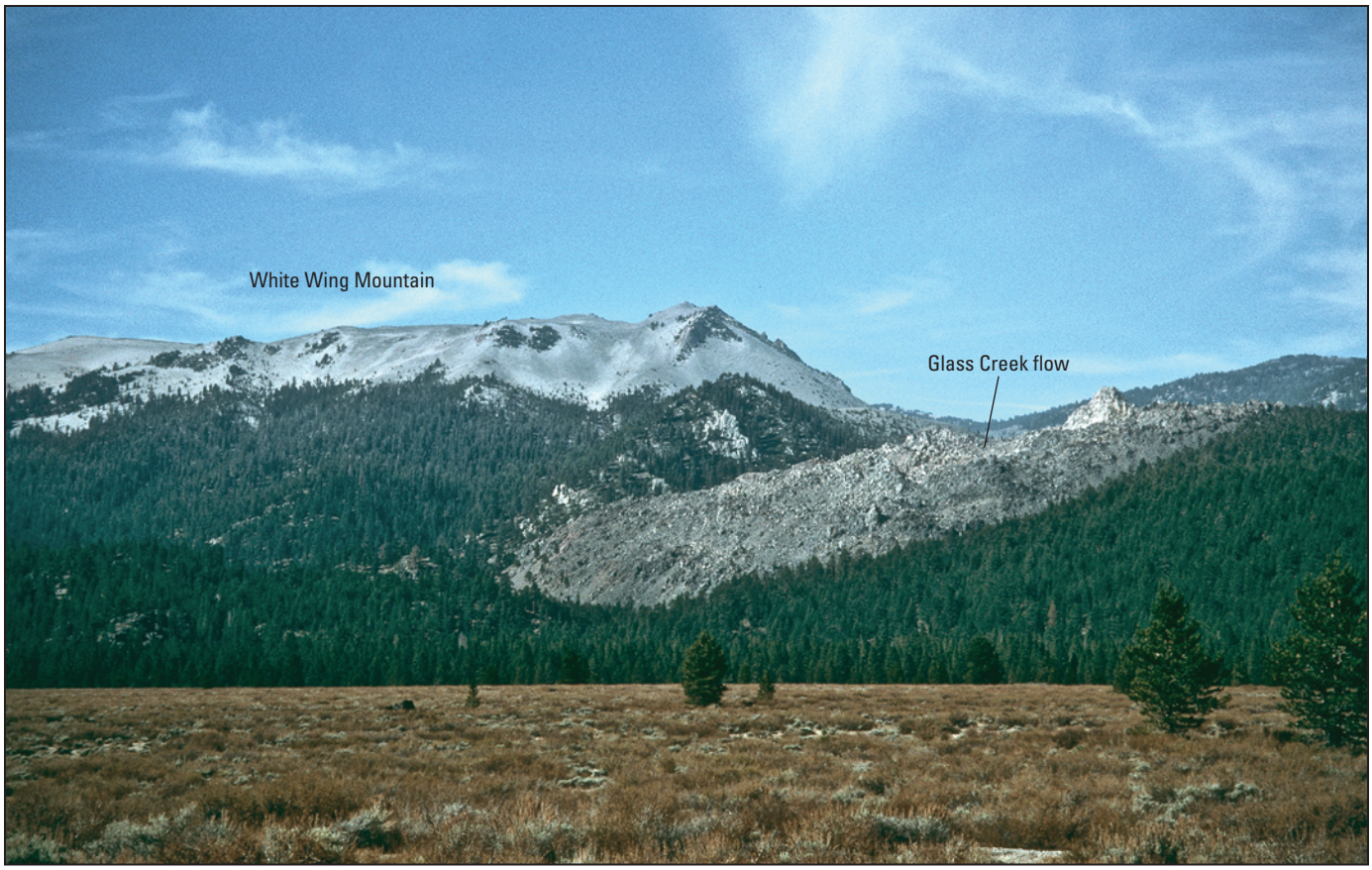

Figure 26. Glass Creek flow (unit ric) draping caldera wall 3 km west of Highway 395 at Crestview. Rugged rhyolitic coulee covers trace of Hartley Springs Fault, which separates Pliocene intermediate lavas that form caldera wall at right from Meozoic granite that forms wall at left. On skyline is granitic White Wing Mountain, thickly mantled with pumiceous fallout, much of it ejected from the nearby vent that subsequently extruded the Glass Creek flow. Tree-ring study of logs and stumps killed by the eruption atop White Wing Mountain pinned the event to late summer 1350 C.E. (Millar and others, 2006). View westward from surface of unit mcv (33 ka). Forested ridge at lower left is unit dnw.

high as 75 m) as well as ~1 km southward, descending 220 m in elevation to foot of caldera wall.

None of the four pumice-fall deposits (Nawotniak and Bursik, 2010) overlie any of the three still-barren lavas, although they blanket Devils Postpile region, Mammoth Mountain, west moat of caldera, and plateaus north of caldera, widely obscuring contacts among older units. Although one vent lies within topographic basin of Long Valley Caldera, all three vents are well outside structural ring-fault margin of caldera (Hildreth, 2004). Although sometimes referred to as "Inyo Domes" or popularly called "Inyo Craters" (presumably in deference to phreatic craters that formed soon after magmatic sequence; see unit pe), all three 1350 C.E. effusive units are pancake-style flow-foliated lava flows with extensive low-angle surfaces of shattered craggy glass. Phenocrysts: products of crystal-poor magma (2–3% phenocrysts) dominate fall deposits and Obsidian flow. Crystal-rich lava (25–40% phenocrysts) makes up 30–40% of Glass Creek flow and more than 50% of Deadman Creek flow, its proportion thus increasing southward along chain. Central areas of latter two flows consist of relatively homogeneous, white, moderately vesicular crystal-rich phase (71.5±0.5% SiO_2), which grades radially into peripheral zones where it is either interlayered with crystal-poor lava or broken up into lenses, blobs, and streaks that were disaggregating into it when frozen (Sampson, 1987). Crystal-poor phase is texturally more heterogeneous, ranging from coarsely to finely vesicular to dense obsidian or microcrystalline felsite; moreover, it is chemically zoned (70–74% SiO_2) as described by Sampson and Cameron (1987) and Vogel and others (1989) and

reviewed by Hildreth (2004). Crystal-rich lava contains 15–20% plagioclase, 10–15% sanidine, 2% biotite, ~2% hornblende, ~1% quartz, ~1% titanomagnetite, and trace amounts of ilmenite, cpx, opx, apatite, zircon, and allanite. Feldspars are as big as 10 mm and biotite and hornblende are commonly >3 mm. Crystal-poor lava contains most of these phases but lacks quartz and allanite, and higher-silica samples along its zoned array also lack hornblende; few of its mafic phenocrysts are larger than 0.5 mm, and most of its feldspars are smaller than 2 mm (though rarely as big as 5 mm). Sparse fine-grained enclaves, dense to vesicular, <1 to 10 cm across, are distributed within crystal-rich rhyolite in high central parts of Deadman Creek and Glass Creek flows, where lavas can be inferred to represent latest material extruded from directly subjacent vents (Varga and others, 1990). Bulk enclave compositions are intermediate (59.5–60.7% SiO_2), but their cargo of abundant disequilibrated phenocrysts from host rhyolite indicates that they are magmatic mixtures of mafic and silicic magma. Mafic contribution may represent seldom-seen source of long-lived thermal flux beneath west moat of Long Valley Caldera

rmf **Alkalic rhyodacite of Mammoth Mountain fumarole (late Pleistocene)—**Moderately porphyritic lava flow (69.9–70.7% SiO_2) that forms 800-m-long dipslope that is referred to as Face Lift planèze (figs. 7, 12). It descends northward from 3,208-m knob to eroded flow front facing McCoy Station reservoir at 2,940 m. Erosionally isolated knob, 400 m north of Mammoth Mountain summit, is upper terminus of Face Lift Express (Chair 3). Dipslope forms glacially eroded planèze 200–350 m wide. Midway up dipslope surface, wispy fumarole issues from joints in lava (and from small artificial pipes) at ~3,030 elevation. Below fumarole, strip of modest acid alteration extends ~200 m downslope, largely confined to surficial debris along a gulch and to films on fractures in the rhyodacitic lava. Flow is mostly dark- or medium-gray vitrophyre, strongly flow foliated, with subordinate layers devitrified, spherulitic, or locally lithophysal; layers are commonly 2–10 cm thick, locally folded convolutely, and ramped into steep inward dips around flow margins. South-facing 25-m-high scarp of knob 3208 is acid-altered, which facilitated glacial excavation of 150-m-wide notch (The Chasm; fig. 12) that separates knob from north scarp of summit dome (units dfl and dsu). Phenocrysts: 10–12% feldspar (0.5–3 mm, rarely 5 mm); ~2% biotite (mph to 2 mm); ≤1% opx (0.3–1.2 mm); sparse Fe-Ti-oxide mph. Also carries mafic blebs and sparse clots of all these minerals in varied proportions. Overlies units dms (68±1 ka) and dfl (61±3 ka). Overlain by remnant outlier of unit dsu (61.4±2 ka). $^{40}Ar/^{39}Ar$ age: 61±1.5 ka

rmk **Rhyolite of Mammoth Knolls (late Pleistocene)—**Bilobate rhyolite dome (76.4–76.8% SiO_2) centered 5.5 km east-northeast of Mammoth Mountain summit. Steep-sided unglaciated dome is 1 by 1.5 km wide and towers 200 m above north edge of Mammoth Lakes business district (fig. 23). Knobs on its rolling upper surface provide 10–20 m local relief. Southeast half has been described as a discrete contiguous dome but, being slightly lower, it may instead be a bulging protrusion rather than having its own independent vent. Exposures are glassy, finely vesicular to micropumiceous, and white to pale gray, weathering tan. At northeast side of dome, pumiceous ejecta form a 50-m-high half-ring, 500 by 800 m across and ~300 m wide at its rim, which was largely constructed during eruption of unit rwm ~50 kyr earlier. Pumice lapilli (and blocks as big as 25 cm) of unit rmk are scattered on surface of older ejecta ring; they also form a linear rib ~3 m high, adjacent to toe of rmk dome, along crater floor inside rwm ring. Phenocrysts: ~15% feldspars (0.2–1.5 mm; more sanidine than plagioclase); 2–3% quartz (0.2–1.5 mm), many embayed; 1–2% biotite (mostly <0.5 mm, rarely up to 1.5 mm); sparse hornblende (<0.5 mm); and trace amounts of Fe-Ti oxides, zircon, apatite, and allanite. Intrudes and marginally overlies unit rwm. Late Pleistocene till of unit gmm banks against south base of dome. K-Ar ages: 97±6 ka (northwest lobe) and 106±2 ka (southeast lobe) (Mankinen and others, 1986). $^{40}Ar/^{39}Ar$ ages: 109±3 ka and 113±1 ka (northwest lobe) and 111±5 ka (southeast lobe) (Heumann and others, 2002; Mahood and others, 2010)

rnc **Rhyolite of north-central chain (middle Pleistocene)—**Northwest-trending alignment of phenocryst-rich rhyolitic domes and one lava flow (73.9–75.3% SiO_2) that crosses north flank of resurgent uplift of Long Valley Caldera. Equivalent to unit Qmr1 of Bailey (1989). Called "moat rhyolite" by Bailey and others (1976) but erupted through Early

rhyolite (unit rer) on central uplift, not in caldera moat. Like other Long Valley rhyolites, unit is subalkaline, contrasting with mildly alkaline domes of Mammoth Mountain. Four extrusive units are defined. (1) Minidome, exposed 2 km north of Little Antelope Valley; crops out only as a 5-m-high subdued ridge within an area 30 by 60 m (UTM 355/7435). Consists of glassy rounded blocks (75.3% SiO_2), micropumiceous and pale gray, weathering tan. Near-primary surface has been exhumed from rhyolite-dominated ashy colluvium that surrounds it. (2) Dome 2395 (UTM 344/755) is 200 m in diameter and has 50 m of relief exposed on its south side. Blocky lava (75.2% SiO_2) is medium-to-pale gray, weathers tan to orange-brown, and (in contrast to subjacent unit rer) displays little flow foliation. Brecciated marginal facies is exposed along steep southwest side. Contains phenocryst-poor mafic enclaves (2–15 cm; 54.9% SiO_2) on its southeast nose. (3) Dome 2415 (UTM 340/764) is 700 m in diameter, nearly circular in plan, and has ~145 m of relief exposed on its northwest slope. Blocky lava (74.6% SiO_2) is glassy, massive or finely pumiceous, and pale gray, weathering tan to pink. (4) Coulee (73.9–74.3% SiO_2), covering ~3 km^2, extends 2 km west from Dome 2415 (its inferred vent site), then 4 km northeastward, descending north slope of caldera's resurgent uplift into its north moat. Maximum relief exposed is ~60 m along gorge just west of dome; far western scarp of coulee, cut by canyon of Dry Creek, has 40 m of relief. Northeast tongue in moat generally has <10 m of exposed relief because lapped by alluvium that further covers most of its distal 1.3-km reach. Outlying knob (UTM 355/787) in north moat, 70 m diameter and 8 m high, is distal extremity of coulee; massive to finely vesicular, glassy outlier is locally flow foliated or brecciated and carries sparse crystal-poor mafic enclaves (5–25 cm; 54.7% SiO_2). Parts of low-relief northeast tongue are strongly hydrated and disintegrate into glassy kernels, suggesting interaction with shallow caldera lake. Lower 10 m of coulee, well exposed along gorge of Dry Creek, is coarse lava-flow breccia (not agglutinated spatter fall as interpreted by Bailey, 1989). Milled during flow, rhyolite blocks are angular to subrounded, commonly 10–50 cm across, and as big as 1 m. Blocks are separated by crush breccia of smaller angular clasts, which are generally weakly to moderately adherent but locally strongly healed to ghost-breccia texture. Mafic enclaves (53.3% SiO_2) are common within rhyolite blocks, in interblock breccia, and widely elsewhere in nonbrecciated parts of coulee; enclaves are angular to rounded, 1–20 cm across, and contain sparse plagioclase and olivine crystals.

Phenocrysts: each rhyolite subunit contains 10–15% feldspar (0.5–5 mm; both sanidine and plagioclase), variously euhedral, sieved, or composite; 1–3% hornblende (0.5–3 mm long); 1–2% biotite (0.2–1.5 mm); sparse rounded quartz as big as 1.5 mm; and rare tiny Fe-Ti oxide mph. Groundmass glassy, dense to finely vesicular; commonly having wavy, collapsed pumiceous texture. All subunits erupted through resurgently deformed unit rer or its pyroclastic subunit rtav. K-Ar age of sanidine from each subunit (Mankinen and others, 1986): (1) 505±15 ka; (2) 527±12 ka; (3) 523±11 ka; (4) 481±10 ka. $^{40}Ar/^{39}Ar$ ages of 570±8 ka were reported by Simon and others (2014) for sanidine from both (3) and (4).

A quartz-rich biotite-granite porphyry of bulk composition (73.9% SiO_2) similar to that of unit rnc was penetrated beneath intracaldera Bishop Tuff in well CP-1 (UTM 360/728) at depths from 1,420 m to 1,847 m (Suemnicht and Varga, 1988), ~1.7 km south of minidome (1). At least 427 m thick (to bottom of hole), porphyry contains euhedral quartz (0.5–1.5 mm), shaggy chloritized biotite (0.5–5 mm long), clay-altered feldspar (mph to 2.5 mm), and sparse tiny Fe-Ti oxide mph. Lacking hornblende, it might be magmatically related to extrusive unit rer rather than to unit rnc, but it fails to provide a convincing chemical match for either

rnd **Rhyolite of North Deadman Creek Dome (Holocene)—**Compact middle Holocene lava dome (74.7% SiO_2) at foot of northwest topographic wall of Long Valley Caldera, on north bank of Deadman Creek, just north of barren and rugged Deadman Creek flow (southernmost of 1350 C.E. chain of Inyo lavas; unit ric). Forested dome is steep-sided, craggy, nearly circular in plan, 600 m in diameter, and has 130 m relief. Pale gray aphyric lava is glassy, block-jointed, flow-foliated, and micropumiceous to massive; sheds coarse talus of angular blocks. Volume of virtually uneroded dome is ~0.03 km^3, and coerupted

ejecta (if any) are not exposed. Phenocrysts: none; but glassy groundmass is rich in feldspar and biotite microlites (<0.1 mm) with sparse feldspar-lath mph (0.1–0.3 mm). Apparently erupted through Mesozoic granite (unit Kjl), exposed in adjacent caldera wall. Overlain by Inyo pumice-fall deposits of 1350 C.E. Undated, but estimated to be roughly 6,000 years old by Miller (1985)

rrc **Alkalic rhyodacite of Reds Creek (late Pleistocene)—**Moderately porphyritic lava flow (70.9–71.2% SiO_2) that crops out only in 200-by-300-m area along gorge of Reds Creek at southwest toe of Mammoth Mountain. Most of exposure is highly flow-foliated, even laminated, cream-white felsite that breaks slabby to platy and forms 20-m-high cliffs on both walls of creek; rusty films are widespread on foliation planes and cross joints, but only upstream-most end of unit is hydrothermally altered like overlying trachydacite (unit dsd) along Reds Creek. Lowermost parts of exposures on both banks are black vitrophyre, 3–8 m thick, hydrated and crumbly, but generally massive with sparse devitrified layers. Phenocrysts: 4–5% feldspar (0.5–2 mm); 1–2% biotite (mph to 1 mm); trace pyroxene mph; sparse Fe-Ti- oxide mph; also contains sparse clusters of feldspar and biotite-feldspar clots. Base not exposed, but probably overlies nearby unit amp (97±1 ka), contact with which is obscured by scree rich in 1350 C.E. Inyo pumice. Overlain by units dsd (87±6 ka) and dwr (73±2 ka). Unit is richest in K_2O and SiO_2 and poorest in MgO and FeO of all units of Mammoth system. $^{40}Ar/^{39}Ar$ age: 83±1 ka

rsq **Alkalic rhyodacite of Quicksilver ski run (late Pleistocene)—**Moderately porphyritic lava flow (70.0–70.3% SiO_2) that issues from beneath Solitude Dome (unit rss) and extends 1.5 km eastward (south of Lincoln Peak) to flow front at ~2,750 m. Crops out patchily through colluvium and bulldozed ski-slope rubble as flow-foliated block-jointed vitrophyre, black to pale gray, but irregularly streaked tan or pink and locally lithophysal. Flow was glacially scoured and plucked distally into a few block-jointed ledges 5–20 m high. Phenocrysts: ~10% feldspar (mph to 3.5 mm); ~2% biotite (0.5–1.5 mm); sparse pyroxenes (0.2–0.7 mm); sparse Fe-Ti oxide mph; and rare hornblende mph. Flow is distinguished from Solitude Dome (unit rss) by paleomagnetic directions; flow also has consistently greater Ba and Zr abundances than unit rss and lower Ti, Mg, Rb, and Sr. Flow overlies unit rce (80±1 ka); also apparently overlies toe of adjacent Lincoln Peak dome (unit dlp; 64±7 ka), but thick colluvial wedge obscures contact. Flow is overlain by dome unit rss (50±3 ka). $^{40}Ar/^{39}Ar$ age of lava flow: 63.7±4 ka

rss **Alkalic rhyodacite of Solitude ski run (late Pleistocene)—**Moderately porphyritic Solitude Dome, knob 3160+, between Lincoln Peak and Mammoth Mountain summit. Dome (70.0– 70.6% SiO_2) lies 500 m northeast of summit (figs. 1, 7), just across ice-excavated trough (The Chasm) that separates it from summit's northeast face (which consists of units dfl and dsu). Flow foliation dips radially on slopes of dome and defines a broad open fold on dome's south face; top central part of dome is more disrupted and may include a final breccia-enveloped protrusion, ~20 m wide and ~80 m long. Exposures are black to pale-gray vitrophyre, only locally oxidized, strongly flow-foliated but also commonly block-jointed; some domains are cream-white and microvesicular; spherulitic, lithophysal, and tan-to-pink flow layers are subordinate. Phenocrysts: 7–12% feldspar (0.5-5 mm); ~2% biotite (mph to 1.5 mm); ≤1% opx (0.5–1.5 mm, rarely as long as 3 mm); sparse Fe-Ti-oxide mph. Also contains sparse feldspar clusters and biotite-oxide-pyroxene-feldspar clots. Overlies units rce (81±1 ka) and dsd (87±6 ka). Dome is distinguished from rhyodacite units rce and rmf by its higher Sr, Ca, Mg, Fe, Ti, and P abundances and lower K, Na, Nb, and Zr. Dome is distinguished from lava-flow unit rsq by greater Mg, Ti, Rb, and Sr abundances, lower Ba and Zr, and by different paleomagnetic directions. Despite chemical and magnetic differences, alkalic rhyodacite units rce (80±1 ka), rsq (63.7±4 ka), and rss evidently issued sequentially at a common vent site. $^{40}Ar/^{39}Ar$ age: 50±3 ka

rwm **Rhyolite of West Moat Coulee (middle Pleistocene)—**Major rhyolite lava flow (72.1–73.4% SiO_2) that forms knobby plateau extending 5 km north-northeast from Mammoth Knolls to Dry Creek. As wide as 2.5 km proximally and 1.5 km distally, flow has steep margins, generally 50–80 m high. Knobs and ridges on its rolling unglaciated surface have 20 m or more of local relief, much of it primary, although its roughness has been subdued

by thick mantle of late Holocene Inyo pumice-fall deposit. Most outcrops are pale gray to white micropumiceous carapace that weathers tan; massive interior felsite is rarely exposed. In drillhole PLV-1 (fig. 6; Benoit, 1984), which was collared on mid-flow surface (550 m southeast of toe of Dry Creek Dome), flow is 574 m thick (more than 5 times its visible thickness), suggesting either that it filled a deep paleovalley (unlike any drainage nearby) or, more likely, that drillhole extended down into intrusive domain that fed surface coulee. Terminal area of flow was cut by resurgent graben faults and eroded by Pleistocene Dry Creek. Outlying remnant of rhyolite unit (~50 m wide) caps mafic lava knoll 2351 (UTM 283/7483), ~750 m northeast of flow's eroded terminus and 40 m higher than alluviated graben floor that separates them. At surface, vent is marked by a 50-m-high half ring of pumiceous ejecta, 500 by 800 m across and ~300 m wide at its rim. Its juvenile ejecta are dominantly ash and lapilli but include finely vesicular blocks up to 30 cm across; accompanying blocks of pumiceous carapace (pale gray but commonly pink internally) are as big as 70 cm. Cognate lithic fragments are angular to subrounded, as big as 55 cm, and include dense gray vitrophyre and flow-foliated felsite. Sparser lithic fragments of mafic lavas, crystal-poor to crystal-rich and as big as 30 cm, range from subrounded to angular or slabby; some correlate chemically with units mkv, msc, and mcl. Absence among lithic ejecta of well-rounded cobbles or of granitoid and metavolcanic clasts suggests that mafic fragments are not derived from till or alluvium but from underlying lava flows. Pumice lapilli (and blocks as big as 25 cm) of unit rmk are scattered across ejecta-ring surface; they also form a linear rib ~3 m high, adjacent to toe of rmk dome, along crater floor inside rwm ring.

Phenocrysts: 15% feldspar (plagioclase and sanidine; 0.3–3 mm); ~7% quartz (0.3–2.5 mm); 2–3% biotite (0.1–1 mm); ~1% hornblende (mostly 0.3–0.6 mm, rarely up to 2 mm long); sparse Fe-Ti oxides (0.1–0.2 mm); and rare pyroxene, zircon, apatite, and allanite mph. Conspicuously contains more hornblende than adjacent rhyolite units rdc and rmk. Overlies units msc (154±2 ka), mcl (~175 ka), and bsm (165±2 ka). Intruded by and overlain by units rmk and rdc. Late Pleistocene till (unit gdc) banks against northwest margin of coulee. $^{40}Ar/^{39}Ar$ ages (all for sanidine): 163±2 ka (proximal) and 161±2 ka (distal) (Mahood and others, 2010); 147±4 ka (proximal) and 151±4 ka (distal outlier) (Heumann and others, 2002). Trough (now traversed by Highway 395) that separates snout of coulee from compositionally identical outlier is part of resurgent graben system, which thus exhibits fault displacement younger than 150,000 years

References Cited

Annen, C., Blundy, J.D., and Sparks, R.S.J., 2006, The genesis of intermediate and silicic magmas in deep crustal hot zones: Journal of Petrology, v. 47, p. 505–539.

Bailey, R.A., 1978, Volcanism, structure, and petrology of Long Valley caldera, California: Baltimore, Md., Johns Hopkins University, Ph.D. dissertation, 112 p.

Bailey, R.A., 1989, Geologic map of Long Valley caldera, Mono-Inyo Craters volcanic chain, and vicinity, eastern California: U.S. Geological Survey Map I-1933, pamphlet 11 p., 2 sheets, scale 1:62,500.

Bailey, R.A., 2004, Eruptive history and chemical evolution of the precaldera and postcaldera basalt-dacite sequences, Long Valley, California; Implications for magma sources, current seismic unrest, and future volcanism: U.S. Geological Survey Professional Paper 1692, 75 p.

Bailey, R.A., Dalrymple, G.B., and Lanphere, M.A., 1976, Volcanism, structure, and geochronology of Long Valley caldera, Mono County, California: Journal of Geophysical Research, v. 81, no. 5, p. 725–744.

Bailey, R.A., Huber, N.K., and Curry, R.R., 1990, The diamicton at Deadman Pass, central Sierra Nevada, California; A residual lag and colluvial deposit, not a 3 Ma glacial till: Geological Society of America Bulletin, v. 102, p. 1165–1173.

Bateman, P.C., 1965, Geology and tungsten mineralization of the Bishop District, Califonia: U.S. Geological Survey Professional Paper 470, 208 p.

Bateman, P.C., 1992a, Plutonism in the central part of the Sierra Nevada batholith, California: U.S. Geological Survey Professional Paper 1483, 186 p.

Bateman, P.C., 1992b, Pre-Tertiary bedrock geologic map of the Mariposa 1º by 2º quadrangle, Sierra Nevada, California: U.S. Geological Survey Map I-1960, scale 1:250,000.

Bateman, P.C., and Busacca, A.J., 1982, Geologic map of the Millerton Lake quadrangle, west-central Sierra Nevada, California: U.S. Geological Survey Map GQ-1548, scale 1:62,500.

Benioff, H., and Gutenberg, B., 1939, The Mammoth "Earthquake Fault" and related features in Mono County, California: Seismological Society of America Bulletin, v. 29, no. 2, p. 333–340.

Benoit, W.R., 1984, Initial results from drillholes PLV-1 and PLV-2 in the western moat of the Long Valley caldera: Geothermal Resources Council Transactions, v. 8, p. 397–402.

Berry, M.E., 1997, Geomorphic analysis of late Quaternary faulting on Hilton Creek, Round Valley and Coyote Warp faults, east-central Sierra Nevada, California, USA: Geomorphology, v. 20, p. 177–195.

Blackwelder, E., 1931, Pleistocene glaciation in the Sierra Nevada and Basin Ranges: Geological Society of America Bulletin, v. 42, p. 865–922.

Brook, C.A., Nokleberg, W.J., and Kistler, R.W., 1974, Nature of the angular unconformity between the Paleozoic metasedimentary rocks and the Mesozoic metavolcanic rocks in the eastern Sierra Nevada, California: Geological Society of America Bulletin, v. 95, p. 571–576.

Browne, B., Bursik, M., Deming, J., Louros, M., Martos, A., and Stine, S., 2010, Eruption chronology and petrologic reconstruction of the ca. 8500 yr B.P. eruption of Red Cones, southern Inyo chain, California: Geological Society of America Bulletin, v. 122, p. 1401–1422.

Bursik, M.I., and Gillespie, A.R., 1993, Late Pleistocene glaciation of Mono Basin, California: Quaternary Research, v. 39, p. 24–35.

Bursik, M., Renshaw, C., McCalpin, J., and Berry, M., 2003, A volcanotectonic cascade; Activation of range front faulting and eruptions by dike intrusion, Mono Basin-Long Valley caldera, California: Journal of Geophysical Research, v. 108, no. B8, 2393, 14 p.

Bursik, M., and Sieh, K., 1989, Range front faulting and volcanism in the Mono Basin, eastern California: Journal of Geophysical Research, v. 94, no. B11, p. 15,587–15,609.

Calvert, A.T., and Lanphere, M., 2006, Argon geochronology of Kilauea's early submarine history: Journal of Volcanology and Geothermal Research, v. 151, p. 1–18.

Carle, S.F., 1988, Three-dimensional gravity modeling of the geologic structure of Long Valley caldera: Journal of Geophysical Research, v. 93, no. B11, p. 13,237–13,250.

Chaudet, R.E., 1986, The petrology and geochemistry of precaldera magmas, Long Valley caldera, eastern California: Blacksburg, Va., Virginia Polytechnic Institute and State University, M.S. thesis, 152 p.

Chelikowski, J.R., 1940, Tectonics of the rhyolite in the Mammoth embayment, California: Journal of Geology, v. 48, p. 421–435.

Clark, D.H., Clark, M.M., and Gillespie, A.R., 1994, Debris-covered glaciers in the Sierra Nevada, California, and their implications for snowline reconstructions: Quaternary Research, v. 41, p. 139–153.

Clark, D.H., and Gillespie, A.R., 1997, Timing and significance of late-glacial and Holocene cirque glaciation in the Sierra Nevada, California: Quaternary International, v. 38–39, p. 21–38.

Clark, M.M., and Gillespie, A.R., 1981, Record of late Quaternary faulting along the Hilton Creek fault in the Sierra Nevada, California: Earthquake Notes, v. 52, no. 1, p. 46.

Clark, M.M., Yount, J.C., Vaughan, P.R., and Zepeda, R.L., 1982, Map showing surface ruptures associated with the Mammoth Lakes, California, earthquakes of 1980: U.S. Geological Survey Map MF-1396, scale 1:24,000.

Cleveland, G.B., 1962, Geology of the Little Antelope Valley clay deposits, Mono County, California: California Division of Mines and Geology Special Report 72, 28 p.

Clow, D.W., and Collum, K.R., 1983, Geology of the volcanic rocks at Devils Postpile, California. [Unpublished report of a joint undergraduate mapping project for Fresno State University, 4 p., instigated by Wymond Eckhardt, then superintendent at Devils Postpile National Monument, the report remains in Monument files and its geologic map was published in Huber and Eckhardt (1985).]

Clynne, M.A., Calvert, A.T., Wolfe, E.W., Evarts, R.C., Fleck, R.J., and Lanphere, M.A., 2008, The Pleistocene eruptive history of Mount St. Helens, Washington, from 300,000 to 12,800 years before present, chap. 28 *of* Sherrod, D.R., Scott, W.E., and Stauffer, P.H., eds., A volcano rekindled; the renewed eruption of Mount St. Helens, 2004–2006: U.S. Geological Survey Professional Paper 1750, p. 593–627.

Clynne, M.A., and Muffler, L.J.P., 2010, Geologic map of Lassen Volcanic National Park and vicinity, California: U.S. Geological Survey Scientific Investigations Map 2899, 110 p., 3 sheets, scale 1:50,000.

Cook, A.C., Hainsworth, L.J., Sorey, M.L., Evans, W.C., and Southon, J.R., 2001, Radiocarbon studies of plant leaves and tree rings from Mammoth Mountain, CA; a long-term record of magmatic CO_2 release: Chemical Geology, v. 177, p. 117–131.

Cousens, B.L., 1996, Magmatic evolution of Quaternary mafic magmas at Long Valley caldera and the Devils Postpile, California; Effects of crustal contamination on lithospheric mantle-derived magmas: Journal of Geophysical Research, v. 101, no. B12, p. 27,673–27,689.

Curry, R.R., 1966, Glaciation about 3,000,000 years ago in the Sierra Nevada: Science, v. 154, p. 770–771.

Curry, R.R., 1968, Quaternary climatic and glacial history of the Sierra Nevada, California: Berkeley, University of California, Ph.D. dissertation, 219 p.

Curry, R.R., 1971, Glacial and Pleistocene history of the Mammoth Lakes Sierra—a geologic guidebook: Missoula, University of Montana, Department of Geology, Geological Series Publication no. 11, 49 p.

Dalrymple, G.B., 1963, Potassium-argon dates of some Cenozoic volcanic rocks of the Sierra Nevada, California: Geological Society of America Bulletin, v. 74, p. 379–390.

Dalrymple, G.B., 1964a, Cenozoic chronology of the Sierra Nevada, California: University of California Publications in Geological Sciences, v. 47, 41 p.

Dalrymple, G.B., 1964b, Potassium-argon dates of three Pleistocene interglacial basalt flows from the Sierra Nevada, California: Geological Society of America Bulletin, v. 75, p. 753–758.

DeGraff, J.M., and Aydin, A., 1987, Surface morphology of columnar joints and its significance to mechanics and direction of joint growth: Geological Society of America Bulletin, v. 99, p. 605–617.

Deming, J.H., 2002, Stratigraphic analysis of Paoha Island and the Red Cones, eastern California; integration with a volcanic database: Buffalo, State University of New York at Buffalo, M.S. thesis, 92 p.

Doell, R.R., Dalrymple, G.B., and Cox, A., 1966, Geomagnetic polarity epochs; Sierra Nevada data, 3: Journal of Geophysical Research, v. 71, no. 2, p. 531–541.

Druitt, T.H., and Kokelaar, B.P., eds., 2002, The eruption of Soufrière Hills Volcano, Montserrat, from 1995 to 1999: London, The Geological Society, Memoir no. 21, 645 p.

Duffield, W.A., and Bacon, C.R., 1981, Geologic map of the Coso volcanic field and adjacent areas, Inyo County, California: U.S. Geological Survey Map I-1200, scale 1:50,000.

Eichelberger, J.C., Lysne, P.C., and Younker, L.W., 1984, Research drilling at Inyo domes, Long Valley, California: Eos, v. 65, p. 721–725.

Eichelberger, J.C., Lysne, P.C., Miller, C.D., and Younker, L.W., 1985, Research drilling at Inyo domes, California; 1984 results: Eos, v. 66, no. 17, p. 186–187.

Eichelberger, J.C., Vogel, T.A., Younker, L.W., Miller, C.D., Heiken, G.H., and Wohletz, K.H., 1988, Structure and stratigraphy beneath a young phreatic vent; South Inyo Crater, Long Valley Caldera, California: Journal of Geophysical Research, v. 93, no. B11, p. 13,208–13,220.

Erwin, H.D., 1934, Geology and mineral resources of northeastern Madera County, California: California Journal of Mines and Geology, v. 30, p. 7–78.

Evans, W.C., Sorey, M.L., Cook, A.C., Kennedy, B.M., Shuster, D.L., Colvard, E.M., White, L.D., and Huebner, M.A., 2002, Tracing and quantifying magmatic carbon discharge in cold groundwaters; Lessons learned from Mammoth Mountain, USA: Journal of Volcanology and Geothermal Research, v. 114, p. 291–312.

Farrar, C.D., Sorey, M.L., Evans, W.C., Howle, J.F., Kerr, B.D., Kennedy, B.M., King, C.-Y., and Southon, J.R., 1995, Forest-killing diffuse CO_2 emission at Mammoth Mountain as a sign of magmatic unrest: Nature, v. 376, p. 675–678.

Farrar, C.D., Sorey, M.L., Roeloffs, E., Galloway, D.L., Howle, J.F., and Jacobson, R., 2003, Inferences on the hydrothermal system beneath the resurgent dome in Long Valley caldera, east-central California, USA, from recent pumping tests and geochemical sampling: Journal of Volcanology and Geothermal Research, v. 127, p. 305–328.

Farrar, C.D., Evans, W.C., Venezky, D.Y., Hurwitz, S., and Oliver, L.K., 2007, Boiling water at Hot Creek—The dangerous and dynamic thermal springs in California's Long Valley caldera: U.S. Geological Survey Fact Sheet 2007–3045, 4 p.

Foulger, G.R., Julian, B.R., Hill, D.P., Pitt, A.M., Malin, P.E., and Shalev, E., 2004, Non-double-couple microearthquakes at Long Valley caldera, California, provide evidence for hydraulic fracturing: Journal of Volcanology and Geothermal Research, v. 132, p. 45–71.

Foulger, G.R., Julian, B.R., Pitt, A.M., and Hill, D.P., 2003, Three-dimensional crustal structure of Long Valley caldera, California, and evidence for the migration of CO_2 under Mammoth Mountain: Journal of Geophysical Research, v. 108, no. B3, 2147, p. 1-16.

Fournier, R.B., 1989, Lithology, mineralogy, and paleontology of Quaternary lake deposits in Long Valley caldera, California: U.S. Geological Survey Open-File Report 89–413, 95 p.

Fowler, A., Wildgoose, M., Zierenberg, R., Schiffman, P., and Suemnicht, G., 2011, Hydrothermal alteration and geochemistry in Core Hole BC 12–31; Implications for segregation of transient flow regimes in the Long Valley geothermal system: Geothermal Resources Council Transactions, v. 35, p. 785–789.

Fullerton, D.S., 1986, Chronology and correlation of glacial deposits in the Sierra Nevada, California, p. 161-169 *in* Sibrava, V., Bowen, D.Q., and Richmond, G.M., eds., Quaternary glaciations in the Northern Hemisphere: Quaternary Science Reviews, v. 5, p. 161–169.

Gerlach, T.M., Doukas, M.P., McGee, K.A., and Kessler, R., 2001, Soil efflux and total emission rates of magmatic CO_2 at the Horseshoe Lake tree kill, Mammoth Mountain, California: Chemical Geology, v. 177, p. 101, p. 116.

Gibbard, P.L., Head, M.J., Walker, M.J.C., and the Subcommission on Quaternary Stratigraphy, 2009, Formal ratification of the Quaternary System/Period and the Pleistocene Series/Epoch with a base at 2.58 Ma: Journal of Quaternary Science, v. 25, no. 2, p. 96–102.

Gibson, R.G., and Naney, M.T., 1992, Textural development of mixed, finely porphyritic silicic volcanic rocks, Inyo domes, eastern California: Journal of Geophysical Research, v. 97, p. 4541–4559.

Gilbert, C.M., 1938, Welded tuff in eastern California: Geological Society of America Bulletin, v. 49, p. 1829–1862.

Gilbert, C.M., 1941, Late Tertiary geology southeast of Mono Lake, California: Geological Society of America Bulletin, v. 52, p. 781–816.

Gillespie, A.R., and Clark, D.H., 2011, Glaciations of the Sierra Nevada, California, USA: Developments in Quaternary Science, v. 15, p. 447–462.

Gillespie, A.R., and Zehfuss, P.H., 2004, Glaciations of the Sierra Nevada, California, USA, *in* Ehlers, J., and Gibbard, P.L., eds., Quaternary glaciations—Extent and chronology; Part II; North America: Amsterdam, Elsevier, Developments in Quaternary Science, v. 2b, p. 51–62.

Goff, F., Wollenberg, H.A., Brookins, D.C., and Kistler, R.W., 1991, A Sr-isotopic comparison between thermal waters, rocks, and hydrothermal calcites, Long Valley caldera, California: Journal of Volcanology and Geothermal Research, v. 48, p. 265–281.

Gradstein, F.M., Ogg, J.G., Smith, A.G., Bleeker, W., and Lourens, L.J., 2004, A new geologic time scale, with special reference to Precambrian and Neogene: Episodes, v. 27, p. 83–100.

Greene, D.C., and Schweickert, R.A., 1995, The Gem Lake shear zone; Cretaceous dextral transpression in the Northern Ritter Range pendant, eastern Sierra Nevada, California: Tectonics, v. 14, p. 945–961.

Greene, D.C., and Stevens, C.H., 2002, Geologic map of Paleozoic rocks in the Mount Morrison pendant, eastern Sierra Nevada, California: California Division of Mines and Geology Map Sheet 53; scale 1:24,000.

Greene, D.C., Stevens, C.H., and Wise, J.M., 1997, The Laurel-Convict fault, eastern Sierra Nevada, California; A Permo-Triassic left-lateral fault, not a Cretaceous intrabatholithic break: Geological Society of America Bulletin, v. 109, no. 4, p. 483–488.

Harris, A.J.L., Rose, W.I., and Flynn, L.P., 2003, Temporal trends in lava dome extrusion at Santiaguito 1922–2000: Bulletin of Volcanology, v. 65, p. 77–89.

Heumann, A., 1999, Timescales of processes within silicic magma chambers: Amsterdam, Vrije Universiteit, Ph.D. dissertation, 200 p.

Heumann, A., and Davies, G.R., 1997, Isotopic and chemical evolution of the post-caldera rhyolitic system at Long Valley, California: Journal of Petrology, v. 38, p. 1661–1678.

Heumann, A., Davies, G.R., and Elliott, T., 2002, Crystallization history of rhyolites at Long Valley, California, inferred from combined U-series and Rb-Sr isotope systematics: Geochimica et Cosmochimica Acta, v. 66, no. 10, p. 1821–1837.

Hildreth, W., 1979, The Bishop Tuff; Evidence for the origin of compositional zonation in silicic magma chambers: Geological Society of America Special Paper 180, p. 43–75.

Hildreth, W., 2004, Volcanological perspectives on Long Valley, Mammoth Mountain, and Mono Craters; several contiguous but discrete systems: Journal of Volcanology and Geothermal Research, v. 136, p. 169–198.

Hildreth, W., and Mahood, G.A., 1986, Ring-fracture eruption of the Bishop Tuff: Geological Society of America Bulletin, v. 97, p. 396–403.

Hildreth, W., and Wilson, C.J.N., 2007, Compositional zoning of the Bishop Tuff: Journal of Petrology, v. 48, p. 951–999.

Hildreth, W., Fierstein, J., Champion, D., and Calvert, A., 2014, Mammoth Mountain and its mafic periphery—A late Quaternary volcanic field in eastern California: Geosphere, v. 10, no. 6., p. 1315–1365.

Hill, D.P., 1976, Structure of Long Valley caldera, California, from a seismic refraction experiment: Journal of Geophysical Research, v. 81, p. 745–753.

Hill, D.P., 1996, Earthquakes and carbon dioxide beneath Mammoth Mountain, California: Seismological Research Letters, v. 67, p. 815.

Hill, D.P., 2006, Unrest in Long Valley caldera, California, 1978-2004, *in* Troise. C., De Natale, G., and Kilburn, C.R.J., eds., Mechanisms of activity and unrest at large calderas: Geological Society of London, Special Publication 269, p. 1–24.

Hill, D.P., Bailey, R.A., Miller, C.D., Hendley, J.W., II, and Stauffer, P.H., 1997, Future eruptions in California's Long Valley area—What's likely?: U.S. Geological Survey Fact Sheet 073–97, 2 p.

Hill, D.P., Bailey, R.A., Hendley, J.W., II, Stauffer, P.H., and Marcaida, M., 2014, California's restless giant—the Long Valley Caldera: U.S. Geological Survey Fact Sheet 2014 3056, 2 p.

Hill, D.P., Dzurisin, D., Ellsworth, W.L., Endo, E.T., Galloway, D.L., Gerlach, T.M., Johnston, M.J.S., Langbein, J., McGee, K.A., Miller, C.D., Oppenheimer, D., and Sorey, M.L., 2002: Response plan for volcano hazards in the Long Valley caldera and Mono Craters region, California: U.S. Geological Survey Bulletin 2185, 57 p.

Hill, D.P., Ellsworth, W.L., Johnston, M.J.S., Langbein, J.O., Oppenheimer, D.H., Pitt, A.M., Reasenberg, P.A., Sorey, M.L., and McNutt, S.R., 1990, The 1989 earthquake swarm beneath Mammoth Mountain, California; an initial look at the 4 May through 30 September activity: Bulletin of the Seismological Society of America, v. 80, no. 2, p. 325–339.

Hill, D.P., Kissling, E., Luetgert, J.H., and Kradolfer, U., 1985, Constraints on the upper crustal structure of the Long Valley–Mono Craters volcanic complex, eastern California, from seismic refraction measurements: Journal of Geophysical Research, v. 90, p. 11,135–11,150.

Hill, D.P., Langbein, J.O., Prejean, S., 2003, Relations between seismicity and deformation during unrest in Long Valley Caldera, California, from 1995 through 1999: Journal of Volcanology and Geothermal Research, v. 127, p. 175–193.

Hill, D.P., and Prejean, S., 2005, Magmatic unrest beneath Mammoth Mountain, California: Journal of Volcanology and Geothermal Research, v. 146, p. 257–283.

Hopson, C.A. 2008, Geologic map of Mount St. Helens, Washington, prior to the 1980 eruption: U.S. Geological Survey Open-File Report 02–468; 2 sheets, scale 1:31,250.

Hoshizumi, H., Uto, K., and Watanabe, K., 1999, Geology and eruptive history of Unzen volcano, Shimabara Peninsula, Kyushu, SW Japan: Journal of Volcanology and Geothermal Research, v. 89, p. 81–94.

Huber, N.K., 1981, Amount and timing of late Cenozoic uplift and tilt of the central Sierra Nevada; evidence from the upper San Joaquin River basin: U.S. Geological Survey Professional Paper 1197, 28 p.

Huber, N.K., and Eckhardt, W.W., 1985, Devils Postpile story: Three Rivers, California, Sequoia Natural History Association, 30 p.

Huber, N.K., and Rinehart, C.D., 1965a, Geologic map of the Devils Postpile quadrangle, Sierra Nevada, California: U.S. Geological Survey Map GQ-437, scale 1:62,500.

Huber, N.K., and Rinehart, C.D., 1965b, The Devils Postpile National Monument: California Division of Mines and Geology, Mineral Information Service, v. 18, no. 6, p. 109–118.

Huber, N.K., and Rinehart, C.D., 1967, Cenozoic volcanic rocks of the Devils Postpile quadrangle, eastern Sierra Nevada, California: U.S. Geological Survey Professional Paper 554-D, 21 p., 1 plate.

Izett, G.A., Obradovich, J.D., and Mehnert, H.H., 1988, The Bishop ash bed (middle Pleistocene) and some older (Pliocene and Pleistocene) chemically and mineralogically similar ash beds in California, Nevada, and Utah: U.S. Geological Survey Bulletin 1675, 37 p.

Julian, B.R., Pitt, A.M., and Foulger, G.R., 1998, Seismic image of a CO_2 reservoir beneath a seismically active volcano: Geophysical Journal International, v. 133, p. F7–F10.

Kane, M.F., Mabey, D.R., and Brace, R., 1976, A gravity and magnetic investigation of the Long Valley caldera, Mono County, California: Journal of Geophysical Research, v. 81, p. 754–762.

Kaye, G., Finnis, K.K., Johnston, D.M., and Paton, D., 2008, Volcanic hazard awareness in the tourism sector in Mammoth Lakes, California: Wellington, New Zealand, Institute of Geological and Nuclear Sciences, GNS Science Report 2008/35, 13 p.

Kaye, G., Cole, J., King, A., and Johnston, D., 2009, Comparison of risk from pyroclastic density current hazards to critical infrastructure in Mammoth Lakes, California, USA, from a new Inyo Craters rhyolite dike eruption versus a dacite dome eruption on Mammoth Mountain: Natural Hazards (Springer), v. 49, p. 541–563.

Kelleher, P.C., and Cameron, K.L., 1990, The geochemistry of the Mono Craters–Mono Lake Islands volcanic complex, eastern California: Journal of Geophysical Research, v. 95, no. B11, p. 17643–17659.

Kesseli, J.E., 1941a, Ice streams in the Sierra Nevada, California: The Geographical Review, v. 31, no. 2, p. 203–227.

Kesseli, J.E., 1941b, Studies in the Pleistocene glaciation of the Sierra Nevada, California: University of California Publications in Geography, v. 6, no. 8, p. 315–362.

Kistler, R.W., 1966, Geologic map of the Mono Craters quadrangle, Mono and Tuolumne Counties, California: U.S. Geological Survey Map GQ-462, scale 1:62,500.

Kistler, R.W., and Swanson, S.E., 1981, Petrology and geochronology of metamorphosed volcanic rocks and a middle Cretaceous volcanic neck in the east-central Sierra Nevada, California: Journal of Geophysical Research, v. 86, p. 10,489–10,501.

Lachenbruch, A.H., Sorey, M.L., Lewis, R.E., and Sass, J.H., 1976a, The near-surface hydrothermal regime of Long Valley caldera: Journal of Geophysical Research, v. 81, no. 5, p. 763–768.

Lachenbruch, A.H., Sass, J.H., Munroe, R.J., and Moses, T.H., Jr., 1976b, Geothermal setting and simple heat conduction models for the Long Valley caldera: Journal of Geophysical Research, v. 81, no. 5, p. 769–784.

Langbein, J.O., 2003, Deformation of the Long Valley caldera, California; inferences from measurements from 1988 to 2001: Journal of Volcanology and Geothermal Research, v. 127, p. 247–267.

Lange, R.A., and Carmichael, I.S.E., 1996, The Aurora volcanic field, California-Nevada: Oxygen fugacity constraints on the development of andesitic magma: Contributions to Mineralogy and Petrology, v. 125, p. 167–185.

LeBas, M.J., Lemaitre, R.W., Streckeisen, A., and Zanettin, B., 1986, A chemical classification of volcanic rocks based on the total alkali–silica diagram: Journal of Petrology, v. 27, p. 745–750.

Lewicki, J.L., Hilley, G.E., Dobeck, L., and Marino, B.D.V., 2012, Eddy covariance imaging of diffuse volcanic CO_2 emissions at Mammoth Mountain, CA, USA: Bulletin of Volcanology, v. 74, p. 135–141.

Lewis, R.E., 1975, Data from a 1,000-foot (305-metre) core hole in the Long Valley caldera, Mono County, California: U.S. Geological Survey Open-File Report 75–683, 16 p.

Lipshie, S.R., 1974, Surficial and engineering geology of the Mammoth Creek area, Mono County, California: University of California at Los Angeles, M.S. thesis, 163 p.

Mahood, G.A., Ring, J.H., Manganelli, S., and McWilliams, M.O., 2010, New $^{40}Ar/^{39}Ar$ ages reveal contemporaneous mafic and silicic eruptions during the past 160,000 years at Mammoth Mountain and Long Valley caldera, California: Geological Society of America Bulletin, v. 122, p. 396–407.

Mankinen, E.A., Grommé, C.S., Dalrymple, G.B., Lanphere, M.A., and Bailey, R.A., 1986, Paleomagnetism and K-Ar ages of volcanic rocks from Long Valley, California: Journal of Geophysical Research, v. 91, no. B1, p. 633–652.

Mastin, L.G., 1991, The roles of magma and groundwater in the phreatic eruptions at Inyo Craters, Long Valley Caldera, California: Bulletin of Volcanology, v. 53, no. 8, p. 579–596.

Mastin, L.G., and Pollard, D.D., 1988, Surface deformation and shallow dike intrusion processes at Inyo Craters, Long Valley, California: Journal of Geophysical Research, v. 93, no. B11, p. 13,221–13,235.

Matthes, F.E., 1960, Reconnaissance of the geomorphology and glacial geology of the San Joaquin basin, Sierra Nevada, California: U.S. Geological Survey Professional Paper 329, 62 p.

Mayo, E.B., 1930, Preliminary report on the geology of southwestern Mono County, California: Mining in California, Report 26 of the State Mineralogist, p. 475–482.

Mayo, E.B., 1934a, Geology and mineral deposits of Laurel and Convict Basins, southwestern Mono County, California: California Journal of Mines and Geology, v. 30, p. 79–87.

Mayo, E.B., 1934b, The Pleistocene Long Valley Lake in eastern California: Science, v. 80, no. 2065, p. 95–96.

Mayo, E.B., 1935, Some intrusions and their wall rocks in the Sierra Nevada: Journal of Geology, v. 43, no. 7, p. 673–689.

Mayo, E.B., 1937, Sierra Nevada pluton and crustal movement: Journal of Geology, v. 45, no. 2, p. 169–192.

Mayo, E.B., Conant, L.C., and Chelikowsky, J.R., 1936, Southern extension of the Mono Craters, California: American Journal of Science, v. 32, p. 81–97.

McConnell, V.S., Shearer, C.K., Eichelberger, J.C., Keskinen, M.J., Layer, P.W., and Papike, J.J., 1995, Rhyolite intrusions in the intracaldera Bishop Tuff, Long Valley caldera, California: Journal of Volcanology and Geothermal Research, v. 67, p. 41–60.

Metz, J., 1987, Physical and chemical evolution of Glass Mountain; Precaldera high-silica rhyolites from the Long Valley magma system: Stanford University, Ph.D. dissertation, 161 p.

Metz, J.M., and Bailey, R.A., 1993, Geologic map of Glass Mountain, Mono County, California: U.S. Geological Survey Map I-1995, scale 1:24,000.

Metz, J.M., and Mahood, G.A, 1985, Precursors to the Bishop Tuff eruption; Glass Mountain, Long Valley, California: Journal of Geophysical Research, v. 90, no. B13, p. 11,121–11,126.

Metz, J.M., and Mahood, G.A, 1991, Development of the Long Valley, California, magma chamber recorded in precaldera rhyolite lavas of Glass Mountain: Contributions to Mineralogy and Petrology, v. 106, p. 379–397.

Millar, C.I., King, J.C., Westfall, R.D., Alden, H.A., and Delany, D.L., 2006, Late Holocene forest dynamics, volcanism, and climate change at White Wing Mountain and San Joaquin Ridge, Mono County, Sierra Nevada, CA, USA: Quaternary Research, v. 66, p. 273–287.

Millar, C.I., and Westfall, R.D., 2008, Rock glaciers and related periglacial landforms in the Sierra Nevada, CA, USA; inventory, distribution and climatic relationships: Quaternary International, v. 188, p. 90–104.

Miller, C.D., 1985, Holocene eruptions at the Inyo volcanic chain, California—Implications for possible eruptions in the Long Valley caldera: Geology, v. 13, p. 14–17.

Moore, J.G., and Dodge, F.C.W., 1980, Late Cenozoic volcanic rocks of the southern Sierra Nevada, California; I., Geology and petrology: Geological Society of America Bulletin, v. 91, no. 9, p. 515–518 and p. 1995–2038.

Morgan, B.A., and Rankin, D.W., 1972, Major structural break between Paleozoic and Mesozoic rocks in the eastern Sierra Nevada, California: Geological Society of America Bulletin, v. 83, p. 3,739–3,744.

Muffler, L.J.P., Clynne, M.A., Calvert, A.T., and Champion, D.E., 2011, Diverse, discrete, mantle-derived batches of basalt erupted along a short normal fault zone; the Poison Lake chain, southernmost Cascades: Geological Society of America Bulletin, v. 123, p. 2177–2200.

Mullineaux, D.R., 1996, Pre-1980 tephra-fall deposits erupted from Mount St. Helens, Washington: U.S. Geological Survey Professional Paper 1563, 99 p.

Nakada, S., Shimizu, H., and Ohta, K., 1999, Overview of the 1990–1995 eruption at Unzen Volcano: Journal of Volcanology and Geothermal Research, v. 89, p. 1–22.

Nawotniak, S.E.K., and Bursik, M., 2010, Subplinian fall deposits of Inyo Craters, California: Journal of Volcanology and Geothermal Research, v. 198, p. 433–446.

Oldow, J.S., 2003, Active transtensional boundary zone between the western Great Basin and Sierra Nevada block, western U.S. Cordillera: Geology, v. 31, p. 1033–1036.

Peck, D.L., and Minakami, T., 1968, The formation of columnar joints in the upper part of Kilauean lava lakes, Hawaii: Geological Society of America Bulletin, v. 79, p. 1151–1166.

Phillips, F.M., Zreda, M.G., Benson, L.V., Plummer, M.A., Elmore, D., and Sharma, P., 1996, Chronology for fluctuations in late Pleistocene Sierra Nevada glaciers and lakes: Science, v. 274, p. 749–751.

Phillips, F.M., Zreda, M., Plummer, M.A., Elmore, D., and Clark, D.H., 2009, Glacial geology and chronology of Bishop Creek and vicinity, eastern Sierra Nevada, California: Geological Society of America Bulletin, v. 121, p. 1013–1033.

Pitt, A.M., and Hill, D.P., 1994, Long-period earthquakes in the Long Valley caldera region, eastern California: Geophysical Research Letters, v. 21, no. 16, p. 1679–1682.

Pitt, A.M., Hill, D.P., Walter, S.W., and Johnson, M.J.S., 2002, Midcrustal, long-period earthquakes beneath northern California volcanic areas: Seismological Research Letters, v. 73, p. 144–152.

Prejean, S., Ellsworth, W.L., Zoback, M., and Waldhouser, F., 2002, Fault structure and kinematics of the Long Valley caldera region, CA, revealed by high-accuracy earthquake hypocenters and focal mechanism stress inversions: Journal of Geophysical Research, v. 107, no. B12, p. 1–19.

Prejean, S., Stork, A., Ellsworth, W., Hill, D., and Julian, B., 2003, High precision earthquake locations reveal seismogenic structure beneath Mammoth Mountain, California: Geophysical Research Letters, v. 30, no. 24, 2247, p. 1–4.

Putnam, W.C., 1949, Quaternary geology of the June Lake district, California: Geological Society of America Bulletin, v. 60, p. 1281–1302.

Putnam, W.C., 1960, Origin of Rock Creek and Owens River gorges, Mono County, California: University of California Publications in Geological Sciences, v. 34, p. 221–280.

Putnam, W.C., 1962, Late Cenozoic geology of McGee Mountain, Mono County, California: University of California Publications in Geological Sciences, v. 40, no. 3, p. 181–207.

Reid, M.R., Coath, C.D., Harrison, T.M., and McKeegan, K.D., 1997, Prolonged residence times for the youngest rhyolites associated with Long Valley caldera; ^{230}Th-^{238}U ion microprobe dating of young zircons: Earth and Planetary Sciences Letters, v. 150, p. 27–39.

Riley, P., Tikoff, B., and Hildreth, W., 2012, Transtensional deformation and structural control of contiguous but independent magmatic systems; Mono-Inyo Craters, Mammoth Mountain, and Long Valley caldera, California: Geosphere, v. 8, no. 4, p. 740–751.

Rinehart, C.D., and Huber, N.K., 1965, The Inyo Crater Lakes—A blast in the past: California Division of Mines and Geology, Mineral Information Service, v. 18, no. 9, p. 169–172.

Rinehart, C.D., and Ross, D.C., 1957, Geology of the Casa Diablo Mountain quadrangle, California: U.S. Geological Survey Map GQ-99, scale 1:62,500.

Rinehart, C.D., and Ross, D.C., 1964, Geology and mineral deposits of the Mount Morrison Quadrangle, Sierra Nevada, California: U.S. Geological Survey Professional Paper 385, 106 p.

Ring, J.H., 2000, Young volcanism in western Long Valley caldera: Stanford University, M.S. thesis, 128 p.

Rivera, T.A., Storey, M., Zeeden, C., Hilgen, F.J., and Kuiper, K., 2011, A refined astronomically calibrated ^{40}Ar/^{39}Ar age for Fish Canyon sanidine: Earth and Planetary Science Letters, v. 311, p. 420–426.

Rogie, J.D., Kerrick, D.M., Sorey, M.L., Chiodini, G., and Galloway, D.L., 2001, Dynamics of carbon dioxide emission at Mammoth Mountain, California: Earth and Planetary Science Letters, v. 188, p. 535–541.

Rood, D.H., Burbank, D.W., and Finkel, R.C., 2011, Chronology of glaciations in the Sierra Nevada, California, from ^{10}Be surface exposure dating: Quaternary Science Reviews, v. 30, p. 646–661.

Ryan, M.P., and Sammis, C.G., 1978, Cyclic fracture mechanisms in cooling basalt: Geological Society of America Bulletin, v. 89, p. 1295–1308.

Sampson, D.E., 1987, Textural heterogeneities and vent area structures in the 600-year-old lavas of the Inyo volcanic chain, eastern California, *in* Fink, J.H., ed., The emplacement of silicic domes and lava flows: Geological Society of America Special Paper 212, p. 89–101.

Sampson, D.E., and Cameron, K.L., 1987, The geochemistry of the Inyo volcanic chain; Multiple magma systems in the Long Valley region, eastern California: Journal of Geophysical Research, v. 92, no. B10, p. 10,403–10,421.

Sarna-Wojcicki, A.M., Reheis, M.C., Pringle, M.S., Fleck, R.J., Burbank, D., Meyer, C.E., Slate, J.L., Wan, E., Budahn, J.R., Troxel, B., and Walker, J.P., 2005, Tephra layers of Blind Spring Valley and related upper Pliocene and Pleistocene tephra layers, California, Nevada, and Utah; Isotopic ages, correlation, and magnetostratigraphy: U.S.; Geological Survey Professional Paper 1701, 63 p.

Savage, J.C., and Clark, M.M., 1982, Magmatic resurgence in Long Valley caldera, California; Possible cause of the 1980 Mammoth Lakes earthquakes: Science, v. 217, no. 4559, p. 531–533.

Sharp, R.P., 1968, Sherwin Till–Bishop Tuff geological relationships, Sierra Nevada, California: Geological Society of America Bulletin, v. 79, p. 351–364.

Sharp, R.P., 1969, Semiquantitative differentiation of glacial moraines near Convict Lake, Sierra Nevada, California: Journal of Geology, v. 77, p. 68–91.

Shelly, D.R., and Hill, D.P., 2011, Migrating swarms of brittle-failure earthquakes in the lower crust beneath Mammoth Mountain, California: Geophysical Research Letters, v. 38, L20307, doi:10.1029/2011GL049336.

Shevenell, L., Goff, F., Grigsby, C.O., Janik, C.J., Trujillo, P.E., Jr., and Counce, D., 1987, Chemical and isotopic characteristics of thermal fluids in the Long Valley caldera lateral flow system, California: Geothermal Resources Council Transactions, v. 11, p. 195–201.

Simon, J.I., Reid, M.R., and Young, E.D., 2007, Lead isotopes by LA-MC-ICPMS; Tracking the emergence of mantle signatures in an evolving silicic magma system: Geochimica et Cosmochimica Acta, v. 71, no. 8, p. 2014–2035.

Simon, J.I., Weis, D., DePaolo, D.J., Renne, P.R., Mundil, R., and Schmitt, A.K., 2014, Assimilation of preexisting Pleistocene intrusions at Long Valley by periodic magma recharge accelerates rhyolite generation: rethinking the remelting model: Contributions to Mineralogy and Petrology, v. 167:955, 35 p.

Smith, R.L., and Bailey, R.A., 1968, Resurgent cauldrons: Geological Society of America Memoir 116, p. 613–662.

Smith, J.L., and Rex, R.W., 1977, Drilling results from the eastern Long Valley caldera: American Nuclear Society Meeting on Energy and Mineral Recovery Research, Golden, Colorado, April 12–14, 1977, p. 529–540.

Sorey, M.L., 1985, Evolution and present state of the hydrothermal system in Long Valley caldera: Journal of Geophysical Research, v. 90, no. B13, p. 11,219–11,228.

Sorey, M.L., Evans, W.C., Kennedy, B.M., Farrar, C.D., Hainsworth, L.J., and Hausback, B., 1998, Carbon dioxide and helium emissions from a reservoir of magmatic gas beneath Mammoth Mountain, California: Journal of Geophysical Research, v. 103, no. B7, p. 15,303–15,323.

Sorey, M.L., Farrar, C.D., Gerlach, T.M., McGee, K.A., Evans, W.C., Colvard, E.M., Hill, D.P., Bailey, R.A., Rogie, J.D., Hendley, J.W., II, and Stauffer, P.H., 2000, Invisible CO_2 gas killing trees at Mammoth Mountain, California: U.S. Geological Survey Fact Sheet 172–96, 2 p.

Sorey, M.L., Kennedy, B.M., Evans, W.C., Farrar, C.D., and Suemnicht, G.A., 1993, Helium isotope and gas discharge variations associated with crustal unrest in Long Valley caldera, California, 1989–1992: Journal of Geophysical Research, v. 98, no. B9, p. 15,871–15,889.

Sorey, M.L., Lewis, R.E., and Olmsted, F.H., 1978, The hydrothermal system of Long Valley caldera, California: U.S. Geological Survey Professional Paper 1044-A, 60 p., 1 plate.

Sorey, M.L., Suemnicht, G.A., Sturchio, N.C., and Nordquist, G.A., 1991, New evidence on the hydrothermal system in Long Valley caldera, California, from wells, fluid sampling, electrical geophysics, and age determinations of hot-spring deposits: Journal of Volcanology and Geothermal Research, v. 48, p. 229–263.

Steiger, R.H., and Jäger, E., 1977, Subcommission on Geochronology—Convention on the use of decay constants in geo- and cosmochronology: Earth and Planetary Science Letters, v. 36, p. 359–362.

Stevens, C.H., and Greene, D.C., 1999, Stratigraphy, depositional history, and tectonic evolution of Paleozoic continental-margin rocks in roof pendants of the eastern Sierra Nevada, California: Geological Society of America Bulletin, v. 111, p. 919–933.

Stuiver, M., and Reimer, P.J., 1993, Extended ^{14}C data base and revised CALIB radiocarbon calibration program: Radiocarbon, v. 35, p. 215–230 (version 5.0).

Suemnicht, G.A., 1987, Results of deep drilling in the western moat of Long Valley, California: Eos, v. 68, no. 40, p. 785, 798.

Suemnicht, G.A., Sorey, M.L., Moore, J.N., and Sullivan, R., 2006, The shallow hydrothermal system of Long Valley caldera, California: Geothermal Resources Council Transactions, v. 30, p. 465–469.

Suemnicht, G.A., and Sorey, M.L., 2007, Long Valley caldera geothermal and magmatic systems: Geothermal Resources Council, Field Trip #1; September 29–30, 2007 for the Annual Meeting, Reno, Nevada; 21 p.

Suemnicht, G.A., and Varga, R.J., 1988, Basement structure and implications for hydrothermal circulation patterns in the western moat of Long Valley caldera, California: Journal of Geophysical Research, v. 93, no. B11, p. 13,191–13,207.

Taylor, G.C., and Bryant, W.A., 1980, Surface rupture associated with the Mammoth Lakes earthquakes of 25 and 27 May, 1980, *in* Sherburne, R.W., ed., Mammoth Lakes, California earthqukes of May 1980: California Division of Mines and Geology Special Report 150, p. 49–67.

Tikoff, B., and Greene, D., 1997, Stretching lineations in transpressional shear zones; An example from the Sierra Nevada Batholith, California: Journal of Structural Geology, v. 19, p. 29–39.

Tikoff, B., and Saint Blanquat, M., 1997, Transpressional shearing and strike-slip partitioning in the Late Cretaceous Sierra Nevada magmatic arc, California: Tectonics, v. 16, p. 442–459.

Tikoff, B., and Teyssier, C., 1992, Crustal-scale, en echelon "P-shear" tensional bridges: A possible solution to the batholithic room problem: Geology, v. 20, p. 927–930.

Tizzani, P., Battaglia, M., Zeni, G., Atzori, S., Berardino, P., and Lanari, R., 2009, Uplift and magma intrusion at Long Valley caldera from InSAR and gravity measurements: Geology, v. 37, p. 63–66.

Varga, R.J., Bailey, R.A., and Suemnicht, G.A., 1990, Evidence for 600-year-old basalt and magma mixing at Inyo Craters volcanic chain, Long Valley caldera, California: Journal of Geophysical Research, v. 95, no. B13, p. 21,441–21,450.

Vogel, T.A., Eichelberger, J.C., Younker, L.W., Schuraytz, B.C., Horkowitz, J.P., Stockman, H.W., and Westrich, H.R., 1989, Petrology and emplacement dynamics of intrusive and extrusive rhyolites of Obsidian Dome, Inyo Craters Volcanic Chain, eastern California: Journal of Geophysical Research, v. 94, p. 17,937–17,956.

Vogel, T.A., Woodburne, T.B., Eichelberger, J.C., and Layer, P.W., 1994, Chemical evolution and periodic eruption of mafic lava flows in the west moat of Long Valley Caldera, California: Journal of Geophysical Research, v. 99, no. B10, p. 19,829–19,842.

Wahrhaftig, C., and Cox, A., 1959, Rock glaciers in the Alaska Range: Geological Society of America Bulletin, v. 70, no. 4, p. 383–436.

Waitt, R.B., and Begét, J.E., 2009, Volcanic processes and geology of Augustine Volcano, Alaska: U.S. Geological Survey Professional Paper 1762, 78 p., 2 plates.

Walker, M., Johnsen, S., Rasmussen, S.O., Popp, T., Steffensen, J.-P., Gibbard, P., Hoek, W., Andrews, J., Björck, S., Cwynar, L.C., Hughen, K., Kershaw, P., Kromer, B., Litt, T., Lowe, D.J., Nakagawa, T., Newnham, R., and Schwander, J., 2009, Formal definition and dating of the GSSP (Global Stratotype Section and Point) for the base of the Holocene using the Greenland NGRIP ice core and selected auxiliary records: Journal of Quaternary Science, v. 24, no. 1, p. 3–17.

Wallace, P.J., Anderson, A.T., Jr., and Davis, A.M., 1999, Gradients in H_2O, CO_2, and exsolved gas in a large-volume silicic magma system; Interpreting the record preserved in melt inclusions from the Bishop Tuff: Journal of Geophysical Research, v. 104, no. B9, p. 20,097–20,122.

Wilson, C.J.N., and Hildreth, W., 1997, The Bishop Tuff; New insights from eruptive stratigraphy: Journal of Geology, v. 105, p. 407–439.

Wilson, C.J.N., and Hildreth, W., 1998, Hybrid fall deposits in the Bishop Tuff, California: A novel pyroclastic depositional mechanism: Geology, v. 26, no. 1, p. 7–10.

Wood, S.H., 1977, Distribution, correlation, and radiocarbon dating of late Holocene tephra, Mono and Inyo Craters, eastern California: Geological Society of America Bulletin, v. 88, p. 89–95.

Table 1. Unit names and petrography.

[Mammoth magmatic system includes the main silicic edifice and contemporaneous basaltic, andesitic, and dacitic units that erupted peripherally. Long Valley rhyolites and nearby Tertiary eruptive units are listed separately. SiO_2 contents are from appendix. Volume percent phenocrysts were estimated visually in thin section. Mineral species, in declining order of abundance, are abbreviated: aln, allanite; bi, biotite; cpx, clinopyroxene; hb, hornblende; ol, olivine; opx, orthopyroxene; ox, Fe-Ti oxides; pl, plagioclase; px, pyroxenes (undivided); qz, quartz; san, sanidine. Other abbreviations: pdc, pyroclastic density current; xen, xenocryst. Three-letter labels appear on maps and diagrams; details of all are given in Description of Map Units. Units amp, bed, and mcl appear in more than one geographic set below]

Map unit	Unit name	Percent SiO_2	Percent phenocrysts
	Mammoth Mountain edifice (25 units)		
dbp	Trachydacite of Bottomless Pit	67	15–20 pl-san-hb-bi-ox
ddl	Trachydacite of lower Dragons Back	66–67	15–22 pl-san-hb-bi-px-ox
ddu	Trachydacite of upper Dragons Back	66–67	17–22 pl-san-hb-bi-px-ox
dfl	Trachydacite of Face Lift	63–65	15–25 pl-san-bi-px-hb-ox
dgr	Trachydacite of Gold Rush Express	68.5–69	20–25 pl-san-bi-hb-px-ox
dlp	Trachydacite of Lincoln Peak	67.5–69	17–25 pl-san-bi-hb-px-ox
dml	Trachydacite of Main Lodge coulee	65.5–68.5	17–27 pl-san-bi-hb-px-ox
dms	Trachydacite of McCoy Station	68.5–69.5	15–20 pl-san-bi-px-hb-ox
dnh	Trachydacite north of Horseshoe Lake	68–68.5	17–20 pl-san-bi-hb-px-ox
dnk	Trachydacite of North Knob	66.5	18–23 pl-san-bi-hb-ox
dom	Trachydacite of Old Mammoth	65.5–66	15–20 pl-san-hb-bi-ox
drc	Trachydacite of upper Reds Creek	63.5–65.5	15–22 pl-san-hb-bi-px-ox
dsd	Trachydacite of South Summit Dome	67–68.5	17–22 pl-san-bi-hb-px-ox
dsk	Trachydacite of Skyline Dome	67–70	15–20 pl-san-bi-px-ox
dsu	Trachydacite of Mammoth Mtn summit	68–69.5	15–20 pl-san-bi-hb-px-ox
dtl	Trachydacite of Twin Lakes outlet	63–64	25–35 pl-san-hb-bi-px-ox
dwr	Trachydacite of White Bark Ridge	68–69.5	13–17 pl-san-bi-hb-px-ox
d61	Trachydacite of Dome 2861	66–67.5	15–20 pl-san-hb-bi-px-ox
d81	Trachydacite of Dome 2781	68.5–69	13–17 pl-san-bi-hb-px-ox
rce	Alkalic rhyodacite of Canyon Express	70–71	5–9 pl-san-bi-ox
rfp	Alkalic rhyodacite pumice fall of Hwy 203	70–71	5–8 pl-san-bi-ox
rmf	Alkalic rhyodacite of Mammoth Mtn fumarole	70–71	12–15 pl-san-bi-px-ox
rrc	Alkalic rhyodacite of Reds Creek	71	5–7 pl-san-px-ox
rsq	Alkalic rhyodacite of Quicksilver Ski Run	70–71	10–15 pl-san-bi-px-ox
rss	Alkalic rhyodacite of Solitude Ski Run	70–71	10–15 pl-san-bi-px-ox
	South moat peripheral eruptive units (15 units)		
aml	Trachyandesite of McLeod Lake	61.5–62.5	3–5 pl-hb-opx-ox
amp	Trachyandesite of Mammoth Pass	57–61.5	1–2 pl-ol-cpx-ox
asr	Trachyandesite of Shady Rest Campground	56.5	<1 pl-cpx-ox
bcd	Basalt of Casa Diablo Hot Springs	51–52	15–20 pl-ol-cpx±ox
bed	Basalt east of Dry Creek (source of bcd)	52	13–18 pl-ol-cpx±ox
bfh	Basalt of Fish Hatchery	49–50	10–15 pl-ol-cpx
bhl	Basalt of Horseshoe Lake	49	18–24 pl-cpx-ol
bmc	Basalt of Mammoth Crest (source of bfh)	49.5–51	10–15 pl-ol-cpx
bsc	Trachybasalt of Sherwin Creek Road	50.5–51	<1 pl-ol-ox
bsr	Trachybasalt of Shady Rest	50.5–51.5	2–4 pl-ol-cpx±ox
mcl	Basaltic trachyandesite of Canyon Lodge	54–56	1–5 pl-ol-cpx±ox
mkv	Basaltic trachyandesite of Knolls Vista	54.5–55	1 pl-ol-cpx-ox
mlc	Basaltic trachyandesite of lower Laurel Creek	52–53	15–20 pl-ol-cpx-ox
mmc	Basaltic trachyandesite of Mammoth Creek	54.5–55	1 pl-ol-cpx-ox
msc	Basaltic trachyandesite of Sawmill Cutoff	52–52.5	2–5 pl-ol-cpx-ox
	West moat peripheral eruptive units (16 units)		
aic	Trachyandesite of Inyo Craters	57.5–59.5	1–2 pl-ol-cpx-ox
bar	Trachybasalt of Arcularius Ranch	50.5–52.5	20–30 pl-ol-cpx±ox
bcf	Trachybasalt south of Crater Flat	51.8	1 pl-ol-cpx

Table 1. Unit names and petrography.—Continued

[Mammoth magmatic system includes the main silicic edifice and contemporaneous basaltic, andesitic, and dacitic units that erupted peripherally. Long Valley rhyolites and nearby Tertiary eruptive units are listed separately. SiO_2 contents are from appendix. Volume percent phenocrysts were estimated visually in thin section. Mineral species, in declining order of abundance, are abbreviated: aln, allanite; bi, biotite; cpx, clinopyroxene; hb, hornblende; ol, olivine; opx, orthopyroxene; ox, Fe-Ti oxides; pl, plagioclase; px, pyroxenes (undivided); qz, quartz; san, sanidine. Other abbreviations: pdc, pyroclastic density current; xen, xenocryst. Three-letter labels appear on maps and diagrams; details of all are given in Description of Map Units. Units amp, bed, and mcl appear in more than one geographic set below]

Map unit	Unit name	Percent SiO_2	Percent phenocrysts
	West moat peripheral eruptive units (16 units)—Contined		
bed	Basalt east of Dry Creek (source of bcd)	52	13–18 pl-ol-cpx±ox
bmn	Trachybasalt northeast of Minaret Summit	51–53	3–8 pl-ol-cpx-ox
bsm	Basalt of Sawmill Cutoff	48.5–49	1–3 pl-ol-cpx
ddc	Trachydacite of Dry Creek	67–67.5	3–5 pl-opx-ox
dnw	Trachydacites of Northwest Moat	60–67	15–25 pl-san-bi-hb-px-ox
mcv	Basaltic trachyandesite south of Crestview	53–54	1–2 pl-ol-cpx-ox
mdm	Basaltic trachyandesite of Deer Mountain	55.5–56	<1 pl-cpx-ol
mdn	Basaltic trachyandesite NE of Deadman Pass	52.5–54	10–15 pl-ol-cpx
mic	Mafic pyroclastic deposit of Inyo Craters	54–56	1–3 pl-ol
mnd	Basaltic trachyandesite NW of Dry Creek	53–54	<1 pl-ol-ox
mor	Basaltic trachyandesite of Owens River Road	51–54	1–5 pl-ol-cpx-ox
msd	Basaltic trachyandesite scoria SE of Dry Creek	52–53	<1 pl-ol
msj	Basaltic andesite of Scenic Loop Road junction	52.8	3–4 ol-pl-cpx
	San Joaquin peripheral eruptive units (8 units)		
a62	Trachyandesite of Cone 2962	57–59	1 pl-ol-cpx-ox
amp	Trachyandesite of Mammoth Pass	57–61	1–2 pl-ol-cpx-ox
apb	Trachyandesite of Pumice Butte	58–59	3–5 pl-ol-cpx-ox
bdc	Trachybasalt west of Deer Creek	51.5	10–15 pl-ol
brc	Basalt of Red Cones	50–51	12–18 pl-ol-cpx-ox
drf	Trachydacite of Rainbow Falls	65.5–67	1–3 pl-bi-opx-hb-ox
mdp	Basaltic trachyandesite of Devils Postpile	54–54.5	9–13 pl-ol-cpx
mss	Basaltic trachyandesite of upper Soda Springs	52.5–53.5	2–5 pl-ol-ox
	Long Valley magmatic system (8 units in map area)		
rbt	Bishop Tuff	71–78	5–25 san-qz-pl-bi-ox-px-aln
rdc	Rhyolite of Dry Creek Dome	76–76.5	15–20 san-pl-qz-bi-hb-ox-aln
rdm	Rhyolite of Deer Mountain	72	20–30 qz-pl-san-bi-hb-ox-px-aln
rer	Early Rhyolite of Bailey	74.5–75.5	0–2 pl-opx-bi
rhc	Rhyolite of Hot Creek flow	76	1 pl-san-bi-px-ox
rmk	Rhyolite of Mammoth Knolls	76.5–77	20 san-qz-pl-bi-hb-ox-aln
rnc	Rhyolite of north-central chain	74–75.5	15–20 pl-san-hb-bi-qz-ox
rwm	Rhyolite of West Moat Coulee	72–73.5	17–25 pl-qz-san-bi-hb-ox-px-aln
	Tertiary eruptive units (32 in map area)		
Tacc	Trachyandesite of Crater Creek	58–63	1 hb-cpx-(qz xens)
Taec	Trachyandesite east of Crestview	57	<1 ol
Tasj	Trachyandesite of San Joaquin River	58–58.3	15–20 pl-cpx-ol-ox
Taww	Trachyandesite north of White Wing Camp	59–60	4–7 ol-pl-cpx
Tbbs	Basalt east of Big Springs	50–51	<1 ol
Tbdp	Trachybasalt of Deadman Pass	50–53	7–20 ol-cpx-ox
Tbld	Basalt south of Lost Dog Lake	52	5–7 ol-ox
Tbmm	Trachybasalt of Mammoth Mine	52	7–10 ol-ox
Tbpl	Trachybasalt east of Pond Lily Lake	49–52	7–12 ol-cpx
Tbrm	Basalt of Red Mountain	50	5–8 ol-ox
Tbtb	Basalt of The Buttresses	46.5–50.5	15–25 cpx-ol±pl
Tb84	Trachybasalt of Cone 8478	49–54	8–15 ol-cpx-pl-ox
Tdlm	Trachydacite of Laurel Mountain	63	5 hb-pl-opx-ox

Table 1. Unit names and petrography.—Continued

[Mammoth magmatic system includes the main silicic edifice and contemporaneous basaltic, andesitic, and dacitic units that erupted peripherally. Long Valley rhyolites and nearby Tertiary eruptive units are listed separately. SiO2 contents are from appendix. Volume percent phenocrysts were estimated visually in thin section. Mineral species, in declining order of abundance, are abbreviated: aln, allanite; bi, biotite; cpx, clinopyroxene; hb, hornblende; ol, olivine; opx, orthopyroxene; ox, Fe-Ti oxides; pl, plagioclase; px, pyroxenes (undivided); qz, quartz; san, sanidine. Other abbreviations: pdc, pyroclastic density current; xen, xenocryst. Three-letter labels appear on maps and diagrams; details of all are given in Description of Map Units. Units amp, bed, and mcl appear in more than one geographic set below]

Map unit	Unit name	Percent SiO_2	Percent phenocrysts
Tdpd	Trachydacite pdc of Deadman Pass	~70	20–25 pl-bi-hb-opx-ox
Tdsd	Trachydacite of Dome 3321 (South Dome)	~70	30–35 pl-bi-hb-opx-ox
Tdsj	Trachydacite block-and-ash-flow deposit of San Joaquin Ridge	~70	30–35 pl-bi-hb-opx-ox
Tdud	Trachydacite complex of upper Deadman Creek	68–71	25–35 pl-bi-hb-ox
Tdww	Trachydacite of White Wing Mountain	67	20–25 pl-bi-hb-ox
Td65	Trachydacite of Dome 2965	64.5	20–25 pl-bi-hb-opx-ox
Td78	Trachydacite of Dome 7835	65	10 bi-hb-pl-ox
Td83	Trachydacite of Dome 8325	66–66.5	10–13 bi-hb-pl-cpx-ox
Tmcl	Basaltic trachyandesite west of Cabin Lake	53	7–10 ol
Tmcm	Basaltic trachyandesite south of Crater Mdw	53	5–7 ol
Tmcr	Basaltic trachyandesite of Mammoth Crest	53	7 ol-ox
Tmcv	Basaltic trachyandesite of Crestview	53–55	7–10 ol-cpx-pl
Tmcw	Basaltic trachyandesite west of Crater Creek	52–53	10 ol-cpx-pl
Tmel	Basaltic trachyandesite of Emerald Lake	52	7–10 ol-cpx
Tmsd	Basaltic trachyandesite south of Deer Creek	53	5–7 ol-cpx
Tmwc	Basaltic trachyandesite west of Castle Lake	53	7 ol
Tmw	Basaltic trachyandesite near Obsidian Flow	53–54.5	10–15 ol-pl-cpx
Tmww	Basaltic trachyandesite of White Wing Mtn	52	5–8 ol-cpx
Trac	Rhyolite tuff of Alpers Canyon	72+	30–45 san-qz-pl-bi-ox

Table 2. $^{40}Ar/^{39}Ar$ ages for Mammoth Mountain and its mafic periphery.

[Samples irradiated at USGS TRIGA reactor using 9.6345 Ma Bodie Hills sanidine as a neutron flux monitor. MSWD, mean square weighted deviation. $^{40}Ar/^{36}Ar$ indicates initial ratio. Samples were groundmass concentrates except those marked as plag (plagioclase) or fsp (sodic sanidine ± minor plagioclase). Preferred ages in bold font. All determinations in USGS lab at Menlo Park, supervised by A.T. Calvert. For details of methods, see Calvert and Lanphere (2006)]

Sample	Map unit	$^{40}Ar/^{39}Ar$ weighted mean plateau age			$^{40}Ar/^{39}Ar$ isotope correlation (isochron) age				$^{40}Ar/^{39}Ar$ total gas age (ka)	Recoil age (ka)
		Age (ka)	%^{39}Ar [steps, °C]	MSWD	Age (ka)	%^{39}Ar [steps, °C]	MSWD	$^{40}Ar/^{36}Ari$		
M-123	mdn	**15.5 ± 1.8**	62.8 [800–950]	0.55	19.8 ± 11.6	62.8 [800–950]	0.98	293.4 ± 12.5	4.2 ± 1.6	
M-124	mcl	**177.2 ± 2.0**	64.5 [700–950]	1.08	182.1 ± 14.8	64.5 [700–950]	1.31	294.2 ± 8.6	171.6 ± 2.2	
M-145 plag	Tasj	**9164 ± 17**	41 [950–1150]	1.89	9188 ± 79	100 [650–1450]	35.7	279.2 ± 27.2	9102 ± 9	
M-168	mdp	**82.1 ± 1.6**	79 [700–1050]	0.61	86.3 ± 4.1	79 [700–1050]	1.35	293.6 ± 3.1	79.9± 1.7	
M-173	bsr	**103.5 ± 1.4**	88 [550–925]	0.9	100.7 ± 6.5	88 [550–925]	1.02	297.6 ± 11.4	100.2 ± 1.5	
M-181	bfh	**92.4 ± 2.5**	100.0 [550–1175]	1.23	98.4 ± 3.1	100.0 [550–1175]	0.72	293.1 ± 1.9	87.5 ± 3.1	
M-182	bsc	**171.8 ± 1.8**	75.1 [650–900]	0.74	159.3 ± 7.1	75.1 [650–900]	0.17	303.5 ± 10.1	168.9 ± 1.7	
M-185	Tbtb	**3754.4 ± 6.9**	46.4 [625–795]	0.96	3754.3 ± 8.0	46.4 [625–795]	1.26	295.3 ± 15.6	3728.4 ± 6.7	
M-219	mcl	**174.6 ± 3.2**	73.0 [550–800]	0.61	166.2 ± 5.1	73.0 [550–800]	0.56	297.0 ± 1.7	161.2 ± 3.4	
M-225 fsp	dnw	**41.7± 0.8**	85 [1125–1450]	1.16	43.8± 2.0	85 {1125–1450]	1.03	284.2± 21.3	38.3± 1.1	
M-240	Tdlm	3558.1 ± 5.8	52 [825–1025]	4.07	3574.5 ± 7.2	52 [825–1025]	1.96	295.9 ± 1.9	3605.6 ± 2.7	**3600.2 ± 42.5**
M-243	bsm	**164.9 ± 2.1**	100 [550–1100]	0.67	169.2 ± 5.8	100 [550–1100]	0.79	294.0 ± 4.2	164.2 ± 2.0	
M-267	mcv	**33.8 ± 1.0**	72 [800–1150]	0.25	35.4 ± 2.9	72 [800–1150]	0.21	294.5 ± 3.7	28.2 ± 1.1	
M-282	bcf	**163.7 ± 1.7**	88 [550–900]	0.2	162.3 ± 3.7	88 [550–900]	0.21	295.9 ± 1.9	158.8 ± 2.1	
M-313	mlc	**129.6 ± 1.2**	92.6 [600–975]	0.95	131.9 ± 2.2	92.6 [600–975]	0.88	293.1 ± 4.1	127.1 ± 1.3	
M-315	mcl	**179.5 ± 2.4**	66 [750–1150]	0.67	183.0 ± 5.0	66 [750–1150]	0.68	294.7 ± 2.3	199.2 ± 2.4	
M-316	bcd	**125.3 ± 1.9**	82 [550–850]	0.67	125.9 ± 7.0	82 [550–850]	0.8	295.3 ± 4.8	115.3 ± 2.2	
M-319	dom	**72.8 ± 0.6**	88.5 [600–850]	0.82	70.5 ± 2.1	88.5 [600–850]	0.87	299.9 ± 9.3	70.6 ± 0.6	
M-322 fsp	d81	**98.9± 7.5**	79 [800–1200]	0.47	72.8± 25.1	79 [800–1200]	0.26	307.7± 26.6	176.0± 7.3	
M-324	msc	**154.2 ± 1.5**	87 [600–1000]	0.96	153.2 ± 4.9	87 [600–1000]	1.08	295.9 ± 3.9	151.5 ± 2.0	
M-329 fsp	rfp	**80.1± 8.3**	80 [900–1225]	0.36	65.3± 31.5	80 [900–1225]	0.34	326.6± 164.8	101.1±14.4	
M-335	mdn	**16.9 ± 1.3**	100 [550–1100]	0.65	16.4 ± 2.1	100 [550–1100]	0.72	295.7 ± 1.3	17.4 ± 1.5	
M-344 fsp	dwr	**73.2 ± 2.0**	87.5 [700–1200]	0.64	75.1 ± 2.7	87.5 [700–1200]	0.5	293.1 ± 11.4	87.7 ± 2.4	
M-347 fsp	dwr	**78.6 ± 11.8**	52.7 [700–1150]	0.34	79.0 ± 13.9	52.7 [700–1150]	0.4	295.3 ± 7.6	89.3 ± 10.3	
M-355	dnk	**60.4 ± 1.2**	88 [550–800]	0.26	62.5 ± 2.6	88 [550–800]	0.13	292.5 ± 7.7	57.3 ± 1.7	
M-359 fsp	rss	**50.3 ± 3.1**	64.7 [600–1175]	0.25	50.4 ± 4.7	64.7 [600–1175]	0.3	295.4 ± 6.4	99.3 ±2.7	
M-365	mss	**121.4 ± 2.1**	96.9 [550–975]	1.49	120.2 ± 4.8	96.9 [550–975]	1.99	296.0 ± 4.5	124.8 ± 1.9	
M-374 fsp	rrc	**83.3 ± 1.1**	67.1 [600–1000]	0.17	84.8 ± 2.2	67.1 [600–1000]	0.005	292.5 ± 8.7	111.1 ± 1.1	
M-375 fsp	dsd	**86.7 ± 6.1**	79 [600–1100]	1.14	100.1 ± 10.1	79 [600–1100]	0.75	288.1 ± 10.9	158.9 ± 5.9	
M-392 fsp	dfl	**61.0 ± 2.7**	78 [600–1175]	0.38	65.2 ± 9.0	78 [600–1175]	0.39	292.7 ± 12.6	73.5 ± 2.5	
M-395 fsp	rce	**79.9 ± 0.7**	69.3 [800–1050]	0.22	80.3 ± 2.4	69.3 [800–1050]	0.29	294.4 ± 14.0	79.3 ± 0.9	
M-400 fsp	rsq	**63.7 ± 3.9**	99 [700–1475]	0.44	61.0 ± 8.9	99 [700–1475]	0.47	297.0 ± 11.7	65.8 ± 4.4	
M-410	bhl	**31.1 ± 1.0**	100 [550–1150]	0.91	30.5 ± 2.1	100 [550–1150]	1.02	295.9 ± 3.8	31.2 ± 1.1	
M-411 fsp	dnh	**64.5± 0.8**	73 [650–1250]	1.14	62.5± 1.2	73 [650–1250]	0.78	301.1± 6.0	68.7± 0.7	
M-416 fsp	dnw	39.6 ± 0.5	63.5 [1125–1400]	2.95	40.5 ± 1.9	63.5 [1125–1400]	3.91	282.7 ± 52.8	37.3 ± 0.3	

Table 2. $^{40}Ar/^{39}Ar$ ages for Mammoth Mountain and its mafic periphery.—Continued

[Samples irradiated at USGS TRIGA reactor using 9.6345 Ma Bodie Hills sanidine as a neutron flux monitor. MSWD, mean square weighted deviation. $^{40}Ar/^{36}Ar$ indicates initial ratio. Samples were groundmass concentrates except those marked as plag (plagioclase) or fsp (sodic sanidine ± minor plagioclase). Preferred ages in bold font. All determinations in USGS lab at Menlo Park, supervised by A.T. Calvert. For details of methods, see Calvert and Lanphere (2006)]

Sample	Map unit	$^{40}Ar/^{39}Ar$ weighted mean plateau age			$^{40}Ar/^{39}Ar$ isotope correlation (isochron) age				$^{40}Ar/^{39}Ar$ total gas age (ka)	Recoil age (ka)
		Age (ka)	%^{39}Ar [steps, °C]	MSWD	Age (ka)	%^{39}Ar [steps, °C]	MSWD	$^{40}Ar/^{36}Ari$		
M-416 fsp	dnw	34.0 ± 13.6	100 [11 crystals]	0.58	48.3 ± 11.7	100 [11 of 11]	4.4	164.6 ± 133.6	42.2 ± 14.4	
M-434 fsp	dlp	**63.7 ± 6.8**	75 [850–1225]	1.62	49.4 ± 21.9	75 [850–1225]	1.8	300.1 ± 16.0	84.3 ± 5.4	
M-447	Tmwo	3125 ± 3	37 [725–820]	0.037	3123 ± 9	37 [725–820]	0.02	297.0 ± 13.2	3140 ± 2	**3153 ± 26**
M-454 fsp	rmf	**61.4 ± 1.5**	64.5 [700–1125]	1.93	62.9 ± 2.9	64.5 [700–1125]	2.18	290.2 ± 16.6	71.8 ± 0.9	
M-463	dtl	**75.9 ± 0.6**	97.0 [550–1000]	0.79	75.1 ± 1.1	97.0 [550–1000]	0.86	298.1 ± 7.3	77.0 ± 0.7	
M-483	aic	**130.8 ± 1.4**	52.1 [750–950]	0.34	133.7 ± 3.9	52.1 [750–950]	0.38	293.3 ± 6.6	132.6 ± 1.0	133.9 ± 1.9
M-487	bdc	**155.3 ± 2.0**	95 [600–1150]	1.57	158.3 ± 4.7	95 [600–1150]	1.64	294.1 ± 4.2	156.8 ± 1.9	
M-494	Tmcm	3377.1 ± 8.8	60 [670–950]	12.28	**3362.6 ± 14.7**	60 [670–950]	8.55	342.7 ± 103.3	3311.9 ± 2.4	
M-523 fsp	dsk	**71.2 ± 1.5**	94.5 [700–1225]	0.2	69.8 ± 5.0	94.5 [700–1225]	0.16	298.8 ± 22.9	79.6 ± 1.9	
M-550	bmc	**92.7 ± 2.4**	96.2 [550–1000]	0.82	92.2 ± 4.5	96.2 [550–1000]	1.04	295.7 ± 3.6	90.6 ± 2.5	
M-613	drf	**98.8 ± 0.6**	100 [550–1150]	1.17	97.6 ± 1.3	100 [550–1150]	1.17	297.1 ± 4.0	99.0 ± 0.6	
M-650	Tasj	**9191.5 ± 14.5**	47 [900–1075]	0.57	9216.4 ± 31.2	47 [900–1075]	0.13	264.6 ± 76.1	9217.2 ± 14.0	
M-815	Tbdp	3711.6 ± 5.5	37 [750–850]	0.25	3708.2 ± 7.9	37 [750–850]	0.14	298.0 ± 9.8	3699.0 ± 4.5	**3700.2 ± 11.6**
M-816	Tbdp	**3277.3 ± 6.7**	88 [700–1025]	1.8	3271.9 ± 7.0	88 [700–1025]	1.68	301.6 ± 12.4	3281.2 ± 5.1	
M-869	dsu	**61.4 ± 2.0**	98 [600–1400]	0.91	60.8 ± 2.7	98 [600–1400]	1.04	295.9 ± 5.6	63.1 ± 2.5	
M-899	amp	**97.3 ± 1.2**	100 [550–1150]	1.18	90.1 ± 3.2	100 [550–1150]	0.67	301.5 ± 5.9	98.5 ± 1.2	
Inyo-4-461	mcl (upper Group II)	**185.9± 1.7**	97 [600–1100]	0.77	185.6 ± 3.8	97 [600–1100]	0.85	295.6 ± 5.3	184.7 ± 2.0	
Inyo-4-824	Group III	**229.9± 6.5**	94 [650–1200]	3.87	217.8 ± 5.2	94 [650–1200]	1.52	298.5 ± 1.9	251.4 ± 5.6	
Inyo-4-918	Group III	**222.5± 5.5**	56 [700–925]	0.35	211.8 ± 13.2	56 [700–925]	0.2	297.5 ± 5.2	220.6 ± 4.4	
Inyo-4-1046	Group IV	**232.6± 4.2**	96 [650–1300]	0.98	224.0 ± 6.9	96 [650–1300]	0.82	296.8 ± 1.9	240.2 ± 5.3	

Table 3. Lengths of lava-flow aprons in Mammoth Lakes region.

Map unit	Length in km
Peripheral units	
amp	9.2 (E)
	>7.3 (SW)
a62	3.5
bar	22.5
bcd	10.5
bfh	18.1
brc	2
bsc	>8
bsm	>4.3
drf	>6
mcl	9.5 (NE)
	8.8 (E)
mcv	9.8
mdp	>7.2
mkv-mmc	>4.5
mor	11.8
Mammoth Mtn	
dml	2.2
dom	4 (?)
dwr	1.5
rce	2.6
Long Valley Rhyolites	
rlm	3.8 (ESE flow, Lookout Mtn)
rhc	4.6
rnc	3.8
rwm	5.3
Neogene units	
Tasj	80
Tbtb	>15 (?)

Produced in the Menlo Park Publishing Service Center, California
Edited by Claire M. Landowski
Cartography and layout by Kathryn Nimz
Manuscript approved for publication January 27, 2015

USGS

Hildreth and Fierstein—**Eruptive History of Mammoth Mountain and its Mafic Periphery, California—Professional Paper 1812**

ISSN 1044-9612 (print)
ISSN 2330-7102 (online)
http://dx.doi.org/10.3133/pp1812

ISBN 978-1-4113-4065-7